Recherche et validation de biomarqueurs de troubles neurologiques dans les fluides biologiques

Ayoub Boulghobra

▶ **To cite this version:**

Ayoub Boulghobra. Recherche et validation de biomarqueurs de troubles neurologiques dans les fluides biologiques. Chimie analytique. Université Paris-Saclay, 2022. Français. ⟨NNT : 2022UPASF071⟩. ⟨tel-04054733⟩

HAL Id: tel-04054733

https://theses.hal.science/tel-04054733v1

Submitted on 1 Apr 2023

HAL is a multi-disciplinary open access archive for the deposit and dissemination of scientific research documents, whether they are published or not. The documents may come from teaching and research institutions in France or abroad, or from public or private research centers.

L'archive ouverte pluridisciplinaire **HAL**, est destinée au dépôt et à la diffusion de documents scientifiques de niveau recherche, publiés ou non, émanant des établissements d'enseignement et de recherche français ou étrangers, des laboratoires publics ou privés.

HAL Authorization

THESE DE DOCTORAT

NNT : 2022UPASF071

Recherche et validation de biomarqueurs de troubles neurologiques dans les fluides biologiques

Search and validation for neurological diseases' biomarkers in biological fluids

Thèse de doctorat de l'université Paris-Saclay

École doctorale n°571 : sciences chimiques : molécules, matériaux, instrumentation et biosystèmes (2MIB)
Spécialité de doctorat : Chimie
Graduate School : Chimie. Référent : Faculté des Sciences d'Orsay

Thèse préparée dans l'unité de recherche **Institut de Chimie Physique (Université Paris Saclay, CNRS)**, sous la direction de **Myriam BONOSE**, Maitresse de conférences

Thèse soutenue à Paris-Saclay, le 28 novembre 2022, par

Ayoub BOULGHOBRA

Composition du Jury

Claire SMADJA Professeure, Université Paris-Saclay	Présidente
Nathalie DELAUNAY Chargée de Recherche, HDR, ESPCI	Rapporteur & Examinatrice
Isabelle FOURNIER Professeure, Université de Lille	Rapporteur & Examinatrice
Myriam BONOSE Maitresse de conférences, Université Paris-Saclay (UMR CNRS 8000)	Directrice de thèse

université PARIS-SACLAY

ÉCOLE DOCTORALE
Sciences Chimiques : Molécules, Matériaux, Instrumentation et Biosystèmes (2MIB)

Titre : Recherche et validation de biomarqueurs de troubles neurologiques dans les fluides biologiques

Mots clés : Biomarqueurs, Liquide céphalorachidien, Diagnostic, HPLC, Spectrométrie de masse.

Résumé : Le diagnostic des erreurs innées du métabolisme de la dopamine et de la sérotonine repose sur la quantification de biomarqueurs dans le liquide céphalorachidien, qui, du fait de sa complexité, n'est réalisable que dans quelques laboratoires dans le monde. La présente thèse a pour but de proposer des méthodes plus accessibles pour le dosage de ces molécules et de mieux comprendre leur stabilité dans le liquide céphalorachidien.

Dans un premier temps, nous avons étudié la stabilité d'un biomarqueur clé dans le diagnostic de ces pathologies, à savoir la tétrahydrobioptérine. En effet, cette dernière est encline à une auto-oxydation spontanée ce qui peut engendrer un biais lors de son dosage dans le liquide céphalorachidien.

Dans un second temps, nous avons décrit et validé deux méthodes de chromatographie liquide à haute performance pour le dosage des métabolites de la dopamine et de la sérotonine : la première avec une détection par fluorescence et la seconde avec une détection par spectrométrie de masse en tandem.

Enfin, nous avons observé le phénomène d'amélioration du signal d'ionisation par electrospray avec de faibles concentrations de phosphate. La nature et le pH du tampon utilisé dans la phase mobile détermine l'intensité de cette amélioration du signal. Après avoir proposé et vérifié plusieurs hypothèses permettant d'expliquer ce phénomène, nous avons mis en évidence le fait qu'il s'agit d'un dessalage avec une diminution des adduits alcalins.

Title : Search and validation of biomarkers of neurological diseases in biological fluids

Keywords: Biomarkers, Cerebrospinal fluid, Diagnosis, HPLC, Mass spectrometry

Abstract: The diagnosis of inborn errors of dopamine and serotonin metabolism relies on the quantification of biomarkers in cerebrospinal fluid. Because of the high complexity of performing this assay, only a few laboratories in the world can realize it. The present thesis aims at proposing convenient methods for the quantification of these molecules and at understanding their stability in cerebrospinal fluid.

First, we studied the stability of a key biomarker in the diagnosis of these illnesses, specifically tetrahydrobiopterin. Indeed, the latter is inclined to spontaneous autoxidation, which may cause bias in the measured cerebrospinal concentrations.

Second, we described and validated two novel methods for the quantification of dopamine and serotonin metabolites in cerebrospinal fluid. Both are based on high-performance liquid chromatography coupled whether to fluorescence detection or to tandem mass spectrometry.

Finally, we observed an enhancement of electrospray ionisation signal when using small concentrations of phosphate.The nature and pH of the buffer used in the mobile phase highly influences the signal increase. After proposing and testing several hypotheses, it has been shown that this phenomenon relies on reducing alkalin ion adducts.

Remerciements

Je tiens à exprimer toute ma gratitude à ma directrice de thèse, Myriam BONOSE, pour sa disponibilité, sa confiance et pour m'avoir encouragé, soutenu et appris tant de choses pendant ces trois années de thèse. Un grand merci pour ta gentillesse, pour ton optimisme sans faille, et pour tes précieux conseils, tant scientifiques que personnels. Je remercie également Antoine PALLANDRE que j'ai côtoyé durant ma thèse. Merci pour avoir partagé tes connaissances scientifiques, pour tes explications sur la politique et pour tes blagues, parfois caustiques, mais toujours drôles. Merci à vous deux pour les discussions scientifiques, grâce à vous, j'ai pu apprendre et évoluer au quotidien au sein du laboratoire. Cela a été un réel plaisir de vous côtoyer et de travailler avec vous durant ces trois années. Je remercie également Fathi MOUSSA pour avoir partagé son expérience.

Je remercie Mesdames Isabelle FOURNIER et Nathalie DELAUNAY qui m'ont fait l'honneur d'être rapporteurs de mon travail de thèse. J'adresse ma profonde reconnaissance à Madame Claire SMADJA pour avoir accepté d'être examinatrice de ma thèse. Je remercie également Monsieur David TOUBOUL pour avoir été le membre extérieur de mon comité de suivi et pour m'avoir conseillé tout au long de ce projet.

Je tiens à remercier les collègues du laboratoire pour avoir fait en sorte que ces trois années soient aussi plaisantes. Merci à Sylvie pour avoir fait partie de mon comité de suivi et pour tes précieux conseils sur l'avancée du projet mais aussi sur les enseignements. Merci à Marie-Claude pour ta bonne humeur, les crêpes, les pauses-café et pour les discussions scientifiques toujours constructives. Merci à Ninette pour ton sens de l'humour, ta bienveillance et pour tes gâteaux toujours réussis (enfin, presque toujours…). Merci à Marine pour ta gentillesse et pour m'avoir fait découvrir une nouvelle façon parfaitement saine de se nourrir. Merci à Alain pour nos discussions toujours très intéressantes. Merci à Kaouther pour ta bienveillance et pour ton aide au quotidien. Merci à Philippe pour tes astuces et tes conseils.

Je voudrais également remercier les doctorants du laboratoire. Merci à Lucie pour les pauses-

goûter, pour ta gentillesse et pour nos discussions profondes sur l'avenir. Merci à Alexandre pour les pasteis de nata et pour nos discussions sur la thèse d'exercice et la thèse de sciences. Merci à Anouchka et Florent, vous êtes les best. Je remercie Taous et Terkia que j'ai côtoyées dans la deuxième moitié de ma thèse. Merci pour votre bonne humeur, pour les pauses-thé et pour les gâteaux. Merci à Lucas pour ton sens de l'humour et ta spontanéité. Je vous souhaite à tous le meilleur.

Je remercie mes amis de l'Institut Galien. Merci à Joanie, Cécile et Marco. J'ai beaucoup rigolé avec vous.

Je remercie mes amis du club jeune de l'AFSEP. Merci à Pauline, Arnaud (alias Tony), Fanny, Laetitia, Elsa et Alexandre. Je ne me suis jamais ennuyé avec vous.

Je remercie également mes amis pharmaciens et qui ont eu le même parcours, depuis le concours en première année jusqu'à la thèse de sciences. Merci à Laurène, Laurie, Amin, Kévin et Guillaume.

Je remercie chaleureusement mes amis Ahmed, Anis, Khaled, Nazim, Ilyas et Réda pour avoir toujours été là pour moi. Les moments passés avec vous ont toujours été très amusants.

Enfin, je tiens à adresser mes plus profonds remerciements à mes parents et à ma sœur. Je vous exprime toute ma gratitude pour m'avoir écouté, soutenu et encouragé tout au long de mes études. Rien n'aurait été possible sans vous.

Curriculum Vitae

Formation

- Diplôme d'Etat de Docteur en Pharmacie (option Industrie) à l'Université Paul Sabatier à Toulouse (2012-2019)
- Master Chimie Analytique Physique et Théorique à Sorbonne Université (2018-2019)
- Doctorat en Chimie Analytique à la Faculté des Sciences d'Orsay, Université Paris Saclay (2019-2022)

Formations doctorales

- Introduction à l'éthique de la recherche et intégrité scientifique, 4 décembre 2019
- Python pour la biologie, 24 mai 2021 - 27 mai 2021
- Ecole thématique : Validation de méthodes, chimiométrie et analyse de données, 14 juin 2022 - 17 juin 2022
- Ecole thématique : Spectrométrie de masse à transformée de Fourrier : Traitement des données très haute résolution, 14 novembre 2022 - 18 novembre 2022

Communications orales

- « Electrospray Ionization Enhancement using Phosphate » ; Analytics 2022 ; Cité des congrès – Nantes (5 – 8 septembre 2022)
- « A new UHPLC-MS/MS platform for metabolic profiling of human cerebrospinal fluid » ; Conférence annuel de la Société Britannique de Spectrométrie de Masse (BMSS42) ; Manchester (13 – 15 septembre 2022)

Posters

- « Quantification of inborn errors of metabolism biomarkers by UHPLC-FD and UHPLC-MS/MS » ; SEP 2021 ; Parc des expositions – Paris (5 – 7 octobre 2021)
- « Diagnosis of orphan diseases by UHPLC-MS/MS-based biomarker quantification in cerebrospinal fluid » ; Conférence annuelle de la Société Américaine de Spectrométrie de Masse (ASMS) ; Présentation en distanciel (31 octobre – 4 novembre 2021)
- « Simultaneous quantification of dopamine and serotonin metabolites in cerebrospinal fluid by UHPLC: MS/MS versus fluorescence detection » ; Conférence annuelle de la Société Américaine de Spectrométrie de Masse (ASMS) ; Minneapolis (2 – 6 juin 2022)
- « Simultaneous quantification of dopamine and serotonin metabolites in cerebrospinal fluid by UHPLC: MS/MS versus fluorescence detection » ; 50ème Symposium internationale sur la chromatographie liquide haute performance (HPLC) ; San Diego (18 – 23 juin 2022)
- « A new UHPLC-MS/MS platform for metabolic profiling of human cerebrospinal fluid » ; Analytics 2022 ; Cité des congrès – Nantes (5 – 8 septembre 2022)

Publications

- Boulghobra, A.; Bonose, M.; Billault, I.; Pallandre, A. A Rapid and Sensitive Method for the Quantification of Dopamine and Serotonin Metabolites in Cerebrospinal Fluid Based on UHPLC with Fluorescence Detection. J. Chromatogr. B 2022, 123264. https://doi.org/10.1016/j.jchromb.2022.123264

- Boulghobra, A.; Abar, T.; Moussa, F.; Baudin, B.; Rodriguez, D.; Pallandre, A.; Bonose, M. Quantification of Monoamine Biomarkers in Cerebrospinal Fluid: Comparison of a UHPLC-MS/MS Method to a UHPLC Coupled to Fluorescence Detection Method. Biomed. Chromatogr., e5502. https://doi.org/10.1002/bmc.5502

- Alhajji, E.; Boulghobra, A.; Bonose, M.; Berthias, F.; Moussa, F.; Maître, P. Multianalytical Approach for Deciphering the Specific MS/MS Transition and Overcoming the Challenge of the Separation of a Transient Intermediate, Quinonoid Dihydrobiopterin. Anal. Chem. 2022. https://doi.org/10.1021/acs.analchem.2c00924

Publications en cours de soumission

- Boulghobra, A.; Bonose, M.; Alhajji, E.; Pallandre, A.; Menet, M-C; Moussa, F. Kinetics of Autoxidation of Tetrahydrobiopterin and Quinonoid Dihydrobiopterin. Anal. Chem.

- Boulghobra, A.; Bonose, M. Quantification of Monoamine Neurotransmitter Metabolites and Cofactors in CSF: State-of-the-art

- Boulghobra, A.; Bonose, M. Electrospray Ionization Enhancement: Phosphate as an Additive to Eliminate Alkali Metal Ion Adducts

Liste des abbréviations

3-OMD	3-*ortho*-méthyl-DOPA
5-HIAA	Acide 5-hydoxyindole acétique
5-HIAL	5-hydroxyindolacétaldéhyde
5-HTP	5-hydroxytryptophane
AADC	Décarboxylase des acides aminés aromatiques
AADC-D	Déficit en décarboxylase des acides aminés aromatiques
AD	Aldéhyde déshydrogénase
AR	Aldose réductase
B	Bioptérine
BH2	7,8-dihydrobioptérine
BH4	Tétrahydrobioptérine
CID	Dissociation induite par collision
COMT	Catéchol-O-méthyl-transférase
CSF	Liquide céphalorachidien
CV	Coefficient de variation
DBH	Dopamine β-hydroxylase
DBH-D	Déficit en dopamine β-hydroxylase
DETAPAC	Acide diéthylenetriaminepentaacétique
DHFR	Dihydrofolate reductase
DHPR	Dihydroptérine réductase
DHPR-D	Déficit en dihydroptérine réductase
DOPA	Dihydroxyphénylalanine
DOPAC	Acide 3,4-dihydroxyphenylacétique
DOPAL	3,4-dihydroxyphenylacétaldehyde
DOPEGAL	3,4-dihydroxyphenylglycoaldéhyde
DTDS	Syndrome de déficience en transporteur de la dopamine
DTT	Dithiothréitol
ECD	Détection électrochimique
EIM	Erreurs innées du métabolisme
EMA	Agence européenne du médicament
ESI	Electrospray
FD	Détection par fluorescence
FIA	Analyse en injection directe

GABA	Acide γ-aminobutyrique
GTP	Guanosine triphosphate
GTPCH	Guanosine-triphosphate cyclohydrolase
GTPCH-D	Déficit en guanosine-triphosphate cyclohydrolase
HILIC	Chromatographie liquide d'interactions hydrophiles
HNF1	Facteur nucléaire des hépatocytes 1
HPA	Acide hydroxyphényl acétique
HPLC	Chromatographie liquide à haute performance
HSP	Protéines de choc thermique
HVA	Acide homovanillique
IPC	Chromatographie d'appariement d'ions
IS	Etalon interne
LCR	Liquide céphalorachidien
L-DOPA	L-dihydroxy-phénylalanine
LLOQ	Lower limit of quantification
LOQ	Limit of quantification
m/z	Rapport masse sur charge
MAO	Monoamine oxydase
MAO-D	Déficit en monoamine oxydase
MF	Facteur matrice
MHPG	3-metoxy-4-hydroxy-phénylglycol
MRM	Suivi de plusieurs réactions de fragmentation en phase gazeuse
MS	Spectrométrie de masse
MS/MS	Spectrométrie de masse en tandem
MWCO	Sueil de masse moléculaire
N	Néoptérine
NH2	Dihydronéoptérine
PAC	Ptérin-4α-carbinolamine
PAH	Phénylalanine hydroxylase
PCD	Ptérine-4α-carbinolamine déhydratase
PCD-D	Déficit en ptérine-4α-carbinolamine déhydratase
PFP	Pentafluorophényle
PLP	Pyridoxal-5-phosphate
PTPS	6-pyruvoyltetrahydropterin synthase
PTPS-D	Déficit en 6-pyruvoyltetrahydropterin synthase
q-BH2	quinonoid-dihydrobioptérine

QC	Solutions de contrôle qualité
R^2	Coefficient de détermination
RPLC	Chromatographie liquide à polarité de phases inversée
Rs	Facteur de résolution
RSD	Coefficent de variation
S/N	Rapport signal sur bruit
SNC	Système nerveux central
SR	Sépiaptérine réductase
SR-D	Déficit en sépiaptérine réductase
SRM	Suivi d'une réaction de fragmentation en phase gazeuse
SS	Solution mère
$t_{½}$	Temps de demi-vie
TH	Tyrosine hydroxylase
TH-D	Déficit en tyrosine hydroxylase
TrpH	Tryptophane hydroxylase
UHPLC	Chromatographie liquide à ultrahaute performance
VMAT2	Transporteur vésiculaire des monoamines
VMAT-D	Déficit en transporteur vésiculaire des monoamines
WS	Solution de travail

Liste des figures

Figure VI.3 Evolution of S/N as a function of the mobile phase pH and of phosphate concentration for HVA (in ammonium formate (A), ammonium acetate (B) and ammonium carbonate (C)) and 3-OMD (in ammonium formate (D), ammonium acetate (E) and ammonium carbonate (F)).

Figure VI.4 Evolution of S/N as a function of phosphate concentration in the mobile phase for 3-OMD (A), 5-HTP (B), 5-HIAA (C), HVA (D) and MHPG (E). The mobile phase consisted of a mixture of pH 5 ammonium acetate with different / methanol (97/3, v/v).

Figure VI.5 Evolution of S/N as a function of the mobile phase pH and of phosphate concentration for BH4 (A), BH2 (B), B (C), N (D) and NH2 (E).

Figure VI.6 Evolution of S/N as a function of phosphate concentration in the mobile phase for 3-OMD (A), 5-HTP (B), MHPG (C), 5-HIAA (D) and HVA (E). The mobile phase consisted of a mixture of 5 mM ammonium acetate with different pHs / methanol (97/3, v/v). ESI was performed in positive mode and MS/MS in MRM mode. Error bars represent the 95% confidence intervals. MS spectra of 3-OMD (A'), 5-HTP (B'), MHPG (C'), 5-HIAA (D') and HVA (E') measured for different phosphate concentration in the mobile phase after positive ESI.

Liste des tableaux

Table des matières

INTRODUCTION GENERALE

Les erreurs innées du métabolisme (EIM) sont des maladies héréditaires causées par des mutations génétiques. Ces mutations sont situées sur des gènes codant pour des protéines enzymatiques ou des transporteurs impliqués dans le métabolisme, engendrant alors une dyshoméostasie de la voie métabolique touchée par la mutation. Ceci entraine alors un trouble métabolique et, *in fine*, l'apparition de symptômes.

Dans le cadre de ce projet de thèse, nous nous intéressons exclusivement aux EIM à l'origine de symptômes neurologiques. Il s'agit de mutations génétiques affectant le métabolisme ou le transport des neurotransmetteurs. En effet, le dysfonctionnement des enzymes et des transporteurs des neurotransmetteurs, plus précisément de la dopamine et de la sérotonine, génère une altération de la neurotransmission au niveau du système nerveux central (SNC) et ainsi, l'apparition de symptômes neurologiques.

Ces symptômes sont de plusieurs types : des symptômes moteurs tels qu'un syndrome parkinsonien ou une dystonie, des retards psychomoteurs, des déficiences intellectuelles, des crises d'épilepsie et une encéphalopathie. La symptomatologie des EIM de la dopamine et de la sérotonine est progressive et commune, quel que soit le gène atteint par la mutation. Ceci rend le diagnostic de certitude hautement complexe. Or, le traitement de ces maladies repose sur la supplémentation en métabolites manquants afin de corriger la synthèse des neurotransmetteurs. Le traitement des EIM est donc spécifique à chaque mutation génétique ce qui fait qu'un diagnostic de certitude est primordial pour permettre une prise en charge efficace des patients.

Afin de poser le diagnostic des EIM de la dopamine et de la sérotonine, des biomarqueurs ont été identifiés et validés dans le liquide céphalorachidien (LCR). Un biomarqueur est une caractéristique biologique mesurable, permettant de distinguer un processus physiologique d'un processus pathologique. Le LCR est le milieu biologique de choix pour le diagnostic de ces maladies. En effet, le SNC étant protégé par la barrière hématoencéphalique, la composition du LCR est le meilleur reflet de l'état physiopathologique alors que d'autres fluides biologiques tels que le sang ou les urines sont impactés par les organes périphériques.

Les biomarqueurs cérébrospinaux des EIM de la dopamine et de la sérotonine se divisent en deux groupes : les métabolites de ces neurotransmetteurs à savoir la 3-*ortho*-méthyl-DOPA (3-OMD), l'acide homovanillique (HVA), le 3-metoxy-4-hydroxy-phénylglycol (MHPG), le 5-hydroxytryptophane (5-HTP) et l'acide 5-hydoxyindole acétique (5-HIAA) ; et les ptérines avec notamment la tétrahydrobioptérine (BH4), la dihydrobioptérine (BH2), la bioptérine (B), la dihydronéoptérine (NH2) et la néoptérine (N).

Actuellement, la quantification de ces biomarqueurs repose sur une séparation par chromatographie liquide à haute performance (HPLC) suivie d'une détection électrochimique (ECD), par fluorescence (FD) ou par spectrométrie de masse en tandem (MS/MS). Récemment, dans le cadre d'un travail de thèse réalisé au sein de notre laboratoire, une méthode de chromatographie liquide ultra-haute performance (UHPLC) a été développée et elle a permis d'analyser simultanément les deux groupes de biomarqueurs. Dans cette méthode, les métabolites de la dopamine et de la sérotonine sont détectés par ECD alors que les ptérines sont détectées par FD après une oxydation en ECD.

Au cours de ce projet de thèse, dans un premier temps, nous nous sommes intéressés à la stabilité des bioptérines et en particulier de la BH4, afin de déterminer les conditions optimales de conservation des échantillons de LCR, en vue du dosage de ces biomarqueurs. Dans un second temps, nous avons comparé la méthode précédemment développée en UHPLC-ECD pour le dosage des métabolites de la dopamine et de la sérotonine à une méthode UHPLC-FD puis à une méthode UHPLC-MS/MS. Enfin dans un troisième temps, l'objectif a été de rechercher de nouveaux biomarqueurs cérébrospinaux des EIM de la dopamine et de la sérotonine. Ce dernier objectif n'a pas pu être atteint au cours des trois années de thèse.

Ce manuscrit s'organise en six chapitres distincts. Le premier chapitre correspond à un rappel bibliographique concernant les EIM de la dopamine et de la sérotonine. Y seront détaillés les déficits enzymatiques et les mutations de transporteurs, leur physiopathologie, leur symptomatologie ainsi que leur traitement. Le second chapitre est un état de l'art des méthodes actuellement décrites pour le dosage des biomarqueurs des EIM de la dopamine et

de la sérotonine. Ce chapitre se présente sous-forme d'une revue bibliographique. Le troisième chapitre détaillera l'étude de la cinétique de dégradation de la BH4 dans différentes conditions. Le suivi de cette cinétique a été réalisé grâce à une méthode HPLC-MS/MS permettant de détecter et de quantifier les produits d'auto-oxydation de la BH4 simultanément. Le quatrième chapitre exposera les travaux de développement et de validation d'une méthode UHPLC-FD pour le dosage des métabolites de la dopamine et de la sérotonine. Dans le cinquième chapitre, sera présenté le développement d'une méthode UHPLC-MS/MS pour le dosage de ces biomarqueurs. Les performances analytiques de cette méthode seront comparées à celles de la méthode UHPLC-FD. Le sixième chapitre correspond à l'étude de l'apport du phosphate en tant qu'additif à la phase mobile en UHPLC-MS/MS pour l'ionisation en electrospray (ESI) des analytes.

CHAPITRE I : SYMPTOMES, DIAGNOSTICS ET TRAITEMENTS DES ERREURS INNEES DU METABOLISME DE LA DOPAMINE ET DE LA SEROTONINE

La fonction cérébrale repose sur des connexions neuronales organisées en voies de neurotransmission. Un même neurone peut faire partie de plusieurs voies de neurotransmission [1–4]. La communication interneurone se fait au moyen d'une structure spécialisée, la synapse [1,2]. Le cerveau humain contient plus de 100 000 milliards de synapses [1]. L'organisation synaptique consiste en un neurone présynaptique qui, sous l'effet d'un potentiel d'action électrique, libère un neurotransmetteur stocké dans des vésicules axonales dans la fente synaptique [1–3]. Le neurotransmetteur se lie alors à un récepteur spécifique localisé sur la membrane du neurone post-synaptique, ce qui entraine une modification de l'activité électrique de ce dernier [5–7]. Ensuite, le stimulus est interrompu par la dégradation et/ou la recapture du neurotransmetteur par le neurone présynaptique [1–3,5–7]. La figure I.1 récapitule l'organisation de la synapse. Les connexions synaptiques formant les différentes voies de neurotransmissions sont capables d'une importante souplesse [1–3]. En effet, elles répondent constamment à la stimulation et peuvent s'adapter à leur environnement [1–3].

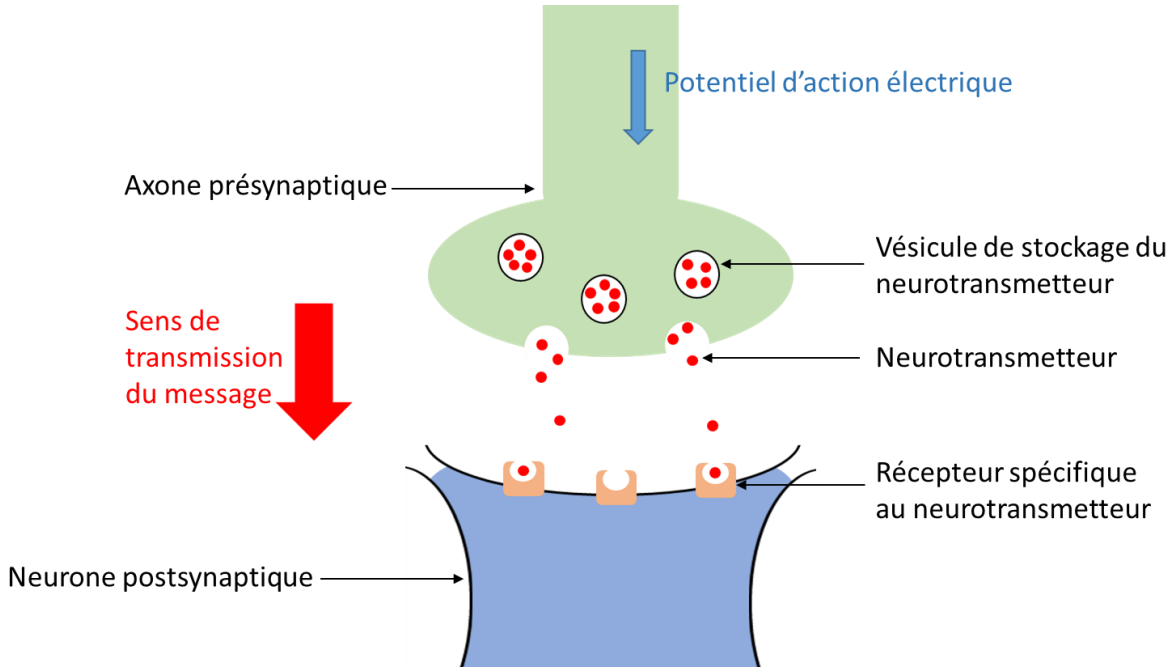

Figure I.1 : Schéma d'une synapse interneurone

Les neurotransmetteurs sont synthétisés dans le neurone puis stockés dans des vésicules. Ils permettent la communication intercellulaire et sont la base des fonctions biologiques

telles que le mouvement musculaire et le développement neuropsychologique [8,9]. Les neurotransmetteurs peuvent être classés en quatre catégories selon leur structure chimique [8,9] :

- Les acides aminés tels que le glutamate, la glycine et l'acide gamma-amino-butyrique (GABA).
- Les monoamines ou amines biogéniques comme la dopamine, la noradrénaline et la sérotonine.
- Les neuropeptides à l'image de la vasopressine.
- Les neurotransmetteurs dit « atypiques » tels que l'acétylcholine, le monoxyde de carbone et l'adénosine triphosphate.

Dans le présent manuscrit, nous nous intéressons exclusivement aux neurotransmetteurs de type monoamine, en particulier la dopamine et la sérotonine. La dopamine est impliquée dans le contrôle du mouvement volontaire, les processus cognitifs tels que l'attention et la mémorisation, le contrôle de la motivation et la sécrétion neuroendocrine de la prolactine [5,10,11]. La sérotonine, quant à elle, participe au contrôle moteur, au contrôle autonome de la respiration et de la température corporelle ainsi qu'à la régulation de l'humeur [12–14].

Les EIM de la dopamine et de la sérotonine sont des maladies neurologiques rares qui apparaissent durant l'enfance [3,15]. Elles sont dues à un dysfonctionnement du métabolisme ou du transport de ces neurotransmetteurs, du fait d'une mutation sur les gènes codant les protéines enzymatiques ou les transporteurs [3,15,16]. La physiopathologie de ces maladies est intrinsèquement liée au gène concerné par la mutation.

I.1. PHYSIOPATHOLOGIE DES ERREURS INNEES DU METABOLISME DE LA DOPAMINE ET DE LA SEROTONINE

Le métabolisme de la dopamine et de la sérotonine est représenté sur la figure I.2 [17,18]. La biosynthèse de la dopamine débute par l'hydroxylation de la phénylalanine en tyrosine qui est, par la suite, hydroxylée en L-dihydroxy-phénylalanine (L-DOPA) par la tyro-

sine hydroxylase (TH). La TH est l'enzyme régulatrice de la voie de biosynthèse de la dopamine. La L-DOPA est ensuite décarboxylée en dopamine par la décarboxylase des acides aminés aromatiques (AADC). Puis, la dopamine est catabolisée par les actions successives de la monoamine oxydase (MAO), l'aldéhyde déshydrogénase (AD) et de la catéchol-O-méthyl-transférase (COMT). La dopamine peut également être hydroxylée en noradrénaline par la dopamine β-hydroxylase (DBH).

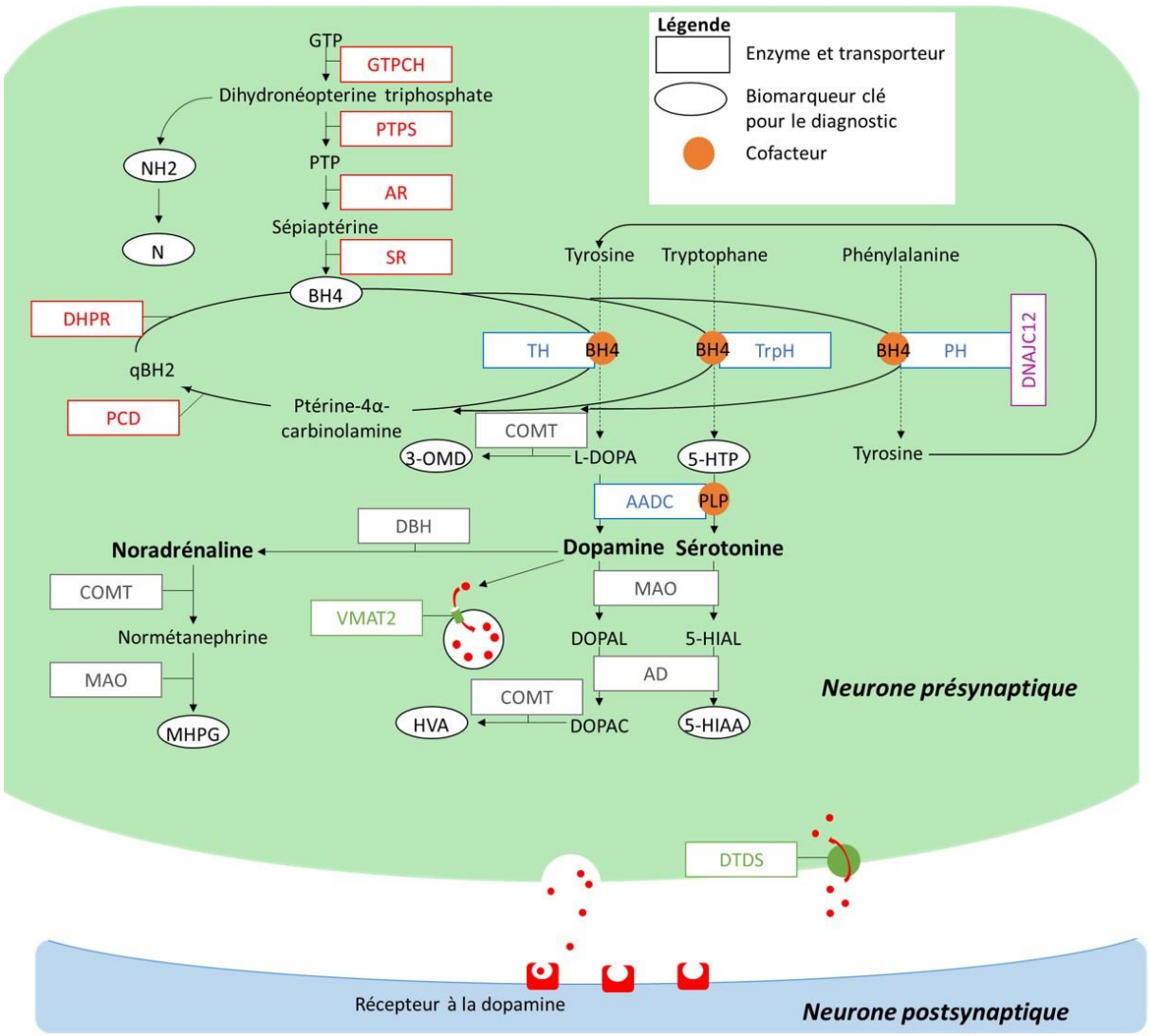

Figure I.2 : Voies métaboliques de la dopamine et de la sérotonine

3-OMD, 3-ortho-méthyl-DOPA ; 5-HIAA, acide 5-hydroy-indole acétique ; 5-HIAL, acide 5-hydroy-indole acétaldéhyde ; 5-HTP, 5-hydroxy-tryptophane ; AADC, décarboxylase des acides aminés aromatiques ; AR, aldose réductase ; AD, aldéhyde déshydrogénase ; BH4, tétrahydrobioptérine ; COMT, catéchol-O-méthyl-transférase ; DBH, dopamine β-hydroxylase ; DHPR, dihydroptéridine réductase ; DTDS, syndrome de déficience en transporteur de la dopamine ; DOPAL, 3,4-dihydroxyphénylacétaldéhyde ; DOPAC, acide 3,4-dihydroxyphénylacétique ; GTP, guanosine-triphosphate ; GTPCH, guanosine-triphosphate cyclohydrolase ; HVA, acide homovanillique ; MAO, monoamine oxydase ; MHPG, 3-methoxy-4-hydroxyphénylglycol ; N, néoptérine ; NH2, dihydronétoptérine ; PCD, ptérine-4α-carbinolamine déhydratase ; PH, phénylalanine hydroxylase ; PTPS, 6-pyruvoyltetrahydropterin synthase ; qBH2, quinonoid dihydrobioptérine TH, tyrosine hydroxylase ; TrpH, tryptophane hydroxylase, VMAT2, transporteur vésiculaire des monoamines.

Concernant la sérotonine, sa biosynthèse commence par l'hydroxylation du tryptophane en 5-hydroxy-tryptophane (5-HTP) par la tryptophane hydroxylase (TrpH) [19,20]. Le 5-HTP est ensuite décarboxylé par l'AADC en sérotonine. De même que pour la dopamine, le

catabolisme de la sérotonine se fait par les actions successives de la MAO et l'AD pour générer l'acide 5-hydroy-indole acétique (5-HIAA) [19,20].

Les principaux cofacteurs de ces voies métaboliques sont le pyridoxal-5-phosphate (PLP) pour l'AADC et la tétrahydrobioptérine (BH4) pour les hydroxylases. La BH4 peut, soit être recyclée après son action de cofacteur par les actions de la ptérine-4α-carbinolamine déhydratase (PCD) et la dihydroptérine réductase (DHPR), soit être synthétisée *de novo* grâce à la guanosine-triphosphate cyclohydrolase (GTPCH), la 6-pyruvoyltetrahydropterin synthase (PTPS), l'aldose réductase (AR) et la sépiaptérine réductase (SR) [21,22].

Dans la physiopathologie des EIM de la dopamine et de la sérotonine, une mutation génétique est à l'origine d'un déficit en enzyme, en transporteur ou en protéine chaperonne. En fonction de la protéine concernée par le déficit, les EIM de la dopamine peuvent être classées en cinq catégories [3,15,16] :

- Les défauts de biosynthèse caractérisés par un déficit enzymatique situé en amont du neurotransmetteur dans la voie métabolique : il s'agit des déficits en TH et en AADC.
- Les altérations du catabolisme de la dopamine et de la sérotonine, à savoir, les déficits en MAO et en DBH.
- Les déficits en transporteurs : le transporteur vésiculaire des monoamines (VMAT2) et le syndrome de déficience en transporteur de la dopamine (DTDS).
- Les défauts de biosynthèse ou de recyclage de la BH4, cofacteur primordiale dans les voies métaboliques de la dopamine et de la sérotonine, les déficiences de : la GTPCH, la PTPS, la SR, la PCD et la DHPR.
- Les déficits en protéine chaperonne, notamment en protéine DNAJC12.

I.2. LES DEFAUTS DE BIOSYNTHESE DE LA DOPAMINE ET DE LA SEROTONINE

Les EIM par défauts de biosynthèse de la dopamine et de la sérotonine correspondent aux déficits en TH (TH-D) et en AADC (AADC-D) [3].

I.2.1. Déficit en tyrosine hydroxylase (TH-D)

La TH catalyse la réaction limitante de la synthèse de la dopamine, l'hydroxylation de la tyrosine en L-DOPA (Figure I.2). La TH-D est causée par une mutation du gène 11p15.5 codant pour cette enzyme [23]. La transmission génétique se fait selon le mode autosomique récessif [23–25]. La TH étant impliquée dans la biosynthèse de la dopamine, son déficit entraine une diminution de la neurotransmission dopaminergique au niveau cérébrale [23–29].

En fonction du tableau clinique, la TH-D peut être subdivisée en deux types : le type A qui correspond à une forme légère à modérée et le type B qui est une forme sévère [23–25]. Dans la TH-D de type A, les patients présentent un développement psychomoteur normal durant les premiers mois de la vie, sans aucun symptôme [23,26–29]. Néanmoins, par la suite, un syndrome extrapyramidal apparait progressivement. Ce syndrome correspond à une hypokinésie, une rigidité du mouvement et une dystonie [23,26–29]. Dans la majorité des cas, ces symptômes moteurs sont symétriques et affectent les jambes ainsi que les bras [23,26–29]. Un léger retard mental peut être décrit chez certains patients atteints de TH-D de type A [23]. Etant donnée l'apparition précoce des symptômes moteurs, les enfants atteints ne peuvent apprendre à marcher sans traitement [23]. Dans la TH-D de type B, les symptômes apparaissent immédiatement après la naissance ou après un intervalle asymptomatique de quelques semaines avec un syndrome extrapyramidal plus marquée que dans la TH-D de type A [23,24,30]. En effet, l'hypokinésie et la rigidité sont plus intenses et la dystonie peut être généralisée [23,24,30]. De plus, des mouvements saccadés excessifs, comprenant notamment des tremblements et des myoclonies, ont également été décrits. Par ailleurs, les patients atteints de TH-D de type B peuvent aussi présenter un retard mental, un ptosis bilatéral ainsi que des crises oculogyres [23,24,30]. Des perturbations du système nerveux autonome incluant hypersudation, hypersalivation et dérégulation de la température corporelle complètent le tableau clinique de la TH-D de type B [23,24,30]. Des crises épileptiques peuvent compliquer ce tableau clinique [23].

I.2.2. Déficit en décarboxylase des acides aminés aromatiques (AADC-D)

L'AADC est l'enzyme catalysant la décarboxylation de la L-DOPA et du 5-HTP en dopamine et en sérotonine, respectivement (Figure I.2) [31,32]. L'AADC-D est caractérisée par une mutation sur le gène en 7p12 avec une transmission autosomique récessive [31–33]. Puisque l'AADC est importante pour la biosynthèse de la dopamine et de la sérotonine, l'AADC-D est à l'origine d'une diminution des neurotransmissions de ces deux neurotransmetteurs [31–36].

Les symptômes résultants incluent un syndrome extrapyramidal progressif comprenant une hypokinésie, une rigidité du mouvement et une dystonie. Les patients atteints d'AADC-D présentent également des atteintes du système nerveux autonome du type hypersudation, dérégulation de la température corporelle et congestion nasal [31–36]. Le déficit de sérotonine engendre des insomnies ainsi que des troubles de l'humeur telle qu'une irritabilité [37–39]. Les symptômes de l'AADC-D apparaissent principalement au cours de la petite enfance (avant 18 mois) ou au cours de l'enfance (entre 18 mois et 10 ans) [31]. Un retard du développement psychomoteur est également retrouvé dans cette erreur innée du métabolisme [31,32].

I.3. LES DEFICITS DE CATABOLISME DE LA DOPAMINE ET DE LA SEROTONINE

Les EIM par déficit de catabolisme de la dopamine et de la sérotonine correspondent aux déficiences en MAO (MAO-D) et en DBH (DBH-D) [3].

I.3.1. Déficit en monoamine oxydase (MAO-D)

La MAO est une enzyme essentielle dans le catabolisme de la dopamine et de la sérotonine (Figure I.2) [40–42]. Elle catalyse la désamination oxydative de la dopamine et de la sérotonine avec transformation de la fonction amine en fonction aldéhyde [40–42]. Il existe deux isoformes de la MAO : la MAO-A et la MAO-B [43]. Les gènes de ces deux isoformes sont situés sur la région Xp11.23 [42,44]. La transmission de la MAO-D est donc liée au chromosome X.

Tandis que le déficit isolé en MAO-B n'entraine pas l'apparition de signes cliniques, le déficit isolé en MAO-A est associé à un retard mental et à de sévères troubles comportementaux à type d'accès agressifs [40–42,44–48]. Dans le déficit en MAO-A, des perturbations du système nerveux autonome ont également été décrites avec une dérégulation de la température corporelle et des troubles gastro-intestinaux [44]. Le déficit combiné en MAO-A et MAO-B entraine, quant à lui, retard mental, épilepsie, épisodes sporadiques d'hypotonie et mouvements stéréotypés [48].

I.3.2. Déficit en dopamine-β-hydroxylase (DBH-D)

La DBH est une enzyme intravésiculaire liée une membrane. Elle catalyse la conversion de la dopamine en noradrénaline (Figure I.2) [49,50]. Le gène de la DBH est localisé dans la région 9q34 [51]. La DBH-D est causée par une mutation sur ce gène et elle présente une transmission autosomique récessive [52]. Cette EIM est à l'origine d'une diminution de la production de noradrénaline au niveau cérébrale [53,54]. La noradrénaline étant le neurotransmetteur du système nerveux sympathique, les principaux symptômes de la DBH-D correspondent à des perturbations du système nerveux autonome avec une diminution de la neurotransmission sympathique alors que la neurotransmission parasympathique n'est pas affectée [53,54].

Les patients atteints de DBH-D présentent des épisodes de syncope dus à une importante hypotension orthostatique associée à un ptosis [52,53]. Ces symptômes apparaissent tardivement durant l'enfance [53]. Le système nerveux sympathique a également une fonction endocrine, dans la mesure où il inhibe la sécrétion d'insuline. Ainsi, dans la DBH-D, une dérégulation de l'homéostasie du glucose a été décrite [55]. En effet, les patients atteints ont une hyperinsulinémie et une résistance périphérique à l'insuline [55].

I.4. LES TRANSPORTOPATHIES

En fonction du gène muté, il existe deux transportopathies décrites parmi les EIM de la dopamine et de la sérotonine : le DTDS et la déficience en VMAT2 (VMAT-D).

I.4.1. Syndrome de déficience en transporteur de la dopamine (DTDS)

La communication synaptique est un processus finement régulé par différent mécanismes d'initiation du potentiel d'action au niveau du neurone présynaptique mais aussi par la fin de la transmission au sein de la synapse [1]. Afin de mettre un terme à une transmission synaptique, le neurotransmetteur subit soit une dégradation, soit une recapture vers le neurone présynaptique [56]. Pour la dopamine, la recapture se fait grâce à un transporteur transmembranaire codé par le gène SLC6A3 [57]. Dans le DTDS, ce gène est muté, ce qui fait que la recapture de la dopamine n'est plus possible [58].

Le neurotransmetteur reste alors dans la fente synaptique et active les récepteurs D2 post-synaptiques [58]. Dans un premier temps, ceci entraine une hyperactivité dopaminergique avec une hyperkinésie et des troubles du sommeil [58]. Dans un second temps, la dopamine se lie aux récepteurs présynaptiques ce qui active une boucle de rétrocontrôle négatif de la biosynthèse du neurotransmetteur. Ceci a pour effet de diminuer la transmission dopaminergique [58].

Les patients atteints de DTDS développent précocement durant l'enfance des troubles du mouvement avec un tableau clinique variable [57–60]. En effet, ce dernier peut être majoritairement choréique et dystonique ou extrapyramidal et dystonique, correspondant à une hyperactivation ou à une diminution de la neurotransmission dopaminergique, respectivement [57–60]. Au fur et à mesure du développement de cette EIM, la symptomatologie choréique laisse place à un syndrome extrapyramidal avec une bradykinésie, une hypomimie et des tremblements [57–60].

I.4.2. Déficit en transporteur vésiculaire des monoamines 2 (VMAT-D)

VMAT2 est un transporteur codé par le gène SLC18A2 qui joue un rôle essentiel dans le remplissage des vésicules présynaptiques en dopamine et en sérotonine [61–63]. La VMAT-D correspond à l'inactivation de ce transporteur suite à une mutation sur le gène SLC18A2 [64]. Cette EIM présente une transmission autosomique récessive [64,65]. Le dysfonctionnement du transporteur VMAT2 fait que le remplissage des vésicules présynaptiques en neurotransmetteur n'est plus possible [61–64]. Ainsi, même si la biosynthèse de dopamine et de sérotonine n'est pas altérée, les vésicules présynaptiques ne sont pas remplies et ne peuvent donc pas libérer de neuromédiateur dans la synapse. La neurotransmission s'en trouve de ce fait fortement diminuée [64].

La symptomatologie de la VMAT-D apparait à un âge particulièrement précoce (4 mois) et comprend des troubles moteurs, des troubles de l'humeur et une dérégulation du système nerveux autonome [64]. Les troubles moteurs correspondent à une hypotonie, une ataxie et une dysarthrie. Les patients atteints de VMAT-D souffrent souvent de dépression clinique. La dérégulation du système nerveux autonome génère, quant à elle, une hypersécretion nasal et oropharyngée, une faible perfusion distale avec des mains et pieds froids et une hypersudation. La VMAT-D entraine également une asthénie, des crises épileptiques, un retard psychomoteur et des troubles du sommeil [64].

I.5. LES DEFICITS DE BIOSYNTHESE OU DE RECYCLAGE DE LA TETRAHYDROBIOPTERINE

La BH4 est le cofacteur des hydroxylases de la tyrosine, la phénylalanine et du tryptophane. Une altération de sa biosynthèse ou de son recyclage au niveau du SNC entraine un déséquilibre des neurotransmissions dopaminergique et sérotoninergique avec l'apparition de symptômes neurologiques [66]. Cinq EIM se caractérisent par un déficit en BH4 : les déficiences en GTPCH (GTPCH-D), PTPS (PTPS-D), SR (SR-D), PCD (PCD-D) et en DHPR (DHPR-D).

I.5.1. Déficit en guanosyl-triphosphate cyclohydrolase (GTPCH-D)

La GTPCH catalyse la transformation du GTP en dihydronéoptérine triphosphate, dans le cadre de la synthèse *de novo* de la BH4 [66]. Cette enzyme est codée par le gène GCH1. La mutation de ce gène entraine un dysfonctionnement de la GTPCH. Celle-ci ne peut alors plus assurer sa fonction de catalyse [66–68]. La biosynthèse de BH4 est donc fortement diminuée et l'activité des hydroxylases, dont elle est le cofacteur, est altérée de manière importante [66]. La GTPCH-D présente deux formes de transmissions génétiques à savoir autosomique dominante et autosomique récessive [68,69].

La forme autosomique dominante, aussi connue sous le nom de syndrome de Segawa [70], se manifeste par des symptômes moteurs comprenant un syndrome extrapyramidal avec une dystonie au niveau des membres, une bradykinésie et des tremblements. Sont également décrits dans cette EIM, des symptômes neuropsychiatriques tels que des troubles du sommeil, une anxiété et une dépression [71]. Ces symptômes apparaissent progressivement dans les dix premières années de la vie [70]. La forme autosomique récessive de la GTPCH-D est plus sévère que la forme autosomique dominante [72]. Elle se manifeste par une hypotonie au niveau du tronc, une dystonie, un syndrome extrapyramidal et des crises oculogyres. Ces symptômes apparaissent dans la période néonatale précoce [69,72].

I.5.2. Déficit en 6-pyruvoyltetrahydropterin synthase (PTPS-D)

Comme la GTPCH, la PTPS est impliquée dans la synthèse *de novo* de la BH4. La déficience en cette enzyme est à l'origine d'une diminution de la synthèse de BH4, entrainant une baisse de l'activité des hydroxylases de la phénylalanine, la tyrosine et du tryptophane [73]. La PTPS-D présente une transmission autosomique récessive [74]. En fonction de la mutation, l'enzyme peut avoir une activité résiduelle plus ou moins importante [75,76]. Les symptômes engendrés dépendent de cette activité résiduelle.

En effet, il existe des formes modérées de PTPS-D caractérisées par un développement neurologique normal [73–76]. Des formes sévères ont également été décrites. Elles se manifestent par des symptômes moteurs tels qu'une hypotonie, une dystonie et un syndrome

extrapyramidal. D'autres symptômes sont également présents dans cette EIM, à savoir des crises épileptiques et un retard mental [75,76]. Ces symptômes apparaissent précocement dans la vie, c'est-à-dire, avant l'âge de 48 mois [74].

I.5.3. Déficit en sépiaptérine réductase (SR-D)

La SR-D est une maladie autosomique récessive causée par une mutation sur le gène SRD codant pour la SR [77,78]. Le début de cette EIM se fait généralement très tôt durant l'enfance, plus précisément, à partir de 7 mois. La symptomatologie peut être variable au cours du temps [77–79]. En effet, le phénotype précoce inclut une hypotonie axiale, un retard de développement des fonctions motrices ainsi que des symptômes psychiatriques tels qu'une irritabilité et des troubles du comportement [77,79–81]. Plus tard, la symptomatologie change avec l'apparition d'une dystonie variant selon un rythme circadien [79].

Comparée aux autres EIM par déficit de BH4, les patients atteints de SR-D sont les seuls à présenter une incapacité pour l'apprentissage cognitif [81,82]. Récemment, des perturbations endocrines ont été décrites dans la SR-D. Il s'agit d'hypoglycémies et de déficiences en hormone de croissance. Ces symptômes sont liés à la déficience en dopamine [83].

I.5.4. Déficit en ptérine-4α-carbinolamine déhydratase (PCD-D)

La PCD est la deuxième enzyme intervenant dans le recyclage de la BH4. Elle catalyse la déshydratation de la ptérine-4α-carbinolamine en quinonoid dihydrobioptérine (q-BH2). Cette dernière se réarrange spontanément en 7,8-BH2. La PCD-D est liée à une mutation sur le gène PCBD1. Cette EIM se caractérise par l'absence de symptômes neurologiques sévères. Elle est donc considérée comme une forme éphémère et bénigne de déficience en BH4, sans réel trouble de la neurotransmission [84].

Néanmoins, il a été décrit que la PCD est un cofacteur de dimérisation du facteur nucléaire des hépatocytes 1 (HNF1) [85]. La PCD-D entraine une diminution de l'activité transcriptionnelle du HNF1. Ainsi, elle est associée à un trouble du développement des cellules hépatiques et pancréatiques, causant un diabète précoce [86,87].

I.5.5. Déficit en dihydroptéridine réductase (DHPR-D)

La dernière enzyme intervenant dans la régénération de la BH4 est la DHPR. Elle assure une production suffisante en cofacteur réduit, à savoir la BH4, et empêche l'accumulation de métabolites toxiques [88]. La DHPR-D est causée par une mutation sur le gène QDPR. Bien que la synthèse *de novo* de la BH4 soit intacte, le développement clinique est généralement plus sévère, comparé aux déficits en biosynthèse de BH4 [89,90]. En effet, l'accumulation de 7,8-BH2 et le blocage de la production de catécholamines et de sérotonine dans le SNC contribuent à la physiopathologie de cette EIM [91].

Les patients atteints de DHPR-D présentent des symptômes précoces comprenant des troubles de l'alimentation durant la période néonatale, une hypersalivation, une microcéphalie et un retard de développement [92,93]. Durant l'enfance, des troubles moteurs apparaissent avec un syndrome extrapyramidal, une hypotonie au niveau du tronc et des tremblements. Des crises épileptiques complètent le tableau clinique [92,93].

I.6. LE DEFICIT EN PROTEINE CHAPERONNE

Le gène DNAJC12 code une protéine chaperonne de la famille des protéines de choc thermique 40 (HSP40). Il a été démontré qu'elle interagit avec les hydroxylases de la phénylalanine, de la tyrosine et du tryptophane [94,95]. La mutation du gène DNAJC12 entraine une déficience dans les neurotransmissions dopaminergique et sérotoninergique. Généralement, les patients présentant cette mutation montrent un large spectre de symptômes cliniques comprenant une dystonie, un retard du langage, une hypertonie, un syndrome extrapyramidal ainsi que des troubles psychiatriques [96]. Par ailleurs, 20 patients ayant cette mutation ne présentent que des troubles neurologiques modérés, voire pas de troubles [97]. Un autre tableau clinique complète cette EIM : il inclut un retard intellectuel modéré et un syndrome extrapyramidal progressif sans dystonie.

I.7. DIAGNOSTIC DES ERREURS INNEES DU METABOLISME DE LA DOPAMINE ET DE LA SEROTONINE

Le diagnostic des EIM de la dopamine et de la sérotonine, dont les symptômes peuvent être très proche, repose sur l'analyse de liquide céphalorachidien (LCR), dans le but de quantifier des biomarqueurs spécifiques des EIM de la dopamine et de la sérotonine. Ces biomarqueurs correspondent aux métabolites et cofacteurs des voies métaboliques des neurotransmetteurs (Figure I.2). Ainsi, chaque EIM présente un profil métabolique cérébrospinal spécifique permettant de la distinguer des autres. Le Tableau I.1 récapitule ces profils métaboliques [3,98].

Les concentrations mesurées pour un échantillon de LCR donné sont comparées aux valeurs normales décrites dans la littérature afin de déterminer le profil métabolique cérébrospinal [99,100]. Sur le plan analytique, la quantification de ces biomarqueurs présente trois défis importants :

- La méthode analytique doit avoir une limite de quantification suffisamment basse pour quantifier les basses concentrations dans le LCR qui peuvent être de l'ordre de la dizaine de nanomolaires.
- La méthode analytique doit nécessiter peu d'échantillon car de faibles volumes d'échantillon sont disponibles par prélèvement.
- La méthode analytique doit être assez rapide pour être appliquée en routine clinique.

Ces défis seront repris de manière plus détaillée dans le chapitre 2, où un état de l'art des méthodes existantes pour l'analyse des biomarqueurs cérébrospinaux sera réalisé.

Tableau I.1 : Profils métaboliques des différentes EIM de la dopamine et de la sérotonine dans le LCR (adapté de [3,98])

Protéine déficiente	Pterines			Métabolites de la dopamine et de la sérotonine					
	BH4	7,8-BH2	NH2	HVA	5-HIAA	HVA/5-HIAA	3-OMD	MHPG	5-HTP
TH	N	N	N	↓	N	↓	N	N	N
AADC	N	N	N	↓	↓	N	↑	N	↑
MAO	N	N	N	↓	↓	N	N	↓	N
DTDS	N	N	N	↑	N	↑	N	N	N
VMAT2	N	N	N	↑	↑	N	N	N	N
GTPCH	↓	N	↓	↓	↓	N	N	N	N
PTPS	↓	N	↑	↓	↓	N	N	N	N
SR	↓	↑	N	↓	↓	N	N	N	N
PCD	↓	N	N	N	N	N	N	N	N
DHPR	↓	↑	N	↓	↓	N	N	N	N
DNAJC	↑	N	N	↓	↓	N	N	N	N

N, Concentration dans les normes ; ↑, Concentration au-dessus des normes ; ↓, Concentration en-dessous des normes.

I.8. TRAITEMENTS DES ERREURS INNEES DU METABOLISME DE LA DOPAMINE ET DE LA SEROTONINE

Le pronostic à long terme dépend de la précocité du diagnostic et de la mise en place du traitement. Etant donné le caractère particulièrement rare des EIM de la dopamine et de la sérotonine, pendant plusieurs années un traitement systématique par L-DOPA a été utilisé [101]. Récemment, cette pratique a été remise en question suite aux avancées considérables dans la compréhension de la physiopathologie de ces maladies, que ce soit d'un point de vue biochimique, génétique ou radiologique [101]. En effet, la L-DOPA ne peut avoir d'efficacité clinique si l'enzyme ou le transporteur déficient se situe en aval dans la voie métabolique (Figure I.2). Par exemple, dans la VMAT-D, l'administration de L-DOPA n'améliore pas le tableau clinique et engendre même une aggravation des symptômes moteurs [102]. Ainsi, bien qu'efficace dans le traitement de certaines EIM de la dopamine et de la sérotonine, il n'est pas recommandé d'administrer la L-DOPA de manière systématique [3,101,102].

De manière générale, le traitement par L-DOPA est recommandé si l'enzyme déficiente se situe en amont de l'hydroxylation de la tyrosine par la TH [102]. La posologie journalière initiale doit être comprise entre 0,5 et 1 mg/Kg. Elle peut être augmentée progressivement jusqu'à un maximum de 10 mg/Kg, si l'amélioration des symptômes n'est pas suffisante [3, 101, 102]. La L-DOPA doit toujours être associée à un inhibiteur de DOPA-décarboxylase périphérique (Carbidopa ou Bensérazide). Ceci évite que la L-DOPA ne soit dégradée en périphérie, augmentant ainsi sa biodisponibilité au niveau de SNC [3,101,102]. A la différence de la maladie de Parkinson, les patients atteints d'EIM ne montrent aucune accoutumance pharmacologique à la L-DOPA. Aucune augmentation de dose n'est donc nécessaire pour maintenir une efficacité constante [3]. Les effets indésirables observés avec ce traitement résultent d'une hyper-réaction des récepteurs à la dopamine et correspondent à des troubles choréiques et des nausées. Ces effets indésirables sont totalement réversibles et peuvent être considérablement réduits en diminuant l'intervalle entre les doses de L-DOPA/Carbidopa ou en utilisant des formes à libération prolongée [103].

Pour le reste des EIM où l'enzyme déficiente se situe en aval de la L-DOPA dans la voie métabolique, le traitement consiste en l'administration d'agoniste dopaminergique, à savoir le Pramipexole, le Ropinirole, la Bromocriptine ou l'Ergotine. Ceci permet de rétablir la neurotransmission dopaminergique au niveau du SNC, réduisant ainsi les symptômes. Il est à noter qu'étant donné l'étiologie génétique des EIM, les traitements doivent être maintenus tout au long de la vie [3, 101, 102].

I.9. REFERENCES BIBLIOGRAPHIQUES

[1] Nestler, E. J.; Hyman, S. E.; Holtzman, D. M.; Malenka, R. C. Synaptic Transmission. In *Molecular Neuropharmacology: A Foundation for Clinical Neuroscience, 3e*; McGraw-Hill Education: New York, NY, 2015.

[2] Pickel, V.; Segal, M. *The Synapse: Structure and Function*; Elsevier, 2013.

[3] Brennenstuhl, H.; Jung-Klawitter, S.; Assmann, B.; Opladen, T. Inherited Disorders of Neurotransmitters: Classification and Practical Approaches for Diagnosis and Treatment. *Neuropediatrics*, 2019, *50* (1), 2–14. https://doi.org/10.1055/s-0038-1673630.

[4] Sieburth, D.; Ch'ng, Q.; Dybbs, M.; Tavazoie, M.; Kennedy, S.; Wang, D.; Dupuy, D.; Rual, J.-F.; Hill, D. E.; Vidal, M.; et al. Systematic Analysis of Genes Required for Synapse Structure and Function. *Nature*, 2005, *436* (7050), 510–517. https://doi.org/10.1038/nature03809.

[5] Greengard Paul. The Neurobiology of Slow Synaptic Transmission. *Science*, 2001, *294* (5544), 1024–1030. https://doi.org/10.1126/science.294.5544.1024.

[6] Manorama Patri ED1 - Thomas Heinbockel ED2 - Antonei B. Csoka. Synaptic Transmission and Amino Acid Neurotransmitters. In *Neurochemical Basis of Brain Function and Dysfunction*; IntechOpen: Rijeka, 2019; p Ch. 2. https://doi.org/10.5772/intechopen.82121.

[7] Sewell, W. F. Neurotransmitters and Synaptic Transmission. In *The Cochlea*; Dallos, P., Popper, A. N., Fay, R. R., Eds.; Springer Handbook of Auditory Research; Springer: New York, NY, 1996; pp 503–533. https://doi.org/10.1007/978-1-4612-0757-3_9.

[8] Webster, R. Neurotransmitter Systems and Function: Overview. In *Neurotransmitters, Drugs and Brain Function*; John Wiley & Sons, Ltd, 2001; pp 1–32. https://doi.org/10.1002/0470846577.ch1.

[9] Gibb, A. J. Neurotransmitter Receptors. In *Neurotransmitters, Drugs and Brain Function*; John Wiley & Sons, Ltd, 2001; pp 57–79. https://doi.org/10.1002/0470846577.ch3.

[10] Carlsson Arvid. A Paradigm Shift in Brain Research. *Science*, 2001, *294* (5544), 1021–1024. https://doi.org/10.1126/science.1066969.

[11] Carlsson, A. Perspectives on the Discovery of Central Monoaminergic Neurotransmission. *Annu. Rev. Neurosci.*, 1987, *10* (1), 19–40. https://doi.org/10.1146/annurev.ne.10.030187.000315.

[12] Daubert, E. A.; Condron, B. G. Serotonin: A Regulator of Neuronal Morphology and Circuitry. *Trends Neurosci.*, 2010, *33* (9), 424–434. https://doi.org/10.1016/j.tins.2010.05.005.

[13] Molliver, M. Serotonergic Neuronal Systems: What Their Anatomic Organization Tells Us about Function. *J Clin Psychopharmacol*, 1987, *7* (6 Suppl), 3S-23S.

[14] Wieland, S.; Lucki, I. Altered Behavioral Responses Mediated by Serotonin Receptors in the Genetically Dystonic (Dt) Rat. *Brain Res. Bull.*, 1991, *26* (1), 11–16. https://doi.org/10.1016/0361-9230(91)90185-M.

[15] Kurian, M. A.; Gissen, P.; Smith, M.; Heales, S. J.; Clayton, P. T. The Monoamine Neurotransmitter Disorders: An Expanding Range of Neurological Syndromes. *Lancet Neurol.*, 2011, *10* (8), 721–733. https://doi.org/10.1016/S1474-4422(11)70141-7.

[16] Ng, J.; Papandreou, A.; Heales, S. J.; Kurian, M. A. Monoamine Neurotransmitter Disorders—Clinical Advances and Future Perspectives. *Nat. Rev. Neurol.*, 2015, *11* (10), 567–584. https://doi.org/10.1038/nrneurol.2015.172.

[17] Meiser, J.; Weindl, D.; Hiller, K. Complexity of Dopamine Metabolism. *Cell Commun. Signal.*, 2013, *11* (1), 34. https://doi.org/10.1186/1478-811X-11-34.

[18] Daubner, S. C.; Le, T.; Wang, S. Tyrosine Hydroxylase and Regulation of Dopamine Synthesis. *Arch. Biochem. Biophys.*, 2011, *508* (1), 1–12. https://doi.org/10.1016/j.abb.2010.12.017.

[19] Tyce, G. Origin and Metabolism of Serotonin. *J Cardiovasc Pharmacol*, 1990, *16 Suppl 3*, S1-7.

[20] Boadle-Biber, M. C. Regulation of Serotonin Synthesis. *Prog. Biophys. Mol. Biol.*, 1993, *60* (1), 1–15. https://doi.org/10.1016/0079-6107(93)90009-9.

[21] Nichol C A; Lee C L; Edelstein M P; Chao J Y; Duch D S. Biosynthesis of Tetrahydrobiopterin by de Novo and Salvage Pathways in Adrenal Medulla Extracts, Mammalian Cell Cultures, and Rat Brain in Vivo. *Proc. Natl. Acad. Sci.*, 1983, *80* (6), 1546–1550. https://doi.org/10.1073/pnas.80.6.1546.

[22] Nichol, C. A.; Smith, G. K.; Duch, D. S. BIOSYNTHESIS AND METABOLISM OF TETRAHYDROBIOPTERIN AND MOLYBDOPTERIN. *Annu. Rev. Biochem.*, 1985, *54* (1), 729–764. https://doi.org/10.1146/annurev.bi.54.070185.003501.

[23] Willemsen, M. A.; Verbeek, M. M.; Kamsteeg, E.-J.; de Rijk-van Andel, J. F.; Aeby, A.; Blau, N.; Burlina, A.; Donati, M. A.; Geurtz, B.; Grattan-Smith, P. J.; et al. Tyrosine Hydroxylase Deficiency: A Treatable Disorder of Brain Catecholamine Biosynthesis. *Brain*, 2010, *133* (6), 1810–1822. https://doi.org/10.1093/brain/awq087.

[24] Hoffmann, G. F.; Assmann, B.; Bräutigam, C.; Dionisi-Vici, C.; Häussler, M.; De Klerk, J. B. C.; Naumann, M.; Steenbergen-Spanjers, G. C. H.; Strassburg, H.-M.; Wevers, R. A. Tyrosine Hydroxylase Deficiency Causes Progressive Encephalopathy and Dopa-Nonresponsive Dystonia. *Ann. Neurol.*, 2003, *54* (S6), S56–S65. https://doi.org/10.1002/ana.10632.

[25] Yeung, W.; Wong, V. C. N.; Chan, K.; Hui, J.; Fung, C.; Yau, E.; Ko, C.; Lam, C.; Mak, C. M.; Siu, S.; et al. Expanding Phenotype and Clinical Analysis of Tyrosine Hydroxylase Deficiency. *J. Child Neurol.*, 2011, *26* (2), 179–187. https://doi.org/10.1177/0883073810377014.

[26] Castaigne, P.; Rondot, P.; Ribadeau-Dumas, J. L.; Saïd, G. Progressive extra-pyramidal disorder in 2 young brothers. Remarkable effects of treatment with L-dopa. *Rev. Neurol. (Paris)*, 1971, *124* (2), 162–166.

[27] Rondot, P.; Aicardi, J.; Goutières, F.; Ziegler, M. [Dopa-sensitive dystonia]. *Rev Neurol Paris*, 1992, *148* (11), 680–686.

[28] Rondot, P.; Ziegler, M. Dystonia--L-Dopa Responsive or Juvenile Parkinsonism? *J Neural Transm Suppl*, 1983, *19*, 273–281.

[29] Schiller, A.; Wevers, R. A.; Steenbergen, G. C. H.; Blau, N.; Jung, H. H. Long-Term Course of l-Dopa-Responsive Dystonia Caused by Tyrosine Hydroxylase Deficiency. *Neurology*, 2004, *63* (8), 1524–1526. https://doi.org/10.1212/01.WNL.0000142083.47927.0A.

[30] Zafeiriou, D. I.; Willemsen, M. A.; Verbeek, M. M.; Vargiami, E.; Ververi, A.; Wevers, R. Tyrosine Hydroxylase Deficiency with Severe Clinical Course. *Mol. Genet. Metab.*, 2009, *97* (1), 18–20. https://doi.org/10.1016/j.ymgme.2009.02.001.

[31] Brun, L.; Ngu, L. H.; Keng, W. T.; Ch'ng, G. S.; Choy, Y. S.; Hwu, W. L.; Lee, W. T.; Willemsen, M. A. A. P.; Verbeek, M. M.; Wassenberg, T.; et al. Clinical and Biochemical Features of Aromatic L-Amino Acid Decarboxylase Deficiency. *Neurology*, 2010, *75* (1), 64. https://doi.org/10.1212/WNL.0b013e3181e620ae.

[32] Swoboda, K. J.; Hyland, K.; Goldstein, D. S.; Kuban, K. C. K.; Arnold, L. A.; Holmes, C. S.; Levy, H. L. Clinical and Therapeutic Observations in Aromatic Amino Acid Decarboxylase Deficiency. *Neurology*, 1999, *53* (6), 1205. https://doi.org/10.1212/WNL.53.6.1205.

[33] Craig, S. P.; Le Van Thai, A.; Weber, M.; Craig, I. W. Localisation of the Gene for Human Aromatic L-Amino Acid Decarboxylase (DDC) to Chromosome 7p13→p11 by in Situ Hybridisation. *Cytogenet. Genome Res.*, 1992, *61* (2), 114–116. https://doi.org/10.1159/000133384.

[34] Haavik, J.; Blau, N.; Thöny, B. Mutations in Human Monoamine-Related Neurotransmitter Pathway Genes. *Hum. Mutat.*, 2008, *29* (7), 891–902. https://doi.org/10.1002/humu.20700.

[35] Hyland, K.; Clayton, P. T. Aromatic L-Amino Acid Decarboxylase Deficiency: Diagnostic Methodology. *Clin. Chem.*, 1992, *38* (12), 2405–2410. https://doi.org/10.1093/clinchem/38.12.2405.

[36] Verbeek, M. M.; Geurtz, P. B. H.; Willemsen, M. A. A. P.; Wevers, R. A. Aromatic L-Amino Acid Decarboxylase Enzyme Activity in Deficient Patients and Heterozygotes. *Mol. Genet. Metab.*, 2007, *90* (4), 363–369. https://doi.org/10.1016/j.ymgme.2006.12.001.

[37] Himmelreich, N.; Montioli, R.; Bertoldi, M.; Carducci, C.; Leuzzi, V.; Gemperle, C.; Berner, T.; Hyland, K.; Thöny, B.; Hoffmann, G. F.; et al. Aromatic Amino Acid Decarboxylase Deficiency: Molecular and Metabolic Basis and Therapeutic Outlook. *Mol. Genet. Metab.*, 2019, *127* (1), 12–22. https://doi.org/10.1016/j.ymgme.2019.03.009.

[38] Wassenberg, T.; Molero-Luis, M.; Jeltsch, K.; Hoffmann, G. F.; Assmann, B.; Blau, N.; Garcia-Cazorla, A.; Artuch, R.; Pons, R.; Pearson, T. S.; et al. Consensus Guideline for the Diagnosis and Treatment of Aromatic L-Amino Acid Decarboxylase (AADC) Deficiency. *Orphanet J. Rare Dis.*, 2017, *12* (1), 12. https://doi.org/10.1186/s13023-016-0522-z.

[39] Pearson, T. S.; Gilbert, L.; Opladen, T.; Garcia-Cazorla, A.; Mastrangelo, M.; Leuzzi, V.; Tay, S. K. H.; Sykut-Cegielska, J.; Pons, R.; Mercimek-Andrews, S.; et al. AADC Deficiency from Infancy to Adulthood: Symptoms and Developmental Outcome in an International Cohort of 63 Patients. *J. Inherit. Metab. Dis.*, 2020, *43* (5), 1121–1130. https://doi.org/10.1002/jimd.12247.

[40] Shih, J. C.; Chen, K.; Ridd, M. J. MONOAMINE OXIDASE: From Genes to Behavior. *Annu. Rev. Neurosci.*, 1999, *22* (1), 197–217. https://doi.org/10.1146/annurev.neuro.22.1.197.

[41] Shih, J. C.; Thompson, R. F. Monoamine Oxidase in Neuropsychiatry and Behavior. *Am. J. Hum. Genet.*, 1999, *65* (3), 593–598. https://doi.org/10.1086/302562.

[42] Sabol, S. Z.; Hu, S.; Hamer, D. A Functional Polymorphism in the Monoamine Oxidase A Gene Promoter. *Hum. Genet.*, 1998, *103* (3), 273–279. https://doi.org/10.1007/s004390050816.

[43] Sanfilippo, C.; Castrogiovanni, P.; Imbesi, R.; Lazzarino, G.; Di Pietro, V.; Li Volti, G.; Tibullo, D.; Barbagallo, I.; Lazzarino, G.; Avola, R.; et al. Sex-Dependent Monoamine Oxidase Isoforms Expression Patterns during Human Brain Ageing. *Mech. Ageing Dev.*, 2021, *197*, 111516. https://doi.org/10.1016/j.mad.2021.111516.

[44] Cheung, N. W.; Earl, J. Monoamine Oxidase Deficiency: A Cause of Flushing and Attention-Deficit/Hyperactivity Disorder? *Arch. Intern. Med.*, 2001, *161* (20), 2503–2504.

[45] Brunner, H. G.; Nelen, M.; Breakefield, X. O.; Ropers, H. H.; van Oost, B. A. Abnormal Behavior Associated with a Point Mutation in the Structural Gene for Monoamine Oxidase A. *Science*, 1993, *262* (5133), 578–580. https://doi.org/10.1126/science.8211186.

[46] Bortolato, M.; Floris, G.; Shih, J. C. From Aggression to Autism: New Perspectives on the Behavioral Sequelae of Monoamine Oxidase Deficiency. *J. Neural Transm.*, 2018, *125* (11), 1589–1599. https://doi.org/10.1007/s00702-018-1888-y.

[47] Bortolato, M.; Shih, J. C. Behavioral Outcomes of Monoamine Oxidase Deficiency: Preclinical and Clinical Evidence. In *International Review of Neurobiology*; Youdim, M. B. H., Douce, P., Eds.; Academic Press, 2011; Vol. 100, pp 13–42. https://doi.org/10.1016/B978-0-12-386467-3.00002-9.

[48] Whibley, A.; Urquhart, J.; Dore, J.; Willatt, L.; Parkin, G.; Gaunt, L.; Black, G.; Donnai, D.; Raymond, F. L. Deletion of MAOA and MAOB in a Male Patient Causes Severe Developmental Delay, Intermittent Hypotonia and Stereotypical Hand Movements. *Eur. J. Hum. Genet.*, 2010, *18* (10), 1095–1099. https://doi.org/10.1038/ejhg.2010.41.

[49] Franco, R.; Reyes-Resina, I.; Navarro, G. Dopamine in Health and Disease: Much More Than a Neurotransmitter. *Biomedicines*, 2021, *9* (2), 109. https://doi.org/10.3390/biomedicines9020109.

[50] Gonzalez-Lopez, E.; Vrana, K. E. Dopamine Beta-Hydroxylase and Its Genetic Variants in Human Health and Disease. *J. Neurochem.*, 2020, *152* (2), 157–181. https://doi.org/10.1111/jnc.14893.

[51] Craig, S. P.; Buckle, V. J.; Lamouroux, A.; Mallet, J.; Craig, I. W. Localization of the Human Dopamine Beta Hydroxylase (DBH) Gene to Chromosome 9q34. *Cytogenet. Genome Res.*, 1988, *48* (1), 48–50. https://doi.org/10.1159/000132584.

[52] Senard, J.-M.; Rouet, P. Dopamine Beta-Hydroxylase Deficiency. *Orphanet J. Rare Dis.*, 2006, *1* (1), 7. https://doi.org/10.1186/1750-1172-1-7.

[53] Garland, E. M.; Biaggioni, I. Dopamine Beta-Hydroxylase Deficiency. In *GeneReviews*®; Adam, M. P., Ardinger, H. H., Pagon, R. A., Wallace, S. E., Bean, L. J., Gripp, K. W., Mirzaa, G. M., Amemiya, A., Eds.; University of Washington, Seattle: Seattle (WA), 1993.

[54] Wassenberg, T.; Deinum, J.; van Ittersum, F. J.; Kamsteeg, E.-J.; Pennings, M.; Verbeek, M. M.; Wevers, R. A.; van Albada, M. E.; Kema, I. P.; Versmissen, J.; et al. Clinical Presentation and Long-Term Follow-up of Dopamine Beta Hydroxylase Deficiency. *J. Inherit. Metab. Dis.*, 2021, *44* (3), 554–565. https://doi.org/10.1002/jimd.12321.

[55] Arnold, A. C.; Garland, E. M.; Celedonio, J. E.; Raj, S. R.; Abumrad, N. N.; Biaggioni, I.; Robertson, D.; Luther, J. M.; Shibao, C. A. Hyperinsulinemia and Insulin Resistance in Dopamine β-Hydroxylase Deficiency. *J. Clin. Endocrinol. Metab.*, 2017, *102* (1), 10–14. https://doi.org/10.1210/jc.2016-3274.

[56] Burchett, S. A.; Hicks, T. P. The Mysterious Trace Amines: Protean Neuromodulators of Synaptic Transmission in Mammalian Brain. *Prog. Neurobiol.*, 2006, *79* (5), 223–246. https://doi.org/10.1016/j.pneurobio.2006.07.003.

[57] Kurian, M. A. *SLC6A3-Related Dopamine Transporter Deficiency Syndrome*; University of Washington, Seattle, Seattle (WA), 1993.

[58] Ford, C. P. The Role of D2-Autoreceptors in Regulating Dopamine Neuron Activity and Transmission. *Ventral Tegmentum Dopamine New Wave Divers.*, 2014, *282*, 13–22. https://doi.org/10.1016/j.neuroscience.2014.01.025.

[59] Kurian, M. A.; Li, Y.; Zhen, J.; Meyer, E.; Hai, N.; Christen, H.-J.; Hoffmann, G. F.; Jardine, P.; von Moers, A.; Mordekar, S. R.; et al. Clinical and Molecular Characterisation of Hereditary Dopamine Transporter Deficiency Syndrome: An Observational Cohort and Experimental Study. *Lancet Neurol.*, 2011, *10* (1), 54–62. https://doi.org/10.1016/S1474-4422(10)70269-6.

[60] Ng, J.; Zhen, J.; Meyer, E.; Erreger, K.; Li, Y.; Kakar, N.; Ahmad, J.; Thiele, H.; Kubisch, C.; Rider, N. L.; et al. Dopamine Transporter Deficiency Syndrome: Phenotypic Spectrum from Infancy to Adulthood. *Brain*, 2014, *137* (4), 1107–1119. https://doi.org/10.1093/brain/awu022.

[61] Patel, J.; Mooslehner, K. A.; Chan, P. M.; Emson, P. C.; Stamford, J. A. Presynaptic Control of Striatal Dopamine Neurotransmission in Adult Vesicular Monoamine Transporter 2 (VMAT2) Mutant Mice. *J. Neurochem.*, 2003, *85* (4), 898–910. https://doi.org/10.1046/j.1471-4159.2003.01732.x.

[62] Truong, J. G.; Newman, A. H.; Hanson, G. R.; Fleckenstein, A. E. Dopamine D2 Receptor Activation Increases Vesicular Dopamine Uptake and Redistributes Vesicular Monoamine Transporter-2 Protein. *Eur. J. Pharmacol.*, 2004, *504* (1), 27–32. https://doi.org/10.1016/j.ejphar.2004.09.049.

[63] Zai, C. C.; Tiwari, A. K.; Mazzoco, M.; de Luca, V.; Müller, D. J.; Shaikh, S. A.; Lohoff, F. W.; Freeman, N.; Voineskos, A. N.; Potkin, S. G.; et al. Association Study of the Vesicular Monoamine Transporter Gene SLC18A2 with Tardive Dyskinesia. *J. Psychiatr. Res.*, 2013, *47* (11), 1760–1765. https://doi.org/10.1016/j.jpsychires.2013.07.025.

[64] Rilstone, J. J.; Alkhater, R. A.; Minassian, B. A. Brain Dopamine–Serotonin Vesicular Transport Disease and Its Treatment. *N. Engl. J. Med.*, 2013, *368* (6), 543–550. https://doi.org/10.1056/NEJMoa1207281.

[65] Rath, M.; Korenke, G. C.; Najm, J.; Hoffmann, G. F.; Hagendorff, A.; Strom, T. M.; Felbor, U. Exome Sequencing Results in Identification and Treatment of Brain Dopamine-Serotonin Vesicular Transport Disease. *J. Neurol. Sci.*, 2017, *379*, 296–297. https://doi.org/10.1016/j.jns.2017.06.034.

[66] Opladen, T.; Hoffmann, G. F.; Blau, N. An International Survey of Patients with Tetrahydrobiopterin Deficiencies Presenting with Hyperphenylalaninaemia. *J. Inherit. Metab. Dis.*, 2012, *35* (6), 963–973. https://doi.org/10.1007/s10545-012-9506-x.

[67] Opladen, T.; Hoffmann, G. F.; Kühn, A. A.; Blau, N. Pitfalls in Phenylalanine Loading Test in the Diagnosis of Dopa-Responsive Dystonia. *Mol. Genet. Metab.*, 2013, *108* (3), 195–197. https://doi.org/10.1016/j.ymgme.2013.01.001.

[68] Garavaglia, B.; Invernizzi, F.; Carbone, M. L. A.; Viscardi, V.; Saracino, F.; Ghezzi, D.; Zeviani, M.; Zorzi, G.; Nardocci, N. GTP-Cyclohydrolase I Gene Mutations in Patients with Autosomal Dominant and Recessive GTP-CH1 Deficiency: Identification and Functional Characterization of Four Novel Mutations. *J. Inherit. Metab. Dis.*, 2004, *27* (4), 455–463. https://doi.org/10.1023/B:BOLI.0000037349.08483.96.

[69] Horvath, G. A.; Stockler-Ipsiroglu, S. G.; Salvarinova-Zivkovic, R.; Lillquist, Y. P.; Connolly, M.; Hyland, K.; Blau, N.; Rupar, T.; Waters, P. J. Autosomal Recessive GTP Cyclohydrolase I Deficiency without Hyperphenylalaninemia: Evidence of a Phenotypic Continuum between Dominant and Recessive Forms. *Mol. Genet. Metab.*, 2008, *94* (1), 127–131. https://doi.org/10.1016/j.ymgme.2008.01.003.

[70] Segawa, M.; Nomura, Y.; Nishiyama, N. Autosomal Dominant Guanosine Triphosphate Cyclohydrolase I Deficiency (Segawa Disease). *Ann. Neurol.*, 2003, *54* (S6), S32–S45. https://doi.org/10.1002/ana.10630.

[71] López-Laso, E.; Sánchez-Raya, A.; Moriana, J. A.; Martínez-Gual, E.; Camino-León, R.; Mateos-González, M. E.; Pérez-Navero, J. L.; Ochoa-Sepúlveda, J. J.; Ormazabal, A.; Opladen, T.; et al. Neuropsychiatric Symptoms and Intelligence Quotient in Autosomal Dominant Segawa Disease. *J. Neurol.*, 2011, *258* (12), 2155–2162. https://doi.org/10.1007/s00415-011-6079-9.

[72] Opladen, T.; Hoffmann, G.; Hörster, F.; Hinz, A.-B.; Neidhardt, K.; Klein, C.; Wolf, N. Clinical and Biochemical Characterization of Patients with Early Infantile Onset of Autosomal Recessive GTP Cyclohydrolase I Deficiency without Hyperphenylalaninemia. *Mov. Disord.*, 2011, *26* (1), 157–161. https://doi.org/10.1002/mds.23329.

[73] Blau, N.; Cotton, R. G. H.; Hyland, K. Tetrahydrobiopterin and Related Biogenic Amines. 53.

[74] Wang, L.; Yu, W.-M.; He, C.; Chang, M.; Shen, M.; Zhou, Z.; Zhang, Z.; Shen, S.; Liu, T.-T.; Hsiao, K.-J. Long-Term Outcome and Neuroradiological Findings of 31 Patients with 6-Pyruvoyltetrahydropterin Synthase Deficiency. *J. Inherit. Metab. Dis.*, 2006, *29* (1), 127–134. https://doi.org/10.1007/s10545-006-0080-y.

[75] Leuzzi, V.; Carducci, C.; Carducci, C.; Pozzessere, S.; Burlina, A.; Cerone, R.; Concolino, D.; Donati, M.; Fiori, L.; Meli, C.; et al. Phenotypic Variability, Neurological Outcome and Genetics Background of 6-Pyruvoyl-Tetrahydropterin Synthase Deficiency. *Clin. Genet.*, 2010, *77* (3), 249–257. https://doi.org/10.1111/j.1399-0004.2009.01306.x.

[76] Niederwieser, A.; Shintaku, H.; Leimbacher, W.; Curtius, H. C.; Hyànek, J.; Zeman, J.; Endres, W. “Peripheral” Tetrahydrobiopterin Deficiency with Hyperphenylalaninaemia

Due to Incomplete 6-Pyruvoyl Tetrahydropterin Synthase Deficiency or Heterozygosity. *Eur. J. Pediatr.*, 1987, *146* (3), 228–232. https://doi.org/10.1007/BF00716465.

[77] Abeling, N. G.; Duran, M.; Bakker, H. D.; Stroomer, L.; Thöny, B.; Blau, N.; Booij, J.; Poll-The, B. T. Sepiapterin Reductase Deficiency an Autosomal Recessive DOPA-Responsive Dystonia. *Mol. Genet. Metab.*, 2006, *89* (1), 116–120. https://doi.org/10.1016/j.ymgme.2006.03.010.

[78] Friedman, J. *Sepiapterin Reductase Deficiency*; University of Washington, Seattle, Seattle (WA), 1993.

[79] Leuzzi, V.; Carducci, C.; Tolve, M.; Giannini, M. T.; Angeloni, A.; Carducci, C. Very Early Pattern of Movement Disorders in Sepiapterin Reductase Deficiency. *Neurology*, 2013, *81* (24), 2141. https://doi.org/10.1212/01.wnl.0000437299.51312.5f.

[80] Friedman, J.; Hyland, K.; Blau, N.; MacCollin, M. Dopa-Responsive Hypersomnia and Mixed Movement Disorder Due to Sepiapterin Reductase Deficiency. *Neurology*, 2006, *67* (11), 2032. https://doi.org/10.1212/01.wnl.0000247274.21261.b4.

[81] Friedman, J.; Roze, E.; Abdenur, J. E.; Chang, R.; Gasperini, S.; Saletti, V.; Wali, G. M.; Eiroa, H.; Neville, B.; Felice, A.; et al. Sepiapterin Reductase Deficiency: A Treatable Mimic of Cerebral Palsy. *Ann. Neurol.*, 2012, *71* (4), 520–530. https://doi.org/10.1002/ana.22685.

[82] Thöny, B.; Blau, N. Mutations in the BH4-Metabolizing Genes GTP Cyclohydrolase I, 6-Pyruvoyl-Tetrahydropterin Synthase, Sepiapterin Reductase, Carbinolamine-4a-Dehydratase, and Dihydropteridine Reductase. *Hum. Mutat.*, 2006, *27* (9), 870–878. https://doi.org/10.1002/humu.20366.

[83] Zielonka, M.; Makhseed, N.; Blau, N.; Bettendorf, M.; Hoffmann, G. F.; Opladen, T. Dopamine-Responsive Growth-Hormone Deficiency and Central Hypothyroidism in Sepiapterin Reductase Deficiency. In *JIMD Reports, Volume 24*; Zschocke, J., Baumgartner, M., Morava, E., Patterson, M., Rahman, S., Peters, V., Eds.; JIMD Reports; Springer: Berlin, Heidelberg, 2015; pp 109–113. https://doi.org/10.1007/8904_2015_450.

[84] Thöny, B.; Neuheiser, F.; Kierat, L.; Rolland, M. O.; Guibaud, P.; Schlüter, T.; Germann, R.; Heidenreich, R. A.; Duran, M.; de Klerk, J. B. C.; et al. Mutations in the Pterin-4α-Carbinolamine Dehydratase (PCBD) Gene Cause a Benign Form of Hyperphenylalaninemia. *Hum. Genet.*, 1998, *103* (2), 162–167. https://doi.org/10.1007/s004390050800.

[85] Mendel Dirk B.; Khavari Paul A.; Conley Pamela B.; Graves Mary K.; Hansen Linda P.; Admon Arie; Crabtree Gerald R. Characterization of a Cofactor That Regulates Dimerization of a Mammalian Homeodomain Protein. *Science*, 1991, *254* (5039), 1762–1767. https://doi.org/10.1126/science.1763325.

[86] Simaite, D.; Kofent, J.; Gong, M.; Rüschendorf, F.; Jia, S.; Arn, P.; Bentler, K.; Ellaway, C.; Kühnen, P.; Hoffmann, G. F.; et al. Recessive Mutations in PCBD1 Cause a New Type of Early-Onset Diabetes. *Diabetes*, 2014, *63* (10), 3557–3564. https://doi.org/10.2337/db13-1784.

[87] Rhee, K.-H.; Stier, G.; Becker, P. B.; Suck, D.; Sandaltzopoulos, R. The Bifunctional Protein DCoH Modulates Interactions of the Homeodomain Transcription Factor HNF1 with Nucleic Acids11Edited by M. Yaniv. *J. Mol. Biol.*, 1997, *265* (1), 20–29. https://doi.org/10.1006/jmbi.1996.0708.

[88] Werner, E. R.; Blau, N.; Thöny, B. Tetrahydrobiopterin: Biochemistry and Pathophysiology. *Biochem. J.*, 2011, *438* (3), 397–414. https://doi.org/10.1042/BJ20110293.

[89] Ponzone, A.; Spada, M.; Ferraris, S.; Dianzani, I.; de Sanctis, L. Dihydropteridine Reductase Deficiency in Man: From Biology to Treatment. *Med. Res. Rev.*, 2004, *24* (2), 127–150. https://doi.org/10.1002/med.10055.

[90] Longo, N. Disorders of Biopterin Metabolism. *J. Inherit. Metab. Dis.*, 2009, *32* (3), 333–342. https://doi.org/10.1007/s10545-009-1067-2.

[91] Hyland, K.; Shoffner, J.; Heales, S. J. Cerebral Folate Deficiency. *J. Inherit. Metab. Dis.*, 2010, *33* (5), 563–570. https://doi.org/10.1007/s10545-010-9159-6.

[92] Coughlin, C. R.; Hyland, K.; Randall, R.; Ficicioglu, C. Dihydropteridine Reductase Deficiency and Treatment with Tetrahydrobiopterin: A Case Report. In *JIMD Reports - Volume 10*; Zschocke, J., Gibson, K. M., Brown, G., Morava, E., Peters, V., Eds.; JIMD Reports; Springer: Berlin, Heidelberg, 2013; pp 53–56. https://doi.org/10.1007/8904_2012_202.

[93] Irons, M.; Levy, H. L.; O'Flynn, M. E.; Stack, C. V.; Langlais, P. J.; Butler, I. J.; Milstien, S.; Kaufman, S. Folinic Acid Therapy in Treatment of Dihydropteridine Reductase Deficiency. *J. Pediatr.*, 1987, *110* (1), 61–67. https://doi.org/10.1016/S0022-3476(87)80289-5.

[94] Dekker, S.; Kampinga, H.; Bergink, S. DNAJs: More than Substrate Delivery to HSPA. *Front. Mol. Biosci.*, 2015, *2*. https://doi.org/10.3389/fmolb.2015.00035.

[95] Sarparanta, J.; Jonson, P. H.; Golzio, C.; Sandell, S.; Luque, H.; Screen, M.; McDonald, K.; Stajich, J. M.; Mahjneh, I.; Vihola, A.; et al. Mutations Affecting the Cytoplasmic Functions of the Co-Chaperone DNAJB6 Cause Limb-Girdle Muscular Dystrophy. *Nat. Genet.*, 2012, *44* (4), 450–455. https://doi.org/10.1038/ng.1103.

[96] Anikster, Y.; Haack, T. B.; Vilboux, T.; Pode-Shakked, B.; Thöny, B.; Shen, N.; Guarani, V.; Meissner, T.; Mayatepek, E.; Trefz, F. K.; et al. Biallelic Mutations in DNAJC12 Cause Hyperphenylalaninemia, Dystonia, and Intellectual Disability. *Am. J. Hum. Genet.*, 2017, *100* (2), 257–266. https://doi.org/10.1016/j.ajhg.2017.01.002.

[97] Blau, N.; Martinez, A.; Hoffmann, G. F.; Thöny, B. DNAJC12 Deficiency: A New Strategy in the Diagnosis of Hyperphenylalaninemias. *Mol. Genet. Metab.*, 2018, *123* (1), 1–5. https://doi.org/10.1016/j.ymgme.2017.11.005.

[98] Hollak, C. E. M.; Lachmann, R. *Inherited Metabolic Disease in Adults: A Clinical Guide*; Oxford University Press, 2016.

[99] Hyland, K. Clinical Utility of Monoamine Neurotransmitter Metabolite Analysis in Cerebrospinal Fluid. *Clin. Chem.*, 2008, *54* (4), 633–641. https://doi.org/10.1373/clinchem.2007.099986.

[100] Hyland, K.; Surtees, R. A. H.; Heales, S. J. R.; Bowron, A.; Howells, D. W.; Smith, I. Cerebrospinal Fluid Concentrations of Pterins and Metabolites of Serotonin and Dopamine in a Pediatric Reference Population. *Pediatr. Res.*, 1993, *34* (1), 10–14. https://doi.org/10.1203/00006450-199307000-00003.

[101] Maas, R. P. P. W. M.; Wassenberg, T.; Lin, J.-P.; van de Warrenburg, B. P. C.; Willemsen, M. A. A. P. L-Dopa in Dystonia. *Neurology*, 2017, *88* (19), 1865. https://doi.org/10.1212/WNL.0000000000003897.

[102] Ng, J.; Heales, S. J. R.; Kurian, M. A. Clinical Features and Pharmacotherapy of Childhood Monoamine Neurotransmitter Disorders. *Pediatr. Drugs*, 2014, *16* (4), 275–291. https://doi.org/10.1007/s40272-014-0079-z.

[103] Birnbacher, R.; Scheibenreiter, S.; Blau, N.; Bieglmayer, C.; Frisch, H.; Waldhauser, F. Hyperprolactinemia, a Tool in Treatment Control of Tetrahydrobiopterin Deficiency: Endocrine Studies in an Affected Girl. *Pediatr. Res.*, 1998, *43* (4), 472–477. https://doi.org/10.1203/00006450-199804000-00006.

CHAPITRE 2 : QUANTIFICATION DES METABOLITES DES NEUROTRANSMETTEURS MONOAMINES ET DES COFACTEURS : ETAT DE L'ART

II.1. PRESENTATION DE L'ARTICLE

Comme indiqué dans le chapitre 1, les erreurs innées du métabolisme de la dopamine et de la sérotonine sont des maladies rares caractérisées par des symptômes neurologiques non spécifiques. Ces symptômes apparaissent précocement au cours de l'enfance et correspondent à des troubles du mouvement, des crises épileptiques, des troubles du sommeil et/ou des retards mentaux. Pour le diagnostic spécifique de ces maladies, des biomarqueurs ont été identifiés et validés dans le liquide céphalorachidien. Ces biomarqueurs se divisent en deux groupes : les métabolites des neurotransmetteurs monoamines et les ptérines. La quantification des biomarqueurs dans le liquide céphalorachidien est basée essentiellement sur l'analyse par chromatographie liquide à haute performance couplée à une détection électrochimique, une détection par fluorescence ou à la spectrométrie de masse en tandem. L'article composant ce chapitre est une revue bibliographique référençant les avancées dans les méthodes de routine proposées pour la quantification de ces analytes dans le liquide céphalorachidien. Il permet d'inventorier et de comparer les différentes méthodes proposées en termes de traitement d'échantillon, de conditions chromatographiques et de modes de détection.

Malgré le large éventail de méthodes proposées, la quantification des biomarqueurs des erreurs innées du métabolisme de la dopamine et de la sérotonine reste un défi important, étant donné les faibles concentrations en analytes retrouvées dans le liquide céphalorachidien.

Statut de l'article : En cours de soumission.

Journal visé : Critical reviews in analytical chemistry

Quantification of monoamine neurotransmitter metabolites and cofactors in CSF: State-of-the-art

A. Boulghobra* and M. Bonose

Institut de Chimie Physique, UMR 8000-Université Paris Saclay

*corresponding author

II.2. ABSTRACT

Inborn errors of monoamine neurotransmitter metabolism are rare diseases characterized by non-specific neurological symptoms. These symptoms appear in early childhood and correspond to movement disorders, epilepsy, sleep disorders and/or mental retardation. Cerebrospinal fluid biomarkers have been identified and validated to allow specific diagnosis of these diseases. Biomarkers of inborn errors of monoamine neurotransmitter metabolites are divided in two groups: monoamine neurotransmitter metabolites and pterins. Biomarkers quantification in cerebrospinal fluid is based on high-performance liquid chromatography separation coupled to electrochemical detection, fluorescence detection or mass spectrometry. The following article reviews the advances in the proposed routine methods for the measurement of these analytes in cerebrospinal fluid. The purpose of this review is to compare the various proposed methods in terms of sample preparation, chromatographic conditions and detection modes. Despite the broad range of proposed methods, quantification of inborn errors of monoamine neurotransmitter biomarkers remains a great challenge, given the complexity of biological fluids and the low amounts of analytes that are present in cerebrospinal fluid.

Keywords: Biomarkers; CSF; monoamine neurotransmitter metabolites; pterins; HPLC

II.3. INTRODUCTION

Monoamine neurotransmitters, namely dopamine and serotonin are a group of molecule involved in numerous functions of the central and peripheral nervous system.[1] Inborn errors of dopamine and serotonin metabolism are rare inherited disorders of metabolism

resulting from single-gene variants.[2] These genes encode enzymes of monoamine neurotransmitter metabolism or neurotransmitter transporters. As a consequence, this metabolism is unbalanced and synaptic transmissions are altered, thus, leading to clinical symptoms such as movement disorders, epilepsy, sleep disorders and/or mental retardation.[3–9]

Clinical symptoms are similar from one genetic mutation to another that is why they provide very low diagnostic specificity.[10–14] However, the diagnosis of inborn errors of dopamine and serotonin metabolism is of paramount importance, since the treatment of each mutation is unique.[3, 15] The latter relies mainly on supplementation with a missing metabolite or cofactor. To diagnose these diseases, biomarkers have been identified and validated in cerebrospinal fluid (CSF).[16–18] Biomarkers of dopamine and serotonin metabolism are classified in two groups: monoamine neurotransmitter metabolites and pterins which correspond to enzymatic cofactors.[16, 18] Quantifying these molecules is an essential element to diagnose inherited disorders of monoamine neurotransmitter disorders.

This quantification relies mostly on high-performance liquid chromatography (HPLC) technique.[16, 19] Even though capillary electrophoresis can be performed, it has limited applicability to CSF samples, given the difficulty to separate the relevant compounds and the high lower limit of quantification (LOQ) reached.[19, 20] Proposed HPLC methods differ mainly in terms of sample treatment, chromatographic conditions and of detection mode where electrochemical detection (ECD), fluorescence detection (FD) and tandem mass spectrometry (MS/MS) can be used.

The following review aims at proposing a state-of-the-art about advances in the quantification of monoamine neurotransmitter metabolites and cofactors in CSF. While comparing the various proposed methods for the measurement of these biomarkers regarding sample preparation, chromatographic conditions and detection modes, we will also focus on the reached performances.

II.4. PRIMARY MONOAMINE NEUROTRANSMITTER DISORDERS

II.4.1. Metabolism of dopamine, serotonin and pterins

II.4.1.1. Metabolism of dopamine

Dopamine is a biogenic monoamine that belongs to catecholamines.[21] Catecholamines consists of a benzene ring with hydroxyl group at position 3 and 4, corresponding to a catechol, with an amino group on the lateral chain.[16, 21] In the central nervous system, dopamine is mainly biosynthesized starting from aromatic amino acids (Figure II.1).[22, 23] In this metabolic pathway, L-phenylalanine is first hydroxylated into L-tyrosine by phenylalanine hydroxylase (PAH).[24] As shown in Figure II.1, L-tyrosine is then converted to L-3,4-dihydroxyphenylalanine (L-DOPA) by tyrosine hydroxylase (TH).[23] The latter is the rate-limiting enzyme of dopamine biosynthesis.[21, 23] L-DOPA is decarboxylated by aromatic amino acids decarboxylase (AADC) to generate dopamine. This neurotransmitter can then be converted by dopamine β-hydroxylase (DBH) to another biogenic monoamine, norepinephrine.[25] Catecholamines catabolism is mainly due to monoamine oxidase (MAO) and catechol-O-methyl transferase (COMT).[16, 22] Concerning dopamine, it undergoes oxidative deamination catalysed by MAO, generating 3,4-dihydroxyphenylacetaldehyde (DOPAL).[26] Then, DOPAL is converted to 3,4-dihydroxyphenylacetic acid (DOPAC) by aldehyde dehydrogenase (AD). Homovanillic acid (HVA) is produced from DOPAC O-methylation by COMT.[16, 22] HVA is a biomarker of inborn errors of dopamine metabolism.[18, 27] L-DOPA can also be metabolized into 3-*ortho*-methyl-DOPA (3-OMD) which is quantified in CSF as part of inborn errors of dopamine metabolism diagnosis.[28] Moreover, norepinephrine is predominantly transformed into 3,4-dihydroxyphenylglycoaldehyde (DOPEGAL) by MAO. DOPEGAL is then reduced to 3,4-dihydroxyphenylglycol (DHPG) by aldehyde reductase (AR). COMT converts DHPG into 3-methoxy-4-hydroxyphenylglycol (MHPG).[22] MHPG is the major catabolite of norepinephrine and it is used as a biomarker in the diagnosis of inborn errors of monoamine metabolism.[16, 18] HVA, MHPG

and 3-OMD are three dopamine metabolites whose cerebrospinal concentrations vary in inborn errors of metabolism which makes them biomarkers of paramount importance for the diagnosis of these diseases.[16, 18, 29, 30]

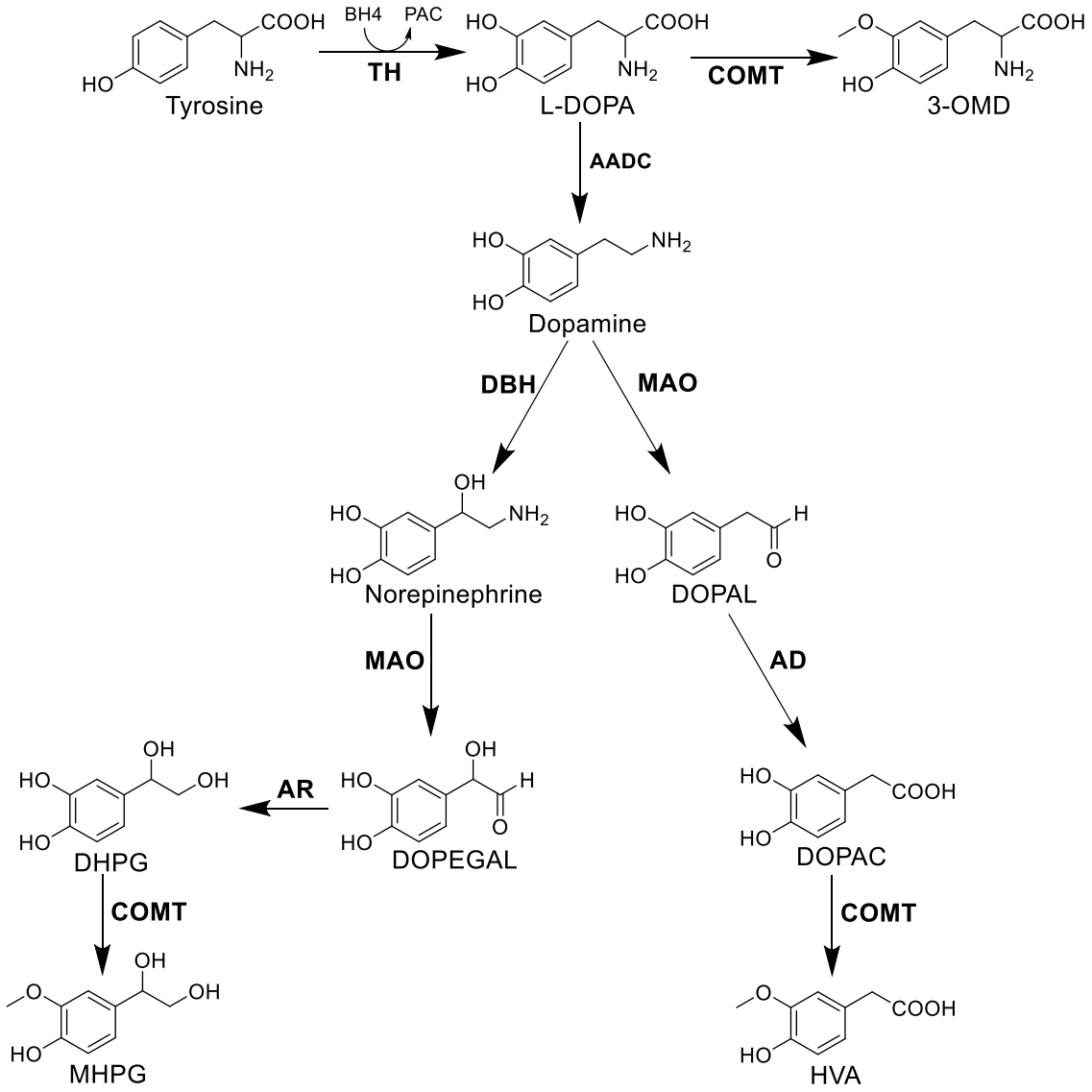

Figure II.1: Dopamine biosynthesis and catabolism pathway.[21–24]

AADC, aromatic L-amino acid decarboxylase; AD, aldehyde dehydrogenase; AR, aldehyde reductase; BH4, tetrahydrobiopterin; COMT, catechol-O-methyl transferase; DBH, dopamine β-hydroxylase; DHPG, 3,4-dihydroxyphenylglycol; DOPAC, 3,4-dihydroxyphenylacetic acid; DOPAL, 3,4-dihydroxyphenylacetaldehyde; DOPEGAL, 3,4-dihydroxyphenylglycoaldehyde; HVA, homovanillic acid; MAO, monoamine oxidase; MHPG, 3-metoxy-4-hydroxyphenylglycol; 3-OMD, 3-*ortho*-methyl-DOPA; PAC, pterin-4α-carbinolamine; TH, tyrosine hydroxylase.

II.4.1.2. Metabolism of serotonin

Serotonin, or 5-hydroxytryptamine, is an indolamine neurotransmitter produced in the central nervous system serotoninergic neurons.[31] It is biosynthesized from tryptophan which is first hydroxylated into 5-hydroxytryptophan (5-HTP) by tryptophan hydroxylase (TPH), then decarboxylated by AADC (Figure II.2).[31, 32] Such as dopamine, serotonin is catabolized by MAO and AD. MAO converts serotonin into 5-hydroxyindolacetaldehyde (5-HIAL), which is oxidized to 5-hydroxyindolacetic acid (5-HIAA) by AD.[31] 5-HTP and 5-HIAA in CSF are important biomarkers for the diagnosis of inborn errors of monoamine metabolism. Indeed, significant modifications in their cerebrospinal concentrations are observed in these illnesses.[16, 18]

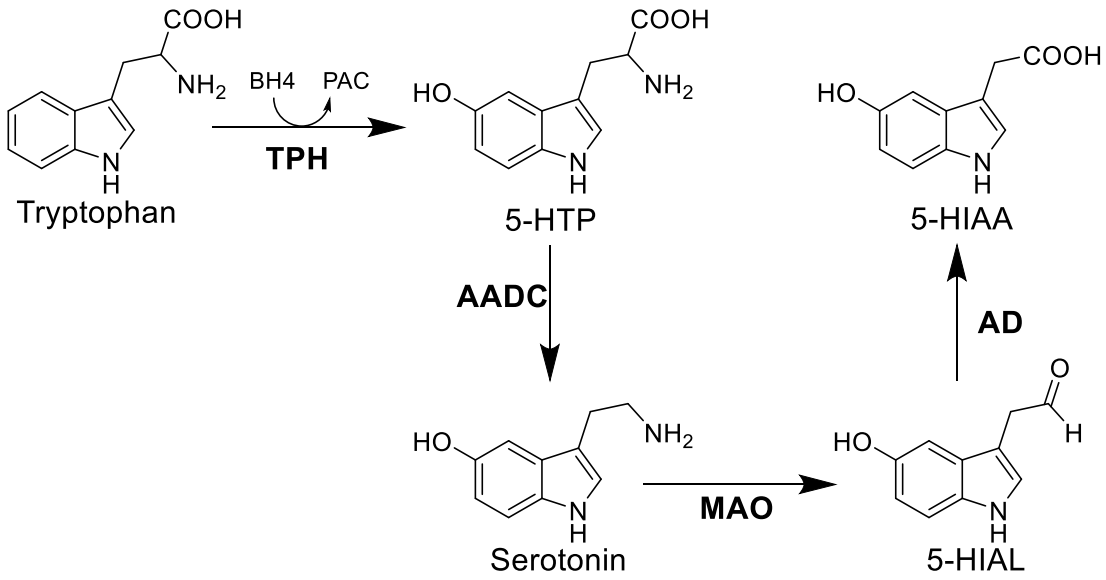

Figure II.2: Serotonin biosynthesis and catabolism pathway.[31, 32]

AADC, aromatic L-amino acid decarboxylase; AD, aldehyde dehydrogenase; BH4, tetrahydrobiopterin; 5-HIAA, 5-hydroxyindolacetic acid; 5-HIAL, 5-hydroxyindolacetaldehyde; 5-HTP, 5-hydroxytryptophan; MAO, monoamine oxidase; PAC, pterin-4α-carbinolamine; TPH, tryptophan hydroxylase.

II.4.1.3. Metabolism of pterins

Pterins are necessary enzymatic cofactors that chemically belongs to 2-aminopteridin-4-one. The most important pterin is tetrahydrobiopterin (BH4), or 6R-2-amino-

5,6,7,8-tetrahydropteridin-4-one.[33, 34] BH4 is a cofactor of enzymatic hydroxylations of aromatic amino acids by PAH, TH and TPH.[33–36] BH4 biosynthesis involves mainly two pathways: *de novo* biosynthesis and salvage pathway. [33, 34] *De novo* biosynthesis starts with the guanosine triphosphate cyclohydrolase-catalysed (GTPCH) metabolism of guanosine triphosphate (GTP) to 7,8-dihydroneopterin triphosphate. The latter is then converted to 6-pyruvoyl-tetrahydropterin by 6-pyruvoyl-tetrahydropterin synthase (PTPS). The last step of BH4 *de novo* biosynthesis is the NADPH-dependent reduction of 6-pyruvoyl-tetrahydropterin to BH4 by sepiapterin reductase (SR). [33–36] In the salvage pathway, sepiapterin is first reduced to 7,8-dihydrobiopterin (BH2) by SR. Second, BH2 is transformed into BH4 in a NADPH-dependent reaction catalysed by dihydrofolate reductase (DHFR).[34, 35] During hydroxylations catalysed by PAH, TH and TPH, BH4 is converted to pterin-4α-carbinolamine. In BH4 recycling pathway, the latter is reduced to quinonoid dihydrobiopterin (q-BH2) by pterin-4-carbinolamine dehydratase (PCD).[33, 34] Dihydropteridine reductase (DHPR) recycles q-BH2 into BH4. [33, 34] BH4, BH2, biopterin (B), dihydroneopterin (NH2) and neopterin (N) are CSF biomarkers of inborn errors of metabolism.[16, 18]

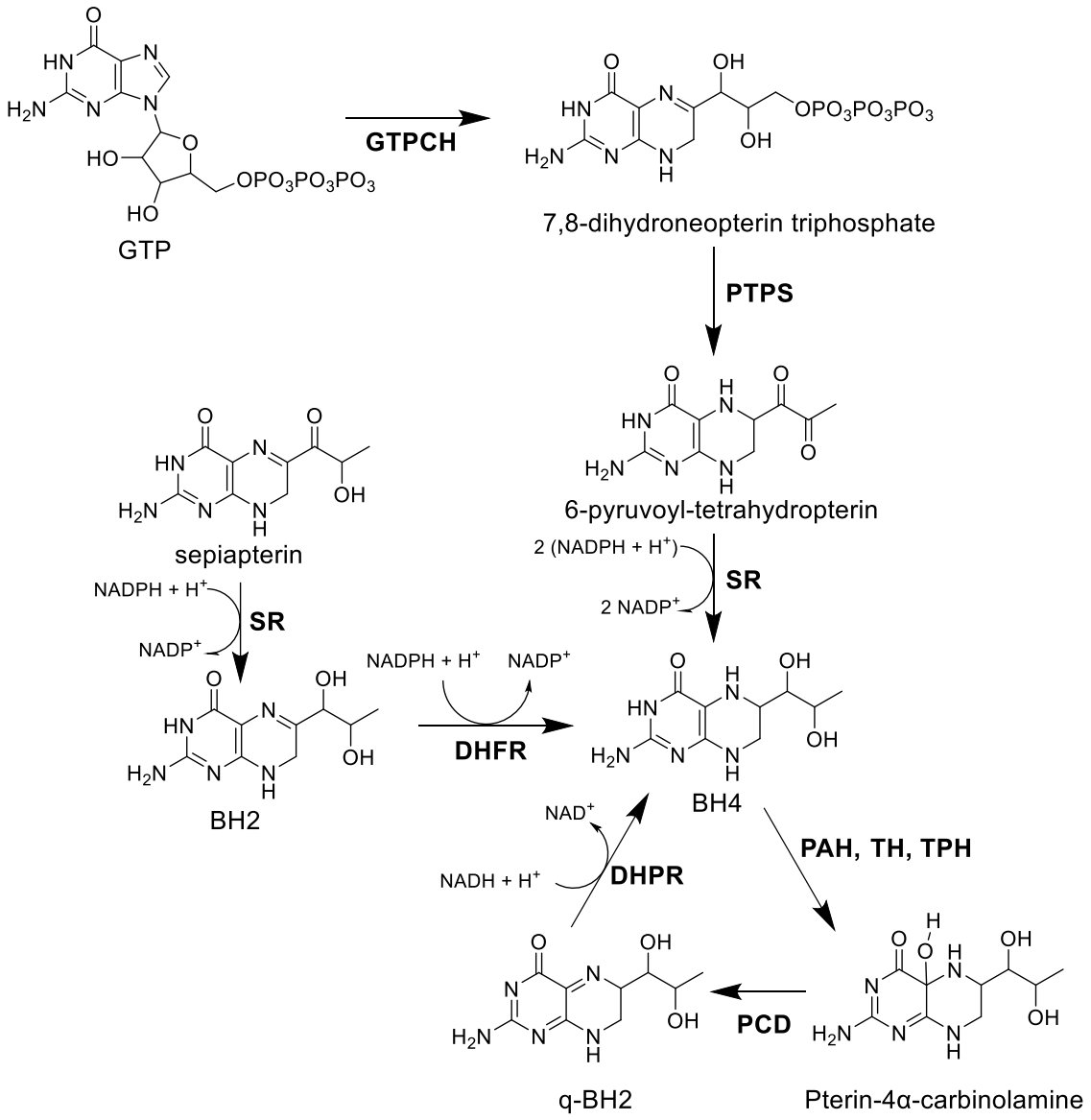

Figure II.3: Metabolism pathway of pterins.[33–36]

BH2, dihydrobiopterin; BH4, tetrahydrobiopterin; DHFR, dihydrofolate reductase; DHPR, dihydropteridine reductase; GTP, guanosine triphosphate; GTPCH, guanosine triphosphate cyclohydrolase; PAH, phenylalanine hydroxylase; PCD, pterin-4-carbinolamine dehydratase; PTPS, 6-pyruvoyl-tetrahydropterin synthase; SR, sepiapterin reductase deficiency; TH, tyrosine hydroxylase; TPH, tryptophan hydroxylase.

II.4.2. Inborn errors of monoamine neurotransmitter metabolism

Inborn errors of monoamine neurotransmitter metabolism correspond to a set of orphan diseases resulting from impaired biosynthesis, catabolism or transport of neurotransmitters and essential cofactors.[3, 4]

II.4.2.1. Pathophysiology

These diseases are based on mutations affecting the genes coding for key proteins in monoamine neurotransmitter metabolism.[3, 4] This causes the dysfunction of the protein and unbalances the metabolism of monoamine neurotransmitter.[3] Depending on the mutated gene, inborn errors of neurotransmitter metabolism are divided into five groups: monoamine biosynthesis disorders, enzyme defects in monoamine catabolism, BH4 synthesis or recycling disorders, monoamine neurotransmitter transportopathies and chaperon-associated disorders.[3, 4]

Concerning monoamine biosynthesis disorders, they are caused by dysfunctions of the enzymes involved in dopamine and serotonin biosynthesis, namely TH and AADC.[37–40] The consequence is that the production of dopamine and serotonin are reduced, generating unbalanced dopaminergic and serotoninergic transmissions in the central nervous system.[37–40] Enzyme defects in monoamine catabolism corresponds to impairment in the activity of whether MAO or DBH.[3]

BH4 synthesis or recycling disorders are caused by mutations on the genes of SR, GTPCH, PTPS, DHPR and PCD. This causes diminution of the production of BH4, essential cofactor of PAH, TH and TPH. Hence the decrease of monoamine neurotransmitter biosynthesis.[3, 4, 16] These mutations are mainly transmitted with an autosomal recessive mode except for GTPCH where two forms have been described: one with an autosomal recessive (AR) transmission and another one with an autosomal dominant (AD) transmission.

Monoamine transportopathies are the consequence of dopamine transporter deficiency syndrome (DTDS) or dysfunction of vesicular monoamine transporter 2

(VMAT2).[5, 41, 42] To date, only one chaperon-associated disorder has been described. It is caused by a mutation on the DNAJC gene.[3] The latter encodes a heat-shock co-chaperone that interacts with hydroxylases involved in monoamine neurotransmitter biosynthesis, namely, PAH, TH and TPH. This mutation inhibits dopamine and serotonin biosynthesis leading to a deficiency of these neurotransmitters.[43, 44]

II.4.2.2. Diagnosis

Inborn errors of monoamine neurotransmitter metabolism impact dopamine and serotonin neurotransmission pathways in the central nervous system, thus, causing neuropsychiatric symptoms:

- Congenital onset neurological symptoms corresponding to floppy infant or developmental delay
- Movement disorders such as dystonia, truncal hypotonia, oculogyric crises, bulbar dysfunction and parkinsonian symptoms
- Autonomous dysregulations like excessive sweating, temperature dysregulation and irritability
- Psychiatric symptoms consisting of sleep disturbances and depression.[3]

These symptoms are common in many inborn errors of dopamine and serotonin metabolism and does not allow to distinguish one specific mutation from the others.[3, 45] Hence, in order to establish a definitive diagnosis and to treat efficiently patients suffering from these diseases, biomarkers quantification in CSF is gold standard.[3, 16, 18, 45] Indeed, as shown in Table II.1, quantification of pterins and neurotransmitter metabolites in CSF is the cornerstone for the diagnosis of inborn errors of monoamine neurotransmitter metabolism.[3, 16, 18, 45, 46]

Table II.1: CSF concentrations of pterins and neurotransmitter metabolites in inborn errors of monoamine neurotransmitter metabolism.[3, 18, 45, 46]

	Pterins			Neurotransmitter metabolites					
Protein defect	BH4	BH2	NH2	HVA	HIAA	HVA/HIAA	3-OMD	5-HTP	MHPG
GTPCH-AR	↓	N	↓	↓	↓	N	N	N	↓
GTPCH-AD	↓	↑	↓	↓	N or ↓	N	N	N	↓
SR	↓	↑	N	↓	↓	N	N	N	↓
PTPS	↓	N	↑	↓	↓	N	N	N	↓
DHPR	↓	↑	N	↓	↓	N	N	N	↓
PCD	↓	N	N	N	N	N	N	N	N
TH	N	N	N	↓	N	↓	N	N	↓
AADC	N	N	N	↓	↓	N	↑	↑	↓
MAO	N	N	N	↓	↓	N	N	N	↓
DTDS	N	N	N	↑	N	↑	N	N	N
VMAT2	N	N	N	↑	↑	N	N	N	N
DNAJC	↑	N	N	↓	↓	N	N	N	N

AADC, aromatic L-amino acid decarboxylase deficiency; B, biopterin; BH2, 7,8-dihydrobiopterin; BH4, tetrahydrobiopterin; DNAJC, DNAJC12 gene mutation; DHPR, dihydropteridine reductase deficiency; DTDS, dopamine transporter deficiency syndrome; GTPCH-AR, autosomal recessive guanosine triphosphate cyclohydrolase deficiency; GTPCH-AD, autosomal dominant guanosine triphosphate cyclohydrolase deficiency; 5-HIAA, 5-hydroxyindol acetic acid; 5-HTP, 5-hydroxytryptophane; HVA, homovanillic acid; MAO, monoamine oxidase deficiency; MHPG, 3-metoxy-4-hydroxyphenylglycol; N, neopterin; NH2, dihydroneopterin; 3-OMD, 3-*ortho*-methyl-DOPA; PCD, pterin-4-carbinolamine dehydratase deficiency; PTPS, 6-pyruvoyl-tetrahydropterin synthase deficiency; SR, sepiapterin reductase deficiency; TH tyrosine hydroxylase deficiency; VMAT2, vesicular monoamine transporter 2.

Table II.1 indicates that the quantification of pterins and neurotransmitter metabolites in CSF samples allows to distinguish any specific mutation from the others, that is why, the quantification of these biomarkers appears as the gold standard diagnostic method.

II.5. DIAGNOSTIC METHOD: VALIDATED BIOMARKERS IN CSF

CSF biomarkers quantification requires to follow strict procedures in terms of sample collection and storage.[47, 48] Many parameters can influence the concentrations of monoamine metabolites and pterins. Indeed, there is a craniocaudal concentration gradient for monoamines, that is why, CSF withdrawal must always be realised at the same lumbar level. Moreover, CSF samples should whether be analysed immediately after collection or stored at -70°C.[47, 48]

II.5.1. Quantification of dopamine and serotonin metabolites

In CSF, dopamine and serotonin metabolites are quantified using separation techniques that are based on high-performance liquid chromatography (HPLC).[16, 19, 48, 49] The main differences between these methods correspond to CSF sample preparation, separation conditions and detection modes.[16, 19, 48, 49]

II.5.1.1. CSF sample preparation

CSF is a biological fluid consisting of an aqueous solution of ions such as sodium and chloride, glucose, proteins and peptides, ascorbic acid, neurotransmitters and their metabolites.[50–53] These compounds may interfere in biomarkers quantification in CSF, that is why sample treatment is paramount. The simplest way to eliminate interferences is to dilute CSF samples in the HPLC mobile phase. It allows to reduce CSF potential interfering compounds and to have a better compatibility with the chromatographic system.[54–58] Some authors described CSF dilution in an antioxidant solution to avoid any degradation of the oxidation incline biomarkers.[54–56] CSF sample treatment is also necessary to eliminate proteins that could interfere in HPLC separation. [16, 49, 59, 60] For that, two strategies are used: one based on protein precipitation, centrifugation and supernatant collection and another one consisting of a filtration on a protein-retaining filters. [54, 57, 58, 61–67] CSF sample preparation procedures are summarized in Table II.2.

Table II.2: CSF sample pre-treatment for the quantification of dopamine and serotonin metabolites

Analysed biomarkers	CSF volume	Sample treatment	Dilution solvent	Ref.
HVA, 5-HIAA, MHPG, 3-OMD	1 mL	Dilution, filtration on 0.45 µm filter	Aqueous solution of 1 g/L ascorbic acid	[54]
HVA, 5-HIAA	1 mL	Dilution	Aqueous solution of 6 mM L-cysteine, 2 mM oxalic acid and 1.3% glacial acetic acid (v/v)	[55]
HVA, 5-HIAA, MHPG	1 mL	Dilution	Aqueous solution of 1 g/L ascorbic acid	[56]
HVA, 5-HIAA, MHPG, 3-OMD, 5-HTP	50 µL	Dilution, ultrafiltration removing any molecule whose weight exceeds 5 kDa	250 nM 2,5-dihydroxybenzoic acid solution in a mixture of 0.05 M sodium citrate pH 5.2 /methanol (97/3, v/v)	[57]
HVA, 5-HIAA, MHPG	200-500 µL	Dilution, filtration removing any molecule whose weight exceeds 10 kDa	Solution of 5-fluorohomovanillic acid at 5 µM	[58]
HVA, 5-HIAA	10 mL	Ultrafiltration removing any molecule whose weight exceeds 30 kDa	No solvent used during sample treatment	[64]

HVA, 5-HIAA	50 µL	Dilution, benzoyl chloride derivatization, protein precipitation, filtration	100 mM sodium tetraborate solution	[61]
HVA, 5-HIAA, MHPG	50 µL	Protein precipitation, centrifugation	0.2 M perchloric acid solution	[63]
HVA, 5-HIAA, MHPG, 3-OMD, 5-HTP	30 µL	Dilution, protein precipitation, centrifugation, evaporation to dryness, sample reconstitution	Water/Acetonitrile/Formic acid/ascorbic acid (96.9/3/0.2/0.02)	[62]
HVA, 5-HIAA	500 µL	pH adjustement at 2-3, gel filtration on Sephadex G-10 column	Formic acid (98%)	[65]
HVA, 5-HIAA, MHPG, 3-OMD, 5-HTP	500 µL	Dilution, centrifugation, filtration on 0.22 µm filter	pH 4.0 sodium acetate-citrate buffer with 1.2 mM EDTA and 1.2 mM 1-heptanosulphonic acid/methanol (91/9)	[66, 67]

EDTA, ethylenediamine-tetraacetic acid; 5-HTP, 5-hydroxytryptophane; 5-HIAA, 5-hydroxyindol acetic acid; HVA, homovanillic acid; MHPG, 3-metoxy-4-hydroxyphenylglycol; 3-OMD, 3-*ortho*-methyl-DOPA.

II.5.1.2. Separation conditions

Table II.3 summarizes the chromatographic conditions that are used to separate inborn errors of dopamine and serotonin biomarkers. The most used chromatographic columns are reversed-phase octadecylsilane (C18) columns.[16, 68, 69] Dopamine and serotonin metabolites are low hydrophobic and low acidic molecules. Therefore, in reversed-phase liquid chromatography (RPLC), the mobile phase must be highly aqueous to allow their separation, whether in isocratic or in gradient modes (Table II.3). Moreover, the mobile phase pH must be controlled with a buffer, since it considerably affects these biomarkers retention. To achieve the separation of these molecules, authors chose specific columns improving the retentions of the analysed biomarkers: polar-embedded C18 stationary phase allows to increase the retention by setting up hydrogen bonds,[54, 57, 62, 70] C18 core-shell silica column improves stationary phase porosity and by this way the surface of contact,[61] or stationary phases with completely different chemistry such as pentafluorophenyl (PFP), porous graphitic carbon, or hydrophilic interaction chromatography (HILIC) columns.[64, 71–74]

Another strategy to perform a reliable separation of dopamine and serotonin metabolites is to use ion-pair chromatography (IPC). The latter is based on the same stationary phases as RPLC, but with an ion-pairing reagent added to the mobile phase. The purpose is to change the retention of the ionic analytes by providing electrostatic interactions of the analytes with the mobile phase.[55, 63, 66, 67] One major problem of IPC is that the column equilibration times are longer than in RPLC because of a slow exchange of the ion-pairing reagent between stationary and mobile phases. Another important problem corresponds to the incompatibility of IPC with some detection modes, especially, mass spectrometry (MS). Indeed, ion-pairing reagents may lead to ion suppression during electrospray ionization (ESI).

Table II.3 indicates isocratic elution mode is more often used than gradient elution. This is due to the fact that isocratic mode is simpler and does not require any extra

equilibration time. It is, therefore, more adapted for routine CSF analysis. Moreover, isocratic mode allows to avoid baseline drift that can be observed in gradient mode particularly with electrochemical and fluorescence detection.[16]

Table II.3: Separation conditions for the quantification of dopamine and serotonin metabolites in CSF samples

Chromatographic mode	Analysed bi-omarkers	Internal standard	Column	Elution mode	Mobile phase	**Analysis time (minutes)**	Ref.
RPLC	HVA, 5-HIAA, MHPG, 3-OMD	N.R	C18 Atlantis T3 (150 x 3.0 mm, 3 µm)	Gradient	pH 4.6; 9.2 mM sodium ace-tate/Acetonitrile	**20**	[54]
IPC	HVA, 5-HIAA	N.R	ESA MD-150 C18 (150 x 3.0 mm)	Isocratic	Aqueous solution of pH 3.1, 75 mM sodium phosphate buffer, 0.5 mM EDTA, 0.8 mM OSA and 5% THF/ acetonitrile (95/5, v/v)	**11**	[55]
RPLC	HVA, 5-HIAA, MHPG	N.R	Apex C18 (250 x 4.6 mm, 5 µm)	Isocratic	pH 5.2 sodium acetate-citrate buffer with 20 mg/L EDTA	**24**	[56]
RPLC	HVA, 5-HIAA, MHPG, 3-OMD, 5-HTP	DHBA	C18 HSS T3 (100 x 2.1 mm, 1.8 µm)	Isocratic	pH 5.2, 0.05 M sodium citrate buffer/methanol (97/3, v/v)	**10**	[57]

RPLC	HVA, 5-HIAA, MHPG	F-HVA	ODS (250 x 4.6 mm, 5 µm)	Isocratic	pH 5.2 sodium acetate-citrate buffer with 0.25 mM EDTA/ methanol (82/8, v/v)	**16-18**	[58]
RPLC	HVA, 5-HIAA	N.R	PFP Hypersil (150 x 2.1 mm, 1.9 µm)	Gradient	Aqueous 0.1% formic acid/ acetonitrile with 0.1% formic acid	**25**	[64]
RPLC	HVA, 5-HIAA	d3-HVA, d5-HIAA	Kinetex C18 (50 x 2.1 mm, 2.6 µm)	Gradient	40 mM ammonium bicarbonate/acetonitrile	**6.5**	[61]
IPC	HVA, 5-HIAA, MHPG	N-methyl-serotonin	Eicom-pak MA-ODS (250 x 4.6 mm, 7 µm)	Isocratic	pH 4.0, 0.1 M potassium phosphate buffer containing 10 µM EDTA and 180 µM sodium 1-octanesulfonate/methanol (89/11, v/v)	**35**	[63]
RPLC	HVA, 5-HIAA, MHPG, 3-OMD, 5-HTP	d4-serotonin, d5-kynurenic acid	Atlantis dC18 (150 x 2.1 mm, 5 µm)	Gradient	Aqueous 0.2% formic acid/ acetonitrile with 0.2% formic acid	**20**	[62]

RPLC	HVA, 5-HIAA	N.R	Nucleosil C18 (150 x 4.6 mm, 5 µm)	Isocratic	pH 3.5 phosphate-citrate buffer/methanol (80/20, v/v)	**N.R**	[65]
IPC	HVA, 5-HIAA, MHPG, 3-OMD, 5-HTP	N.R	Nucleosil C18 (250 x 5 mm, 5 µm)	Isocratic	pH 4.0 sodium acetate-citrate buffer with 1.2 mM EDTA and 1.2 mM 1-heptanosulphonic acid/methanol (91/9)	**25**	[66, 67]

DHBA, 2,5-dihydroxybenzoic acid; EDTA, ethylenediamine-tetraacetic acid; 5-HTP, 5-hydroxytryptophane; 5-HIAA, 5-hydroxyindol acetic acid; HVA, homovanillic acid; IPC, ion pair chromatography; MHPG, 3-metoxy-4-hydroxyphenylglycol; N.R, not reported; 3-OMD, 3-*ortho*-methyl-DOPA; OSA, octanesulphonic acid; RPLC, reversed-phase liquid chromatography.

II.5.1.3. Detection modes used

Dopamine and serotonin metabolites can be detected by different detection modes: electrochemical detection (ECD), fluorescence detection (FD) and tandem mass spectrometry (MS/MS).[16, 54, 68, 75] Monoamine biomarkers are electroactive molecules that can be oxidized. The oxidation generates a current that is measured in ECD and it is proportionally correlated to the amount of analyte.[76–78] Two types of ECD are available for these molecules: coulometry and amperometry. Coulometry is the most widely used, since it is more sensitive and selective than amperometry.[16, 59] Indeed, coulometry allows to reach lower LOQ (lower limit of quantification) and it is less susceptible to interferences. ECD does not require any derivatization step. Nevertheless, attenuation of ECD signal was described because of the electrode contamination by adsorbed compounds. Thus, the electrode must be cleaned up frequently to avoid any signal loss.[75, 79] As shown in Table II.4, ECD is the most widely used detector for the quantification of dopamine and serotonin metabolites in CSF.

Monoamine biomarkers are native fluorescent molecules, but with low quantum yields, that is why most of the FD-based methods requires a derivatization step.[16, 68] Because of the low repeatability and robustness of this step, it is not compatible with CSF routine analysis. However, Akiyama *et al.* proposed a HPLC-FD method based on monoamine biomarkers native fluorescence.[54] FD of dopamine and serotonin metabolites is performed in UV light and the obtained LOQ are compatible with CSF analysis and inborn errors of metabolism diagnosis (Table II.4). FD allows to reach high specificity. Compared to ECD, FD appears more reliable and less incline to fluctuations which makes it more adapted to CSF analysis.[16, 54, 80]

The last detection mode that can be considered in monoamine biomarkers quantification is MS/MS.[62, 64] MS/MS is used in single reaction monitoring (SRM) or multiple reaction monitoring (MRM) modes. These modes are based on selecting one (SRM) or more (MRM) mass transitions. A mass transition corresponds to the fragmentation of a precursor ion into a product ion. Therefore, MS/MS is highly specific and provides

structural information. Moreover, it allows to reach high sensitivity.[16, 62] MS/MS is usually used with ESI in negative mode, given that monoamine neurotransmitter are low acidic molecules.[64] Nevertheless, ESI can also be used in positive mode especially for the ionisation of 5-HIAA, 5-HTP and 3-OMD.[62] Sensitivity highly depends on ionisation efficiency in the ESI source and it is influenced by many factors such as mobile phase composition or matrix interference. Indeed, ESI-MS/MS signal can be importantly suppressed or enhanced by matrix effect. Hence, the importance of sample treatment and of using internal standards.[81]

LOQ is a critical parameter to determine if a chromatographic method is compatible with inborn errors of metabolism diagnosis. Indeed, monoamine biomarkers' cerebrospinal concentration can be lower than 10 nM in pathological states.[18, 57] Therefore, the aforementioned method must reach LOQ of 10 nM at the highest to allow diagnosis. Table II.4 indicates that either ECD, FD or MS/MS are adapted to the quantification of monoamine biomarkers in CSF, in terms of LOQ. When considering, the injection volume, MS/MS detection appears as the most satisfactory since it uses the lowest CSF volume (15 µL) and it reaches the lowest LOQ.[62]

Table II.4: Detection conditions of dopamine and serotonin metabolites quantified in CSF

Analysed biomarkers	Detection mode	Detection conditions	LOQ (nM)	Injection volume (µL)	Ref.
HVA, 5-HIAA, MHPG, 3-OMD	FD	λ_{ex} = 270 nm, λ_{em} = 320 nm for HVA MHPG and 3-OMD λ_{ex} = 280 nm, λ_{em} = 345 nm for 5-HIAA	HVA (**16**), 5-HIAA(**4**), MHPG (**25**), 3-OMD (**16**)	20	[54]
HVA, 5-HIAA	ECD	Second analytical cell potential : + 300mV	HVA (**5**), 5-HIAA (**5**)	20	[55]
HVA, 5-HIAA, MHPG	ECD	Second analytical cell potential : + 450mV	N.R	50	[56]
HVA, 5-HIAA, MHPG, 3-OMD, 5-HTP	ECD	Second analytical cell potential : + 400mV	HVA (**15**), 5-HIAA (**10**), MHPG (**5**), 3-OMD (**5**), 5-HTP (**5**)	50	[57]
HVA, 5-HIAA, MHPG	ECD	Flow cell potential : +750 mV	HVA (**20**)*, 5-HIAA (**10**)*, MHPG (**8**)*	100	[58]

HVA, 5-HIAA	MS/MS	Negative electrospray ionisation, SRM transitions: 181 > 137 for HVA 190 > 146 for 5-HIAA	HVA (**100**), 5-HIAA (**25**)	15	[64]
HVA, 5-HIAA	MS/MS	Positive electrospray ionisation, SRM transitions: 304 > 105 for HVA 313 > 105 for 5-HIAA	HVA (**24**), 5-HIAA (**11**)	N.R	[61]
HVA, 5-HIAA, MHPG	ECD	Flow cell potential : +700 mV	N.R	15	[63]
HVA, 5-HIAA, MHPG, 3-OMD, 5-HTP	MS/MS	Negative electrospray ionisation, MRM transitions: 181 > 122 for HVA, 263 > 165 for MHPG. Positive electrospray ionisation, MRM transitions: 212 > 195 for 3-OMD 221 > 204 for 5-HTP, 192 > 146 5-HIAA	HVA (**20**), 5-HIAA (**5**), MHPG (**1**), 3-OMD (**1**), 5-HTP (**1**)	15	[62]
HVA, 5-HIAA	ECD	Flow cell potential : +700 mV for HVA and +500 mV for 5-HIAA	N.R	50-100	[65]

HVA, 5-HIAA, MHPG, 3-OMD, 5-HTP	ECD	Flow cell potential : +400 mV	HVA (**9**), 5-HIAA (**4.6**), MHPG (**3**), 3-OMD (**2.4**), 5-HTP (**1.3**)	30	[66, 67]

*The reported values correspond to limits of detection.

ECD, electrochemical detection; FD, fluorescence detection; 5-HTP, 5-hydroxytryptophane; 5-HIAA, 5-hydroxyindol acetic acid; HVA, homovanillic acid; LOQ, lower limit of quantification; MHPG, 3-metoxy-4-hydroxyphenylglycol; MRM, multiple reaction monitoring; MS/MS, tandem mass spectrometry; N.R, not reported; 3-OMD, 3-*ortho*-methyl-DOPA; SRM, single reaction monitoring.

II.5.2. Quantification of pterins

Pterins, namely BH4, BH2, B, NH2 and N are enzymatic cofactors used as CSF biomarkers in the diagnosis of inborn errors of dopamine and serotonin metabolism.[16, 18]

II.5.1.1. CSF sample preparation

In order to quantify pterins in CSF samples, a sample preparation step is necessary. As with monoamine biomarkers, the purpose of CSF sample treatment is to avoid any interference. It aims at stabilizing pterins as well. Indeed, reduced pterins, especially BH4 are incline to autoxidation.[82–85] The latter may generate BH2 and B formation and by this way, leads to artificial fluctuations in the concentrations of BH4, BH2 and B, and possibly to misdiagnosis.[85–87] To limit BH4 autoxidation in CSF samples, antioxidant are added during sample preparation (Table II.5).

Table II.5 indicates that CSF sample preparation in the quantification of pterins consists mainly of adding antioxidant and in protein elimination. Antioxidants used corresponds to ascorbic acid, dithiothreitol (DTT) and/or diethylenetriaminepentaacetic acid (DETAPAC).[62, 88–91] Some proposed methods did not use any antioxidant, but authors demonstrated BH4 concentration does not significantly decrease in the storage conditions used.[57, 92]

Table II.5: CSF sample pre-treatment for the quantification of pterins

Analysed biomarkers	CSF volume	Sample treatment	Dilution solvent	Ref.
BH4, BH2, B, NH2, N	50 µL	Dilution, ultrafiltration removing any molecule whose weight exceeds 5 kDa	250 nM 2,5-dihydroxybenzoic acid solution in a mixture of pH 7.4 ; 0.05 M sodium citrate/methanol (97/3, v/v)	[57]
N, B	500 µL	Dilution, centrifugation, filtration on 0.22 µm filter	pH 4.0 sodium acetate-citrate buffer with 1.2 mM EDTA and 1.2 mM 1-heptanosulphonic acid/methanol (91/9)	[66, 67]
BH4, BH2, N	30 µL	Dilution	Aqueous solution of internal standards and 0.2% DTT	[88]
BH2, B, N	30 µL	Dilution, protein precipitation, centrifugation, evaporation to dryness, sample reconstitution	Water/Acetonitrile/Formic acid/ascorbic acid (96.9/3/0.2/0.02)	[62]
BH4, BH2, B, N	1 mL	Addition of antioxidants	Addition of 1 mg DTT and 1 mg DETAPAC	[89]

BH4, BH2, B, NH2, N	100 µL	Dilution, ultrafiltration removing any molecule whose weight exceeds 5 kDa	pH 7.4 ; 0.05 M sodium citrate/methanol (97/3, v/v)	[92]
B, N	250 µL	Dilution	Aqueous solution of 0.1 M HCl, 0.2% I_2/0.4%KI, 1% ascorbic acid	[90]

B, biopterin; BH2, 7,8-dihydrobiopterin; BH4, tetrahydrobiopterin; DETAPAC, diehtylenetriaminepantaacetic acid; DTT, dithiothreitol; EDTA, ethylenediamine-tetraacetic acid; N, neopterin; NH2, dihydroneopterin.

II.5.1.2. Chromatographic conditions

Pterins are low hydrophobic basic molecules that can be separated in classical RPLC using a C18-based stationary phase.[93–96] Given the structural proximity of these biomarkers, some proposed methods are based on IPC to achieve an efficient separation.[66, 67] As for monoamine biomarkers, polar-embedded C18 stationary phases are commonly used since they allow to set up hydrogen bonds in addition to hydrophobic effect, to achieve the separation of pterins (Table II.6).[57, 62, 92, 95]

Moreover, the retention of pterins highly depends on the mobile phase pH that is why buffer are used to set the pH and to improve retention factors repeatability. Table II.6 indicates isocratic mode is more often used for pterins analysis in CSF than gradient elution. This is explained by the fact that it is simpler, faster and more easily applicable to routine analysis than gradient elution.

Another pterin that could have a great importance in diagnosing inborn errors of dopamine and serotonin is q-BH2, since it is involved in pterins metabolism (Figure II.3).[97, 98] However, q-BH2 is a highly unstable molecule that can hardly be separated from BH4.[85, 87]

Table II.6: Separation conditions for the quantification of pterins in CSF samples

Chromato-graphic mode	Analysed bi-omarkers	Internal standard	Column	Elution mode	Mobile phase	**Analysis time (minutes)**	Ref.
RPLC	BH4, BH2, B, NH2, N	DHBA	C18 HSS T3 (100 x 2.1 mm, 1.8 µm)	Isocratic	pH 5.2, 0.05 M sodium citrate buffer/methanol (97/3, v/v)	**10**	[57]
IPC	N, B	N.R	Nucleosil C18 (250 x 5 mm, 5 µm)	Isocratic	pH 4.0 sodium acetate-citrate buffer with 1.2 mM EDTA and 1.2 mM 1-heptanosulphonic acid/methanol (91/9)	**25**	[66, 67]
RPLC	BH4, BH2, N	^{15}N-BH2 ^{15}N-neopterin	EZfaast AAA-MS (250 x 2 mm, 4 µm)	Gradient	Water containing 0.1% formic acid and 0.1% heptafluorobutyric acid/methanol	**10**	[88]

RPLC	BH2, B, N	d4-dopa-mine, d4-ty-rosine	Atlantis dC18 (150 x 2.1 mm, 5 µm)	Gradient	Aqueous 0.2% formic acid/ ace-tonitrile with 0.2% formic acid	**20**	[62]
RPLC	BH4, BH2, B, N	N.R	Apex C18 (250 x 4.6 mm, 5 µm)	Isocratic	pH 5.2 sodium acetate-citrate buffer with 20 mg/L EDTA	**24**	[89]
RPLC	BH4, BH2, B, NH2, N	Lumazine	Atlantis dC18 (150 x 4.6 mm, 3 µm)	Isocratic	pH 7.4, 0.05 M sodium citrate buffer/methanol (97/3, v/v)	**16**	[92]
RPLC	B, N	N.R	UltraPure Torsic acid	Isocratic	pH 3.5 ammonium phosphate	**14**	[90]

B, biopterin; BH2, 7,8-dihydrobiopterin; BH4, tetrahydrobiopterin; DHBA, 2,5-dihydroxybenzoic acid; IPC, ion pair chromatography; EDTA, eth-ylenediamine-tetraacetic acid; N, neopterin; NH2, dihydroneopterin; N.R, not reported, RPLC, reversed-phase liquid chromatography.

II.5.1.3. Detection modes used

Pterins can be detected by various detection modes. For CSF analysis, proposed methods are based on FD, ECD coupled with FD or on MS/MS (Table II.7).[16, 18, 19, 99] Indeed, only oxidized pterins, namely B and N, are fluorescent and emit at 450 nm when excited at 350 nm.[100–103] In order, to quantify reduced pterins by FD, authors propose a post-column oxidation, whether electrochemical by using ECD or chemical oxidation with an oxidant.[57, 89, 92] MS/MS is proposed for pterin quantification in SRM or MRM modes.[95, 104–106] MS/MS does not require any post-column oxidation improving by this way repeatability. SRM or MRM modes also allows to improve method specificity and sensitivity.[62, 88]

Pterins' concentration in CSF can reach less than 5 nM in pathological states, that is why, LOQ is determinant to consider a method adapted to inborn errors of dopamine and serotonin metabolism.[18, 57] In fact, LOQ must not be higher than 5 nM. Table II.7 shows all proposed methods are compatible with pterins quantification in CSF, in terms of LOQ.

Table II.7: Detection conditions of pterins quantified in CSF

Analysed biomarkers	Detection mode	Detection conditions	LOQ (nM)	Injection volume (µL)	Ref.
BH4, BH2, B, NH2, N	ECD-FD	Post-column electrochemical oxidation and FD Flow cell potential: +400 mV λ_{ex} = 350 nm, λ_{em} = 450 nm	BH4 **(4.2)**, BH2 **(3.2)**, B **(1.6)**, NH2 **(3.2)**, N **(2.4)**	50	[57]
B, N	FD	λ_{ex} = 350 nm, λ_{em} = 450 nm	B **(0.8)**, N **(0.6)**	20	[66, 67]
BH4, BH2, N	MS/MS	Positive electrospray ionisation, SRM transitions: 242 > 166 for BH4, 240 > 165 for BH2, 254 > 206 for N	BH4 **(3.0)**, BH2 **(3.0)**, N **(3.0)**	10	[88]
BH2, B, N	MS/MS	Positive electrospray ionisation, MRM transitions: 240 > 196 for BH2, 238 > 178 for B, 254 > 236 for N	BH2 **(1.0)**, B **(1.0)**, N **(0.5)**	15	[62]

BH4, BH2, B, N	FD	Post-column oxidation and FD λ_{ex} = 348 nm, λ_{em} = 444 nm	BH4 **(0.7)***, BH2 **(0.7)***, B **(0.7)***, N **(0.5)***	100	[89]
BH4, BH2, B, NH2, N	ECD-FD	Post-column oxidation and FD Flow cell potential: +400 mV λ_{ex} = 350 nm, λ_{em} = 450 nm	BH4 **(5.0)**, BH2 **(5.0)**, B **(3.6)**, NH2 **(4.5)**, N **(2.7)**	100	[92]
B, N	FD	λ_{ex} = 350 nm, λ_{em} = 450 nm	B **(0.65)**, N **(0.21)**	250	[90]

*The reported values correspond to limits of detection.

B, biopterin; BH2, 7,8-dihydrobiopterin; BH4, tetrahydrobiopterin; ECD, electrochemical detection; FD, fluorescence detection; LOQ, lower limit of quantification; MS/MS, tandem mass spectrometry; N, neopterin; NH2, dihydroneopterin.

II.6. CONCLUSIONS AND PERSPECTIVES

A wide range of methods are developed for measuring either monoamine neurotransmitter metabolites or pterins in CSF. In this article, we reviewed the various features of these methods, namely, sample treatment, chromatographic conditions and detection modes. Therefore, it allows to choose analytical conditions for upcoming method development.

The current trend is to simultaneously quantify these two sets of biomarkers.[57, 62, 66] This allows a higher applicability in routine and a faster diagnosis of inborn errors of monoamine neurotransmitter metabolism. However, it is highly challenging since both groups of molecules does not have the same physicochemical properties. Moreover, the proposed methods are increasingly based on MS/MS detection, the latter reaching higher sensitivity and specificity than other detection modes.[16, 62]

CSF remains the gold standard biological fluid for the diagnosis of inborn errors of monoamine neurotransmitter metabolism. However, CSF collection relies on an invasive procedure, that is why biomarkers are quantified in simpler to collect biological fluids such as urine, plasma and blood, even though diagnosis specificity is reduced.[3, 16]

From an analytical point of view, rapid and comprehensive analytical methods measuring simultaneously at least 20 molecules are more and more proposed, thus allowing a fast and reliable diagnosis. In perspective, diagnosis of inborn errors of metabolism is expected to be improved by new biomarkers validation, thanks to both targeted and untargeted metabolomics studies whether in CSF or in other biological fluids. This may also allow to identify other metabolic diseases and to treat them efficiently.

II.7. REFERENCES

[1] Nestler, E. J.; Hyman, S. E.; Holtzman, D. M.; Malenka, R. C. Synaptic Transmission. In *Molecular Neuropharmacology: A Foundation for Clinical Neuroscience*; McGraw-Hill Education: New York, NY, **2015**.

[2] Burton, B. K. Inborn Errors of Metabolism in Infancy: A Guide to Diagnosis. *PEDIATRICS*, **1998**, *102* (6), e69–e69. https://doi.org/10.1542/peds.102.6.e69.

[3] Brennenstuhl, H.; Jung-Klawitter, S.; Assmann, B.; Opladen, T. Inherited Disorders of Neurotransmitters: Classification and Practical Approaches for Diagnosis and Treatment. *Neuropediatrics*, **2019**, *50* (01), 002–014. https://doi.org/10.1055/s-0038-1673630.

[4] Kurian, M. A.; Gissen, P.; Smith, M.; Heales, S. J.; Clayton, P. T. The Monoamine Neurotransmitter Disorders: An Expanding Range of Neurological Syndromes. *Lancet Neurol.*, **2011**, *10* (8), 721–733. https://doi.org/10.1016/S1474-4422(11)70141-7.

[5] Ng, J.; Zhen, J.; Meyer, E.; Erreger, K.; Li, Y.; Kakar, N.; Ahmad, J.; Thiele, H.; Kubisch, C.; Rider, N. L.; et al. Dopamine Transporter Deficiency Syndrome: Phenotypic Spectrum from Infancy to Adulthood. *Brain*, **2014**, *137* (4), 1107–1119. https://doi.org/10.1093/brain/awu022.

[6] Murphy, D. L.; Andrews, A. M.; Wichems, C. H.; Li, Q.; Tohda, M.; Greenberg, B. Brain Serotonin Neurotransmission: An Overview and Update with an Emphasis on Serotonin Subsystem Heterogeneity, Multiple Receptors, Interactions with Other Neurotransmitter Systems, and Consequent Implications for Understanding the Actions of Serotonergic Drugs. *J. Clin. Psychiatry*, **1998**, *59* (Suppl 15), 4–12.

[7] Kurian, M. A.; Li, Y.; Zhen, J.; Meyer, E.; Hai, N.; Christen, H.-J.; Hoffmann, G. F.; Jardine, P.; Moers, A. von; Mordekar, S. R.; et al. Clinical and Molecular Characterisation of Hereditary Dopamine Transporter Deficiency Syndrome: An Observational Cohort and Experimental Study. *Lancet Neurol.*, **2011**, *10* (1), 54–62. https://doi.org/10.1016/S1474-4422(10)70269-6.

[8] Beaulieu, J.-M.; Gainetdinov, R. R. The Physiology, Signaling, and Pharmacology of Dopamine Receptors. *Pharmacol. Rev.*, **2011**, *63* (1), 182–217. https://doi.org/10.1124/pr.110.002642.

[9] Vallone, D.; Picetti, R.; Borrelli, E. Structure and Function of Dopamine Receptors. *Neurosci. Biobehav. Rev.*, **2000**, 8.

[10] Opladen, T.; Hoffmann, G.; Hörster, F.; Hinz, A.-B.; Neidhardt, K.; Klein, C.; Wolf, N. Clinical and Biochemical Characterization of Patients with Early Infantile Onset of Autosomal Recessive GTP Cyclohydrolase I Deficiency without Hyperphenylalaninemia. *Mov. Disord.*, **2011**, *26* (1), 157–161. https://doi.org/10.1002/mds.23329.

[11] Bonafé, L.; Thöny, B.; Penzien, J. M.; Czarnecki, B.; Blau, N. Mutations in the Sepiapterin Reductase Gene Cause a Novel Tetrahydrobiopterin-Dependent Monoamine-Neurotransmitter Deficiency without Hyperphenylalaninemia. *Am. J. Hum. Genet.*, **2001**, *69* (2), 269–277. https://doi.org/10.1086/321970.

[12] Leuzzi, V.; Carducci, C.; Carducci, C.; Pozzessere, S.; Burlina, A.; Cerone, R.; Concolino, D.; Donati, M. A.; Fiori, L.; Meli, C.; et al. Phenotypic Variability, Neurological Outcome and Genetics Background of 6-Pyruvoyl-Tetrahydropterin Synthase Deficiency. *Clin. Genet.*, **2010**, *77* (3), 249–257. https://doi.org/10.1111/j.1399-0004.2009.01306.x.

[13] Manegold, C.; Hoffmann, G. F.; Degen, I.; Ikonomidou, H.; Knust, A.; Laaß, M. W.; Pritsch, M.; Wilichowski, E.; Hörster, F. Aromatic L-Amino Acid Decarboxylase Deficiency: Clinical Features, Drug Therapy and Follow-Up. *J. Inherit. Metab. Dis.*, **2009**, *32* (3), 371–380. https://doi.org/10.1007/s10545-009-1076-1.

[14] Willemsen, M. A.; Verbeek, M. M.; Kamsteeg, E.-J.; de Rijk-van Andel, J. F.; Aeby, A.; Blau, N.; Burlina, A.; Donati, M. A.; Geurtz, B.; Grattan-Smith, P. J.; et al. Tyrosine Hydroxylase Deficiency: A Treatable Disorder of Brain Catecholamine Biosynthesis. *Brain*, **2010**, *133* (6), 1810–1822. https://doi.org/10.1093/brain/awq087.

[15] Saudubray, J.-M.; Garcia-Cazorla, À. Inborn Errors of Metabolism Overview: Pathophysiology, Manifestations, Evaluation, and Management. *Inborn Errors Metab.*, **2018**, *65* (2), 179–208. https://doi.org/10.1016/j.pcl.2017.11.002.

[16] Jung-Klawitter, S.; Kuseyri Hübschmann, O. Analysis of Catecholamines and Pterins in Inborn Errors of Monoamine Neurotransmitter Metabolism—From Past to Future. *Cells*, **2019**, *8* (8), 867. https://doi.org/10.3390/cells8080867.

[17] Wester, P.; Bergström, U.; Eriksson, A.; Gezelius, C.; Hardy, J.; Winblad, B. Ventricular Cerebrospinal Fluid Monoamine Transmitter and Metabolite Concentrations Reflect Human Brain Neurochemistry in Autopsy Cases. *J. Neurochem.*, **1990**, *54* (4), 1148–1156. https://doi.org/10.1111/j.1471-4159.1990.tb01942.x.

[18] Hyland, K.; Surtees, R. A. H.; Heales, S. J. R.; Bowron, A.; Howells, D. W.; Smith, I. Cerebrospinal Fluid Concentrations of Pterins and Metabolites of Serotonin and Dopamine in a Pediatric Reference Population. *Pediatr. Res.*, **1993**, *34* (1), 10–14. https://doi.org/10.1203/00006450-199307000-00003.

[19] Bicker, J.; Fortuna, A.; Alves, G.; Falcão, A. Liquid Chromatographic Methods for the Quantification of Catecholamines and Their Metabolites in Several Biological Samples—A Review. *Anal. Chim. Acta*, **2013**, *768*, 12–34. https://doi.org/10.1016/j.aca.2012.12.030.

[20] Vlčková, M.; Schwarz, M. A. Determination of Cationic Neurotransmitters and Metabolites in Brain Homogenates by Microchip Electrophoresis and Carbon Nanotube-Modified Amperometry. *J. Chromatogr. A*, **2007**, *1142* (2), 214–221. https://doi.org/10.1016/j.chroma.2006.12.040.

[21] Bergquist, J.; Ściubisz, A.; Kaczor, A.; Silberring, J. Catecholamines and Methods for Their Identification and Quantitation in Biological Tissues and Fluids. *J. Neurosci. Methods*, **2002**, *113* (1), 1–13. https://doi.org/10.1016/S0165-0270(01)00502-7.

[22] Meiser, J.; Weindl, D.; Hiller, K. Complexity of Dopamine Metabolism. *Cell Commun. Signal.*, **2013**, *11* (1), 34. https://doi.org/10.1186/1478-811X-11-34.

[23] Daubner, S. C.; Le, T.; Wang, S. Tyrosine Hydroxylase and Regulation of Dopamine Synthesis. *Arch. Biochem. Biophys.*, **2011**, *508* (1), 1–12. https://doi.org/10.1016/j.abb.2010.12.017.

[24] Kobe, B.; Jennings, I. G.; House, C. M.; Michell, B. J.; Goodwill, K. E.; Santarsiero, B. D.; Stevens, R. C.; Cotton, R. G. H.; Kemp, B. E. Structural Basis of Autoregulation of Phenylalanine Hydroxylase. *Nat. Struct. Biol.*, **1999**, *6* (5), 442–448. https://doi.org/10.1038/8247.

[25] Senard, J.-M.; Rouet, P. Dopamine Beta-Hydroxylase Deficiency. *Orphanet J. Rare Dis.*, **2006**, *1* (1), 7. https://doi.org/10.1186/1750-1172-1-7.

[26] Graves, S. M.; Xie, Z.; Stout, K. A.; Zampese, E.; Burbulla, L. F.; Shih, J. C.; Kondapalli, J.; Patriarchi, T.; Tian, L.; Brichta, L.; et al. Dopamine Metabolism by a Monoamine Oxidase Mitochondrial Shuttle Activates the Electron Transport Chain. *Nat. Neurosci.*, **2020**, *23* (1), 15–20. https://doi.org/10.1038/s41593-019-0556-3.

[27] Molero-Luis, M.; Serrano, M.; Ormazábal, A.; Pérez-Dueñas, B.; García-Cazorla, À.; Pons, R.; Artuch, R. Homovanillic Acid in Cerebrospinal Fluid of 1388 Children with Neurological Disorders. *Dev. Med. Child Neurol.*, **2013**, *55* (6), 559–566. https://doi.org/10.1111/dmcn.12116.

[28] Antkiewicz-Michaluk, L.; Ossowska, K.; Romańska, I.; Michaluk, J.; Vetulani, J. 3-Methoxytyramine, an Extraneuronal Dopamine Metabolite Plays a Physiological Role in the Brain as an Inhibitory Regulator of Catecholaminergic Activity. *Eur. J. Pharmacol.*, **2008**, *599* (1), 32–35. https://doi.org/10.1016/j.ejphar.2008.09.033.

[29] Stanley, M.; Traskman-Bendz, L.; Dorovini-Zis, K. Correlations between Aminergic Metabolites Simultaneously Obtained from Human CSF and Brain. *Life Sci.*, **1985**, *37* (14), 1279–1286. https://doi.org/10.1016/0024-3205(85)90242-5.

[30] Marín-Valencia, I.; Serrano, M.; Ormazabal, A.; Pérez-Dueñas, B.; García-Cazorla, A.; Campistol, J.; Artuch, R. Biochemical Diagnosis of Dopaminergic Disturbances in

Paediatric Patients: Analysis of Cerebrospinal Fluid Homovanillic Acid and Other Biogenic Amines. *Clin. Biochem.*, **2008**, *41* (16), 1306–1315. https://doi.org/10.1016/j.clinbiochem.2008.08.077.

[31] Jonnakuty, C.; Gragnoli, C. What Do We Know about Serotonin? *J. Cell. Physiol.*, **2008**, *217* (2), 301–306. https://doi.org/10.1002/jcp.21533.

[32] Zhang, X.; Beaulieu, J.-M.; Sotnikova, T. D.; Gainetdinov, R. R.; Caron, M. G. Tryptophan Hydroxylase-2 Controls Brain Serotonin Synthesis. *Science*, **2004**, *305* (5681), 217. https://doi.org/10.1126/science.1097540.

[33] Werner, E. R.; Blau, N.; Thöny, B. Tetrahydrobiopterin: Biochemistry and Pathophysiology. *Biochem. J.*, **2011**, *438* (3), 397–414. https://doi.org/10.1042/BJ20110293.

[34] Thöny, B.; Auerbach, G.; Blau, N. Tetrahydrobiopterin Biosynthesis, Regeneration and Functions. *Biochem. J.*, **2000**, *347* (1), 1–16. https://doi.org/10.1042/bj3470001.

[35] Nichol, C. A.; Smith, G. K.; Duch, D. S. BIOSYNTHESIS AND METABOLISM OF TETRAHYDROBIOPTERIN AND MOLYBDOPTERIN. *Annu. Rev. Biochem.*, **1985**, *54* (1), 729–764. https://doi.org/10.1146/annurev.bi.54.070185.003501.

[36] Kaufman, S. New Tetrahydrobiopterin-Dependent Systems. *Annu. Rev. Nutr.*, **1993**, *13* (1), 261–286. https://doi.org/10.1146/annurev.nu.13.070193.001401.

[37] Pons, R.; Syrengelas, D.; Youroukos, S.; Orfanou, I.; Dinopoulos, A.; Cormand, B.; Ormazabal, A.; Garzía-Cazorla, A.; Serrano, M.; Artuch, R. Levodopa-Induced Dyskinesias in Tyrosine Hydroxylase Deficiency. *Mov. Disord.*, **2013**, *28* (8), 1058–1063. https://doi.org/10.1002/mds.25382.

[38] Willemsen, M. A.; Verbeek, M. M.; Kamsteeg, E.-J.; de Rijk-van Andel, J. F.; Aeby, A.; Blau, N.; Burlina, A.; Donati, M. A.; Geurtz, B.; Grattan-Smith, P. J.; et al. Tyrosine Hydroxylase Deficiency: A Treatable Disorder of Brain Catecholamine Biosynthesis. *Brain*, **2010**, *133* (6), 1810–1822. https://doi.org/10.1093/brain/awq087.

[39] Swoboda, K. J.; Hyland, K.; Goldstein, D. S.; Kuban, K. C. K.; Arnold, L. A.; Holmes, C. S.; Levy, H. L. Clinical and Therapeutic Observations in Aromatic Amino Acid Decarboxylase Deficiency. *Neurology*, **1999**, *53* (6), 1205. https://doi.org/10.1212/WNL.53.6.1205.

[40] Brun, L.; Ngu, L. H.; Keng, W. T.; Ch'ng, G. S.; Choy, Y. S.; Hwu, W. L.; Lee, W. T.; Willemsen, M. A. A. P.; Verbeek, M. M.; Wassenberg, T.; et al. Clinical and Biochemical Features of Aromatic L-Amino Acid Decarboxylase Deficiency. *Neurology*, **2010**, *75* (1), 64. https://doi.org/10.1212/WNL.0b013e3181e620ae.

[41] Yildiz, Y.; Pektas, E.; Tokatli, A.; Haliloglu, G. Hereditary Dopamine Transporter Deficiency Syndrome: Challenges in Diagnosis and Treatment. *Neuropediatrics*, **2017**, *48* (1), 49–52. https://doi.org/10.1055/s-0036-1593372.

[42] Rilstone, J. J.; Alkhater, R. A.; Minassian, B. A. Brain Dopamine–Serotonin Vesicular Transport Disease and Its Treatment. *N. Engl. J. Med.*, **2013**, *368* (6), 543–550. https://doi.org/10.1056/NEJMoa1207281.

[43] Dekker, S.; Kampinga, H.; Bergink, S. DNAJs: More than Substrate Delivery to HSPA. *Front. Mol. Biosci.*, **2015**, *2*, 35. https://doi.org/10.3389/fmolb.2015.00035.

[44] Sarparanta, J.; Jonson, P. H.; Golzio, C.; Sandell, S.; Luque, H.; Screen, M.; McDonald, K.; Stajich, J. M.; Mahjneh, I.; Vihola, A.; et al. Mutations Affecting the Cytoplasmic Functions of the Co-Chaperone DNAJB6 Cause Limb-Girdle Muscular Dystrophy. *Nat. Genet.*, **2012**, *44* (4), 450–455. https://doi.org/10.1038/ng.1103.

[45] Hoffmann, F. G.; Blau, N. *Congenital Neurotransmitter Disorders: A Clinical Approach*; Nova Publishers. Inc.: Huppauge, NY, 2014.

[46] Hollak, C. E. M.; Lachmann, R. *Inherited Metabolic Disease in Adults: A Clinical Guide*; Oxford University Press, **2016**.

[47] Hyland, K. The Lumbar Puncture for Diagnosis of Pediatric Neurotransmitter Diseases. *Ann. Neurol.*, **2003**, *54* (S6), S13–S17. https://doi.org/10.1002/ana.10627.

[48] Burlina, A. B.; Celato, A.; Polo, G.; Edini, C.; Burlina, A. P. The Utility of CSF for the Diagnosis of Primary and Secondary Monoamine Neurotransmitter Deficiencies. *EJI-FCC*, **2017**, *28* (1), 64–76.

[49] Peaston, R. T.; Weinkove, C. Measurement of Catecholamines and Their Metabolites. *Ann. Clin. Biochem.*, **2004**, *41* (Pt 1), 17–38. https://doi.org/10.1258/000456304322664663.

[50] Brinker, T.; Stopa, E.; Morrison, J.; Klinge, P. A New Look at Cerebrospinal Fluid Circulation. *Fluids Barriers CNS*, **2014**, *11* (1), 10. https://doi.org/10.1186/2045-8118-11-10.

[51] Bonadio, W. A.; Stanco, L.; Bruce, R.; Barry, D.; Smith, D. Reference Values of Normal Cerebrospinal Fluid Composition in Infants Ages 0 to 8 Weeks. *Pediatr. Infect. Dis. J.*, **1992**, *11* (7).

[52] Hladky, S. B.; Barrand, M. A. Mechanisms of Fluid Movement into, through and out of the Brain: Evaluation of the Evidence. *Fluids Barriers CNS*, **2014**, *11* (1), 26. https://doi.org/10.1186/2045-8118-11-26.

[53] Spector, R.; Robert Snodgrass, S.; Johanson, C. E. A Balanced View of the Cerebrospinal Fluid Composition and Functions: Focus on Adult Humans. *Exp. Neurol.*, **2015**, *273*, 57–68. https://doi.org/10.1016/j.expneurol.2015.07.027.

[54] Akiyama, T.; Hayashi, Y.; Hanaoka, Y.; Shibata, T.; Akiyama, M.; Nakamura, K.; Tsuyusaki, Y.; Kubota, M.; Yoshinaga, H.; Kobayashi, K. Simultaneous Measurement of Monoamine Metabolites and 5-Methyltetrahydrofolate in the Cerebrospinal Fluid of Children. *Clin. Chim. Acta*, **2017**, *465*, 5–10. https://doi.org/10.1016/j.cca.2016.12.005.

[55] Hubbard, K. E.; Wells, A.; Owens, T. S.; Tagen, M.; Fraga, C. H.; Stewart, C. F. Determination of Dopamine, Serotonin, and Their Metabolites in Pediatric Cerebrospinal Fluid by Isocratic High Performance Liquid Chromatography Coupled with Electrochemical Detection. *Biomed. Chromatogr.*, **2010**, *24* (6), 626–631. https://doi.org/10.1002/bmc.1338.

[56] Hyland, K.; Smith, I.; Howells, D. W.; Clayton, P. T.; Leonard, J. V. *The Determination of Pterins, Biogenic Amine Metabolites, and Aromatic Amino Acids in Cerebrospinal Fluid using Isocratic Reverse Phase Liquid Chromatography with in Series Dual Cell Coulometric Electrochemical and Fluorescence Detection:- Use in the Study Of Inborn Errors of Dihydropteridine Reductase and 5,Lo-Methylenetetrahydrofolate Reductase*; De Gruyter, 2019; pp 85–100.

[57] Lo, A.; Guibal, P.; Doummar, D.; Rodriguez, D.; Hautem, J.-Y.; Couderc, R.; Billette De Villemeur, T.; Roze, E.; Chaminade, P.; Moussa, F. Single-Step Rapid Diagnosis of Dopamine and Serotonin Metabolism Disorders. *ACS Omega*, **2017**, *2* (9), 5962–5972. https://doi.org/10.1021/acsomega.7b01008.

[58] Scheinin, M.; Chang, W.-H.; Kirk, K. L.; Linnoila, M. Simultaneous Determination of 3-Methoxy-4-Hydroxyphenylglycol, 5-Hydroxyindoleacetic Acid, and Homovanillic Acid in Cerebrospinal Fluid with High-Performance Liquid Chromatography Using Electrochemical Detection. *Anal. Biochem.*, **1983**, *131* (1), 246–253. https://doi.org/10.1016/0003-2697(83)90162-8.

[59] Sabbioni, C.; Saracino, M. A.; Mandrioli, R.; Pinzauti, S.; Furlanetto, S.; Gerra, G.; Raggi, M. A. Simultaneous Liquid Chromatographic Analysis of Catecholamines and 4-Hydroxy-3-Methoxyphenylethylene Glycol in Human Plasma: Comparison of Amperometric and Coulometric Detection. *27th Int. Symp. High-Perform. Liq.-Phase Sep. Relat. Tech. Part III*, **2004**, *1032* (1), 65–71. https://doi.org/10.1016/j.chroma.2004.01.008.

[60] Sakaguchi, Y.; Yoshida, H.; Hayama, T.; Itoyama, M.; Todoroki, K.; Yamaguchi, M.; Nohta, H. Selective Liquid-Chromatographic Determination of Native Fluorescent Biogenic Amines in Human Urine Based on Fluorous Derivatization. *J. Chromatogr. A*, **2011**, *1218* (33), 5581–5586. https://doi.org/10.1016/j.chroma.2011.05.076.

[61] Cox, J. M.; Butler, J. P.; Lutzke, B. S.; Jones, B. A.; Buckholz, J. E.; Biondolillo, R.; Talbot, J. A.; Chernet, E.; Svensson, K. A.; Ackermann, B. L. A Validated LC–MS/MS Method for Neurotransmitter Metabolite Analysis in Human Cerebrospinal Fluid Using Benzoyl Chloride Derivatization. *Bioanalysis*, **2015**, *7* (19), 2461–2475. https://doi.org/10.4155/bio.15.170.

[62] Galla, Z.; Rajda, C.; Rácz, G.; Grecsó, N.; Baráth, Á.; Vécsei, L.; Bereczki, C.; Monostori, P. Simultaneous Determination of 30 Neurologically and Metabolically Important

Molecules: A Sensitive and Selective Way to Measure Tyrosine and Tryptophan Pathway Metabolites and Other Biomarkers in Human Serum and Cerebrospinal Fluid. *J. Chromatogr. A*, **2021**, *1635*, 461775. https://doi.org/10.1016/j.chroma.2020.461775.

[63] Koyama, E.; Minegishi, A.; Ishizaki, T. Simultaneous Determination of Four Monoamine Metabolites and Serotonin in Cerebrospinal Fluid by “High-Performance” Liquid Chromatography with Electrochemical Detection; Application for Patients with Alzheimer’s Disease. *Clin. Chem.*, **1988**, *34* (4), 680–684. https://doi.org/10.1093/clinchem/34.4.680.

[64] Suominen, T.; Uutela, P.; Ketola, R. A.; Bergquist, J.; Hillered, L.; Finel, M.; Zhang, H.; Laakso, A.; Kostiainen, R. Determination of Serotonin and Dopamine Metabolites in Human Brain Microdialysis and Cerebrospinal Fluid Samples by UPLC-MS/MS: Discovery of Intact Glucuronide and Sulfate Conjugates. *PLoS ONE*, **2013**, *8* (6), e68007. https://doi.org/10.1371/journal.pone.0068007.

[65] Westerink, B. H. C. Correlation between High-Performance Liquid Chromatography and Automated Fluorimetric Methods for the Determination of Dopamine, 3, 4-Dihydroxyphenylacetic Acid, Homovanillic Acid and 5-Hydroxyindoleacetic Acid in Nervous Tissue and Cerebrospinal Fluid. *J. Chromatogr. B. Biomed. Sci. App.*, **1982**, *233* (1), 69–77. https://doi.org/10.1016/S0378-4347(00)81732-6.

[66] Ormazabal, A.; García-Cazorla, A.; Fernández, Y.; Fernández-Álvarez, E.; Campistol, J.; Artuch, R. HPLC with Electrochemical and Fluorescence Detection Procedures for the Diagnosis of Inborn Errors of Biogenic Amines and Pterins. *J. Neurosci. Methods*, **2005**, *142* (1), 153–158. https://doi.org/10.1016/j.jneumeth.2004.08.007.

[67] Batllori, M.; Molero-Luis, M.; Ormazabal, A.; Casado, M.; Sierra, C.; García-Cazorla, A.; Kurian, M.; Pope, S.; Heales, S. J.; Artuch, R. Analysis of Human Cerebrospinal Fluid Monoamines and Their Cofactors by HPLC. *Nat. Protoc.*, **2017**, *12* (11), 2359–2366. https://doi.org/10.1038/nprot.2017.103.

[68] Tsunoda, M. Recent Advances in Methods for the Analysis of Catecholamines and Their Metabolites. *Anal. Bioanal. Chem.*, **2006**, *386* (3), 506–514. https://doi.org/10.1007/s00216-006-0675-z.

[69] Bergquist, J.; Ściubisz, A.; Kaczor, A.; Silberring, J. Catecholamines and Methods for Their Identification and Quantitation in Biological Tissues and Fluids. *J. Neurosci. Methods*, **2002**, *113* (1), 1–13. https://doi.org/10.1016/S0165-0270(01)00502-7.

[70] Gabler, J.; Miller, A.; Wang, S. A Simple Liquid Chromatography-Tandem Mass Spectrometry Method for Measuring Metanephrine and Normetanephrine in Urine: *Clin. Chem. Lab. Med.*, **2011**, *49* (7), 1213–1216. https://doi.org/10.1515/CCLM.2011.195.

[71] He, X.; Gabler, J.; Yuan, C.; Wang, S.; Shi, Y.; Kozak, M. Quantitative Measurement of Plasma Free Metanephrines by Ion-Pairing Solid Phase Extraction and Liquid Chromatography–Tandem Mass Spectrometry with Porous Graphitic Carbon Column. *J. Chromatogr. B*, **2011**, *879* (23), 2355–2359. https://doi.org/10.1016/j.jchromb.2011.06.013.

[72] Törnkvist, A.; Sjöberg, P. J. R.; Markides, K. E.; Bergquist, J. Analysis of Catecholamines and Related Substances Using Porous Graphitic Carbon as Separation Media in Liquid Chromatography–Tandem Mass Spectrometry. *J. Chromatogr. B*, **2004**, *801* (2), 323–329. https://doi.org/10.1016/j.jchromb.2003.11.036.

[73] Peaston, R. T.; Graham, K. S.; Chambers, E.; van der Molen, J. C.; Ball, S. Performance of Plasma Free Metanephrines Measured by Liquid Chromatography–Tandem Mass Spectrometry in the Diagnosis of Pheochromocytoma. *Clin. Chim. Acta*, **2010**, *411* (7), 546–552. https://doi.org/10.1016/j.cca.2010.01.012.

[74] Kumar, A.; Hart, J. P.; McCalley, D. V. Determination of Catecholamines in Urine Using Hydrophilic Interaction Chromatography with Electrochemical Detection. *J. Chromatogr. A*, **2011**, *1218* (25), 3854–3861. https://doi.org/10.1016/j.chroma.2011.04.034.

[75] Gu, Q.; Shi, X.; Yin, P.; Gao, P.; Lu, X.; Xu, G. Analysis of Catecholamines and Their Metabolites in Adrenal Gland by Liquid Chromatography Tandem Mass Spectrometry. *Anal. Chim. Acta*, **2008**, *609* (2), 192–200. https://doi.org/10.1016/j.aca.2008.01.017.

[76] Vaarmann, A.; Kask, A.; Mäeorg, U. Novel and Sensitive High-Performance Liquid Chromatographic Method Based on Electrochemical Coulometric Array Detection for Simultaneous Determination of Catecholamines, Kynurenine and Indole Derivatives of Tryptophan. *J. Chromatogr. B*, **2002**, *769* (1), 145–153. https://doi.org/10.1016/S1570-0232(01)00639-0.

[77] Bielavská, M.; Kassa, J. Simultaneous Determination of Dopamine, Serotonin and Their Metabolites in the Rat Brain by HPLC Method with Coulometric Detection. *Collect. Czechoslov. Chem. Commun.*, **2000**, *65* (10), 1677–1682. https://doi.org/10.1135/cccc20001677.

[78] Alvarez, J.-C.; Bothua, D.; Collignon, I.; Advenier, C.; Spreux-Varoquaux, O. Simultaneous Measurement of Dopamine, Serotonin, Their Metabolites and Tryptophan in Mouse Brain Homogenates by High-Performance Liquid Chromatography with Dual Coulometric Detection. *Biomed. Chromatogr.*, **1999**, *13* (4), 293–298. https://doi.org/10.1002/(SICI)1099-0801(199906)13:4<293::AID-BMC863>3.0.CO;2-R.

[79] Manica, D. P.; Mitsumori, Y.; Ewing, A. G. Characterization of Electrode Fouling and Surface Regeneration for a Platinum Electrode on an Electrophoresis Microchip. *Anal. Chem.*, **2003**, *75* (17), 4572–4577. https://doi.org/10.1021/ac034235f.

[80] Fujino, K.; Yoshitake, T.; Kehr, J.; Nohta, H.; Yamaguchi, M. Simultaneous Determination of 5-Hydroxyindoles and Catechols by High-Performance Liquid Chromatography

with Fluorescence Detection Following Derivatization with Benzylamine and 1,2-Diphenylethylenediamine. *J. Chromatogr. A*, **2003**, *1012* (2), 169–177. https://doi.org/10.1016/S0021-9673(03)01180-4.

[81] Zhang, M.-Y.; Beyer, C. E. Measurement of Neurotransmitters from Extracellular Fluid in Brain by in Vivo Microdialysis and Chromatography–Mass Spectrometry. *Hyphenated Tech. Pharm. Biomed. Anal.*, **2006**, *40* (3), 492–499. https://doi.org/10.1016/j.jpba.2005.07.025.

[82] Armarego, W. L. F.; Randles, D.; Taguchi, H. Peroxidase Catalysed Aerobic Degradation of 5,6,7,8-Tetrahydrobiopterin at Physiological PH. *Eur. J. Biochem.*, **1983**, *135* (3), 393–403. https://doi.org/10.1111/j.1432-1033.1983.tb07666.x.

[83] Archer, M. C.; Vonderschmitt, D. J.; Scrimgeour, K. G. Mechanism of Oxidation of Tetrahydropterins. *Can. J. Biochem.*, **1972**, *50* (11), 1174–1182. https://doi.org/10.1139/o72-160.

[84] Buglak, A. A.; Telegina, T. A.; Vechtomova, Y. L.; Kritsky, M. S. Autoxidation and Photooxidation of Tetrahydrobiopterin: A Theoretical Study. *Free Radic. Res.*, **2020**, 1–23. https://doi.org/10.1080/10715762.2020.1860213.

[85] Davis, M. D.; Kaufman, S.; Milstien, S. The Auto-Oxidation of Tetrahydrobiopterin. *Eur. J. Biochem.*, **1988**, *173* (2), 345–351. https://doi.org/10.1111/j.1432-1033.1988.tb14004.x.

[86] Kaufman, S. The Nature of the Primary Oxidation Product Formed from Tetrahydropteridines during Phenylalanine Hydroxylation. *J. Biol. Chem.*, **1961**, *236* (3), 804–810. https://doi.org/10.1016/S0021-9258(18)64312-1.

[87] Kirsch, M.; Korth, H.-G.; Stenert, V.; Sustmann, R.; de Groot, H. The Autoxidation of Tetrahydrobiopterin Revisited: Proof of Superoxide Formation From Reaction of Tetrahydrobiopterin With Molecular Oxygen*. *J. Biol. Chem.*, **2003**, *278* (27), 24481–24490. https://doi.org/10.1074/jbc.M211779200.

[88] Arning, E.; Bottiglieri, T. LC-MS/MS Analysis of Cerebrospinal Fluid Metabolites in the Pterin Biosynthetic Pathway. *JIMD Rep. Vol. 29*, **2014**, 1–9. https://doi.org/10.1007/8904_2014_336.

[89] Howells, D. W.; Smith, I.; Hyland, K. Estimation of Tetrahydrobiopterin and Other Pterins in Cerebrospinal Fluid Using Reversed-Phase High-Performance Liquid Chromatography with Electrochemical and Fluorescence Detection. *J. Chromatogr. B. Biomed. Sci. App.*, **1986**, *381*, 285–294. https://doi.org/10.1016/S0378-4347(00)83594-X.

[90] Verbeek, M. M.; Blom, A. M.; Wevers, R. A.; Lagerwerf, A. J.; van de Geer, J.; Willemsen, M. A. A. P. Technical and Biochemical Factors Affecting Cerebrospinal Fluid 5-MTHF, Biopterin and Neopterin Concentrations. *Mol. Genet. Metab.*, **2008**, *95* (3), 127–132. https://doi.org/10.1016/j.ymgme.2008.07.004.

[91] Howells, D. W.; Hyland, K. Direct Analysis of Tetrahydrobiopterin in Cerebrospinal Fluid by High-Performance Liquid Chromatography with Redox Electrochemistry: Prevention of Autoxidation during Storage and Analysis. *Clin. Chim. Acta*, **1987**, *167* (1), 23–30. https://doi.org/10.1016/0009-8981(87)90081-7.

[92] Guibal, P.; Lévêque, N.; Doummar, D.; Giraud, N.; Roze, E.; Rodriguez, D.; Couderc, R.; Billette De Villemeur, T.; Moussa, F. Simultaneous Determination of All Forms of Biopterin and Neopterin in Cerebrospinal Fluid. *ACS Chem. Neurosci.*, **2014**, *5* (7), 533–541. https://doi.org/10.1021/cn4001928.

[93] Allegri, G.; Costa Netto, H. J. B.; Ferreira Gomes, L. N. L.; Costa de Oliveira, M. L.; Scalco, F. B.; de Aquino Neto, F. R. Determination of Six Pterins in Urine by LC–MS/MS. *Bioanalysis*, **2012**, *4* (14), 1739–1746. https://doi.org/10.4155/bio.12.131.

[94] Fekkes, D.; Voskuilen-Kooijman, A. Quantitation of Total Biopterin and Tetrahydrobiopterin in Plasma. *Clin. Biochem.*, **2007**, *40* (5), 411–413. https://doi.org/10.1016/j.clinbiochem.2006.12.001.

[95] Santagata, S.; Di Carlo, E.; Carducci, C.; Leuzzi, V.; Angeloni, A.; Carducci, C. Development of a New UPLC-ESI-MS/MS Method for the Determination of Biopterin and Neopterin in Dried Blood Spot. *Clin. Chim. Acta*, **2017**, *466*, 145–151. https://doi.org/10.1016/j.cca.2017.01.019.

[96] Guibal, P.; Lo, A.; Maitre, P.; Moussa, F. Pterin Determination in Cerebrospinal Fluid: State of the Art. *Pteridines*, **2017**, *28* (2), 83–89. https://doi.org/10.1515/pterid-2017-0001.

[97] Ponzone, A.; Spada, M.; Ferraris, S.; Dianzani, I.; de Sanctis, L. Dihydropteridine Reductase Deficiency in Man: From Biology to Treatment. *Med. Res. Rev.*, **2004**, *24* (2), 127–150. https://doi.org/10.1002/med.10055.

[98] Haavik, J.; Flatmark, T. Isolation and Characterization of Quinonoid Dihydropterins by High-Performance Liquid Chromatography. *J. Chromatogr. A*, **1983**, *257*, 361–372. https://doi.org/10.1016/S0021-9673(01)88192-9.

[99] Hyland, K. Estimation of Tetrahydro, Dihydro and Fully Oxidised Pterins by High-Performance Liquid Chromatography Using Sequential Electrochemical and Fluorometric Detection. *J. Chromatogr. B. Biomed. Sci. App.*, **1985**, *343*, 35–41. https://doi.org/10.1016/S0378-4347(00)84565-X.

[100] Fukushima, T.; Nixon, J. C. [55] Chromatographic Analysis of Pteridines. In *Methods in Enzymology*; Academic Press, 1980; Vol. 66, pp 429–436. https://doi.org/10.1016/0076-6879(80)66485-4.

[101] Zurflüh, M. R.; Giovannini, M.; Fiori, L.; Fiege, B.; Gokdemir, Y.; Baykal, T.; Kierat, L.; Gärtner, K. H.; Thöny, B.; Blau, N. Screening for Tetrahydrobiopterin Deficiencies Using

Dried Blood Spots on Filter Paper. *New Dev. Phenylketonuria Tetrahydrobiopterin Res.*, **2005**, *86*, 96–103. https://doi.org/10.1016/j.ymgme.2005.09.011.

[102] Werner, E. R.; Wachter, H.; Werner-Felmayer, G. Determination of Tetrahydrobiopterin Biosynthetic Activities by High-Performance Liquid Chromatography with Fluorescence Detection. In *Methods in Enzymology*; Academic Press, 1997; Vol. 281, pp 53–61. https://doi.org/10.1016/S0076-6879(97)81008-7.

[103] Kośliński, P.; Jarzemski, P.; Markuszewski, M. J.; Kaliszan, R. Determination of Pterins in Urine by HPLC with UV and Fluorescent Detection Using Different Types of Chromatographic Stationary Phases (HILIC, RP C8, RP C18). *J. Pharm. Biomed. Anal.*, **2014**, *91*, 37–45. https://doi.org/10.1016/j.jpba.2013.12.012.

[104] Burton, C.; Shi, H.; Ma, Y. Simultaneous Detection of Six Urinary Pteridines and Creatinine by High-Performance Liquid Chromatography-Tandem Mass Spectrometry for Clinical Breast Cancer Detection. *Anal. Chem.*, **2013**, *85* (22), 11137–11145. https://doi.org/10.1021/ac403124a.

[105] Burton, C.; Shi, H.; Ma, Y. Development of a High-Performance Liquid Chromatography – Tandem Mass Spectrometry Urinary Pterinomics Workflow. *Anal. Chim. Acta*, **2016**, *927*, 72–81. https://doi.org/10.1016/j.aca.2016.05.005.

[106] Yuan, T.-F.; Huang, H.-Q.; Gao, L.; Wang, S.-T.; Li, Y. A Novel and Reliable Method for Tetrahydrobiopterin Quantification: Benzoyl Chloride Derivatization Coupled with Liquid Chromatography-Tandem Mass Spectrometry Analysis. *Free Radic. Biol. Med.*, **2018**, *118*, 119–125. https://doi.org/10.1016/j.freeradbiomed.2018.02.035.

CHAPITRE 3 : ETUDE DE LA CINETIQUE D'AUTO-OXYDATION DE LA TETRAHYDROBIOPTERINE PAR CHROMATOGRAPHIE LIQUIDE COUPLEE A LA SPECTROMETRIE DE MASSE EN TANDEM

III.1. PRESENTATION DE L'ARTICLE

Après avoir référencé les méthodes disponibles pour le dosage des biomarqueurs des erreurs innées du métabolisme, il est apparu qu'un des composés les plus importants pour le diagnostic, à savoir la tétrahydrobioptérine (H4Bip), est instable et encline à l'auto-oxydation. Nous nous sommes intéressés à la quinonoid dihydrobioptérine (qH2Bip), intermédiaire éphémère jouant un rôle crucial dans les hydroxylations dépendantes de la H4Bip. En effet, la qH2Bip pourrait avoir un intérêt dans le diagnostic ou dans le suivi thérapeutique des erreurs innées du métabolisme. Cependant, à l'heure actuelle, il n'existe aucune étude décrivant son potentiel dans le suivi clinique et ce, principalement pour deux raisons : la difficulté de séparer la quinonoid dihydrobioptérine des autres bioptérines et son caractère hautement éphémère avec une demi-vie de dégradation entre 0,9 et 5 minutes. Ainsi, il n'existe aucune méthode chromatographique permettant la mise en évidence de la formation de la qH2Bip, que ce soit dans un milieu biologique ou en solution pure.

Sur la base de la découverte récente d'une transition spécifique de la quinonoid dihydrobioptérine en spectrométrie de masse en tandem, nous avons développé une méthode de chromatographie liquide couplée à la spectrométrie de masse en tandem permettant d'analyser cet intermédiaire, la tétrahydrobioptérine et les autres produits d'auto-oxydation en moins de 3,5 minutes. Cette méthode a été appliquée à l'étude de l'auto-oxydation de la tétrahydrobioptérine en fonction de la nature et du pH du tampon. Ceci a permis de démontrer que la voie d'auto-oxydation ainsi que la demi-vie de la tétrahydrobioptérine dépend fortement de la nature et du pH du milieu. Par ailleurs, nous avons observé que la demi-vie apparente de la quinonoid dihydrobioptérine est bien plus élevée que celles décrites dans la littérature. Il apparait donc, que pour améliorer l'exactitude du diagnostic des déficiences en tétrahydrobioptérine et du suivi thérapeutique, les méthodes d'analyse de cette ptérine doivent permettre la quantification de la quinonoid dihydrobioptérine.

Statut de l’article : Soumis.

Journal visé : Analytical Chemistry

Kinetics of autoxidation of tetrahydrobiopterin and quinonoid dihydrobiopterin

A. Boulghobra, M. Bonose, E. Alhajji, A. Pallandre, M-C. Menet, F. Moussa

Institut de Chimie Physique, UMR 8000-Université Paris Saclay

III.2. ABSTRACT

In humans, quinonoid dihydrobiopterin (qH2Bip) is a transient intermediate that plays a central role in the physiologically essential tetrahydrobiopterin (H4Bip) dependent hydroxylation reactions. Surprisingly, more than half a century later, from the discovery of the physiological role of H4Bip until the recent advances of gene therapy in genetic disorders of dopamine and serotonin, qH2Bip has never been considered in the diagnosis and therapeutic monitoring of H4Bip deficiency. This is mainly due to the difficulty of separating qH2Bip from H4Bip, and to its supposed very short half-life that would vary from 0.9 to 5 minutes, according to previ-ous studies. Indeed, no current method of pterins determination, even by LC-MS/MS, allows the determination of qH2Bip in bio-logical medium or simply in pure solution. Based on the recent discovery of the specific MS/MS transition of qH2Bip, here we developed an UHPLC-MS/MS method able to separate this intermediate from H4Bip and other oxidation products in less than 3.5 minutes. The application of this method to the investigation of H4Bip autoxidation shows that for a considered buffer, the autoxidation pathway and qH2Bip half-life strongly depends on pH of the medium. Most importantly, the obtained data confirm that qH2Bip half-life is much longer than previously reported and mostly longer than that of H4Bip, irrespective of the considered conditions. Hence, in order to improve the accuracy in terms of diagnosis of H4Bip defects, quality control of H4Bip-based drugs, pharmacokinetics, and therapeutic monitoring during H4Bip supplementation, analysis methods of this pterin should consider, henceforth, the quantification of qH2Bip.

III.3. INTRODUCTION

In living organisms, tetrahydrobiopterin (H4Bip) is the cofactor of several essential hydroxylation reactions. [1–3] H4Bip deficiencies have a serious impact on health, with various pathophysiological disorders, ranging from neurotransmission disorders to cardiovascular diseases, neurodegenerative diseases (Parkinson's, Alzheimer's, etc.), depression, inflammatory diseases and cell growth.[3] Nowadays, the physiopathology of H4Bip remains an active field of research in human medicine as reflected in the recent description of a new genetic disorder,[4] the renewed interest to its role in vitiligo,[5, 6] or the new discoveries related to its role in autoimmunity and cancer,[7] and in kidney injury in diabetes.[8]

Since the elucidation of H4Bip structure,[2] it is widely assumed that the first step of the H4Bip-dependent hydroxylation reac-tions involves the oxidation of H4Bip into a short-lived intermediate, quinonoid dihydrobiopterin (qH2Bip).[3] H4Bip is then regenerated by enzymatic reduction of the latter thanks to dihydro-pteridine reductase (DHPR) (Figure III.1).[3]

In the absence of rapid reduction, qH2Bip may rearrange to 7,8-dihydrobiopterin (H2Bip) (Figure III.1), a more stable con-former as reflected in the increase of the latter in case of DHPR deficiency.[9-15] Hence, the determination of these pterins in biological media including H4Bip, H2Bip, and their precursor dihydro-neopterin (H2Nptr) is of importance for both diagnosis and monitoring the efficacy of H4Bip supplementation in patients with genetic defects.[12-14] However, the determination of H4Bip in biological fluids is quite difficult due to its proneness to autoxidation (Figure III.1).[15–17]

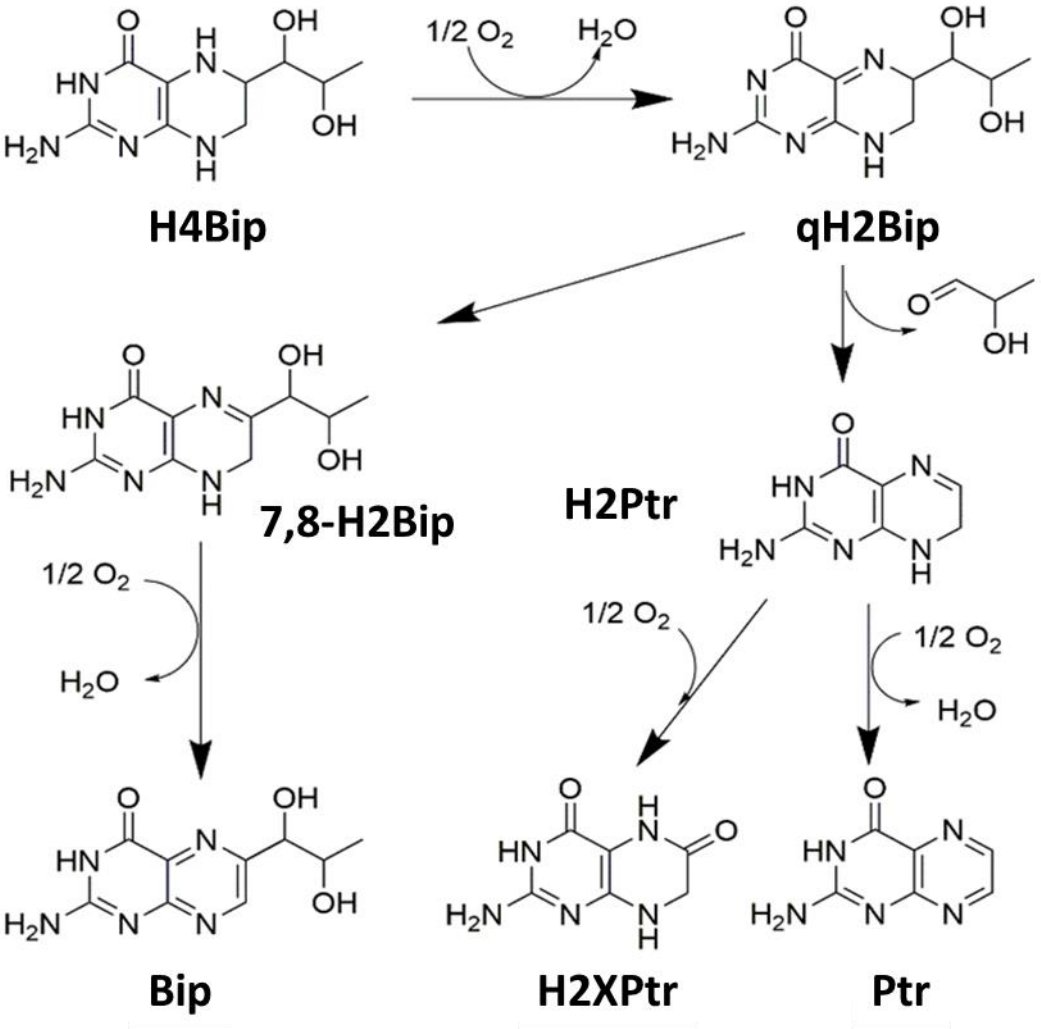

Figure III.1: Autoxidation pathways of tetrahydrobiopterine (H4Bip) according to references 6 and 20.
qH2Bip (quinonoid dihydrobiopterin); 7,8-H2Bip (7,8-dihydrobiopterin); H2Ptr (dihydropterin); Bip (Biopterin); H2XPtr (dihydro-xanthopterin); and Ptr (Pterin).

Under aerobic conditions and in the absence of rapid enzymatic reduction, the first step of H4Bip autoxidation leads to qH2Bip production that would then rapidly undergo two competing autoxidation pathways (Figure III.1).[2,18-23] qH2Bip could either isomerize into 7,8-H2Bip or lose the side chain at C-6 lead-ing to dihydro-pterin (H2Ptr) formation.[20] Then, 7,8-H2Bip and H2Ptr would oxidize into biopterin (Bip), and pterin (Ptr) or dihydro-xanthopterin (H2Xptr), respecti-vely.[23]

Considered together, these observations underline the central role of qH2Bip in the oxidation pathway of H4Bip and the physiopathology of H4Bip-dependent hydroxylation reac-tions. They also strongly suggest that precise determination of qH2Bip is necessary to get definite insights in this field.

Surprisingly, while the occurrence of qH2Bip in the H4Bip oxidation process was proposed since 1963,[2] only a few attempts have been made to synthetize[24] or to separate and directly characterize this transient intermediate.[25,26] Although these studies indirectly confirmed that the first step of H4Bip oxidation led to the release of qH2Bip, they showed that it was difficult to separate it from H4Bip.[26] Consequently, in the era of gene therapy of dopamine and seroto-nin disorders,[27] no current method of pterins determination,[17,28] even using LC-MS/MS[29-35] al-lows to directly determine qH2Bip, to our knowledge.

Available data on qH2Bip remain scarce and conflicting.[18,20] The autoxidation pathway itself has been sometimes ques-tioned[18,20] and the half-life of qH2Bip would be very short and may vary from 0.9[24] to 5 min[25] as a function of pH and the type of buffer.[20] Besides, in biological samples, H4Bip would oxidize within minutes, without molar relationship between H4Bip loss and the increase in concentrations of 7,8-H2Bip and Bip.[16]

By using a multiple analytical approach, it has been recently demonstrated that 7,8-H2Bip iso-mers can be distinguished thanks to their MS/MS transitions.[36] Based on these findings, here we developed a HPLC-MS/MS method able to separate all autox-idation products of H4Bip, including qH2Bip, in order to revisit the autoxidation pathway and kinetics of this essential cofactor as a function of pH and the type of buffer.

III.4. EXPERIMENTAL SECTION

Reagents

All standards including H4Bip, H2Bip, Bip, and Nptr were purchased from Sigma and were used without further purification. Standard solutions (SS, 1 mM) of H4Bip, H2Bip, Bip, and Nptr (0.25 mM, used as internal standard (IS)) were prepared in pH 2.8, 0.05 M ammonium formate, aliquoted, and immediately stored at -20°C.

Materials

HPLC-MS/MS analysis were carried out on a Shimadzu Nexera LC-20A system connected to a Shimadzu LCMS-8040 triple quadrupole.

HPLC-MS/MS method

Chromatographic separations were performed on a 100 x 2.1 mm; 3 µm Atlantis T3 C18 column (Waters, St-Quentin en Yvelines, France). The mobile phase consisted of a mixture of pH 2.8, 0.05M, ammonium formate/methanol (97/3; v/v). The flow rate was set at 0.4 mL/min and the column temperature was maintained at 30 °C.

MS/MS experiments were performed in positive electrospray ionization (ESI) mode with multiple reaction monitoring (MRM). ESI source voltage was set at 4.5 kV, heat block temperature at 400°C and desolvation temperature at 250°C. Nitrogen was used as drying gas at a flow rate of 15 L/min. Nitrogen was also used as nebulizing gas at 3 L/min. Argon was used for collision induced dissociation.

Sample preparation for autoxidation kinetic studies

Kinetics studies were conducted in three different 0.1 M ammonium-based buffers including formate, acetate, and citrate, at three different pH each (≤ 3.0, 5.4, and 7.4).

Working solutions (WS) for HPLC-MS/MS autoxidation kinetics' studies are prepared by appropriate dilution of defrosted aliquots of SS in the considered buffer. The obtained WS are

then installed at 10 °C in the autosampler and 10 µL are injected into the chromatograph at regular time intervals. For kinetic studies, the final concentrations of H4Bip and Nptr in the WS were set at 1.00 and 0.25 µM, respectively.

Pterins' autoxidation reaction order, rate constants, and half-lives

In order to estimate autoxidation reaction orders of H4Bip and qH2Bip, we selected the most appropriate function in terms of correlation coefficient (R^2) to modeling their kinetics of decrease. Depending on whether the model is linear or exponential, the autoxidation reaction order will be 0 or 1, respectively.[37,38] For a linear model, the corresponding equation to calculate the half-life follows the Equation 1, whereas it follows the Equation 2 for an exponential model (Scheme 1), where A(t) is the measured area at t hours, A_0 the area at t = 0 hour, k the rate constant, and $t_{½}$ the half-life.[37,38]

Scheme 1. Equation models for half-life determination

$$\textbf{Equation 1}: A\,(t) = A_0 - kt \;\; ; \;\; t_{\frac{1}{2}} = \frac{A_0}{2k}$$

$$\textbf{Equation 2}: A\,(t) = A_0 e^{-kt} \;\; ; \;\; t_{\frac{1}{2}} = \frac{\ln(2)}{k}$$

Bip and 7,8-H2Bip quantification

In order to quantify Bip and 7,8-H2Bip release during H4Bip autoxidation, we checked the linearity and the precision of the LC-MS/MS proposed method for both products.

III.5. RESULTS AND DISCUSSION

III.5.1. LC-MS/MS method development

III.5.1.1. Selecting MS/MS conditions

In order to develop an MS/MS method we used the product ions scan mode by selecting the $[M+H]^+$ parent ion and scanning from *m/z* 50 to *m/z* corresponding to the parent ion for each pterin with collision energies values ranging from 10 to 35 V. For H4Bip, H2Bip, Bip, and Nptr, the selected precursor, fragment ions and collision energies were optimized by flow injection analysis (FIA) of 5 µM standard solutions. For qH2Bip, H2Ptr, H2Xptr, and Ptr, the acquisition parameters were optimized on a degraded 20 µM H4BIP solution (incubation at room temperature in the dark during 3 hours) after HPLC separation. The MRM transitions of the studied pterins are summarized in Table III.1.

Table III.1: MS/MS transitions of targeted pterins (most intense fragment in bold)

Analyte	Retention time (min)	MRM transitions				
		Parent ion (*m/z*)	Fragment ions (*m/z*)	Q1 potential (V)	Collision energy (V)	Q3 potential (V)
H4Bip	0.93	242	**166**	-27.0	-20.0	-30.0
			206	-13.0	-18.0	-21.0
qH2Bip	1.05	240	**166**	-27.0	-15.0	-16.0
H2Ptr	1.43	166	**107**	-19.0	-23.0	-11.0
			121	-18.0	-21.0	-20.0
N	1.46	254	**206**	-29.0	-16.0	-25.0
			236	-29.0	-19.0	-21.0
H2Bip	2.76	240	**196**	-27.0	-14.0	-20.0
			165	-27.0	-21.0	-16.0
H2Xptr	2.88	182	**154**	-14.0	-19.0	-28.0
			137	-14.0	-22.0	-25.0
Bip	3.12	238	**220**	-27.0	-16.0	-23.0
			178	-27.0	-21.0	-19.0
Ptr	3.13	164	**119**	-12.0	-25.0	-22.0
			92	-12.0	-33.0	-16.0

Except for qH2Bip, we used two MRM transitions for each pterin, the first one, corresponding to the most intense fragment, for identification and quantification, and the second one, less intense, for identification confirmation. For qH2Bip, we used only the previously deciphered characteristic MRM transition (*m/z*, 240>166).[36]

III.5.1.2. Selecting separation conditions

H4Bip and its oxidation products are low hydrophobic basic compounds, which can be easily separated in hydrophilic interactions liquid chromatography (HILIC) mode or in reversed phase (RP) mode by using a polar embedded C18 column thus avoiding the addition of ion pairing reagents.[40] However, HILIC mode separations may suffer from mobile-phase/solvent of injection incompatibility for such water-soluble solutes.[40] Hence, we selected a polar embedded C18 stationary phase, allowing for the separation of pterins in the RP mode[40] with a classical formate-based mobile phase compatible with the ESI ionization source. For this purpose, we used a 2,1 x 50 mm, 3 µm Atlantis T3 column (Waters, St-Quentin en Yvelines, France) with a mixture of pH 2.8, 0.05 M ammonium formate/methanol (97/3, v/v) as mobile phase.

III.5.1.3. Separating the autoxidation products

The evolution of the chromatographic profiles of ammonium formate-based WS of H4Bip as a function of pH and incubation time is shown in figure III.2. Under the proposed chromatographic conditions, the MRM mode allows for the specific detection of most if not all autoxidation products of H4Bip including 7,8-H2Bip isomers, H2Ptr, Bip, H2Xptr, and Ptr in less than 3.5 minutes (Figure III.2). Most importantly, this figure clearly shows that qH2Bip is efficiently separated from H4Bip and 7,8-H2Bip under the proposed chromatographic conditions. These results confirm the predictions from previous work on the separation and identification of qH2Bip. Notably, the characteristic transitions of qH2Bip (*m/z*, 240>166) and 7,8-H2Bip (*m/z*, 240>196) enable to unambiguously identify both isomers and to separate them from H4Bip by HPLC-MS/MS. To the best of our knowledge this is the first time that qH2Bip is separated and unambiguously identified by HPLC-MS/MS thus offering the possibility of studying its autoxidation kinetics (Figure III.2). Interestingly, these chromatograms also clearly show that qH2Bip is

still present in the medium after 1.6 hours (Figure III.2c) of incubation thus confirming that the half-life of this transient intermediate is significantly higher than that previously reported.[20,24,25]

As stationary phase, we also tried a 50 x 2.1 mm, 1.8 µm HSS T3 column assumed to be the UHPLC counterpart of the Atlantis T3 column. However, this stationary phase failed to separate qH2Bip from H4Bip probably due to some differences in the chemical composition between HSS T3 and Atlantis T3 stationary phases especially in terms of carbon load, and to less extent extra-column void volume effects.

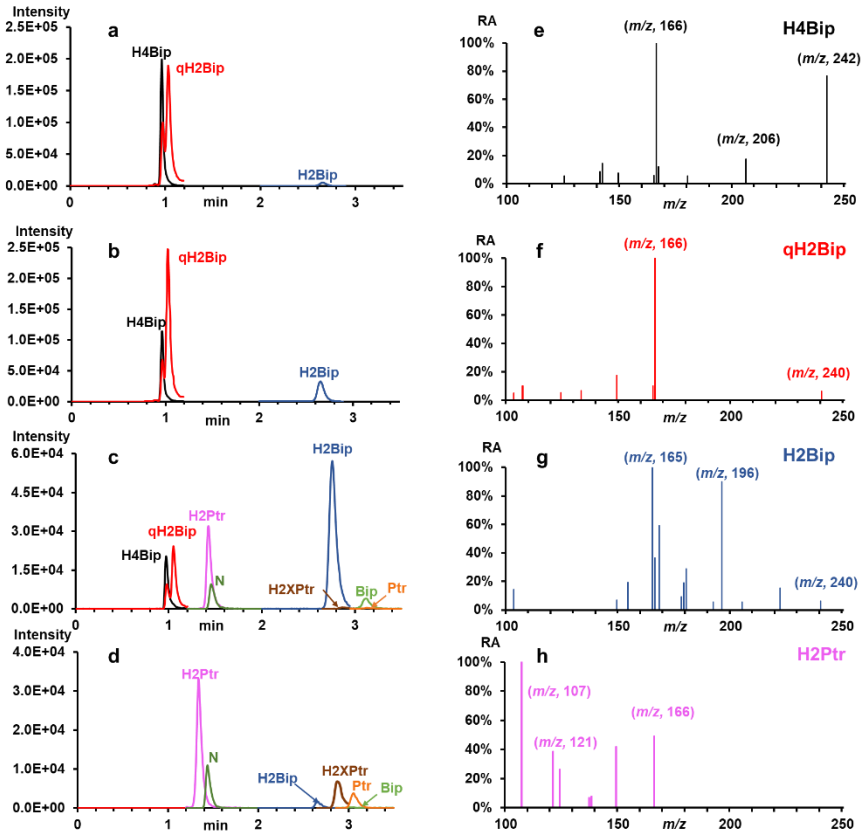

Figure III.2. Chromatographic profiles of H4Bip working solutions (WS) prepared and incubated in the ammonium formate buffer: (a) pH 2.8, first injection after the preparation of the WS (time 0 hour); (b) after 1 hour of incubation in the same buffer; (c) pH 5.4, after 1.6 hours of incubation; (d) pH 7.4, after 49.4 hours of incubation. (e-h) MS/MS spectra of H4Bip, qH2Bip, 7,8-H2Bip, and H2Ptr, respectively. RA: Relative abundance. Chromatographic conditions: 100 x 2.1 mm, 3 µm Atlantis T3 column; mobile phase: pH 2.8, 0.05 M ammonium formate /methanol (97/3, v/v) at a flow rate of 0.4 mL/min, 30 °C. Injection volume, 10 µL.

Under the proposed chromatographic conditions, in spite of the coelution of some autoxidation products, the resolution is clear between the critical pair of peaks with the same MS/MS transitions (*m/z*, 240>166) corresponding to the fragmentation of H4Bip in the ion source and the preexisting qH2Bip in the WS.

It is possible to use an Atlantis T3 column with larger dimensions than that proposed herein in order to increase the efficiency of the separation and thus the resolution. It is also possible to optimize the mobile phase and elution conditions in order to better separate the autoxidation products. However, the proposed column geometry is enough to separate under isocratic elution the critical pair corresponding to H4Bip and qH2Bip peaks in a short run-time convenient for autoxidation kinetic studies, which are our main objectives.

Likewise, it is possible to enhance the detection sensitivity by increasing the concentration of methanol at the column outlet in order to improve the yield of ionization in the ESI source. However, this will need an additional pumping system, while the sensitivity of the proposed method is sufficient to detect all oxidation products of H4Bip, without need for additional material.

III.5.2. Autoxidation kinetics

According to previous studies, the oxidation pathway of H4Bip and qH2Bip may vary as a function of pH and the type of buffer.[19] However, the data related to H4Bip stability and qH2Bip half-life remain scarce and conflicting [19, 24, 25]. Hence, we used the proposed LC-MS/MS method to further investigate this issue.

III.5.2.1. Selecting pH and buffers

In order to investigate the autoxidation pathway of H4Bip, and qH2Bip half-life we selected 3 pH levels covering acidic and neutral conditions. We first selected pH 2.8, which is the pH of the mobile phase of the proposed method. This pH is the most suitable one for the protonation

and MS/MS detection of these basic compounds, whilst considering the stationary phase stability under acidic conditions. We also selected pH 5.4 because this pH is commonly used for the RP-LC separation of pterins in biological media.[17, 33-35] Finally, we choose to investigate the autoxidation of H4Bip at physiological pH i.e. pH 7,4. Also, this latter pH is the only condition enabling fluorescence detection of H4BIP after post-column electro-oxidation.[17]

In order to investigate the effects of buffer type, we chose three ammonium-based buffers. Ammonium formate was selected because it is the main constituent of the proposed mobile phase and the most widely used volatile buffer for HPLC-MS separations.[29-35] We also selected ammonium acetate because it is frequently used for the analysis of pterins in biological samples.[37] Finally, we selected ammonium citrate because of its good buffer capacity in the selected entire pH range and because of its chelating properties. Citrate buffer is also used for pterins determination in biological media.[17] For obvious reasons of incompatibility with the ionization source, we avoided using phosphate buffers.

III.5.2.2. H2Bip and Bip quantification

As H4BIP would oxidize within minutes, without molar relationship between H4Bip loss and the increase in concentrations of 7,8-H2Bip and Bip [11] we aimed to quantify both oxidation products under the selected autoxidation conditions. For this purpose, we checked the linearity of the proposed method between 5 and 1000 nM ($y = 0.006x - 0.021$, $n = 6$, and $y = 0.005x + 0.057$, $n = 6$, with $R^2 > 0.99$ for 7,8-H2Bip and Bip, respectively). The accuracy of the method has been investigated at two concentration levels, 5 and 1000 nM. The relative standard deviations were lower than 5% for both compounds in all instances (supporting information).

III.5.2.3. Autoxidation at pH ≤ 3.0

The autoxidation kinetics under acidic conditions is shown in figure III.3 (panels a-c). The kinetic parameters clearly differ as a function of the type of buffer (Table III.2). However, the autoxidation pathway remains the same regardless the type of buffer. The first autoxidation product is qH2Bip, which converts to H2Bip, which slowly oxidizes to yield Bip. In all cases, the other autoxidation products, H2Ptr, Ptr, and H2Xptr are very low and remain below the limit

of quantitation. Hence, under these conditions qH2Bip is mainly converted into H2Bip. In fact, the autoxidation kinetics evolves as a function of the type of buffer (Table III.2).

Table III.2: H4B autoxidation parameters as a function of pH and buffer's type.

		H4Bip				qH2Bip				Product (%/H4Bip)
pH	Buffer (Ammo-nium)	**Half-life (min)**	Time in-terval (hours)	Reaction order	Rate constant (h^{-1})	**Half-life (min)**	Time in-terval (hours)	Reaction order	Rate constant (h^{-1})	
2.8	Formiate	**87**	0 - 3.4	1	0.5	**111**	0.8 - 3.9	1	0.4	qH2Bip, 7,8-H2Bip (30%), Bip (40%), H2Xptr, Ptr
		33	3.4 - 8.7		1.3	**37**	3.9 - 9		1.1	
3.0	Acetate	**25**	0 - 4	1	1.7	**34**	0 - 6.6	1	1.2	qH2Bip, 7,8-H2Bip (58%), Bip (15%), H2Xptr, Ptr
2.8	Citrate	**83**	0 – 3.6	1	0.5	**120**	0 - 29	1	0.3	qH2Bip, 7,8-H2Bip (80%), Bip (7%), H2Xptr, Ptr
5.4	Formiate	**66**	0 - 2.3	0	2.5*	**79**	0 - 2.7	0	1.8*	qH2Bip, 7,8-H2Bip (15%), H2Ptr, Bip (18%), H2Xptr, P
		15	2.3 - 3.9	1	3.3	**16**	2.7 - 3.9	1	2.7	
	Acetate	**22**	0 - 3	1	1.9	**20**	0 – 3.5	1	2.1	qH2Bip, H2Ptr, 7,8-H2Bip (64%), Bip (12%), H2Xptr, Ptr
	Citrate	**23**	0 - 3	1	1.8	**29**	0 - 3	1	1.4	qH2Bip, 7,8-H2Bip (34%), H2Ptr, Bip (7%), H2Xptr, Ptr
7.4	Formiate	**147**	0.3 - 5.7	1	0.3	**135**	0.3 - 6.4	1	0.3	qH2Bip, H2Ptr, H2Xptr, 7,8-H2Bip (5%), Ptr, Bip (<1%)
		69	5.7 - 14.3		0.6	**75**	6.4 - 14.8		0.6	
	Acetate	**37**	0 - 6	1	1.1	**35**	0 - 6.6	1	1.2	qH2Bip, H2Ptr, H2Xptr, 7,8-H2Bip (9%), Ptr, Bip (3%)
	Citrate	**57**	0 - 6	1	0.7	**154**	0 - 5	0	0.6*	qH2Bip, H2Ptr, 7,8-H2Bip (30%), H2Xptr, Ptr, Bip (<1%)

*rate constants for reaction orders are in mol.L-1.h-1

** %H4Bip (The percentages of 7,8-H2Bip and Bip are calculated relative to the initial concentration of H4Bip).

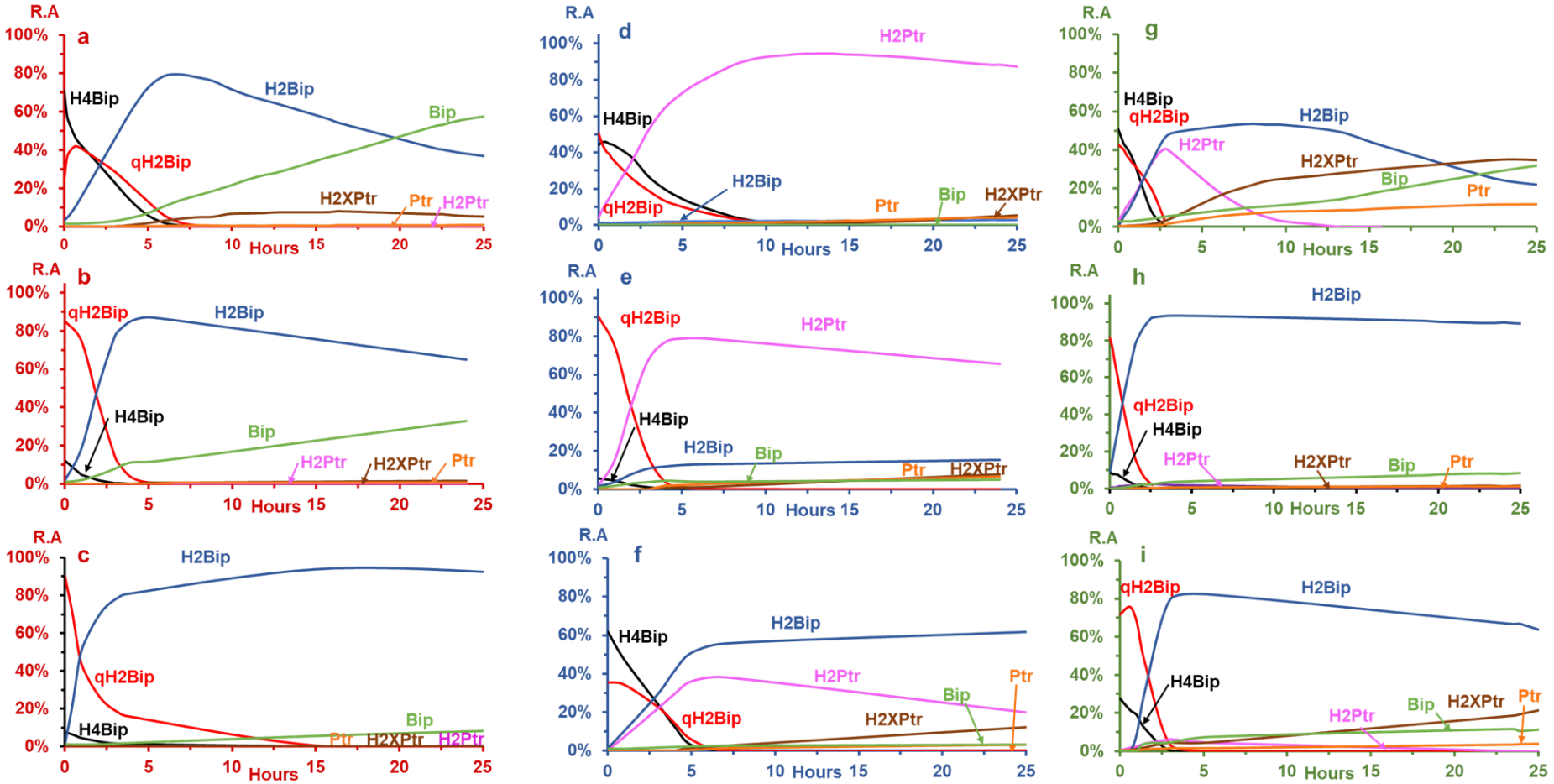

Figure III.3. H4Bip autoxidation kinetics in: (a) pH 2.8, 0.05 M ammonium formate, (b) pH 3.0, 0.1 M acetic acid, (c) pH 2.8, 0.05 M ammonium citrate, (d) pH 7.4, 0.05 M ammonium formate, (e) pH 7.4, 0.05 M ammonium acetate, (f) pH 7.4, 0.05 M ammonium citrate, (g), pH 5.4, 0.05 M ammonium formate, (h) pH 5.4, 0.05 M ammonium acetate, and (i) pH 5.4, 0.05 M ammonium citrate. (R.A) represents the relative abundance of the considered peak.

Formate buffer. Under these conditions (Figure III.3a), H4Bip decreases bi-exponentially. From 0 to 3.4 hours, the first half-life is 87 minutes. The second half-life, from 3.4 to 8.7 hours, drops to 33 minutes. Under the same conditions qH2Bip first increases from 0 h to 0.8 hours and then starts decreasing bi-exponentially, like that occurs for H4Bip, to yield H2Bip.

Between 0.8 and 3.9 hours, the first half-life of qH2Bip is 111 minutes while the second one drops to 37 minutes between 3.9 and 9 hours. Meanwhile, 7,8-H2Bip starts increasing from 0 to 4.9 hours and then begins decreasing to yield mainly Bip. If we consider the time interval going from 12.5 to 16.1 hours, only 57% of 7,8-H2Bip is oxidized into Bip. Besides, 7,8-H2Bip degradation temporally coincides with an obvious H2Xptr increase (Figure III.2a), which suggests that a little part of 7,8-H2Bip is oxidized into H2Xptr.

Acetate buffer. As compared to formate buffer, an acceleration of the autoxidation kinetics is observed in presence of acetic acid. H4Bip decreases exponentially between 0 and 4 hours with a half-life of 25 minutes (Figure III.3b, Table III.2). Concomitantly, qH2Bip decreases between 0 and 5 hours with a half-life of 34 minutes (Figure III.3b, Table III.2). Meanwhile, 7,8-H2Bip increases from 0 h to 5 hours and then starts decreasing until the end of the study (25 h). Under these conditions, Bip, resulting from the autoxidation of 7,8-H2Bip increases during the whole kinetic study (0 h–25 h).

Citrate buffer. In citrate buffer at pH 2.8 (Figure III.2c), the autoxidation of H4Bip is similar to formate buffer. Indeed, its oxidation products are the same, namely: qH2Bip, 7,8-H2Bip and Bip. Moreover, H4Bip decreases following an exponential model until 3.6 h which corresponds to the last moment where it is detected. The measured half-life is of 83 minutes. Concerning qH2Bip, it starts decreasing exponentially at the beginning of the kinetic study. Its half-life is of 120 minutes. These two half-lives are very close to the ones measured in ammonium formate at the same pH.

While these results confirm that the kinetics of autoxidation of H4Bip under acidic conditions differ according to the type of buffer, they show that the apparent half-life of qH2Bip is significantly longer than that previously reported [19,24,25] and longer than that of H4Bip.

III.5.2.4. Autoxidation at pH 7.4

The autoxidation kinetics under neutral conditions is shown in figure III.3 (Panels d-f, Table III.2). As compared to acidic conditions, the oxidation pathway and kinetics at neutral pH change drastically (Table III.2).

Formate buffer. In this buffer, qH2Bip is always the first oxidation product, however, instead of converting into 7,8-H2Bip like that occurs under acidic conditions (Figure III.3a), this isomer mainly oxidizes by losing its side chain to yield H2Ptr (Figure III.3d). Under these conditions, H2Ptr remains quite stable until the 25th hour. H4Bip autoxidation starts at 0.3 hours after a short plateau where less than 5% of H4Bip decrease is observed. Then H4Bip decreases bi-exponentially with half-lives longer than those observed under acidic conditions (Table III.2). Likewise, qH2Bip decreases bi-exponentially with a first half-life of 135 minutes between 0.3 and 6.4 hours and a second half-life of 75 minutes between 6.4 and 14.8 hours (Table III.2). Under these conditions (Figure III.3d), the level of other oxidation products, remains negligible.

Acetate buffer. The main differences with formate buffer lie in the kinetics of H4Bip and qH2Bip degradation (Table III.2) as well as in the subsequent oxidation of H2Ptr. In contrast to what occurs in formate buffer, in this buffer, the oxidation products, notably Ptr, and H2Xptr increases as a function of the incubation time, although very slowly (Figure III.3e). The increase of these products may be attributed to the oxidation of a little part of H2Ptr, as previously suggested.[25] Likewise, there is a production of 7,8-H2Bip through qH2Bip isomerization, but at a relatively low rate. Finally, in this medium, 7,8-H2Bip produced through qH2Bip conversion remains quite stable until the 25th hour.

Citrate buffer. The results observed in citrate buffer at neutral pH (Figure III.3f) indicate the degradation of qH2Bip produces a mixture of 7,8-H2Bip and H2Ptr (Figure III.3f). Besides, under these conditions, only 7,8-H2Bip remains stable while H2Ptr decreases to yield H2Xptr (Figure III.3f). Hence, the stability of H4Bip and qH2Bip under acidic pH in citrate buffer is not simply due to the chelation of metal ions present in the medium. Because, in this case, their stability should increase with pH, like that usually occurs for citrates/metal complexes. Then, the remarkable stability of these pterins in citrate buffer under acidic conditions is probably due the direct complexation of protonated pterins by citrate ions, which protect them from autoxidation. The deprotonation of the heterocyclic nitrogen atoms of these pterins with pH increase, could explain the instability of H4Bip at neutral pH, through complexes dissociation and citrate ions release.

III.5.2.5. Autoxidation at pH 5.4

At this pH, kinetics of autoxidation is faster (Table III.2), but, again, the pathway differs as a function of the type of buffer (Figure III.3g-i)**.**

Formate buffer. In this buffer, the breakdown of H4Bip and qH2Bip rapidly yields a mixture of 7,8-H2Bip and H2Ptr. While the latter rapidly autoxidize yielding H2Xptr and Ptr, the former slowly oxidizes to yield Bip (Figure III.3g).

Acetate buffer. Like that occurs at more acidic pH (Figure III.3b), qH2Bip mainly isomerizes into H2Bip, but, in contrast to what occurs at acidic pH, the latter is more stable at this pH (Figure III.3h).

Citrate buffer. At this pH, the oxidation pathway is similar to that of acetate buffer (Figure III.3h), but 7,8-H2Bip is significantly less stable under these conditions (Figure III.3i).

III.5.2.6 Effects of H4Bip concentration

Although the results obtained by HPLC-MS/MS confirm the apparent half-life of qH2Bip is higher than the one measured for H4Bip, there is a difference between the obtained half-lives

and the ones described in the litterature. Since the used H4Bip concentrations are variable from one study to another, these differences could be attributed to this factor. To check this hypothesis, we studied the effect of H4Bip concentration on the half-lives of both pterins in formate buffer.

As expected, the obtained data confirm the hypothesis. Half-lives increase significantly with increasing H4Bip concentration (Figure III.4, and Table III.3).

III.5.3. General comments

In 1963, 7,8-H2Bip was identified as the stable product of qH2Bip rearrangement in pH 6.8, 0.1 M phosphate buffer.[2] Twenty years later this assignment has been questioned because aerobic oxidation of H4Bip in pH 7.6, 0.1 M Tris buffer, mainly leads to H2Ptr.[18] Since then, the authors of the former study monitored spectrophotometrically the rearrangement of qH2Bip in various buffer solutions and reported half-lives values from 1.2 to 2.0 minutes.[20] They stated that in phosphate buffer at pH 6.8, the predominant product of the aerobic oxidation of H4Bip is H2Bip, whereas in Tris buffer at pH 7.6, the analogous reaction yields H2P.[20] The authors concluded that the pH of the solution is not the only factor that determines which pathway the rearrangement of qH2Bip follows.[20] The temperature of the reaction solution and the type of buffer present during the rearrangement of qH2Bip can also play important roles in determining the distribution of products.[20] However, all these data were obtained at neutral pH and were only based on the spectrophotometrically detection of H4Bip autoxidation products.

While confirming the important role of the type of buffer, the results of the present study clearly show that, for a considered type of buffer the kinetics and the autoxidation pathway strongly depend of pH (Figure III.3, Table III.2). Overall, these results show that in presence of a simple monoacidic buffer, such as formate or acetate, the autoxidation of H4Bip at acidic pH (i.e. ≤ 3.0) leads mainly to the production of 7,8-H2Bip after isomerization of qH2Bip (Figure III.3a, b). In neutral media, however, the loss of qH2Bip side chain leading to H2Ptr is the most likely pathway (Figure III.3d, e). These data mostly agree with that is generally observed after che-

mical oxidation.[10] At intermediate pH (Figure III.3g), a mixture of both 7,8-petrins can be observed. In the presence of a buffer with chelating power such as citrate buffer, however, these rules become obsolete as shown in Figure III.3 (panels c, f, and i).

Considered together all these results still do not explain why it is 7,8-H2Bip which is predominantly excreted, in vivo.[10-12] In this context, it has been previously suggested that qH2Bip isomerization into 7,8-H2Bip is slower than the loss of the lateral chain leading to H2Ptr and that is why the isomerization only occurs when qH2Bip is stable enough not to be oxidized into H2Ptr.[22] The results of the present study obtained in formate and acetate buffers showing the stability of H2Ptr under neutral conditions with a negligible yield of 7,8-H2Bip (Figure III.3d, e) clearly invalidate this hypothesis. The results obtained herein strongly suggests that the *in vivo* microenvironment of qH2Bip should be considered to explain why DHPR-deficient patients, who cannot reduce qH2Bip to H4Bip, excrete 7,8-H2Bip and not H2Ptr. Indeed, the *in vivo* microenvironment of qH2Bip, notably its binding to hydroxylases could slow or even inhibit the loss of the alkyl side chain like that occurs with citrate ions at acidic pH (Figure III.3c).

III.6. CONCLUSIONS

The results of the present study show that qH2Bip half-lives are significantly longer than those previously reported.[20,24,25] More importantly, these results show that the apparent half-life of qH2Bip is almost always greater than that of H4Bip regardless of the type of buffer, (Table III.2). As discussed previously, this phenomenon is not surprising, since qH2Bip is the first step of autoxidation of the H4Bip. Thus, as long as there is H4Bip in the medium, there will necessarily be production of qH2Bip.

Since the half-life of qH2Bip is equivalent, even longer than that of H4Bip, it becomes obvious that any study relating to stability, quality control of H4Bip-based drugs, pharmacokinetics, or therapeutic monitoring of H4Bip supplementation should consider, henceforth, the quantification of qH2Bip. It is simply a matter of giving qH2Bip the consideration it deserves.

III.7. REFERENCES

(1) Fukuda, T. Conversion of phenylalanine into tyrosine in the silkworm larva (Bombyx mori). *Nature* **1956**, 177(4505):429-30. https://doi.10.1038/177429b0

(2) Kaufman, S. The structure of the phenylalanine-hydroxylation cofactor. *P.N.A.S.* **1963**, 50, 1085–1093. https://doi:10.1073/pnas.50.6.1085

(3) Himmelreich, N.; Blau, N.; b, Thöny, B. Molecular and metabolic bases of tetrahydrobiopterin (BH4) deficiencies. *Molecular Genetics and Metabolism* **2021**, 13, 2, 123-136. https://doi.org/10.1016/j.ymgme.2021.04.003

(4) Rilstone, J. J.; Alkhater, R. A.; and Minassian, B. A. Brain dopamine-ne-serotonin vesicular transport disease and its treatment. *N. Engl. J. Med.* **2013**, 368, 543-550. https://doi.org/10.1056/NEJMoa1207281

(5) Telegina, T. A.; Lyudnikova, T. A.; Buglak, A. A.; Vechtomova, Y. L.; Biryukov, M. V.; Demin, V. V.; Kritsky, M. S. Transformation of 6-tetrahydrobiopterin in aqueous solutions under UV-irradiation. *Journal of Photochemistry and Photobiology A: Chemistry* **2018**, 354, 155–162. https://doi.org/10.1016/j.jphotochem.2017.07.029

(6) Buglak, A. A.; Telegina, T. A. Vechtomova, Y; L.; Kritsky, M; S. Autoxidation and photooxidation of tetrahydrobiopterin: a theoretical study. *Free Radical Research* **2021**, 55, 5, 499-509. https://doi.org/10.1080/10715762.2020.1860213

(7) Cronin, S.J.F.; Seehus, C.; Weidinger, A. *et al.* The metabolite BH4 controls T cell proliferation in autoimmunity and cancer. *Nature* **2018**, 563**,** 564–568. https://doi.org/10.1038/s41586-018-0701-2

(8) Deng, C.; Wang, S.; Niu, Z.; Ye, Y.; Gao, L. Newly established LC-MS/MS method for measurement of plasma BH4 as a predictive biomarker for kidney injury in diabetes. Free Radical Biology and Medicine **2022,** 178, 1-6.

(9) Archer, M. C.; Scrimgeour, K. G. Rearrangement of Quinonoid Dihydropteridines to 7,8-Dihydropteridines. *Canadian Journal of Biochemistry* **1970**. https://doi.org/10.1139/o70-049.

(10) Kaufman, S.; Holtzman, N. A.; Milstien, S.; Butler, I. J.; Krumholz, A. Phenylketonuria Due to a Deficiency of Dihydropteridine Reductase. *N Engl J Med* **1975**, *293* (16), 785–790. https://doi.org/10.1056/NEJM197510162931601.

(11) Koslow, S. H.; Butler, I. J. Biogenic amine synthesis defect in dihydropteridine reductase deficiency. *Science* **1977**, 198(4316):522-523. doi: 10.1126/science.20665.

(12) Brennenstuhl, H.; Jung-Klawitter, S.; Assmann, B.; Opladen, T. Inherited Disorders of Neurotransmitters: Classification and Practical Approaches for Diagnosis and Treatment. *Neuropediatrics* **2019**, *50* (01), 002–014. https://doi.org/10.1055/s-0038-1673630.

(13) Jung-Klawitter, S.; Kuseyri Hübschmann, O. Analysis of Catecholamines and Pterins in Inborn Errors of Monoamine Neurotransmitter Metabolism—From Past to Future. *Cells* **2019**, *8* (8), 867. https://doi.org/10.3390/cells8080867.

(14) International Working Group on Neurotransmitter Related Disorders. Consensus guideline for the diagnosis and treatment of tetrahydrobiopterin (H4BIP) deficiencies. *Orphanet Journal of Rare Diseases* **2020**, 15(1).

(15) Fukushima, T.; Nixon, J. C. Analysis of Reduced Forms of Biopterin in Biological Tissues and Fluids. *Anal. Biochem*. **1980**, *102*, 176–188. https://doi.org/10.1016/0003-2697(80)90336-X

(16) Howells, D. W.; Hyland, K. Direct analysis of tetrahydrobiopterin in cerebrospinal fluid by high-performance liquid chromatography with redox electrochemistry: Prevention of autoxidation during storage and analysis. *Clinica Chimica Acta* **1987**, 167, 23-30. DOI: 10.1016/0009-8981(87)90081-7

(17) Guibal, P.; Lo, A.; Maitre, P.; and Moussa, F. Pterin determination in cerebrospinal fluid: state of the art. *Pteridines* **2017**, 28(2): 83–89. https://doi.org/10.1515/pterid-2017-0001

(18) Armarego, W. L. F.; Randles, D.; Taguchi, H. Peroxidase Catalysed Aerobic Degradation of 5,6,7,8-Tetrahydrobiopterin at Physiological PH. *European Journal of Biochemistry* **1983**, *135* (3), 393–403. https://doi.org/10.1111/j.1432-1033.1983.tb07666.x.

(19) Benkovic, S. J.; Sammons, D.; Armarego, W. L. F.; Waring, P.; Inners, R. Tautomeric Nature of Quinonoid 6,7-Dimethyl-7,8-Dihydro-6H-Pterin in Aqueous Solution: A Nitrogen-15 NMR Study. *J. Am. Chem. Soc.* **1985**, *107* (12), 3706–3712. https://doi.org/10.1021/ja00298a048

(20) Davis, M. D.; Kaufman, S.; Milstien, S. The Auto-Oxidation of Tetrahydrobiopterin. *European Journal of Biochemistry* **1988**, *173* (2), 345–351. https://doi.org/10.1111/j.1432-1033.1988.tb14004.x.

(21) Kirsch, M.; Korth, H.-G.; Stenert, V.; Sustmann, R.; de Groot, H. The Autoxidation of Tetrahydrobiopterin Revisited: Proof of Superoxide Formation From Reaction Of Tetrahydrobiopterin With Molecular Oxygen*. *Journal of Biological Chemistry* **2003**, *278* (27), 24481–24490. https://doi.org/10.1074/jbc.M211779200.

(22) Archer, M. C.; Vonderschmitt, D. J.; Scrimgeour, K. G. Mechanism of Oxidation of Tetrahydropterins. *Canadian Journal of Biochemistry* **2011**. https://doi.org/10.1139/o72-160.

(23) Buglak, A. A.; Telegina, T. A.; Vechtomova, Y. L.; Kritsky, M. S. Autoxidation and Photooxidation of Tetrahydrobiopterin: A Theoretical Study. *null* **2020**, 1–23. https://doi.org/10.1080/10715762.2020.1860213.

(24) Matsuura, S.; Murata, S.; Sugimoto, T. Quinonoid dihydrobiopterin, an important metabolic intermediate of biopterin cofactor in the aromatic hydroxylation of amino acids. *Tetrahedron Letters* **1986**, 27, 5, 585-588. https://doi.org/10.1016/S0040-4039(00)84047-2

(25) Haavik, J.; Flatmark. Isolation and characterization of tetrahydropterin oxidation products generated in the tyrosine 3-monooxygenase (tyrosine hydroxylase) reaction. Eur J Biochem. 1987 Oct 1;168(1):21-6. doi: 10.1111/j.1432-1033.1987.tb13381.x.

(26) Heales, S.; Hyland, K. Determination of Quinonoid Dihydrobiopterin by High-Performance Liquid Chromatography and Electrochemical Detection. *Journal of Chromatography B: Biomedical Sciences and Applications* **1989**, *494*, 77–85. https://doi.org/10.1016/S0378-4347(00)82658-4.

(27) Pearson, T.S.; Gupta, N.; San Sebastian, W.; et al. Gene therapy for aromatic L-amino acid decarboxylase deficiency by MR-guided direct delivery of AAV2-AADC to midbrain dopaminergic neurons. *Nat Commun*. **2021**;12(1):4251. https://doi.org/10.1038/s41467-021-24524-8.

(28) Batllori, M.; Molero-Luis, M.; Ormazabal, A.; Casado, M.; Sierra, C.; García-Cazorla, A.; Kurian, M.; Pope, S.; Heales, S. J.; Artuch, R. Analysis of Human Cerebrospinal Fluid Monoamines and Their Cofactors by HPLC. *Nat Protoc* **2017**, *12* (11), 2359–2366. https://doi.org/10.1038/nprot.2017.103.

(29) Fismen, L.; Eide, T.; Djurhuus, R.; Svardal, A. M. Simultaneous quantification of tetrahydrobiopterin, dihydrobiopterin, and biopterin by liquid chromatography coupled to electrospray tandem mass spectrometry**.** *Analytical Biochemistry* **2012**, 430, 163–170.

(30) Allegri, G.; Costa Netto, H. J. B.; Ferreira Gomes, L. N. L.; Costa de Oliveira, M. L.; Scalco, F. B.; de Aquino Neto, F. R. Determination of Six Pterins in Urine by LC–MS/MS. *Bioanalysis* **2012**, *4* (14), 1739–1746. https://doi.org/10.4155/bio.12.131.

(31) Arning, E.; Bottiglieri, T. LC-MS/MS Analysis of Cerebrospinal Fluid Metabolites in the Pterin Biosynthetic Pathway. In *JIMD Reports, Volume 29*; Morava, E., Baumgartner, M., Patterson, M., Rahman, S., Zschocke, J., Peters, V., Eds.; JIMD Reports; Springer: Berlin, Heidelberg, **2016**; pp 1–9. https://doi.org/10.1007/8904_2014_336.

(32) Burton, C.; Shi, H.; Ma, Y. Development of a high-performance liquid chromatography – tandem mass spectrometry urinary pterinomics workflow. *Analytica Chimica Acta* **2016**, 927, 72-81. DOI: 10.1016/j.aca.2016.05.005

(33) Xiong, X.; Liu, Y. Chromatographic behavior of 12 polar pteridines in hydrophilic interaction chromatography using five different HILIC columns coupled with tandem mass spectrometry. *Talanta* **2016**, 150, 493-502. DOI: 10.1016/j.talanta.2015.12.066

(34) Galla, Z.; Rajda, C.; Rácz, G.; Grecsó, N.; Baráth, Á.; Vécsei, L.; Bereczki, C.; Monostori, P. Simultaneous determination of 30 neurologically and metabolically important molecules: A sensitive and selective way to measure tyrosine and tryptophan pathway metabolites and other biomarkers in human serum and cerebrospinal fluid. . J Chromatogr A. **2021**, 1635:461775. https://doi.org/10.1016/j.chroma.2020.461775

(35) Galla, Z.; Rácz, G.; Grecsó, N.; Baráth, Á.; Kósa, M.; Bereczki, C.; Monostori, P. Improved LC-MS/MS method for the determination of 42 neurologically and metabolically important molecules in urine. J Chromatogr B Analyt Technol Biomed Life Sci. **2021** Jun 25;1179:122846. https://doi.org/10.1016/j.jchromb.2021.122846.

(36) Alhajji, E.; Boulghobra, A.; Bonose, M.; Berthias, F.; Moussa, F.; Maître, P. Multianalytical Approach for Deciphering the Specific MS/MS Transition and Overcoming the Challenge of the Separation of a Transient Intermediate, Quinonoid Dihydrobiopterin. Anal. Chem. **2022**. https://doi.org/10.1021/acs.analchem.2c00924

(37) Espenson, J. H. *Chemical Kinetics and Reaction Mechanisms*; McGraw-Hill: Primis Custom: New York, **2002**.

(38) McNaught, A. D. (comp); International Union of Pure and Applied Chemistry, O. (United K. eng; Wilkinson, A. (comp). Compendium of Chemical Terminology. IUPAC Recommendations. **1997**.

(39) Guibal, P.; Lévêque, N.; Doummar, D.; Giraud, N.; Roze, E.; Rodriguez, D.; Couderc, R.; Billette De Villemeur, T.; Moussa, F. Simultaneous Determination of All Forms of Biopterin and Neopterin in Cerebrospinal Fluid. *ACS Chem. Neurosci.* **2014**, *5* (7), 533–541. https://doi.org/10.1021/cn4001928.

(40) Lo, A.; Guibal, P.; Doummar, D.; Rodriguez, D.; Hautem, J.-Y.; Couderc, R.; Billette De Villemeur, T.; Roze, E.; Chaminade, P.; Moussa, F. Single-Step Rapid Diagnosis of Dopamine and Serotonin Metabolism Disorders. *ACS Omega* **2017**, *2* (9), 5962–5972. https://doi.org/10.1021/acsomega.7b01008.

III.8. SUPPORTING INFORMATION

LC-MS/MS to revisit the autoxidation of tetrahydrobiopterin: giving quinonoid dihydrobiopterin the consideration it deserves

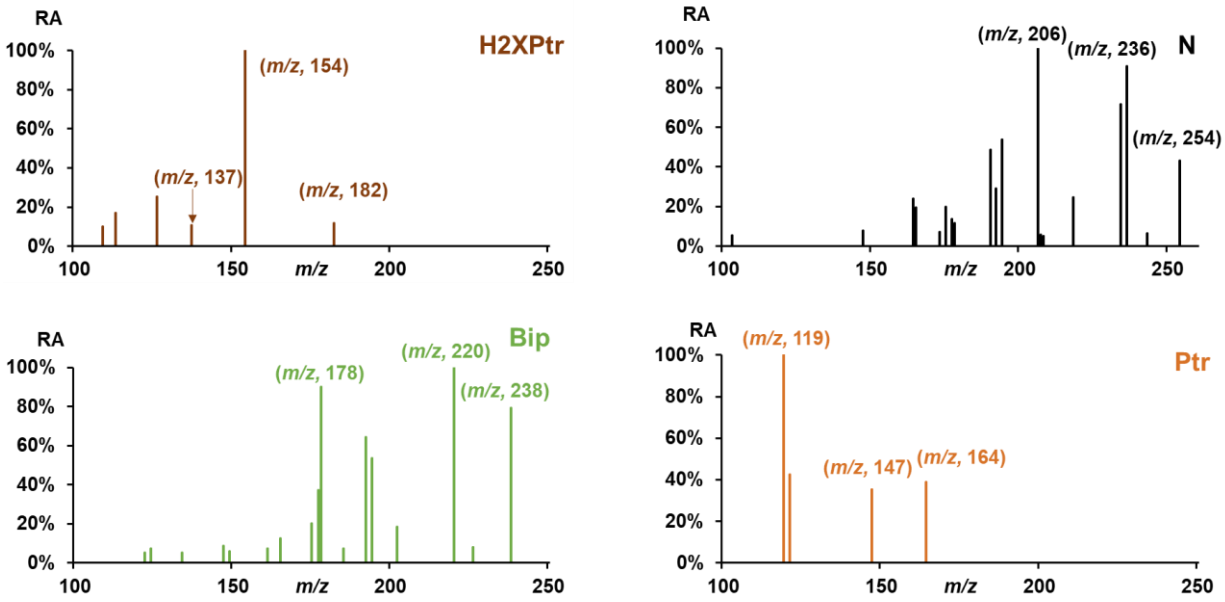

Figure III.4: MS/MS spectra of H2XPtr, N (Neopterin), Bip, and Ptr. RA: Relative abundance

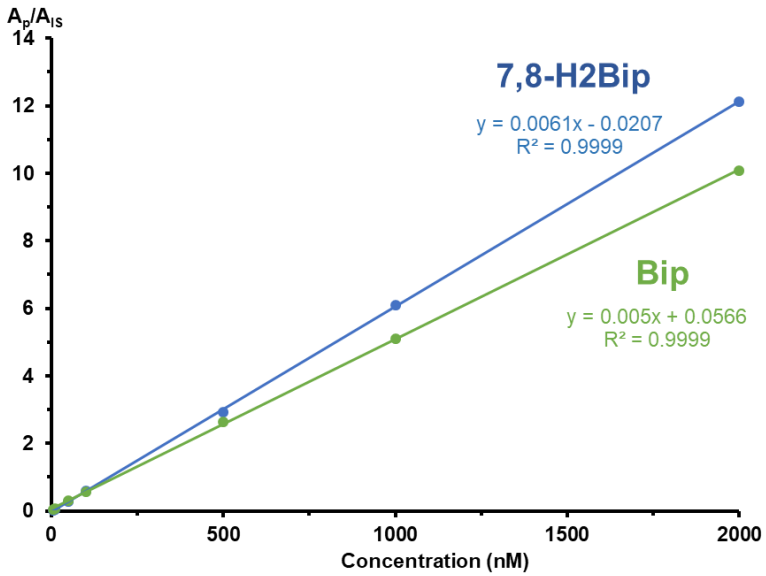

Figure III.5: Linearity validation for 7,8-H2Bip and Bip

Table III.3: Repeatability validation for 7,8-H2Bip and Bip

7,8-H2Bip		Bip	
Concentration (nM)	RSD (n = 6)	Concentration (nM)	RSD (n = 6)
5	3.7%	50	1.7%
50	0.6%	100	0.9%
100	0.3%	500	2.4%
500	0.8%	1000	0.6%
1000	0.6%	2000	0.8%
2000	0.9%		

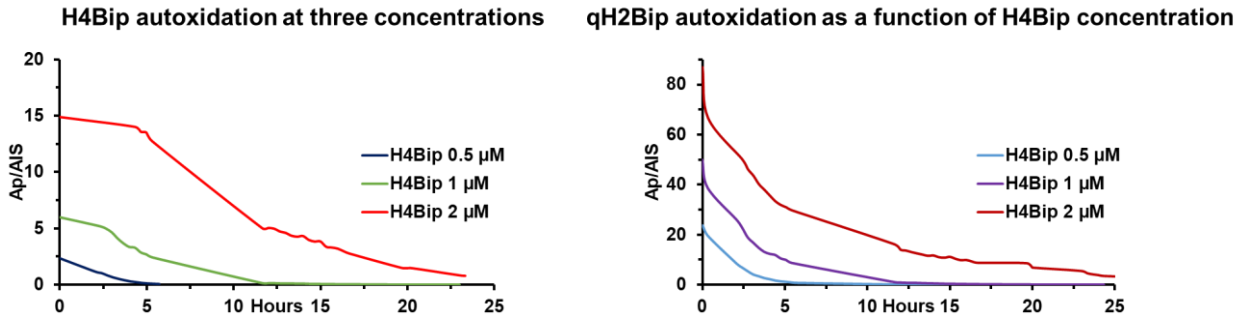

Figure III.6: H4Bip and qH2Bip autoxidation kinetics as a function of H4Bip concentration

Table SI2: H4Bip and qH2Bip kinetic parameters as a function of H4Bip concentration

	H4Bip		qH2Bip	
H4Bip concen-tration (µM)	**Half-life (min)**	Time interval (hours)	**Half-life (min)**	Time interval (hours)
0.5	**85**	0.3 - 3.4	**66**	0.3 - 5.8
	53	3.4 - 5.8		
1	**193**	0.7 - 5.4	**129**	0.7 - 14.3
	107	5.4 - 14.3		
2	**299**	3.4 - 12.0	**406**	3.4 - 23.3
	245	12.0 – 23.3		

CHAPITRE 4 : UNE METHODE RAPIDE ET SENSIBLE POUR LA QUANTIFICATION DES METABOLITES DE LA DOPAMINE ET DE LA SEROTONINE DANS LE LIQUIDE CEPHALORACHIDIEN

IV.1. PRESENTATION DE L'ARTICLE

Après avoir mis au point une méthode indicatrice de stabilité pour le suivi de l'auto-oxydation de la tétrahydrobioptérine, nous nous sommes intéressés au dosage des métabolites de la dopamine et de la sérotonine. En effet, le diagnostic des erreurs innées du métabolisme repose sur la quantification de ces biomarqueurs dans le liquide céphalorachidien, en particulier l'acide homovanillique, la 3-*ortho*-méthyl-DOPA, le 3-méthoxy-4-hydroxy-phényl-glycol, le hydroxy-tryptophane et l'acide 5-hydroxy-indole acétique. Dans l'article qui suit, nous proposons une nouvelle méthode basée sur la chromatographie liquide ultrahaute performance couplée à une détection par fluorescence pour quantifier ces cinq analytes dans le liquide céphalorachidien. Cette méthode sépare efficacement les cinq molécules en moins de 10 minutes. Il s'agit d'une méthode facile à mettre en place en routine clinique et basée sur un instrument peu coûteux.

La méthode proposée a été validée en termes de linéarité, d'exactitude, de précision, d'effet matrice et de limite basse de quantification. En fonction du composé, les limites basses de quantification obtenues sont entre 1 nM et 5 nM, permettant de doser des concentrations aussi basses que dans le liquide céphalorachidien. Par ailleurs, l'applicabilité de la méthode a été vérifiée sur 10 échantillons de liquide céphalorachidien. Les résultats obtenus ont montré une capacité de la méthode à différencier clairement les échantillons sains des échantillons pathologiques, démontrant ainsi, sa pertinence pour le diagnostic des erreurs innées du métabolisme de la dopamine et de la sérotonine. Par conséquent, la méthode de chromatographie liquide ultra-haute performance couplée à la détection par fluorescence est une alternative fiable au standard actuel basé sur une détection électrochimique.

Statut de l'article : Publié

Journal : Journal of chromatography B

A rapid and sensitive method for the quantification of dopamine and serotonin metabolites in cerebrospinal fluid based on UHPLC with fluorescence detection

Ayoub Boulghobra, Myriam Bonose, Isabelle Billault, Antoine Pallandre

Affiliation

Institut de Chimie Physique, Université Paris-Saclay, CNRS UMR 8000, 91405, Université Paris Saclay, France

IV.2. ABSTRACT

Inborn errors of dopamine and serotonin metabolism are diseases caused by deficiencies in enzymes belonging to metabolic pathways. The specific diagnosis of these inborn illnesses is based on the identification and quantification of biomarkers in cerebrospinal fluid (CSF), especially: 5-hydroxy-tryptophane (5-HTP), 5-hydroxy-indol-acetic acid (5-HIAA), 3-ortho-methyl-DOPA (3-OMD), homovanillic acid (HVA) and 3-methoxy-4-hydroxyphenylglycol (MHPG). In the present work, we propose a novel ultrahigh performance liquid chromatography (UHPLC) method coupled to fluorescence detection (FD) to quantify simultaneously the five dopamine and serotonin metabolites. This method efficiently separates the five molecules in less than 10 minutes. A complete validation of the proposed method was performed in terms of accuracy, linearity, precision, and lower limit of quantification (LLOQ). Depending on the compound, the obtained LLOQs are between 1 nM and 5 nM, thus allowing to measure concentrations as low as in CSF samples. We also verified the method applicability by analyzing 10 CSF samples in triplicates. The obtained results showed satisfactory repeatability and an ability of this method to clearly distinguish healthy samples from pathologic samples, hence, demonstrating, the method suitability for diagnosing inborn errors of dopamine and serotonin

metabolism. Therefore, the proposed UHPLC-FD method appears as a reliable alternative to the current gold standard for the quantification of these biomarkers, which is based on UHPLC coupled to electrochemical detection (ECD).

IV.3. INTRODUCTION

Inherited disorders of dopamine and serotonin metabolism are rare inborn errors of monoamine neurotransmitter biosynthesis and catabolism [1]. They result from single gene variants. These genes encode enzymes involved in dopamine and serotonin metabolic pathways, or proteins in neurotransmitter transport [2].

Dopamine brain neurotransmission pathways are mainly involved in the initiation and regulation of movement [3–5] whereas serotonin pathways are essential for mood regulation [6, 7]. Therefore, clinical symptoms resulting from inherited disorders of dopamine and serotonin metabolisms correspond to movement disorders such as dystonia and parkinsonian syndrome, sleep disorders, , and/or mental retardation [8–10].

Since the majority of inherited disorders of dopamine and serotonin metabolism lead to the reduction of brain transmission mediated by these two neurotransmitters, resulting neurological symptoms are similar regardless of the enzyme gene affected by the mutation [11–15]. Consequently, clinical diagnosis of each inherited disorder of metabolism is difficult. Moreover, this diagnosis is of paramount importance because the treatment of each mutation is unique [2, 16]. The treatment relies mainly on supplementation with a missing metabolite.

Given the complexity of diagnosing dopamine and serotonin inherited metabolic disorders only on clinical symptoms basis, cerebrospinal fluid (CSF) biomarkers have been identified [17]. The biomarkers correspond to metabolites produced from dopamine and serotonin biochemical pathways during the biosynthesis or the degradation of these two neurotransmitters [17]. Indeed, in these disorders, the mutation of the gene encoding an enzyme causes the inactivation of the latter. It leads to the modification of brain metabolite concentrations. Such molecules

have to be eliminated from the brain towards CSF. It has been shown that the brain and CSF concentrations are directly correlated, thus, the reliability of these biomarkers in diagnosing inborn errors of dopamine and serotonin metabolism [18–21].

Quantifying these compounds in CSF is a key element for an early diagnosis of dopamine and serotonin inherited metabolic disorders [22, 23]. There are mostly two groups of CSF biomarkers for these diseases [17, 20, 22, 24]: cofactors like biopterins and metabolites. In the present work, we focused on dopamine and serotonin metabolites (Figure IV.1) since they are robust biomarkers, especially: homovanillic acid (HVA), 5-hydroxyindoleacetic acid (5-HIAA), 3-orthomethyl-DOPA (3-OMD), 5-hydroxy-tryptophan (5-HTP) and 3-methoxy-4-hydroxyphenylglycol (MHPG) [17, 22, 24]. As shown in Figure IV.1, 5-HIAA and 5-HTP are serotonin metabolites, and HVA, 3-OMD, and MHPG are dopamine ones. Variations in the concentrations of these five compounds have been observed in numerous inborn errors of serotonin and dopamine metabolism (Table IV.1) [22, 25].

Currently, the standard techniques to quantify these five biomarkers in CSF are ultrahigh performance liquid chromatography coupled to electrochemical detection (UHPLC-ECD) or to tandem mass spectrometry (MS/MS) [17, 24, 26–29]. These methods allow for the quantification of the five metabolites in CSF within a single run. Since these biomarkers are at a minimum concentration of 10 nM in the CSF of patients [17, 24, 30], we aim to put forward a reliable and easy-to-handle alternative detection to ECD and to MS/MS. For this purpose, we propose a novel UHPLC with fluorescence detection (FD) method for the quantification of dopamine and serotonin metabolites. This work allows to compare FD to ECD, especially in terms of lower limit of quantification (LLOQ).

Table IV.1: Variations in CSF neurotransmitter metabolites' concentrations in inborn errors of serotonin and dopamine metabolism, adapted from [26].

Enzyme defect	**HVA**	**5-HIAA**	**HVA/5-HIAA**	**3-OMD**	**5-HTP**	**MHPG**
GTPCH	↓	↓	↓	N	N	↓
PTPS	↓	↓	N	N	N	↓
PCD	N	N	N	N	N	N
DHPR	↓	↓	N	N	N	↓
SR	↓	↓	N	N	N	↓
TH	↓	N	↓	N	N	↓
AADC	↓	↓	↓	↑	↑	↓
DTDS	↑	N	↑	N	N	N

GTPCH (guanosine triphosphate-cyclohydrolase autosomal recessive deficiency), PTPS (6-pyruvoyl-tetrahydropterin synthase deficiency), PCD (pterin-4α-carbinolamine dehydratase deficiency), DHPR (dihydropteridine reductase deficiency), SR (sepiapterin reductase deficiency), TH (tyrosine hydroxylase deficiency), AADC (aromatic amino acids decarboxylase deficiency), DTDS (dopamine transporter deficiency syndrome), N (physiological concentration), ↑ (higher concentration than the physiological one) and ↓ (lower concentration than the physiological one).

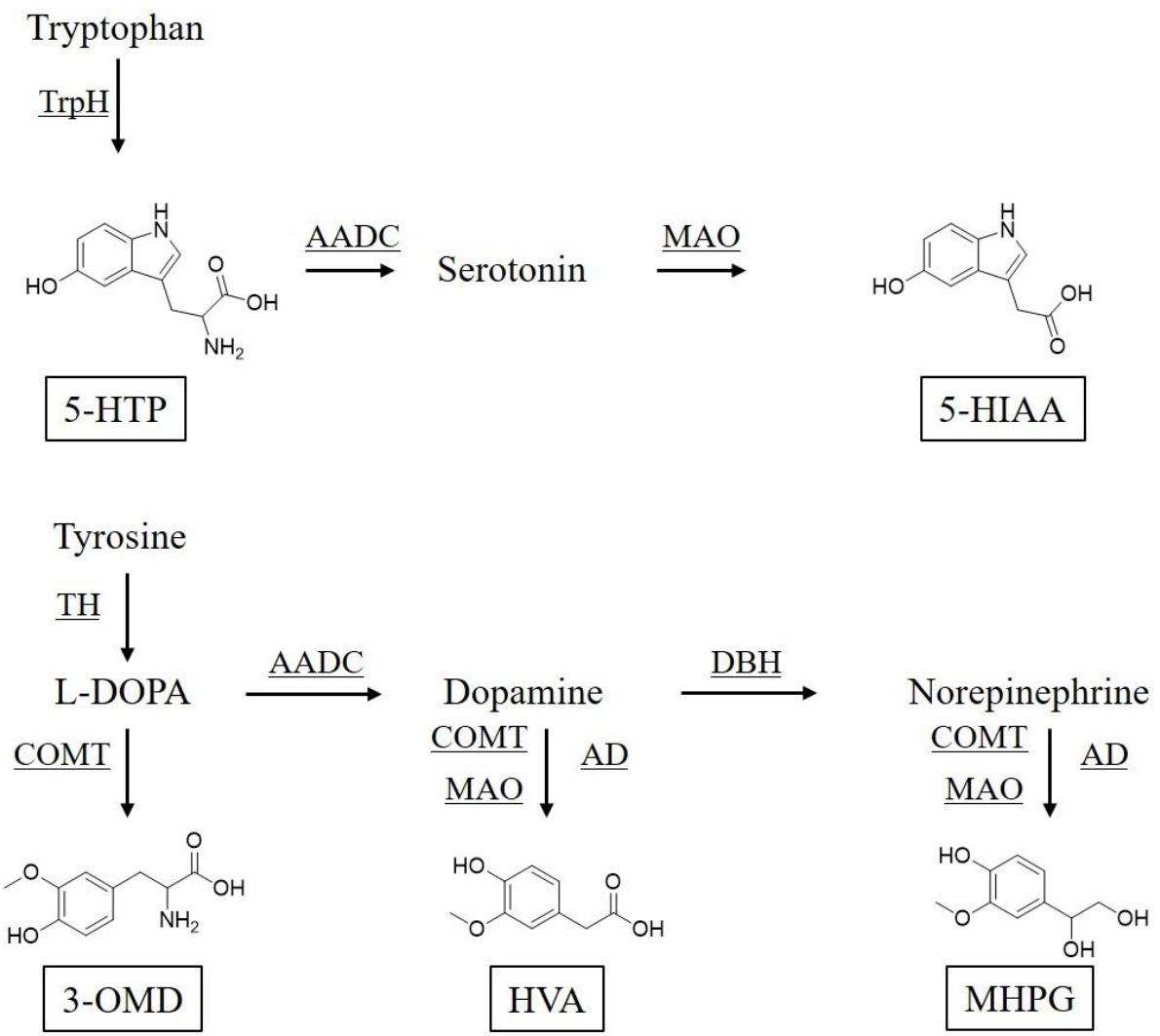

Figure IV.1: Serotonin and dopamine metabolism pathways, adapted from [17].

TrpH (Tryptophan hydroxylase), 5-HTP (5-hydroxytryptophan), AADC (aromatic amino acid decarboxylase), MAO (monoamine oxidase), 5-HIAA (5-hydroxyindole acetic acid), TH (Tyrosine hydroxylase), L-DOPA (L-dihydroxyphenylalanine), COMT (catechol-O-methyl transferase), 3-OMD (3-ortho-methyl-DOPA), AD (aldehyde dehydrogenase), HVA (homovanillic acid), DBH (Dopamine β-hydroxylase) and MHPG (3-methoxy-4-hydroxyphenylglycol).

IV.4. EXPERIMENTAL SECTION

Reagents: Water was obtained from a LabWater purification system (Veolia). Methanol was HPLC grade (Carlo Erba). Formic acid was 99% purity (Carlo Erba). The standards of HVA (purity ≥ 97%), 5-HIAA (purity ≥ 98%), 5-HTP (purity ≥ 98%), 3-OMD (purity ≥ 98%), and MHPG as a hemipiperazinium salt (purity ≥ 98%) were purchased from Sigma (Germany) and were used without further purification.

Materials: The fluorimeter used to measure the excitation and emission spectra was a Horiba Fluoromax. Preliminary HPLC-FD analyses were carried out on a Dionex HPLC system connected to a Jasco FP 920 fluorescence detector. For HPLC coupled to PDA detection, we used a ThermoScientific Ultimate 3000 system. UHPLC-FD separations were carried out on a Shimadzu Nexera LC-40 system with an RF-20A Shimadzu fluorescence detector.

Calibration standards and quality control samples: Stock solutions of each metabolite of interest were prepared from weighed standards and solubilized in ultrapure water. Stock solutions were aliquoted and stored at -20°C. Working solutions correspond to a mixture of the stock solutions of the five biomarkers, diluted in 0.05 M, pH 5.4 ammonium formate/ methanol (97/3; v/v) to obtain a final concentration of 10 µM. The obtained working solution was then diluted in artificial cerebrospinal fluid [31] to prepare the calibration standards.

Quantification of the analytes in CSF samples was made according to calibration curves obtained in artificial cerebrospinal fluid, to be certain that endogenous metabolites would not skew the quantification results.

Quality control samples (QC) were prepared by mixing and diluting stock solutions in artificial cerebrospinal fluid [31].

CSF samples: CSF samples were collected between 2019 and 2020 by lumbar puncture as part of classical diagnostic procedure at Armand-Trousseau hospital, Paris, France. Indeed, in the present article, we studied the CSF remaining after the biochemical and microbiological analysis, that is why, in accordance with the French Code de la Santé Publique, no approval

by ethical committee is needed. The study was conducted in accordance with the methodology MR-004 of the French Commission national de l'informatique et des libertés. Written informed consent of parents or legal representatives was obtained prior to sample collection. The patients included were children with neurological symptoms, namely, epilepsy, movement disorders, and/or severe cephalalgia. Patients were excluded, if there was a traumatic lumbar puncture with observed blood in the CSF sample and/or if samples were inadequately stored. CSF samples were frozen immediately after collection with liquid nitrogen and then stored at -80°C. These samples were collected from patients aged between 9 days and 17.6 years.

Internal standard choice: In order to choose the most versatile internal standard (IS), four molecules were preliminarily selected because of their structural similarity to dopamine and serotonin metabolites: 4-hydroxy-benzoic acid, gallic acid, 2-hydroxy-phenyl acetic acid, and 4-hydroxy-phenyl acetic acid. Gallic acid was excluded since it eluted at the void time. 4-hydroxy-benzoic acid exhibited a lack of fluorescence emission, that is why it was not chosen. 4-hydroxy-phenyl acetic acid coeluted with 5-HTP, thus, it was excluded. 2-hydroxy-phenyl acetic acid (HPA) met all the criteria since it was correctly separated from the analytes with a resolution factor (Rs) of 3.3 and it emitted at the same λex/λem combinations as the five biomarkers.

Sample preparation: Sample preparation consisted in diluting calibration standards, QC samples, standard addition samples, and CSF samples (1/1, v/v) in a 1 µM solution of HPA in the mobile phase. The obtained solution was filtered on a 5000 Da molecular weight cutoff (MWCO) PES Vivaspin filter (Sartorius) by centrifugation (20 min at 12 000 G, 4°C). The filtrate was then injected in the UHPLC system.

Liquid chromatography method: UHPLC separation was performed with C18 UPLC HSS T3 (100 x 2.1; 1.8 µm) column (Waters) which is adapted to the retention of polar molecules. The mobile phase was a mixture of ammonium formate 0.05 M, pH 5.4/ methanol (97/3; v/v) used at a flow rate of 0.4 mL/min. The column temperature was maintained at 30°C, and the injection volume was of 10 µL. The analysis time was of 10 minutes.

Fluorescence detection: FD was performed in multi-channel mode by using λex = 280 nm and four λem simultaneously: 310 nm, 320 nm, 330 nm, and 340 nm. This allows to measure an emission profile for each biomarker. The fluorescence cell was maintained at 15°C.

Method validation: The proposed UHPLC-FD method was validated according to the guideline of bioanalytical method validation of the European medicine agency (EMA) [32].

Method specificity relies on both retention factor and fluorescence profile. The linearity of the method was validated with at least eleven levels in the concentration range between LLOQ and 4000 nM. Six measurements were done at each level and at three different days. HPA was used as IS at a constant concentration of 500 nM.

Accuracy was determined by performing six independent measurements per level at four concentration levels corresponding to the LLOQ, three times the LLOQ (low QC), 1000 nM (medium QC) and 4000 nM (high QC). These determinations were performed in six different sets of analyses by changing the operator and/or the day. Recoveries corresponding to the ratio of the calculated concentration to the theoretical one, were determined. The UHPLC-FD method precision was validated within-run and between-run on the same concentration levels as accuracy by calculating relative standard deviation (RSD) at each level. LLOQ for each biomarker corresponds to the lowest concentration where linearity, accuracy, and precision are validated.

Matrix effect was verified by performing standard additions to a CSF pool. The use of a CSF pool is justified by the fact that, for authentic CSF samples, the available volume is not sufficient for standard addition experiment. Five concentration levels were measured with six replicates per level. Matrix factors were calculated for each concentration. They correspond to the ratio of the IS-normalized peak area in the presence of matrix, to the IS-normalized peak area in the absence of matrix. Carry-over effect was checked by analyzing blank samples consisting in the mobile phase immediately after the 4000 nM concentration standard.

Sample stability was verified on QC samples. These samples were analyzed six times per level at four concentration levels. The same samples were reanalyzed following the same procedure

after 24 hours at 4°C, away from the light, in the auto-sampler rack. Recoveries were determined before and after the storage time.

IV.5. Results and Discussion

IV.5.1. Fluorescence detection

FD relies on choosing the matching excitation and emission wavelengths. To determine the optimum λex, we realized the absorption spectra of each serotonin and dopamine metabolite (Figure S3). These spectra were obtained with a PDA module after UHPLC separation of a standard solution. They show that all of the compounds of interest have similar absorption profiles. Indeed, there is one absorption band with a maximum between 274 nm and 280 nm regardless of the biomarker. The second step consisted in determining the optimal emission wavelength. For this purpose, we recorded emission spectra with λex = 280 nm (Figure IV.2). These emission spectra indicate that dopamine metabolites, namely HVA, MHPG, and 3-OMD emit almost 8 times less than serotonin metabolites, considering their respective emission maxima. Excitation spectra confirm that λex = 280 nm is satisfactory for the five biomarkers. Moreover, the maximum emission wavelength for HVA, MHPG, and 3-OMD is 312-313 nm, while it is 337 nm for 5-HTP and 349 nm for 5-HIAA.

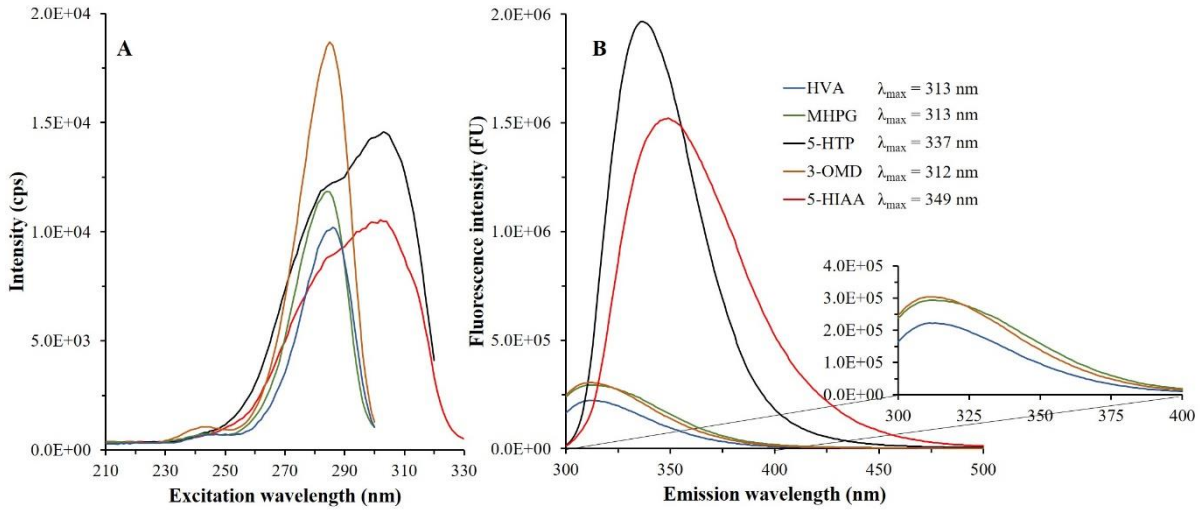

Figure IV.2: Excitation (A) and emission (B) spectra of serotonin and dopamine metabolites measured from standard solutions at a concentration of 1000 nM in the mobile phase used for chromatographic separation. The emission spectra were determined with λ_{ex}=280 nm. The excitation spectra were measured at maximum emission wavelength of each compound.

IV.5.2. Separation conditions

The metabolites of dopamine and serotonin are low hydrophobic acidic compounds, that are usually separated in reversed-phase liquid chromatography by using a C18 column adapted to the analysis of polar molecules. Thus, an ACQUITY UPLC HSS T3 column (100 x 2.1; 1.8 µm) was chosen for the separation of these molecules.

Concerning the elution mode, isocratic mode was selected as it is the most adapted for routine analysis because of its simplicity, and it does not require any additional equilibration time.

To reach a rapid and efficient separation of the biomarkers, we tested several ammonium formate based mobile phases, in which we adjusted the aqueous phase pH at 2.8, 5.0, 5.2, 5.4, 5.6, and 7.4 and the proportion of methanol at 1%, 3%, and 5%, respectively (Figure S.2). The pKa of each biomarker are as follows: HVA (3.7), 5-HIAA (4.2), 3-OMD (1.8 for the carboxylic acid function and 9.3 for the amino function), 5-HTP (2.2 for the carboxylic acid function and 9.2 for the amino function). MHPG does not exhibit any ionizable function in the studied pH range. 3-OMD and 5-HTP are in zwitterionic form in the studied pH range, and MHPG is not ionized, that is why pH variation weakly influences their retention. Moreover, for 5-HIAA and HVA, the pKa are included in the studied pH range. Therefore, pH strongly influences the ionized proportions and the retentions of both analytes. The fastest separation was performed

at a pH of 5.4 with 3% of methanol, that is why this mobile phase was selected for further studies (Figure S.2).

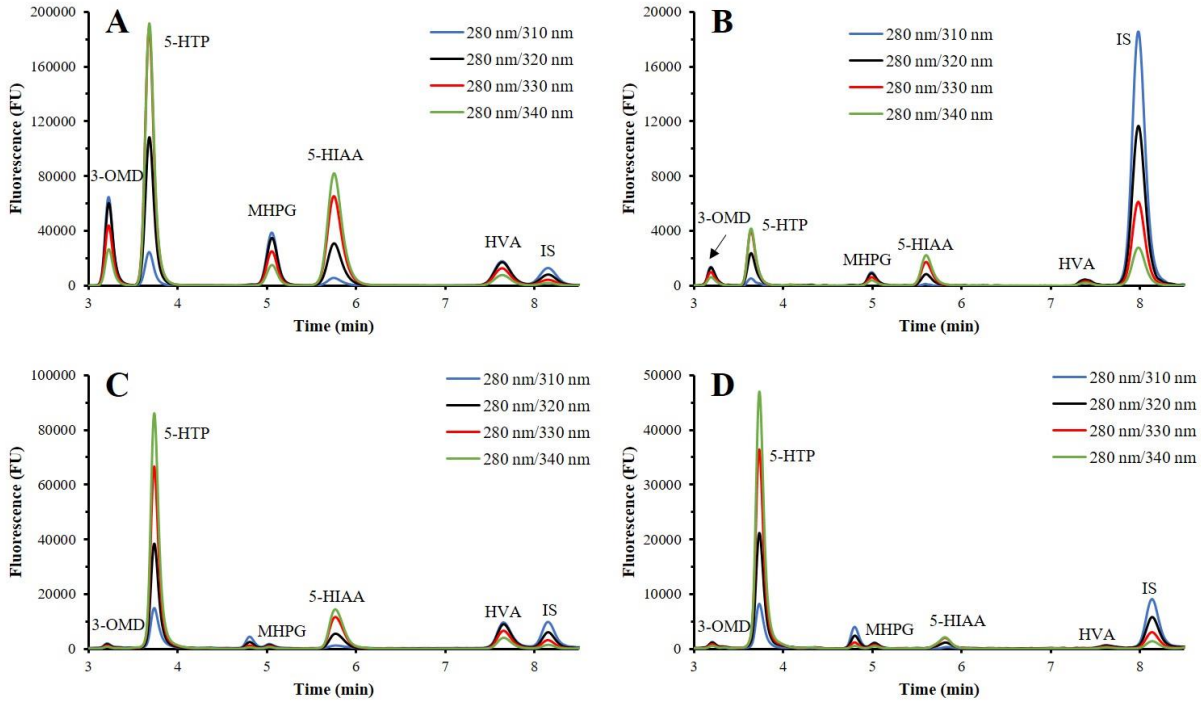

Figure IV.3: Chromatograms obtained with the presented UHPLC-FD method: (A) medium QC, (B) 10 nM calibration solution, (C) normal CSF sample collected from a 1.5-years old person and (D) pathological CSF sample collected from a 17.6-years old patient with suspected guanosine triphosphate cyclohydrolase deficiency.

Figure IV.3 shows the proposed UHPLC-FD method allows the separation of the five serotonin and dopamine metabolites in less than 10 minutes. We verified the absence of endogenous interferences by analyzing authentic CSF samples. Figure IV.3C and Figure IV.3D indicate the five biomarkers and the IS are separated from CSF endogenous molecules since no coelution is observed. Therefore, by combining both retention factors and fluorescence profiles, the UHPLC-FD method allowed for the specific quantification of dopamine and serotonin metabolites.

Preliminary analysis of the five standards showed they are quantifiable at concentrations as low as 10 nM (Figure IV.3B). Thus, the obtained method can be validated. Moreover, thanks to the detection of four different fluorescence channels, we simultaneously analyzed

the five dopamine and serotonin metabolites to measure their respective LLOQs. Based on the signal-to-noise ratio (S/N), the optimum λem for the analysis of dopamine-derived compounds is 330 nm (Table S1). For 5-HIAA and 5-HTP, quantification was performed at λem of 340 nm. λem = 350 nm was also tested, and it did not exhibit significantly higher fluorescence than 340 nm.

IV.5.3. Method validation

Method validation aims to provide evidence that the obtained results during routine analysis are close enough to the true concentration in a sample. For the proposed UHPLC-FD method, we validated the following parameters: accuracy, precision, linearity, LLOQ, matrix effect, and carry-over. For this analytical method validation, all the measured solutions correspond to a mixture of the five biomarkers. The concentration ranges have been chosen depending on the CSF levels of each metabolite [22,24].

To ensure the linearity of the proposed method, in accordance with the EMA guideline of bioanalytical method validation [32], thanks to the linear model, we back-calculated concentrations for each run, and we estimated recoveries in relation to theoretical concentrations. All the recoveries were in the range 100+/-15% and 100+/-20% for the LLOQs. In addition to the guideline requirements, we compared the experimental error variance with the lack of fit variance by using a variance comparison Fisher-Snedecor test. If the two variances are not statistically different from one another ($P > 0.05$), it indicates that the chosen linear model fits [33,34]. Linearity was then validated for the five analytes of interest between the LLOQ and 4000 nM (Figure IV.4).

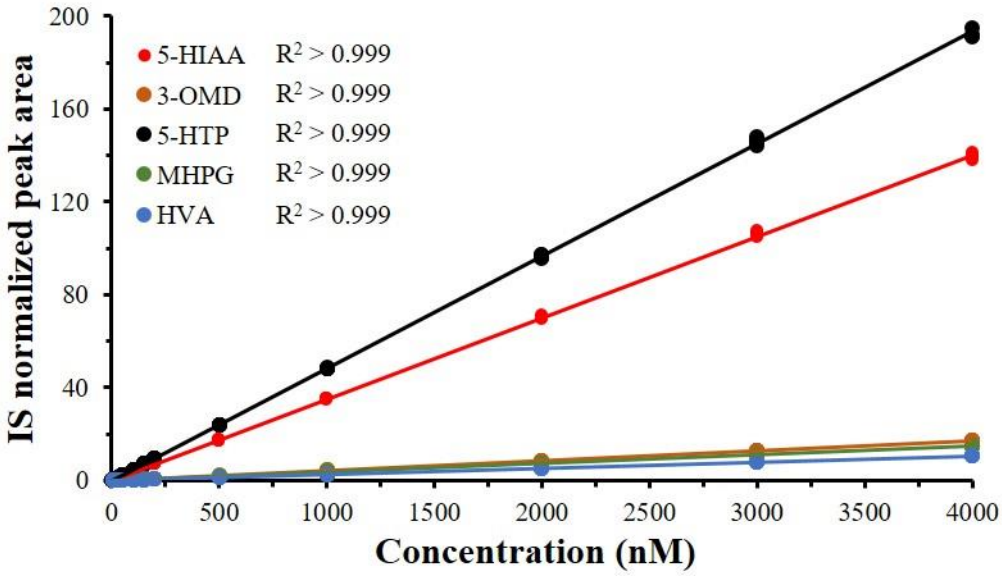

Figure IV.4: Linearity for the five biomarkers of interest between the LLOQ and 4000 nM in calibration solutions by the proposed UHPLC-FD method.

To observe a possible matrix effect of the presented method, standard addition experiment was performed on a CSF pool with added concentrations ranging between 0 and 2000 nM (Table IV.2). Table IV.2 shows matrix factors were all in the range of 1 +/- 0.15, indicating that the matrix effect was negligible for the proposed UHPLC-FD method.

Sample stability was determined on QC samples by comparing recoveries before and after a 24-hours storage time at 4°C in the dark. Regardless of the analyte, all recoveries were in the 100 +/- 15% range, whether before or after the storage time. Thus, dopamine and serotonin metabolites appear stable in the proposed storage conditions for at least 24 hours.

Table IV.2: Matrix effect validation results of the UHPLC-FD method for 5-HIAA, 3-OMD, 5-HTP, MHPG and HVA quantification.

Standard addition experiment										
Added concentration (nM)	5-HIAA		3-OMD		5-HTP		MHPG		HVA	
	MF	RSD (%)	**MF**	RSD (%)	**MF**	RSD (%)	**MF**	RSD (%)	**MF**	RSD (%)
0	**0.86**	1.0	**1.00**	1.5	**0.88**	2.6	**0.94**	2.7	**0.86**	1.2
100	**0.87**	0.4	**0.91**	0.3	**0.88**	1.1	**0.96**	0.5	**0.88**	0.5
200	**0.94**	0.6	**0.96**	0.7	**1.04**	0.6	**0.99**	0.9	**0.94**	0.5
400	**1.08**	0.6	**1.10**	0.3	**1.13**	0.7	**1.13**	0.8	**1.06**	0.4
1000	**0.93**	0.6	**0.95**	0.3	**0.96**	0.7	**0.96**	0.6	**0.94**	0.3
2000	**0.95**	0.6	**0.97**	0.4	**0.98**	0.8	**0.97**	0.6	**0.95**	0.3

MF: Matrix factor: ratio of the IS-normalized peak area in the presence of matrix, to the IS-normalized peak area in the absence of matrix.

To validate the accuracy of the method, we analyzed six sets of six replicates for each QC sample. As indicated in Table IV.3, the obtained recoveries were between 80-120% for the LLOQs and between 85-115% for the other concentrations. Table IV.3 shows the proposed UHPLC-FD method meets the requirements of the guideline of bioanalytical method validation [32]. Hence, accuracy is validated for all of our five compounds.

For precision validation, based on the same six sets of six replicates as for accuracy, we calculated RSDs for QC samples (Table IV.3). The measured variation appears acceptable for the five biomarkers regardless of the concentration level, since RSDs are lower than 20% for the LLOQ and lower than 15% for the other concentrations [32].

The LLOQs that can be reached by the proposed UHPLC-FD method correspond to the lowest concentration where linearity, accuracy, and precision are validated. These LLOQs are summarized in Table IV.4 and compared with the ones obtained by Akiyama et al. in HPLC-FD [35], by Galla et al. in HPLC-MS/MS [29], and by Lo et al. in UHPLC-ECD [24], after considering injection volumes. Table IV.4 shows that FD, whether in HPLC or in UHPLC, is suitable for IEM diagnosis since the LLOQs are lower than the lowest metabolite concentration which can be found in CSF and that, regardless of the biomarker.

Table IV.3: Accuracy and precision validation results of the UHPLC-FD method for 3-OMD, 5-HTP, MHPG, 5-HIAA and HVA quantification.

			Accuracy		**Precision**	
Analyte	Level	Concentration (nM)	Intra-day recovery (%) (n = 6)	Inter-day recovery (%) (n = 6 x 6)	Intra-day RSD (%) (n = 6)	Inter-day RSD (%) (n = 6 x 6)
5-HIAA	LLOQ	1	112.5	111.3	2.3	2.2
	3LLOQ	3	97.2	96.1	1.9	1.4
	Medium	1000	103.6	104.5	1.0	1.4
	High	4000	100.3	99.3	1.1	1.1
HVA	LLOQ	5	99.8	97.5	3.1	2.1
	3LLOQ	15	104.8	102.4	2.0	2.5
	Medium	1000	112.9	110.1	0.6	1.8
	High	4000	105.4	104.4	1.1	0.5
5-HTP	LLOQ	1	95.1	92.2	3.0	1.0
	3LLOQ	3	99.2	103.0	1.8	3.2
	Medium	1000	105.7	107.5	1.0	1.8
	High	4000	103.3	102.4	1.0	1.0
3-OMD	LLOQ	1	108.6	110.8	5.1	1.1
	3LLOQ	3	102.8	104.7	4.0	0.9
	Medium	1000	110.4	110.9	0.7	1.0
	High	4000	105.7	105.6	1.1	0.4
MHPG	LLOQ	2.5	95.1	92.6	3.7	1.1
	3LLOQ	7.5	103.1	98.1	2.8	4.4
	Medium	1000	100.1	99.8	0.8	1.6
	High	4000	93.5	94.8	1.1	1.4

Table IV.4: Comparison of the LLOQs of serotonin and dopamine metabolites obtained by HPLC-FD [35], UHPLC-ECD [24], LC-MS/MS [29] and the proposed UHPLC-FD method after taking into account the injection volume.

	LLOQ values (**femtomoles**)

Analyte	HPLC-FD	HPLC-MS/MS	UHPLC-ECD	**UHPLC-FD**
5-HIAA	80	75	500	**10**
HVA	320	300	750	**50**
5-HTP	/	15	250	**10**
3-OMD	320	15	250	**10**
MHPG	5000	15	250	**25**
Injection volume	20 µL	15 µL	50 µL	**10 µL**
Chromatographic run time	20 min	20 min	10 min	**10 min**

The proposed method reaches lower LLOQs for the five metabolites of interest for an analysis time of 10 minutes versus 20 minutes for the HPLC-FD method [35]. Indeed, thanks to the transfer from HPLC to UHPLC and to the use of the latest-generation FD, lower LLOQs are obtained in the present study. Besides, Akiyama et al. [35] performed separation using acetonitrile as eluting solvent, whereas methanol was used in the proposed method. Methanol being less eluting in reversed-phase liquid chromatography; separation is achieved by using a higher proportion than with acetonitrile which allows for fluorescence enhancement. Moreover, the HPLC-FD method [35] is based on elution gradient, whereas the UHPLC-FD method is in isocratic mode, which is faster since it does not require any extra equilibration time, thus, more suitable for routine analysis. Furthermore, the proposed UHPLC-FD method reaches lower LLOQs than those reported by Lo et al. [24] obtained by UHPLC-ECD. Indeed, for example, the proposed method allows to quantify amounts 50 times lower for 5-HIAA and 15 times lower for HVA.

Compared to the HPLC-MS/MS method described by Galla et al. [29], the present UHPLC-FD method reaches lower LLOQs for all dopamine and serotonin metabolites, except for MHPG, whose LLOQ is lower by HPLC-MS/MS. However, the method proposed by Galla et al. simultaneously quantifies 30 molecules in 20 minutes which is a definite advantage.

Therefore, FD appears as the most sensitive detector in order to quantify dopamine and serotonin metabolites. Besides, it should be noted that the LLOQs reached in UHPLC-ECD [24] and in HPLC-MS/MS [29] are obtained with an injection volume of 50 and 15 microliters, res-

pectively; whereas in the presented UHPLC-FD method, the injection volume is only 10 microliters. That is of great importance since CSF samples are precious, and analysts need a certain volume to perform complementary analysis. Consequently, the proposed method is more sensitive than HPLC-FD [35], HPLC-MS/MS [29], and UHPLC-ECD [24], and it allows to use less CSF sample volume.

IV.5.4. Application to CSF samples

Given that the presented UHPLC-FD method was validated, we verified its applicability to authentic CSF samples. For this purpose, we analyzed 10 CSF samples obtained from 10 patients. Two of the obtained chromatograms (Figure IV.3C and D) show that the five metabolites are well separated and they can be quantified. The obtained quantification results for the analyzed CSF samples are summarized in Figure IV.5. Each concentration corresponds to a mean of a set of three measures. RSD was calculated for each set of analyses to evaluate the variability of the method on CSF samples. All the obtained RSDs are lower than 10% regardless of the quantified biomarker, indicating the method repeatability is satisfactory on authentic CSF samples. The measured concentrations were compared to the age-dependent physiologic concentrations (dashed lines in Figure IV.5) in order to establish a diagnosis.

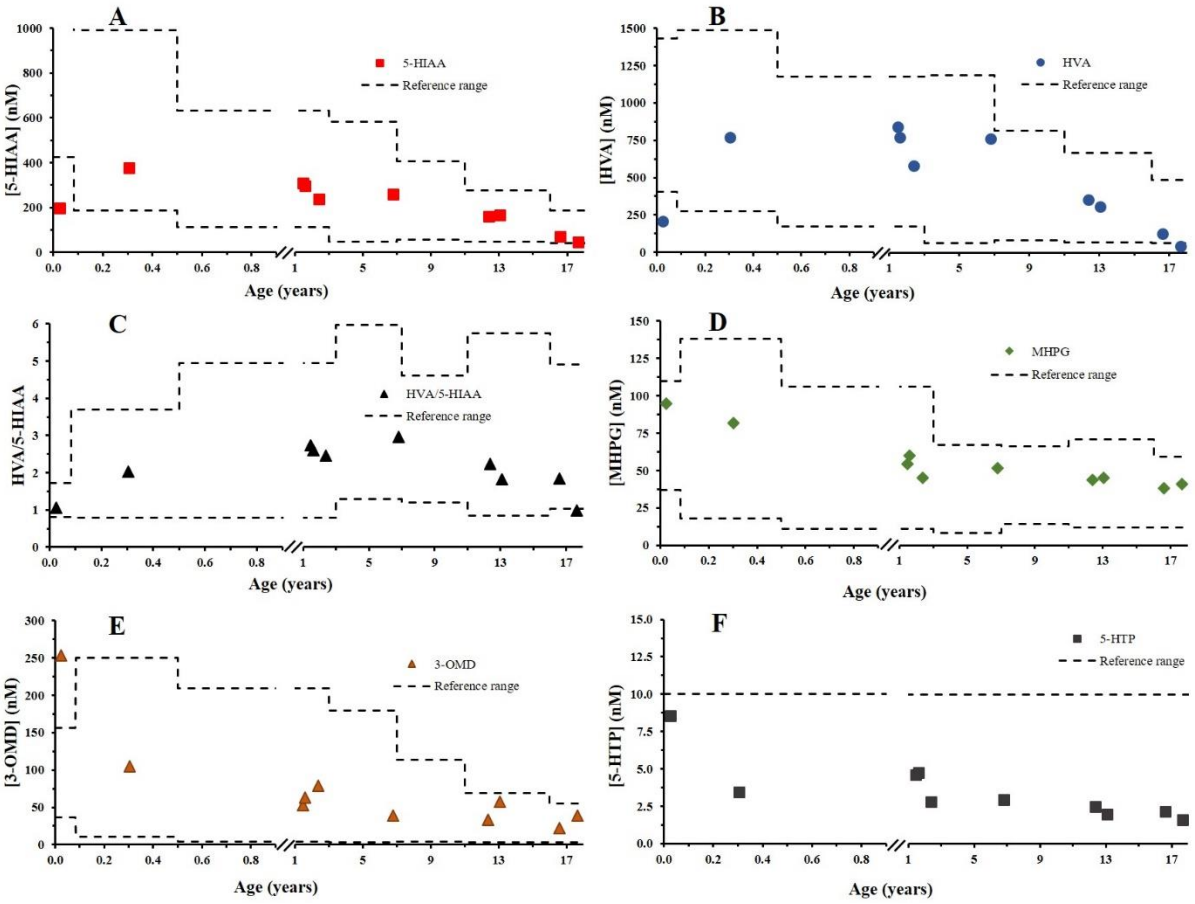

Figure IV.5: Concentrations of dopamine and serotonin metabolites in CSF samples obtained by the presented UHPLC-FD method and age-dependent reference ranges described by Lo et al. [25] for 5-HIAA, HVA, HVA/5-HIAA, MHPG and 3-OMD and by Hyland et al. for 5-HTP [23].
Dashed lines correspond to reference ranges.

Figure IV.5 indicates the presented UHPLC-FD method is suitable for dopamine and serotonin metabolites quantification in CSF for diagnostic purpose. Furthermore, the measured concentrations in 10 CSF samples were compared to reference values of each biomarker [22,24], in order to establish a probable diagnosis. In all the analyzed samples, the concentrations of biomarkers are in the physiologic norms except in two CSF samples. For the first one, the patient is a nine-days-old infant whose CSF has low levels of 5-HIAA and HVA and a high level of 3-OMD [24]. The probable diagnosis appears to be aromatic amino acids decarboxylase (AADC) deficiency. The second pathological sample corresponds to a 17.6-years-old patient with low levels of 5-HIAA, HVA, and HVA/5-HIAA, which corresponds to the metabolic profile of guanosine triphosphate cyclohydrolase (GTPCH) deficiency. Therefore, the proposed

UHPLC-FD method can differentiate between pathological samples and healthy samples. Hence, its suitability for inborn errors of dopamine and serotonin metabolism diagnosis.

IV.6. CONCLUSION

We developed a simple and sensitive UHPLC-FD method for the simultaneous quantification of five inborn errors of metabolism biomarkers. With these chromatographic conditions, efficient separation is achieved in less than 10 minutes. The method underwent a complete validation according to the EMA guideline on bioanalytical method validation. This method has sufficiently LLOQs ranging between 1 and 5 nM, and it allows to reliably quantify these biomarkers in CSF samples. It enables to distinguish between healthy samples and pathological ones. Therefore, the method diagnostic suitability was established.

The proposed UHPLC-FD method appears as a reliable alternative to UHPLC-ECD and to HPLC-MS/MS methods for analyzing CSF samples as part of the diagnosis of inherited disorders of metabolism, especially considering that the proposed method enables to use only 10 microliters of CSF sample, which is five times less than the method validated in UHPLC-ECD. The small volume consumption is a major improvement since CSF is commonly used for complementary analysis.

IV.7. REFERENCES

[1] B.K. Burton, Inborn Errors of Metabolism in Infancy: A Guide to Diagnosis, PEDIATRICS. 102 (1998) e69–e69. https://doi.org/10.1542/peds.102.6.e69.

[2] H. Brennenstuhl, S. Jung-Klawitter, B. Assmann, T. Opladen, Inherited Disorders of Neurotransmitters: Classification and Practical Approaches for Diagnosis and Treatment, Neuropediatrics. 50 (2019) 002–014. https://doi.org/10.1055/s-0038-1673630.

[3] U. Ungerstedt, M. Herrera-Marschitz, T. Zetterström, Dopamine Neurotransmission and Brain Function, in: R.M. Buijs, P. Pévet, D.F. Swaab (Eds.), Chemical Transmission in the Brain: The Role of Amines, Amino Acids and Peptides, Elsevier, 1982: pp. 41–49. https://doi.org/10.1016/S0079-6123(08)64189-8.

[4] D. Vallone, R. Picetti, E. Borrelli, Structure and function of dopamine receptors, Neuroscience and Biobehavioral Reviews. (2000) 8.

[5] J.-M. Beaulieu, R.R. Gainetdinov, The Physiology, Signaling, and Pharmacology of Dopamine Receptors, Pharmacol Rev. 63 (2011) 182–217. https://doi.org/10.1124/pr.110.002642.

[6] E.J. Van Bockstaele, D.M. Cestari, V.M. Pickel, Synaptic structure and connectivity of serotonin terminals in the ventral tegmental area: potential sites for modulation of mesolimbic dopamine neurons, Brain Research. 647 (1994) 307–322. https://doi.org/10.1016/0006-8993(94)91330-7.

[7] D.L. Murphy, A.M. Andrews, C.H. Wichems, Q. Li, M. Tohda, B. Greenberg, Brain serotonin neurotransmission: An overview and update with an emphasis on serotonin subsystem heterogeneity, multiple receptors, interactions with other neurotransmitter systems, and consequent implications for understanding the actions of serotonergic drugs, The Journal of Clinical Psychiatry. 59 (1998) 4–12.

[8] M.A. Kurian, P. Gissen, M. Smith, S.J. Heales, P.T. Clayton, The monoamine neurotransmitter disorders: an expanding range of neurological syndromes, The Lancet Neurology. 10 (2011) 721–733. https://doi.org/10.1016/S1474-4422(11)70141-7.

[9] M.A. Kurian, Y. Li, J. Zhen, E. Meyer, N. Hai, H.-J. Christen, G.F. Hoffmann, P. Jardine, A. von Moers, S.R. Mordekar, F. O'Callaghan, E. Wassmer, E. Wraige, C. Dietrich, T. Lewis, K. Hyland, S.J. Heales, T. Sanger, P. Gissen, B.E. Assmann, M.E. Reith, E.R. Maher, Clinical and molecular characterisation of hereditary dopamine transporter deficiency syndrome: an

observational cohort and experimental study, The Lancet Neurology. 10 (2011) 54–62. https://doi.org/10.1016/S1474-4422(10)70269-6.

[10] J. Ng, A. Papandreou, S.J. Heales, M.A. Kurian, Monoamine neurotransmitter disorders—clinical advances and future perspectives, Nat Rev Neurol. 11 (2015) 567–584. https://doi.org/10.1038/nrneurol.2015.172.

[11] T. Opladen, G. Hoffmann, F. Hörster, A.-B. Hinz, K. Neidhardt, C. Klein, N. Wolf, Clinical and biochemical characterization of patients with early infantile onset of autosomal recessive GTP cyclohydrolase I deficiency without hyperphenylalaninemia, Movement Disorders. 26 (2011) 157–161. https://doi.org/10.1002/mds.23329.

[12] L. Bonafé, B. Thöny, J.M. Penzien, B. Czarnecki, N. Blau, Mutations in the Sepiapterin Reductase Gene Cause a Novel Tetrahydrobiopterin-Dependent Monoamine-Neurotransmitter Deficiency without Hyperphenylalaninemia, The American Journal of Human Genetics. 69 (2001) 269–277. https://doi.org/10.1086/321970.

[13] V. Leuzzi, C. Carducci, C. Carducci, S. Pozzessere, A. Burlina, R. Cerone, D. Concolino, M. Donati, L. Fiori, C. Meli, A. Ponzone, F. Porta, P. Strisciuglio, I. Antonozzi, N. Blau, Phenotypic variability, neurological outcome and genetics background of 6-pyruvoyl-tetrahydropterin synthase deficiency, Clinical Genetics. 77 (2010) 249–257. https://doi.org/10.1111/j.1399-0004.2009.01306.x.

[14] M.A. Willemsen, M.M. Verbeek, E.-J. Kamsteeg, J.F. de Rijk-van Andel, A. Aeby, N. Blau, A. Burlina, M.A. Donati, B. Geurtz, P.J. Grattan-Smith, M. Haeussler, G.F. Hoffmann, H. Jung, J.B. de Klerk, M.S. van der Knaap, F. Kok, V. Leuzzi, P. de Lonlay, A. Megarbane, H. Monaghan, W.O. Renier, P. Rondot, M.M. Ryan, J. Seeger, J.A. Smeitink, G.C. Steenbergen-Spanjers, E. Wassmer, B. Weschke, F.A. Wijburg, B. Wilcken, D.I. Zafeiriou, R.A. Wevers, Tyrosine hydroxylase deficiency: a treatable disorder of brain catecholamine biosynthesis, Brain. 133 (2010) 1810–1822. https://doi.org/10.1093/brain/awq087.

[15] C. Manegold, G.F. Hoffmann, I. Degen, H. Ikonomidou, A. Knust, M.W. Laaß, M. Pritsch, E. Wilichowski, F. Hörster, Aromatic l-amino acid decarboxylase deficiency: clinical features, drug therapy and follow-up, Journal of Inherited Metabolic Disease. 32 (2009) 371–380. https://doi.org/10.1007/s10545-009-1076-1.

[16] J.-M. Saudubray, À. Garcia-Cazorla, Inborn Errors of Metabolism Overview: Pathophysiology, Manifestations, Evaluation, and Management, Pediatric Clinics. 65 (2018) 179–208. https://doi.org/10.1016/j.pcl.2017.11.002.

[17] S. Jung-Klawitter, O. Kuseyri Hübschmann, Analysis of Catecholamines and Pterins in Inborn Errors of Monoamine Neurotransmitter Metabolism—From Past to Future, Cells. 8 (2019) 867. https://doi.org/10.3390/cells8080867.

[18] M. Stanley, L. Traskman-Bendz, K. Dorovini-Zis, Correlations between aminergic metabolites simultaneously obtained from human CSF and brain, Life Sciences. 37 (1985) 1279–1286. https://doi.org/10.1016/0024-3205(85)90242-5.

[19] P. Wester, U. Bergström, A. Eriksson, C. Gezelius, J. Hardy, B. Winblad, Ventricular Cerebrospinal Fluid Monoamine Transmitter and Metabolite Concentrations Reflect Human Brain Neurochemistry in Autopsy Cases, Journal of Neurochemistry. 54 (1990) 1148–1156. https://doi.org/10.1111/j.1471-4159.1990.tb01942.x.

[20] K. Hyland, R.A.H. Surtees, S.J.R. Heales, A. Bowron, D.W. Howells, I. Smith, Cerebrospinal Fluid Concentrations of Pterins and Metabolites of Serotonin and Dopamine in a Pediatric Reference Population, Pediatric Research. 34 (1993) 10–14. https://doi.org/10.1203/00006450-199307000-00003.

[21] C.M. Banki, G. Molnár, Cerebrospinal fluid 5-hydroxyindoleacetic acid as an index of central serotonergic processes, Psychiatry Research. 5 (1981) 23–32. https://doi.org/10.1016/0165-1781(81)90057-3.

[22] K. Hyland, Clinical Utility of Monoamine Neurotransmitter Metabolite Analysis in Cerebrospinal Fluid, Clinical Chemistry. 54 (2008) 633–641. https://doi.org/10.1373/clinchem.2007.099986.

[23] I.P. Kema, E.G.E. de Vries, F.A.J. Muskiet, Clinical chemistry of serotonin and metabolites, Journal of Chromatography B: Biomedical Sciences and Applications. 747 (2000) 33–48. https://doi.org/10.1016/S0378-4347(00)00341-8.

[24] A. Lo, P. Guibal, D. Doummar, D. Rodriguez, J.-Y. Hautem, R. Couderc, T. Billette De Villemeur, E. Roze, P. Chaminade, F. Moussa, Single-Step Rapid Diagnosis of Dopamine and Serotonin Metabolism Disorders, ACS Omega. 2 (2017) 5962–5972. https://doi.org/10.1021/acsomega.7b01008.

[25] C.E.M. Hollak, R. Lachmann, Inherited Metabolic Disease in Adults: A Clinical Guide, Oxford University Press, 2016.

[26] A. Ormazabal, A. García-Cazorla, Y. Fernández, E. Fernández-Álvarez, J. Campistol, R. Artuch, HPLC with electrochemical and fluorescence detection procedures for the diagnosis of inborn errors of biogenic amines and pterins, Journal of Neuroscience Methods. 142 (2005) 153–158. https://doi.org/10.1016/j.jneumeth.2004.08.007.

[27] J. Bicker, A. Fortuna, G. Alves, A. Falcão, Liquid chromatographic methods for the quantification of catecholamines and their metabolites in several biological samples—A review, Analytica Chimica Acta. 768 (2013) 12–34. https://doi.org/10.1016/j.aca.2012.12.030.

[28] S. Parrot, P.-C. Neuzeret, L. Denoroy, A rapid and sensitive method for the analysis of brain monoamine neurotransmitters using ultra-fast liquid chromatography coupled to electrochemical detection, Journal of Chromatography B. 879 (2011) 3871–3878. https://doi.org/10.1016/j.jchromb.2011.10.038.

[29] Z. Galla, C. Rajda, G. Rácz, N. Grecsó, Á. Baráth, L. Vécsei, C. Bereczki, P. Monostori, Simultaneous determination of 30 neurologically and metabolically important molecules: A sensitive and selective way to measure tyrosine and tryptophan pathway metabolites and other biomarkers in human serum and cerebrospinal fluid, Journal of Chromatography A. 1635 (2021) 461775. https://doi.org/10.1016/j.chroma.2020.461775.

[30] J. Van Der Heyden, J. Rotteveel, R. Wevers, Decreased homovanillic acid concentrations in cerebrospinal fluid in children without a known defect in dopamine metabolism, European Journal of Paediatric Neurology. 7 (2003) 31–37. https://doi.org/10.1016/S1090-3798(02)00137-X.

[31] J.H. An, Y. Su, T. Radman, M. Bikson, Effects of glucose and glutamine concentration in the formulation of the artificial cerebrospinal fluid (ACSF), Brain Research. 1218 (2008) 77–86. https://doi.org/10.1016/j.brainres.2008.04.007.

[32] Bioanalytical method validation, European Medicines Agency. (2018). https://www.ema.europa.eu/en/bioanalytical-method-validation (accessed March 28, 2021).

[33] P. Araujo, Key aspects of analytical method validation and linearity evaluation, Journal of Chromatography B. 877 (2009) 2224–2234. https://doi.org/10.1016/j.jchromb.2008.09.030.

[34] A.G. González, M.Á. Herrador, A practical guide to analytical method validation, including measurement uncertainty and accuracy profiles, TrAC Trends in Analytical Chemistry. 26 (2007) 227–238. https://doi.org/10.1016/j.trac.2007.01.009.

[35] T. Akiyama, Y. Hayashi, Y. Hanaoka, T. Shibata, M. Akiyama, K. Nakamura, Y. Tsuyusaki, M. Kubota, H. Yoshinaga, K. Kobayashi, Simultaneous measurement of monoamine metabolites and 5-methyltetrahydrofolate in the cerebrospinal fluid of children, Clinica Chimica Acta. 465 (2017) 5–10. https://doi.org/10.1016/j.cca.2016.12.005.

IV.8. SUPPORTING INFORMATION

A rapid and sensitive method for the quantification of dopamine and serotonin metabolites in cerebrospinal fluid based on UHPLC with fluorescence detection

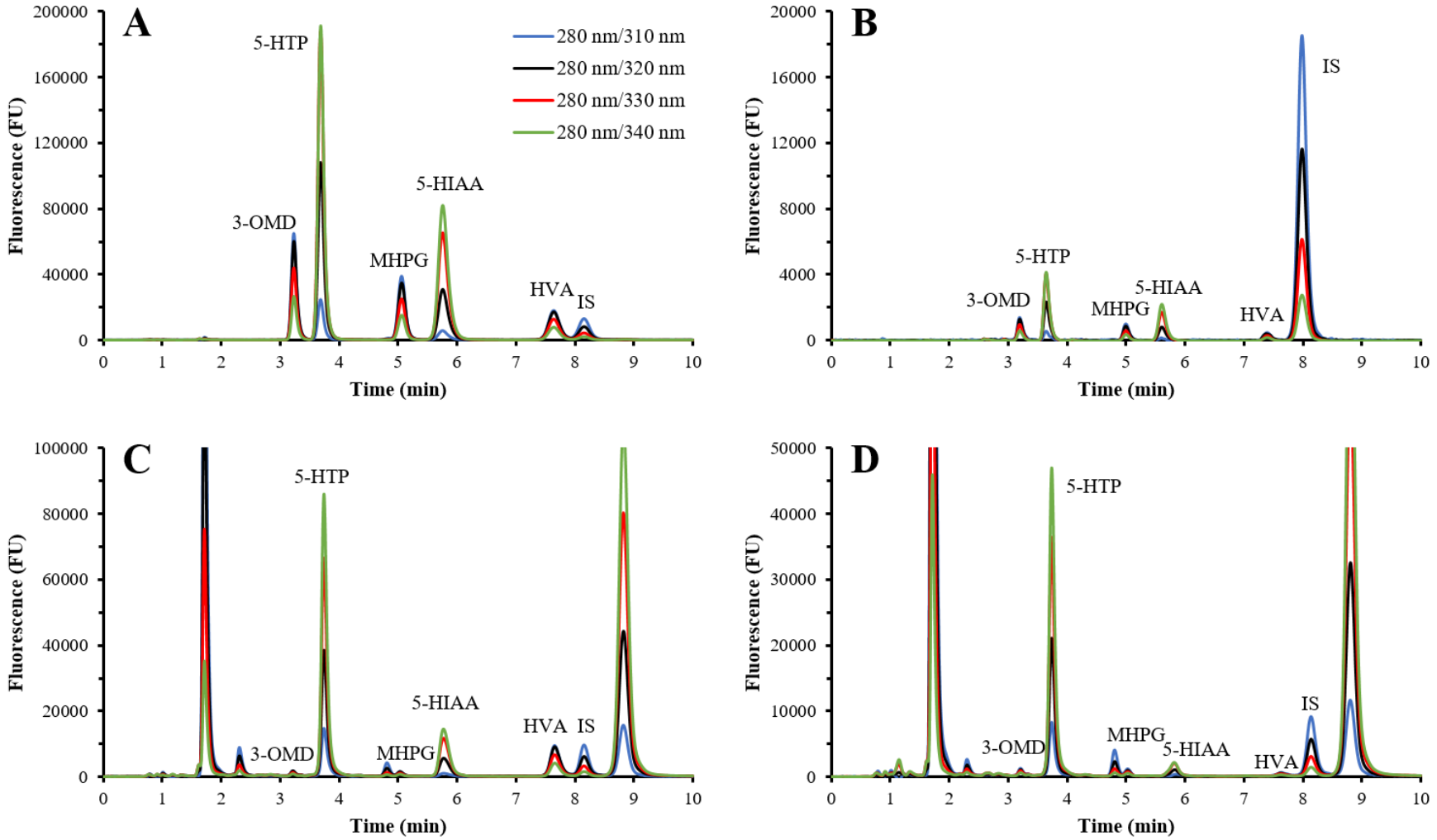

Figure IV.6: Full chromatograms obtained with the presented UHPLC-FD method: (A) medium QC, (B) 10 nM calibration solution, (C) normal CSF sample collected from a 1.5-years old person and (D) pathological CSF sample collected from a 17.6-years old patient with suspected guanosine triphosphate cyclohydrolase deficiency.

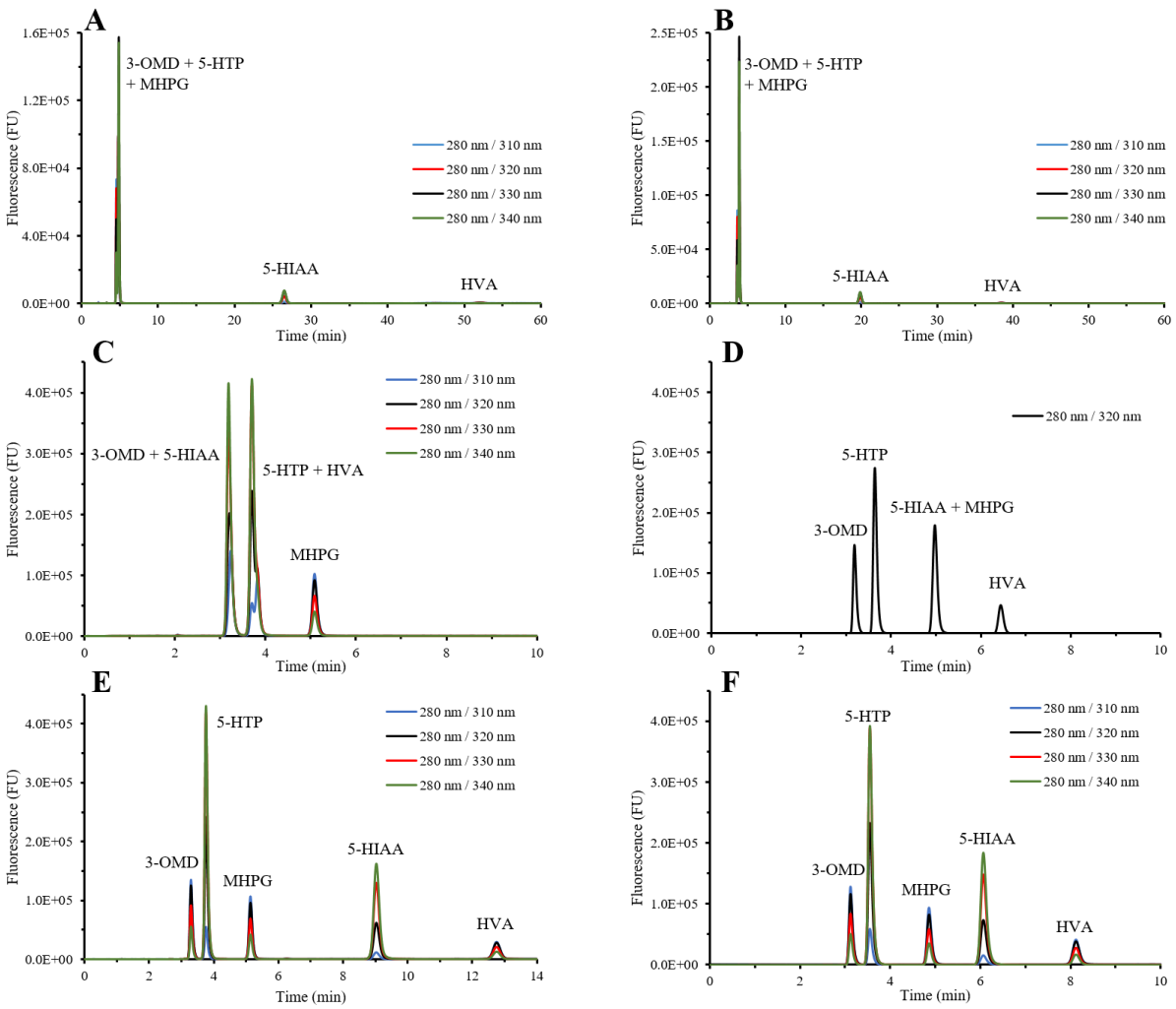

Figure IV.7: Chromatograms obtained as part of method development with various mobile phases: (A) 50 mM pH 2.8 ammonium formate / methanol (97/3, v/v), (B) 50 mM pH 2.8 ammonium formate / methanol (95/5, v/v), (C) 50 mM pH 7.4 ammonium formate / methanol (97/3, v/v), (D) 50 mM pH 5.6 ammonium formate / methanol (97/3, v/v), (E) 50 mM pH 5.0 ammonium formate / methanol (97/3, v/v), (F) 50 mM pH 5.2 ammonium formate / methanol (97/3, v/v)

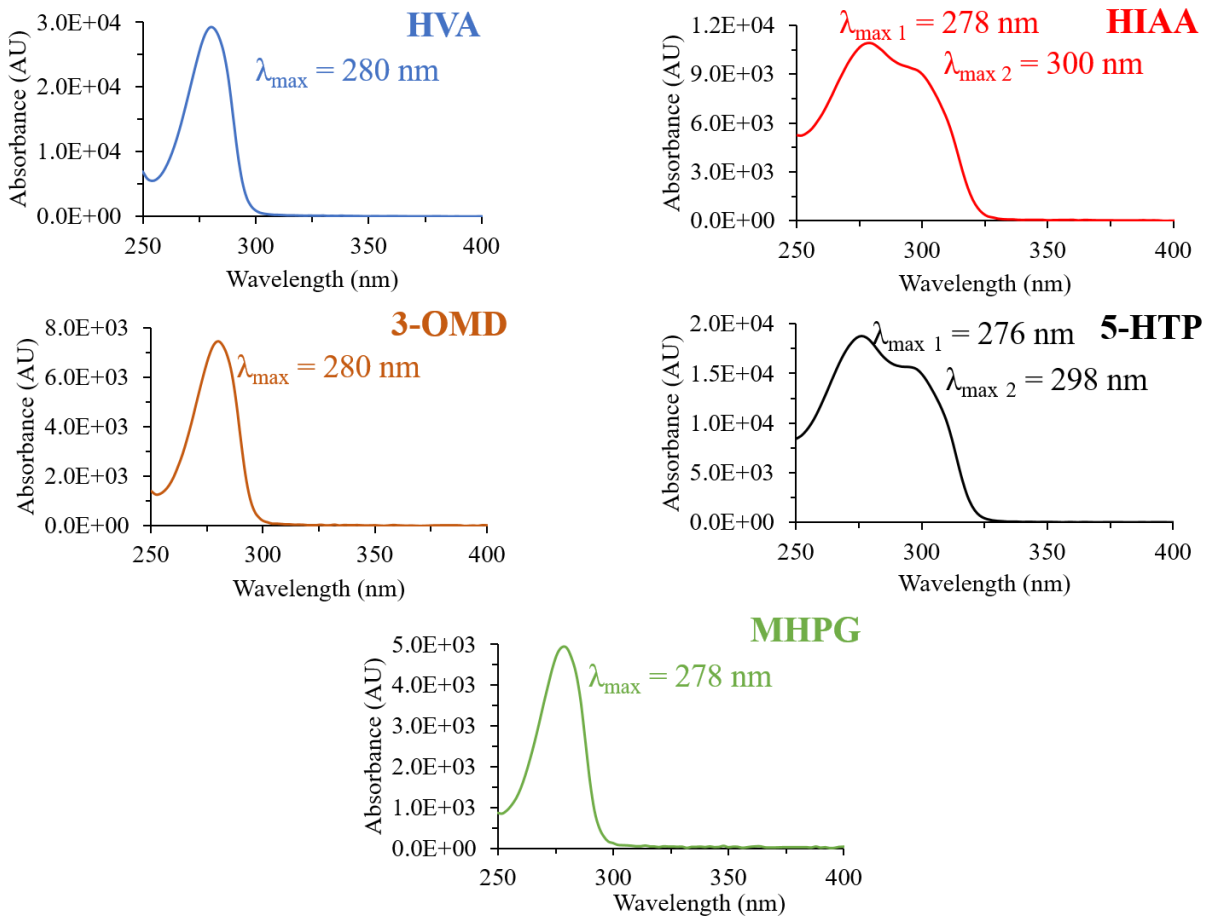

Figure IV.8: Absorption spectra of 5-HTP, 5-HIAA, 3-OMD, MHPG and HVA, obtained with a PDA module.

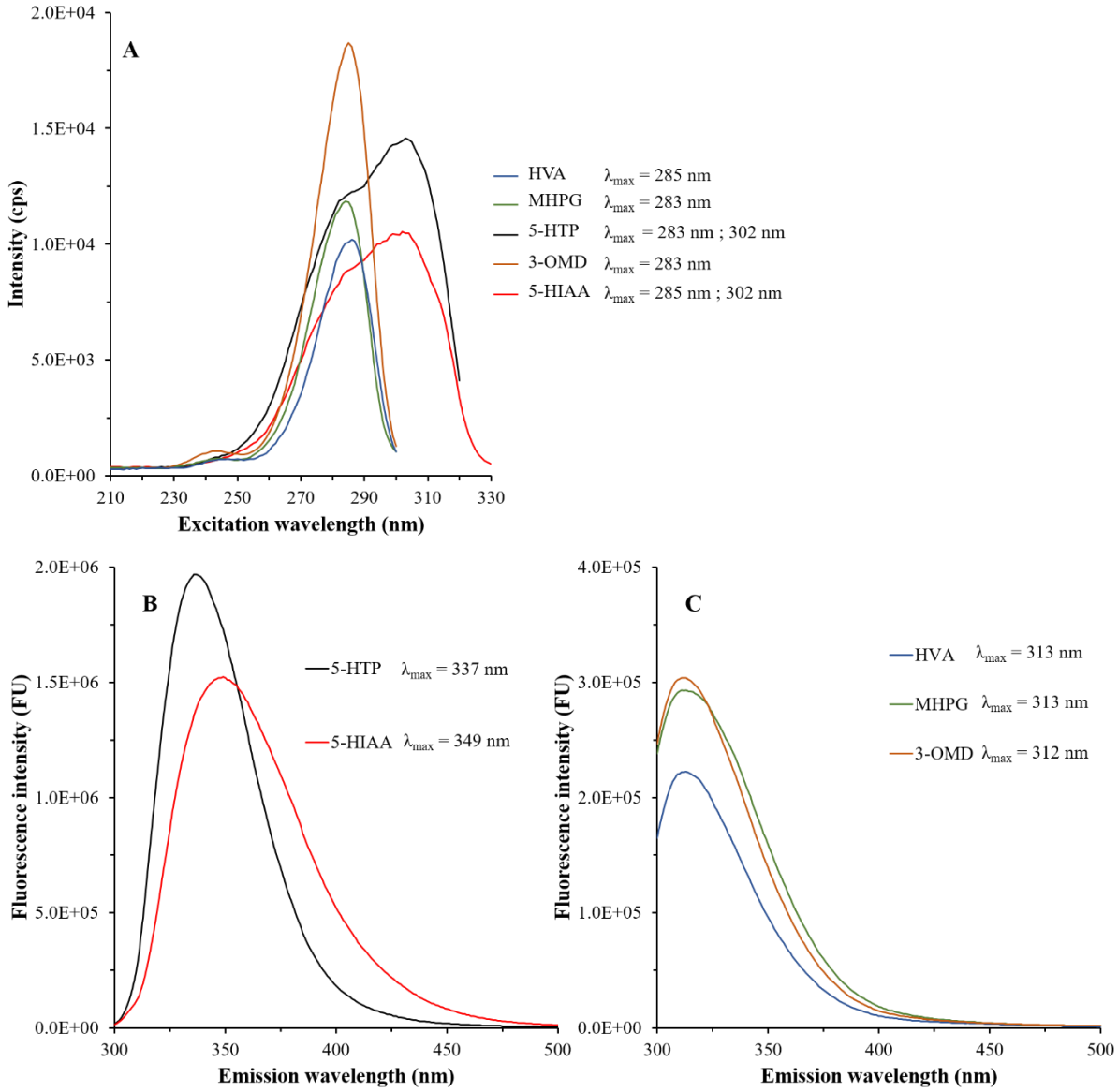

Figure IV.9: Excitation (A) and emission (B and C) spectra of serotonin and dopamine metabolites measured from standard solutions at a concentration of 1000 nM in the mobile phase used for chromatographic separation. The emission spectra were determined with λ_{ex}=280 nm. The excitation spectra were measured at maximum emission wavelength of each compound.

Table S1: Comparison of the signal to noise ratio for HVA, 3-OMD and MHPG for the λ_{ex} = 280 nm; three different λ_{em}: 310 nm, 320 nm, 330 nm

		280 nm / 310 nm			280 nm / 320 nm			280 nm / 330 nm		
Molecule	Concentration (nM)	Signal	Noise	S/N	Signal	Noise	S/N	Signal	Noise	S/N
HVA	10	455	95	4.8	447	65	6.9	366	45	8.1
MHPG		891	95	9.4	751	65	11.6	588	45	13.1
3-OMD		1393	95	14.7	1302	65	20.0	982	45	21.8
HVA	25	1091	121	9.0	1054	96	11.0	795	64	12.4
MHPG		2095	121	17.3	1826	96	19.0	1357	64	21.2
3-OMD		3354	121	27.7	3161	96	32.9	2320	64	36.3
HVA	50	2190	99	22.1	2132	84	25.4	1605	49	32.8
MHPG		4232	99	42.7	3824	84	45.5	2746	49	56.0
3-OMD		6723	99	67.9	6270	84	74.6	4641	49	94.7

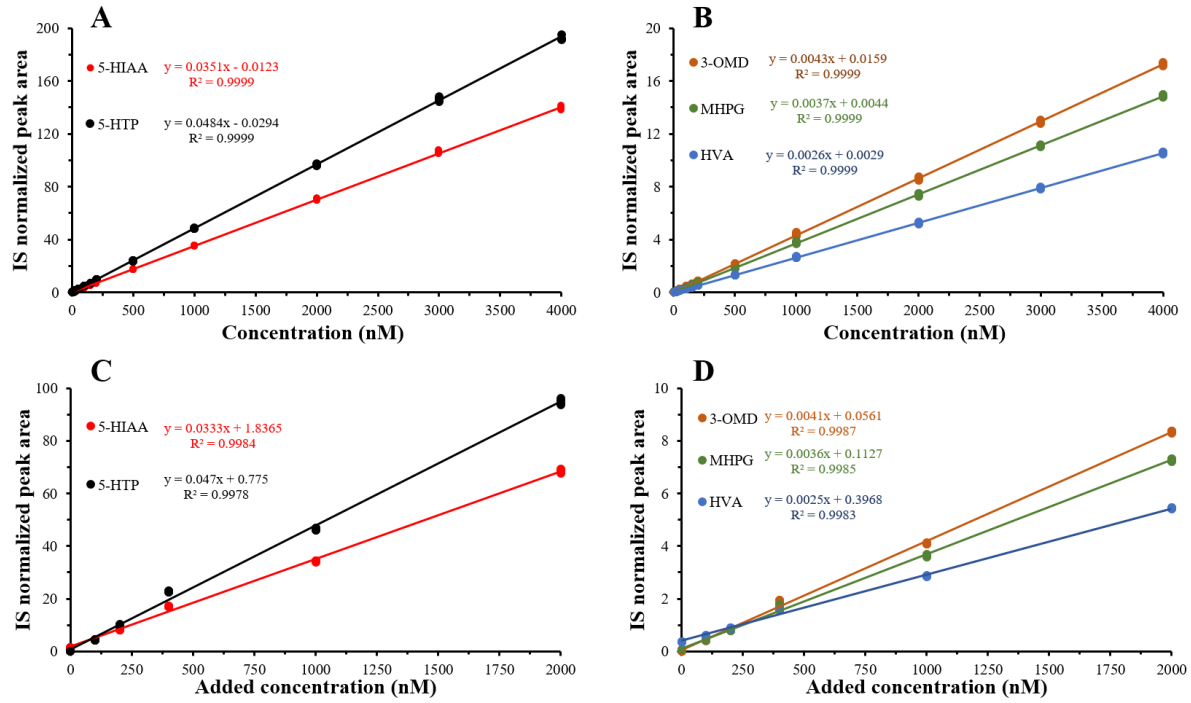

Figure IV.10: Calibration ranges for the five biomarkers between the LLOQ and 4000 nM in calibration solutions (A and B) and standard addition measurement in a CSF pool (C and D) by the proposed UHPLC-FD method

CHAPITRE 5 : QUANTIFICATION DES BIOMARQUEURS DE TYPE MONOAMINE DANS LE LIQUIDE CEPHALORACHIDIEN : COMPARAISON DE DEUX METHODES DE CHROMATOGRAPHIE LIQUIDE ULTRA-HAUTE PERFORMANCE

V.1. PRESENTATION DE L'ARTICLE

Nous disposons désormais d'une méthode de chromatographie liquide couplée à une détection par fluorescence permettant de quantifier les biomarqueurs de type monoamine dans le liquide céphalorachidien. Compte tenu du développement et de l'accessibilité financière des spectromètres de masse qui permettent un gain en sélectivité et en sensibilité lors des analyses, nous voulons comparer la méthode UHPLC-FD à une méthode ou la détection se fait par spectrométrie de masse en tandem. Pour cela, dans l'article qui suit, nous avons développé une nouvelle méthode de chromatographie liquide ultra-haute performance couplée à la spectrométrie de masse en tandem pour l'analyse des biomarqueurs de type monoamine. La détection se fait en mode MRM (multiple reaction monitoring) en utilisant deux transitions spécifiques à chaque analyte. L'ionisation est effectuée en electrospray en polarité positive.

Comme précédemment, cette méthode a été validée en termes de linéarité, d'exactitude, de précision, d'effet matrice et de limites basses de quantification. Ces dernières étaient entre 0,5 nM et 10 nM, selon le composé. Les performances analytiques des deux méthodes, notamment concernant les limites basses de quantification, sont adaptées au dosage des biomarqueurs dans le liquide céphalorachidien. Les deux méthodes ont été appliquées à l'analyse de 30 échantillons de liquide céphalorachidien. Les concentrations obtenues par les deux méthodes ont montré une corrélation satisfaisante et sont comparables aux normes décrites dans la littérature. Ainsi, les deux méthodes sont adaptées au diagnostic des erreurs innées du métabolisme. Par ailleurs, le mode MRM présente une spécificité supérieure qu'en détection par fluorescence ce qui permet d'avoir une analyse plus rapide (6 minutes et 10 minutes, respectivement). Néanmoins, la détection par fluorescence est réalisée sur une instrumentation moins couteuse que la spectrométrie de masse en tandem.

Statut de l'article : Accepté, en cours de publication

Journal : Biomedical Chromatography

Quantification of monoamine biomarkers in cerebrospinal fluid: comparison of a UHPLC-MS/MS method to a UHPLC coupled to fluorescence detection method

Authors

Ayoub Boulghobra[1], Taous Abar[1], Fathi Moussa[1], Bruno Baudin[2], Diana Rodriguez[2], Antoine Pallandre[1], Myriam Bonose[1]

Affiliation

[1]Université Paris-Saclay, CNRS, Institut de Chimie Physique, UMR8000, 91405 Orsay, FRANCE

[2]Services de Neuropédiatrie et de Biochimie, Groupe Hospitalier Trousseau Laroche-Guyon, 26 avenue du Dr Arnold Netter, 75012 Paris, France

V.2. ABSTRACT

Inborn errors of monoamine neurotransmitter metabolism are rare genetic diseases classified as catecholamine and serotonin metabolism disorders or neurotransmitter transportopathies. To diagnose these orphan diseases, monoamine metabolites have been identified and validated as cerebrospinal fluid (CSF) biomarkers: 5-hydroxy-tryptophane, 5-hydroxy-indol-acetic acid, 3-ortho-methyl-DOPA, homovanillic acid, and 3-methoxy-4-hydroxyphenylglycol. The present work presents a UHPLC-MS/MS method developed for the quantification of these me-

tabolites in CSF and compares it to a previously described UHPLC-FD method. MS/MS detection was performed in positive electrospray ionization and multiple reaction monitoring (MRM) mode.

The UHPLC-MS/MS and UHPLC-FD methods were validated in terms of accuracy, linearity, precision, and matrix effect. The lower limits of quantification (LLOQ) were ranging between 0.5 nM and 10 nM and between 1 and 5 nM for the UHPLC-MS/MS method and the UHPLC-FD one, respectively. We verified the applicability of both methods by analyzing 30 CSF samples. The measured concentrations were comparable to the reference values described in the literature. The two methods allowed to distinguish pathological samples from healthy ones for clinical diagnosis. UHPLC-MS/MS and UHPLC-FD methods exhibit very close LLOQs. As UHPLC-MS/MS method is more selective, it allows faster analysis with 6 minutes per run versus 10 minutes for the UHPLC-FD method.

Keywords:

Cerebrospinal fluid, Monoamine biomarkers, UHPLC, MS/MS, Fluorescence detection.

V.3. INTRODUCTION

Inborn errors of monoamine neurotransmitter diseases are rare genetic disorders that affect pediatric patients in particular (Jeanmonod et al., 2022; Saudubray & Garcia-Cazorla, 2018; Walterfang et al., 2013; Pearl et al., 2007). They are classified as catecholamines and serotonin metabolism disorders or neurotransmitter transportopathies (Opladen et al., 2016; Burton, 1998; Ng et al., 2014). Defects in biosynthesis, degradation, and transport of dopamine and serotonin lead to clinical symptoms (Garcia-Cazorla & Duarte, 2014; Kurian et al., 2011; Marecos et al., 2014; Sedel et al., 2007). These clinical symptoms, such as movement disorders or epilepsy, are common to other neurological illnesses like cerebral palsy or encephalopathies (Brennenstuhl et al., 2019; Burton, 1998; Kurian et al., 2011; Ng et al., 2014). Consequently, the diagnosis of inborn errors of monoamine neurotransmitter metabolism is highly complex (Brennenstuhl et al., 2019; Hyland, 1999; Kuster et al., 2018).

Definitive diagnosis necessitates the analysis of cerebrospinal fluid (CSF) samples, in order to quantify dopamine and serotonin metabolites which are validated biomarkers for these diseases (Banki & Molnár, 1981; Stanley et al., 1985). The main analytes to consider are: homovanillic acid (HVA), 3-ortho-methyl-DOPA (3-OMD), 3-methoxy-4-hydroxy-phenyl-glycol (MHPG), 5-hydroxy-indole acetic acid (5-HIAA) and 5-hydroxy-tryptophan (5-HTP) (Hyland et al., 1993). Measurement of these biomarkers allows determination of metabolite profiles that distinguish between genetic mutation of enzymes and transporters, hence carrying out a definitive diagnosis (Brennenstuhl et al., 2019; Hyland, 2008). This is of great importance since each enzyme or transporter deficiency may require specific treatment (Birnbacher et al., 1998; Brennenstuhl et al., 2019; Maas et al., 2017).

Monoamine metabolite quantification in CSF presents three main challenges. First, biomarkers can be at concentrations as low as 10 nM in CSF samples, especially for certain enzyme defects (Bicker et al., 2013; Hyland, 2008; Jung-Klawitter & Kuseyri Hübschmann, 2019). Therefore, for diagnostic purposes, a lower limit of quantification (LLOQ) of 10 nM must be targeted during analytical method development. Second, CSF sample treatment is a critical step since

it aims to reduce any interference and matrix effect while being adapted to routine use. Thus, it has to be sufficiently fast and easy-to-handle (Bicker et al., 2013; Jung-Klawitter & Kuseyri Hübschmann, 2019). Third, since the diagnosis of inborn errors of monoamine neurotransmitters is mainly performed for pediatric patients, CSF sample volume must be considered. Indeed, in the pediatric population, especially infants, collected CSF volume can be lower than 300 µL (Cameron et al., 2019). Thus, the smallest possible sample volume has to be used in monoamine metabolite quantification to allow confirming the first analysis or to perform further investigations.

As part of the diagnosis of inborn errors of monoamine neurotransmitter metabolism, CSF analysis is mainly based on high-performance liquid chromatography (HPLC) or ultrahigh-performance liquid chromatography (UHPLC) coupled to whether electrochemical detection (ECD), fluorescence detection (FD) or tandem mass spectrometry (MS/MS) (Hyland et al., 1993; Bicker et al., 2013; Jung-Klawitter & Kuseyri Hübschmann, 2019; Cameron et al., 2019; Ormazabal et al., 2005; Lo et al., 2017; Galla et al., 2021; Boulghobra et al., 2022; Akiyama et al., 2017). Indeed, given the electroactivity of monoamine metabolites, ECD has been widely used for the analysis of dopamine and serotonin metabolites in CSF (Hyland et al., 1993; Lo et al., 2017; Ormazabal et al., 2005). Moreover, these biomarkers exhibit a native fluorescence. Thus HPLC-FD methods are also described as an alternative to ECD and avoid some drawbacks of ECD, such as possible signal attenuation because of analyte adsorption onto the electrode and the necessary frequent cleaning of the electrochemical cell (Jung-Klawitter & Kuseyri Hübschmann, 2019; Boulghobra et al., 2022; Akiyama et al., 2017). MS/MS detection can also be coupled to chromatographic separation enabling to reach high selectivity and sensitivity for such diagnosis (Galla et al., 2021; Jung-Klawitter & Kuseyri Hübschmann, 2019).

In order to set up a comparison of the detection modes that may be used in the analysis of monoamine metabolites, in the present work, a UHPLC-MS/MS method is proposed and compared to the previously described UHPLC-FD method (Boulghobra et al., 2022). We focused the comparison on the possible alternative and more convenient detectors than ECD. Similar

to the previously proposed UHPLC-FD method (Boulghobra et al., 2022), the UHPLC-MS/MS method underwent complete validation in terms of linearity, accuracy, precision, LLOQ, and matrix effect. The applicability of both methods was verified on the same 30 CSF samples. The reached performances of the two methods were compared regarding their analytical performances (sensitivity and selectivity) and their efficiency for clinical diagnosis.

V.4. MATERIALS AND METHODS

V.4.1. Chemicals and reagents

All solvents used were HPLC grade. Ultrapure water was obtained from a LabWater purification system (Veolia). Ammonium formate, ammonium acetate, and ammonium carbonate were ordered from Sigma-Aldrich (Kappelweg, Germany).

The standards of HVA (purity ≥ 97%), 5-HIAA (purity ≥ 98%), 5-HTP (purity ≥ 98%), 3-OMD (purity ≥ 98%), and MHPG as a hemipiperazinium salt (purity ≥ 98%) were ordered from Sigma-Aldrich (Kappelweg, Germany) and were used without further purification. Standards labeled with stable isotopes were HIAA-d6 and HVA-d5 were purchased as 100 µg/mL solutions in methanol from Sigma-Aldrich (Kappelweg, Germany).

V.4.2. Instruments

UHPLC-FD separations were carried on a Shimadzu Nexera LC-40 system with a Shimadzu RF-20A fluorescence detector with a fluorescence cell at 15°C. A Horiba Fluoromax fluorimeter was used to measure excitation and emission spectra, to adjust FD conditions. UHPLC-MS/MS analyses were performed on a Shimadzu LCMS-8040 system.

V.4.3. Calibration standards and quality control samples

Stock solutions of each analyzed biomarker were prepared in ultrapure water. Stock solutions were aliquoted and stored at -20°C. The working solution was prepared by mixing the stock solutions and by diluting them in the mobile phase to reach a final concentration of 10 µM. The obtained solution was diluted in artificial cerebrospinal fluid (An et al., 2008) to prepare the

calibration solutions. Quality control (QC) samples consisted of mixtures of stock solutions diluted in artificial cerebrospinal fluid (An et al., 2008).

V.4.4. CSF samples

In the present study, 30 CSF samples were analyzed. These samples were collected between 2019 and 2020 by lumbar puncture at Armand-Trousseau hospital (Paris, France). Indeed, in the present article, we studied the remaining CSF volume after the biochemical and microbiological analyses; that is why, in accordance with the French Code de la Santé Publique, no approval by ethical committee is needed. The study was conducted according to the methodology MR-004 of the French Commission national de l'informatique et des libertés. 17 female patients and 13 male patients were included. The patients included were children with neurological symptoms, namely, epilepsy, movement disorders, and/or severe cephalalgia. Written informed consent of parents or legal representatives was obtained prior to sample collection. Patients were excluded if there was a traumatic lumbar puncture with observed blood in the CSF sample and/or if samples were inadequately stored. CSF samples were frozen immediately after collection with liquid nitrogen and then stored at -80°C. These samples were collected from patients aged between 9 days and 32.4 years.

V.4.5. Sample preparation

For UHPLC-MS/MS analysis, calibration standards, QC samples, standard addition samples, and authentic CSF samples were diluted (1/1, v/v) in a solution of 5-HIAA-d6 and HVA-d5 at 200 nM and 300 nM, respectively, prepared beforehand in a mixture of ultrapure water/methanol (94/6, v/v). The diluted sample was then filtered on a 5000 Da molecular weight cutoff (MWCO) PES Vivaspin filter (Sartorius) by centrifugation (20 min at 12 000 G, 4°C). The filtrate was then injected into the UHPLC system.

V.4.6. UHPLC methods

Chromatographic separation was carried out with an Acquity UPLC HSS T3 column (2.1 x 100 mm, 1.8µm; Waters) protected by an Acquity UPLC HSS T3 Vanguard pre-column (2.1 x 5 mm, 1.8µm; Waters) maintained at 30°C. Elution was performed in isocratic mode. The mobile phase consisted of a mixture of ammonium formate 50 mM, pH 5.4 / methanol (97/3, v/v), and ammonium carbonate 5 mM, pH 7 / methanol (97/3, v/v) for FD and MS/MS, respectively. In both methods, the flow rate was 0.4 mL/min, and the injection volume was of 10 µL.

V.4.7. MS/MS method

MS/MS detection was performed using positive electrospray ionization (ESI). ESI conditions were optimized as follows: heat block and desolvation line were at a temperature of 300°, N2 was used as both nebulizing gas and drying gas at a flow rate of 3 L/min and 15 L/min, respectively, ESI voltage was set at 4.5 kV for 5-HIAA and 1.5 kV for the other biomarkers, conversion dynode voltage was 6 kV, and detector voltage was 1.7 kV.

Dopamine and serotonin metabolites were quantified in multiple reaction monitoring (MRM) mode with two mass transitions for each analyte. Argon was used as collision-induced dissociation (CID) gas at a pressure of 230 kPa.

Table V.1: Retention times and MRM conditions for each analyzed biomarker and internal standard in positive ESI.

Analyte	Retention time (min)	MRM transitions					Internal standard
		Parent ion (m/z)	Fragment ions (m/z)	Q1 Voltage (V)	Collision energy (V)	Q3 Voltage (V)	
5-HIAA-d6	2.7	198	**151**	-22	-17	-28	-
			123	-22	-31	-22	
5-HIAA	2.8	192	**146**	-15	-15	-14	5-HIAA-d6
			118	-22	-32	-21	
HVA-d5	3.2	205	**141**	-23	-17	-26	-
			126	-11	-32	-24	
3-OMD	3.3	212	195	-24	-11	-21	5-HIAA-d6
			153	-24	-18	-27	
HVA	3.3	200	**137**	-11	-18	-24	HVA-d5
			122	-24	-32	-23	
5-HTP	3.7	221	**204**	-25	-13	-22	5-HIAA-d6
			162	-12	-20	-17	
MHPG	5.1	167	135	-19	-16	-25	5-HIAA-d6
			107	-19	-16	-19	

Bold transitions were used for quantification.

Table V.1 summarizes the MRM transitions and retention times for each analyte and the internal standards (IS). For each analyte, the MRM signal was acquired on a time segment corresponding to the retention time +/- 0.4 min. Product ion spectra of each analyte and IS are shown in Figure V.5 (Supplementary material). These spectra were obtained by flow injection analysis of standard solutions of each biomarker and internal standard at a concentration of 25 µM for all the analytes, except HVA and HVA-d5, that were at 100 µM. For each product ion spectrum, the two most intense fragments were identified, and optimization was set up on the voltage of the first and third quadrupoles and the collision energy. It consists in choosing the voltages and collision energies, allowing to reach the optimal signal to noise ratio (S/N) for each mass transition.

V.4.8. Fluorescence detection

As described previously (Boulghobra et al., 2022), FD was performed in multichannel detection mode with an excitation wavelength of 280 nm, the maximum absorption wavelength for the five biomarkers, and four different emission wavelengths corresponding to 310 nm, 320 nm, 330 nm, and 340 nm. This method (Boulghobra et al., 2022) was validated according to the guideline of bioanalytical method validation of the European medicine agency (EMA) (Bioanalytical Method Validation, 2018).

V.4.9. UHPLC-MS/MS method validation

The proposed UHPLC-MS/MS method was validated according to the guideline of bioanalytical method validation of the EMA (Bioanalytical Method Validation, 2018).

MRM transitions and retention factors allow for the reliable identification of each biomarker, hence the validation of selectivity. The method linearity was verified with at least eleven levels ranging between LLOQ and 4000 nM. Six replicates were done at each concentration level and on four different days.

Since the unavailability of CSF samples depleted in dopamine and serotonin metabolites, the validation of accuracy and precision was performed on artificial CSF samples corresponding to QC samples. Accuracy was validated by setting up six independent analyses per concentration level at four concentrations: the LLOQ, three times the LLOQ (low QC), 1000 nM (medium QC), and 4 000 nM (high QC). Six sets of measurements were performed by changing the day and/or the operator. Recoveries were then determined by calculating the ratio of the measured concentration to the theoretical one.

The method precision was validated on the same sets of measures as accuracy. Within-run and between-run relative standard deviations (RSD) were calculated at each concentration level. The LLOQ of each biomarker is the lowest concentration where linearity, precision, and accuracy are verified.

Matrix effect validation relied on a standard addition experiment. Standard additions of the biomarkers were performed on a mixture of five CSF samples, and five concentration levels were measured in six replicates. Matrix factors were calculated for each concentration as follows: matrix factor = (IS-normalized peak area in the CSF) / (IS-normalized peak area in the mobile phase). Carry-over effect was verified by injecting ultrapure water immediately after the analysis of CSF samples and after the analysis of the 4 000 nM standard solution.

All statistical calculations were carried out using Microsoft Excel 2016 software.

V.4.10. Comparison of UHPLC-MS/MS to UHPLC-FD

In order to compare the proposed UHPLC-MS/MS method to the previously described UHPLC-FD method (Boulghobra et al., 2022), the same 30 CSF samples were analyzed by both methods in triplicates. The five biomarkers of interest were quantified in these samples, and we calculated the determination coefficients for each analyte.

V.5. RESULTS AND DISCUSSION

V.5.1. MS/MS conditions

In the present work, MS/MS method was optimized for dopamine and serotonin metabolites. First, we assessed positive and negative ESI. We observed that positive ionization exhibited a higher signal than negative ionization for all the biomarkers and internal standards. Therefore, positive ESI appeared more efficient for detecting the analytes.

MRM transitions were identified thanks to product ion spectra in positive mode (Supplementary Figure V.5). For each biomarker and internal standard, two transitions were identified: the most intense one was used for quantification, and the other one for confirming identification (Table V.1). Based on the identified MRM transitions of each analyte, ESI conditions were also optimized to reach the highest signal intensity.

V.5.2. UHPLC conditions

The analyzed dopamine and serotonin metabolites are low acidic polar compounds. The most adapted column for their separation is the ACQUITY UPLC HSS T3, that is why it was selected at the beginning of method development. Mobile phase optimization was set up on an ACQUITY UPLC HSS T3 column with the following dimensions: 50 x 2.1 mm; 1.8 µm. For that purpose, we tested 20 different mobile phases by varying methanol proportion and the buffer nature, pH and ionic strength. Ammonium acetate, formate, and carbonate at pHs ranging between 4.6 and 7 and at an ionic strength between 1 and 50 mM were evaluated.

Given the high specificity of two MRM transitions, mobile phase choice was based on the optimal S/N rather than chromatographic separation. Indeed, efficient separation (resolution factors higher than 1.5) was reached in both ammonium acetate and ammonium formate at pHs between 4.6 and 5.4 with 3% methanol. Nevertheless, the LLOQs reached using these mobile phases were not compatible with biomarkers quantification in CSF. However, the highest S/N for all the analytes was obtained in 5 mM pH 7 ammonium carbonate with 3% methanol; that is why this mobile phase was selected for further studies.

Using the chosen mobile phase, 3-OMD, HVA, and HVA-d5 coeluted, and their respective MRM transitions were detected simultaneously on the chromatogram. Consequently, the obtained peaks were defined by less than 20 points which might be insufficient for quantitative analysis. In fact, as a consequence of this lack of peak definition, imprecise peak areas were obtained with RSD > 15%. To improve chromatographic peak definition as well as separation, a longer column was used (100 x 2.1 mm; 1.8 µm). That enabled us to reach a satisfactory peak definition with at least 30 points per peak, hence allowing for a reliable quantitative analysis.

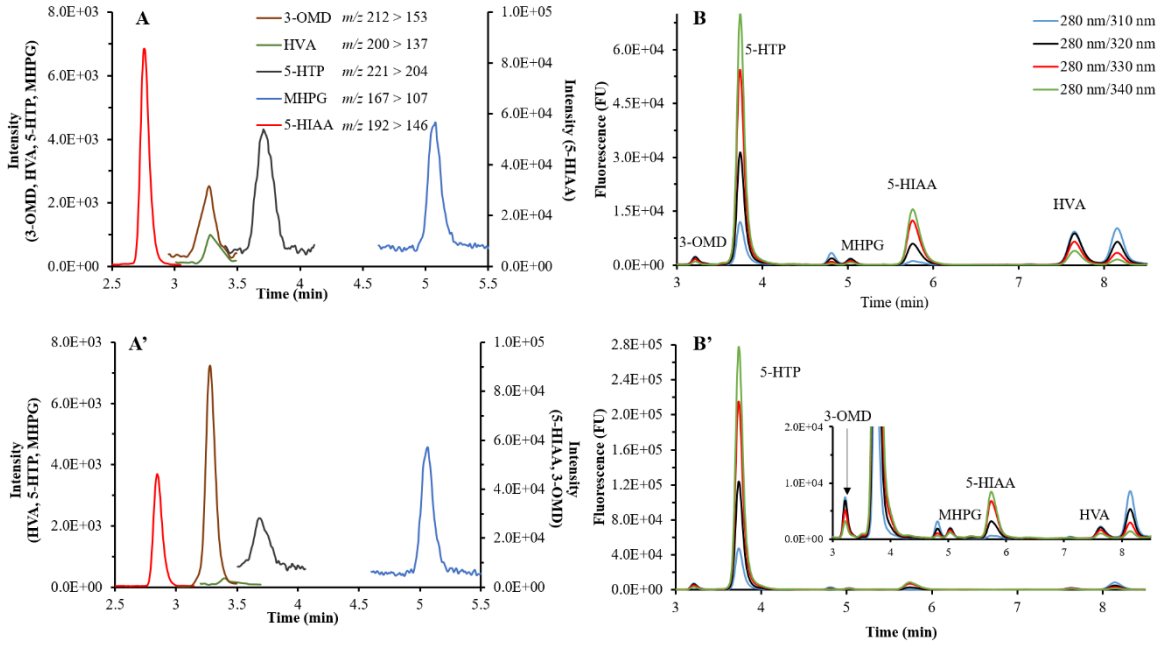

Figure V.1: Chromatograms obtained for a normal CSF sample collected from a 1.6-year old person analyzed by UHPLC-MS/MS (A) and UHPLC-FD (B) and for a pathological CSF sample collected from a 9-day-old infant with suspected aromatic amino acid decarboxylase deficiency analyzed by UHPLC-MS/MS (A') and UHPLC-FD (B').
Aromatic amino acid decarboxylase deficiency induces high cerebrospinal concentration of 3-OMD and low concentrations of 5-HIAA and HVA.

Figure V.1 shows chromatograms of two CSF samples obtained by the selected UHPLC-MS/MS conditions (A for CSF 1 and A' for CSF 2) and by UHPLC-FD (B for CSF 1 and B' for CSF 2). Figure 1A and A' indicate the proposed UHPLC-MS/MS method detects the analytes

in CSF samples. Thus, it is adapted for the analysis of dopamine and serotonin metabolites in CSF samples. Moreover, compared to the previously described UHPLC-FD method (Boulghobra et al., 2022), it allows for faster analysis with 6 minutes per run in UHPLC-MS/MS. In contrast, the analysis time was of 10 minutes in UHPLC-FD. This is due to the fact that with an optical detection such as fluorescence, complete chromatographic separation of the analytes must be achieved, whereas it is not necessary for MS/MS since two selective MRM transitions are used for each biomarker.

V.5.3. UHPLC-MS/MS method validation

The proposed UHPLC-MS/MS method underwent a complete validation according to the EMA guideline of bioanalytical method validation. Linearity was validated by back-calculating the concentration of each analyte. Recoveries were then estimated by considering the theoretical concentration. All these recoveries were between 85% and 115% and between 80% and 120% for the LLOQ. Thus, linearity was verified according to the EMA guideline (Bioanalytical Method Validation, 2018) for the five biomarkers between the LLOQ and 4000 nM (Figure V.2). Besides the guideline requirements for linearity validation, Figure V.2 shows all determination coefficients (R^2) are higher than 0.99, regardless of the analyzed biomarker.

To verify a possible matrix effect, a standard addition experiment was performed on a pooled CSF sample with five concentration levels and six replicated per level. Matrix factors were calculated for each replicate (Table 2). According to the EMA guideline on bioanalytical method validation, matrix effect was validated since the RSD for each concentration level was lower than 15%. Moreover, Table 2 shows all the obtained matrix factors are between 0.85 and 1.15, indicating that the proposed UHPLC-MS/MS method exhibits a negligible matrix effect. The carry-over effect was also verified because no peak was detected in the blank chromatogram analyzed immediately after CSF samples and after the 4 000 nM standard solution.solution.

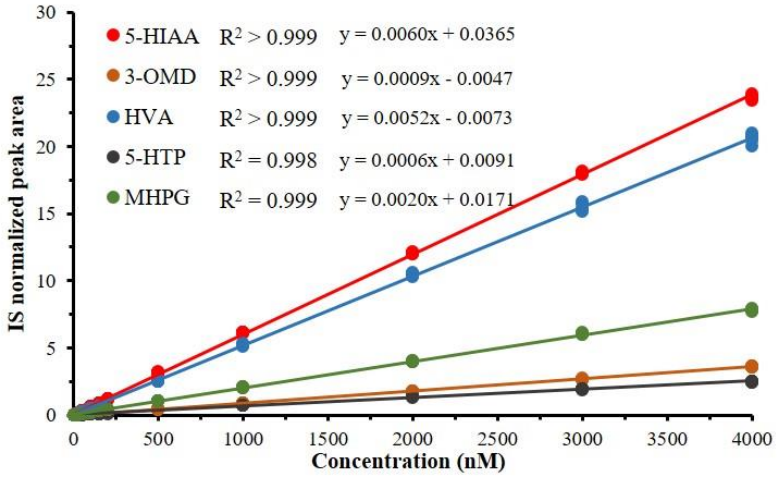

Figure V.2: Linearity for the five biomarkers of interest between the LLOQ and 4000 nM in calibration solutions measured by the proposed UHPLC-MS/MS method.

Table V.2: Matrix effect validation results of the UHPLC-MS/MS method for 5-HIAA, 3-OMD, 5-HTP, MHPG, and HVA quantification.

Standard addition experiment										
Added concentration (nM)	5-HIAA		3-OMD		5-HTP		MHPG		HVA	
	MF	RSD (%)	**MF**	RSD (%)	**MF**	RSD (%)	**MF**	RSD (%)	**MF**	RSD (%)
0	**1.13**	1.3	**0.88**	1.1	**0.97**	5.3	**0.99**	1.4	**1.05**	0.8
100	**1.09**	0.8	**1.10**	1.1	**0.93**	1.2	**1.10**	0.9	**0.92**	1.1
200	**1.03**	0.7	**1.00**	1.1	**0.87**	1.7	**0.98**	0.9	**0.86**	0.6
400	**1.09**	0.4	**1.10**	1.4	**0.92**	1.2	**1.12**	1.0	**0.85**	3.4
2000	**1.12**	1.2	**1.15**	0.9	**0.97**	1.2	**1.14**	0.9	**0.85**	0.8

MF: Matrix factor: ratio of the IS-normalized peak area in the presence of matrix to the IS-normalized peak area in the absence of matrix.

Table V.3: Accuracy and precision validation results of the UHPLC-MS/MS method for 3-OMD, 5-HTP, MHPG, 5-HIAA, and HVA quantification.

Analyte	Level	Concentration(nM)	**Accuracy**		**Precision**	
			Intra-day recovery (%) (n=6)	Inter-day recovery (%) (n=6x6)	Intra-day RSD (%) (n=6)	Inter-day RSD (%) (n=6x6)
5-HIAA	LLOQ	0.5	101.6	104.6	1.8	3.5
	3LLOQ	1.5	96.4	101.2	2.9	5.6
	Medium	500	104.3	110.9	1.3	5.1
	High	2000	103.7	107.7	1.3	2.5
HVA	LLOQ	10	108.3	112.4	2.5	1.6
	3LLOQ	30	107.2	105.6	3.2	3.8
	Medium	500	104.7	102.7	1.8	4.4
	High	2000	100.3	99.1	3.0	0.9
5-HTP	LLOQ	1	98.2	99.6	3.2	1.7
	3LLOQ	3	99.0	98.0	3.0	4.5
	Medium	500	104.6	101.7	4.0	8.4
	High	2000	102.7	104.1	1.8	9.3
3-OMD	LLOQ	1	95.4	98.1	2.4	2.9
	3LLOQ	3	103.8	103.7	2.9	1.2
	Medium	500	96.8	96.1	4.2	9.9
	High	2000	97.6	97.3	1.6	7.6
MHPG	LLOQ	1	102.3	101.9	3.2	5.9
	3LLOQ	3	111.8	104.6	2.8	7.1
	Medium	500	106.6	94.7	1.8	7.1
	High	2000	100.1	91.6	1.7	9.5

The method accuracy was validated by analyzing six sets of six replicates at four concentration levels corresponding to QC samples. Table V.3 indicates the obtained recoveries are all in the range of 100+/-15%; hence the UHPLC-MS/MS method accuracy is verified. For precision validation, for the same analysis as for accuracy, we determined intraday and inter-day RSDs.

Table V.3 shows all these RSDs are lower than 15%. Therefore, the UHPLC-MS/MS method meets the requirements of the EMA guideline on bioanalytical method validation in terms of accuracy and precision.

For each biomarker, the LLOQ corresponds to the lowest concentration for which accuracy, precision, and linearity are validated. Table V.3 indicates the proposed UHPLC-MS/MS method reaches the targeted LLOQ (10 nM) for all the analytes. Thus, the method allows for quantifying biomarkers concentration as low as in CSF. It is, therefore, adapted for CSF analysis.

V.5.4. Analysis of authentic CSF samples

The proposed UHPLC-MS/MS method being validated; it was applied to 30 authentic CSF samples collected from 30 different patients. Samples were analyzed in triplicates, and the mean concentration of each biomarker was compared to reference ranges as described in the literature (Hyland, 2008; Lo et al., 2017). Figure 3 shows the obtained concentrations for CSF samples.

Figure 3 indicates that the obtained concentrations by the presented UHPLC-MS/MS method are comparable to the reference ranges described in the literature, demonstrating that it is suitable for diagnosing inborn errors of dopamine and serotonin metabolism.

Moreover, Figure 3 shows the proposed method allows distinguishing between healthy and pathological samples, confirming that it is adapted to diagnosis. Indeed, the metabolic profile of each patient was compared to the diagnostic guideline for inherited disorders of neurotransmitter metabolism.

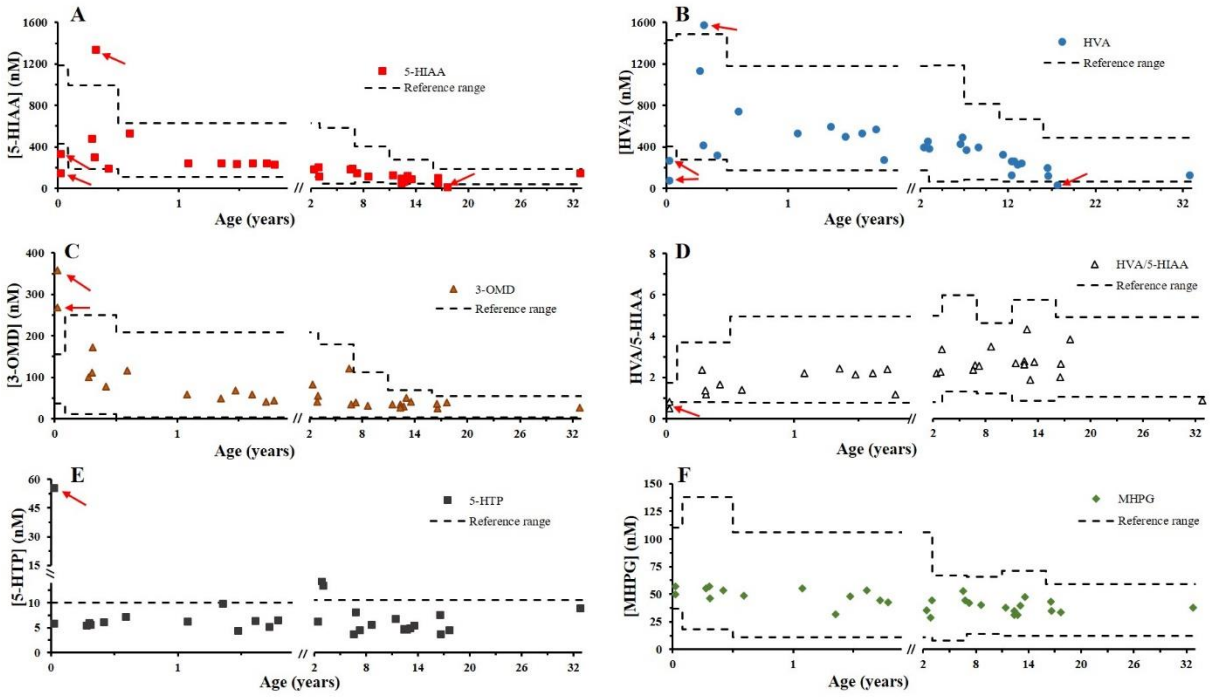

Figure V.3: Concentrations of dopamine and serotonin metabolites in 30 CSF samples obtained by the presented UHPLC-MS/MS method and age-dependent reference ranges described by Lo et al., 2017 for 5-HIAA, HVA, HVA/5-HIAA, MHPG, and 3-OMD and by Hyland, 2008 for 5-HTP. Red arrows indicate the pathological concentrations.

Four CSF samples were found to be pathological. Two 9-day-old patients had aromatic L-amino acid decarboxylase deficiency (AADC) with unequivocal metabolic profiles (Wassenberg et al., 2021), considering the remarkably low concentrations of HVA (268.8 and 72.6 nM) and 5-HIAA (327.4 and 141.5 nM) and the significantly high concentrations of 3-OMD (268.7 and 359.0 nM). Another patient aged of 3 months had a pathological CSF sample with a metabolic profile that may correspond to a vesicular monoamine transporter 2 (VMAT2) deficiency with high amounts of both HVA (1575.8 nM) and 5-HIAA (1333.2 nM) (Brennenstuhl et al., 2019; Rilstone et al., 2013). The fourth patient is a 17-year-old teenager for whom the diagnosis was ambiguous since only HVA and 5-HIAA were significantly low, which may correspond to many inborn errors of monoamine neurotransmitter metabolism, namely guanosyltriphosphate cyclohydrolase (GTPCH), dihydropterin reductase (DHPR) or 6-pyruvoyl tetrahydropterin synthase (PTPS) deficiencies or DNAJC12 mutation (Brennenstuhl et al., 2019; Hollak & Lachmann, 2016; Hyland et al., 1993). It should be noted that the treatments of the four

suspected inborn errors of dopamine and serotonin metabolism have similarities since they all include the administration of L-DOPA combined with Carbidopa (Brennenstuhl et al., 2019). Therefore, although further investigations need to be set up for a definitive diagnosis, treatment may be started based on the measured biomarkers by the UHPLC-MS/MS method.

Thus, the proposed UHPLC-MS/MS method for the quantification of dopamine and serotonin metabolites is suitable for the clinical diagnosis of inborn errors of neurotransmitter metabolism.

V.5.5. Comparison of UHPLC-MS/MS and UHPLC-FD methods

In order to compare UHPLC-MS/MS and UHPLC-FD methods, since both are aimed at clinical use, we correlated the diagnosis performed by the two methods. Such as UHPLC-MS/MS, UHPLC-FD method allowed to identify four pathological CSF samples with the very same metabolic profiles. This indicates a satisfactory correlation in terms of definitive diagnosis between the two analytical methods and, more importantly, that the measured concentrations by both methods are comparable to the norms described in the literature (Hyland, 2008; Lo et al., 2017).

The quantification results were also correlated between the two methods for each analyte in the 30 CSF samples (Figure V.4). Determination coefficients (R^2) were calculated for each analyte. Figure V.4 shows that measured concentrations by UHPLC-MS/MS and UHPLC-FD are correlated for 5-HIAA, HVA, 3-OMD, and MHPG ($R^2 > 0.75$). However, for 5-HTP, the measured concentrations by UHPLC-MS/MS and UHPLC-FD are different for a given CSF sample. This is explained by the fact that a coelution is observed in the UHPLC-FD chromatograms. Indeed, the unidentified peak appears to interfere significantly with 5-HTP's peak. This sheds light on the fact that the selectivity of the quantified biomarkers is higher with the UHPLC-MS/MS method allowing a specific identification of each analyte thanks to the retention factor and two MRM transitions. Therefore, the measured concentrations by UHPLC-MS/MS should be the closest to the true concentrations of 5-HTP in the CSF samples.

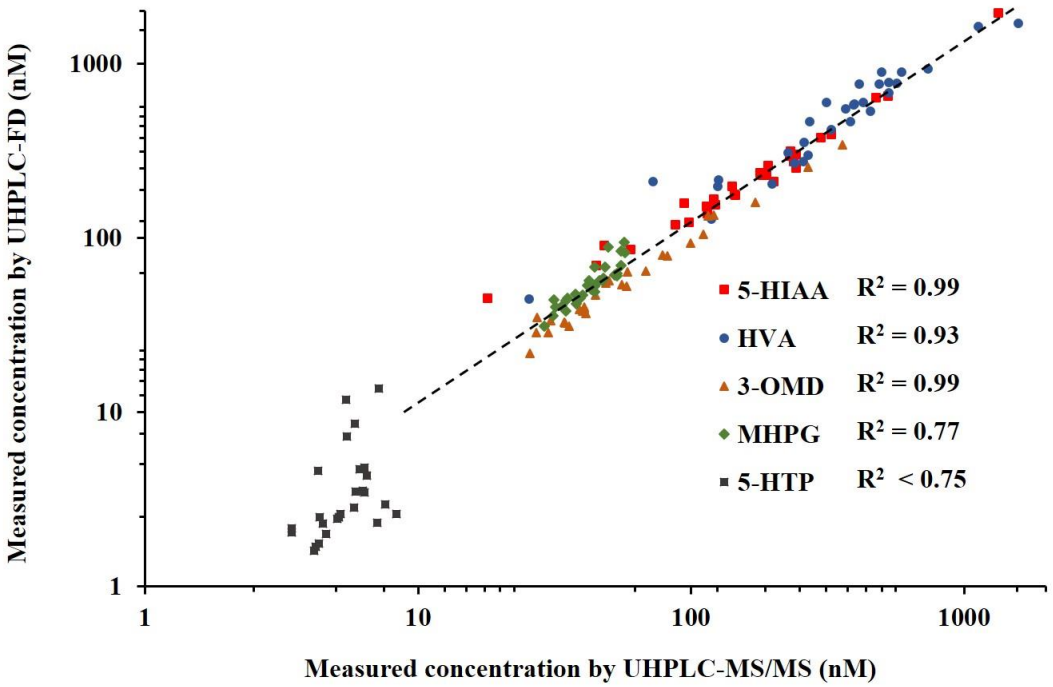

Figure V.4: Correlation for the measured concentrations of 5-HIAA, HVA, 3-OMD, MHPG, and 5-HTP by UHPLC-MS/MS and UHPLC-FD for 30 CSF samples. The two axes are in a logarithmic scale.

In terms of sensitivity, as shown in Table V.4, both UHPLC-MS/MS and UHPLC-FD methods are adapted for clinical use. Indeed, a 10 nM LLOQ is required for each analyte to allow a reliable diagnosis, and Table V.4 indicates that the reached LLOQs for both methods are less than or equal to 10 nM.

Even though both methods reach the targeted LLOQ for clinical use, Table V.4 shows differences depending on the quantified biomarker. UHPLC-MS/MS and UHPLC-FD methods reach the same LLOQ for 5-HTP and 3-OMD. UHPLC-MS/MS method is more sensitive for 5-HIAA and MHPG, while the UHPLC-FD method exhibit a lower LLOQ for HVA. Therefore, the UHPLC-MS/MS is as sensitive as the UHPLC-FD method, except for HVA.

Table V.4: Comparison of the LLOQs of serotonin and dopamine metabolites obtained by UHPLC-MS/MS and UHPLC-FD.

	LLOQ values (nM)	
Analyte	UHPLC-MS/MS	UHPLC-FD
5-HIAA	0.5	1
HVA	10	5
5-HTP	1	1
3-OMD	1	1
MHPG	1	2.5

V.5.6. Comparison to existing methods

Based on the critical analytical performances for diagnostic purposes, namely LLOQ, injection volume, and analysis time, three methods were identified in the literature as state-of-the-art for the quantification of monoamine biomarkers in CSF (Boulghobra et al., 2022; Galla et al., 2021; Lo et al., 2017). These methods have demonstrated their clinical suitability and correspond to the three possible detection modes: MS/MS (Galla et al., 2021), FD (Boulghobra et al., 2022), and ECD (Lo et al., 2017).

Table V.5: Comparison of the sensitivity, injection volume, and analysis time obtained by UHPLC-FD (Boulghobra et al., 2022), HPLC-MS/MS (Galla et al., 2021), and UHPLC-ECD (Lo et al., 2017).

	LLOQ values (**femtomoles**)			
Analyte	**UHPLC-MS/MS**	**UHPLC-FD**	HPLC-MS/MS	UHPLC-ECD
5-HIAA	**5**	**10**	75	500
HVA	**100**	**50**	300	750
5-HTP	**10**	**10**	15	250
3-OMD	**10**	**10**	15	250
MHPG	**10**	**25**	15	250
Injection volume	**10 µL**	**10 µL**	15 µL	50 µL
Chromatographic run time	**6 min**	**10 min**	20 min	10 min

Table 5 shows the proposed UHPLC-MS/MS method allows for the fastest analysis with 6 minutes per run. Compared to the HPLC-MS/MS method proposed by Galla et al. (Galla et al., 2021), this is explained by the use of UHPLC, whereas compared to the previously described UHPLC-FD method (Boulghobra et al., 2022) or the UHPLC-ECD method of Lo et al. (Lo et al., 2017), the shorter analysis time is due to the use of MS/MS detection in MRM mode allowing for the quantification of the analytes without an efficient chromatographic separation. Moreover, the proposed UHPLC-MS/MS method, such as the previously described UHPLC-FD method (Boulghobra et al., 2022), is based on the injection of only 10 µL of sample, which is a definite advantage compared to both HPLC-MS/MS (Galla et al., 2021) and UHPLC-ECD (Lo et al., 2017) methods. Concerning the sensitivity, the described UHPLC-MS/MS method reaches the lowest LLOQs except for HVA.

V.6. CONCLUSIONS

We developed an analytical method based on UHPLC-MS/MS for the quantification of monoamine metabolites in CSF. The method was fully validated and compared to a previously developed UHPLC-FD method. The two assays meet the clinical diagnosis requirements in terms of sensitivity, accuracy, precision, and selectivity. Moreover, the measured concentrations are comparable with reference amounts described in the literature. Therefore, both compared methods are adapted to routine use.

Nevertheless, UHPLC-MS/MS is the most specific method based on both chromatographic retention and two MRM transitions. Moreover, the LLOQs of the two methods are quite similar and suitable for the diagnosis of inborn errors of monoamine neurotransmitter metabolism. Furthermore, the developed UHPLC-MS/MS method allows for a faster analysis than the UHPLC-FD one, with 6 minutes and 10 minutes per run, respectively. The correlation of the measured concentrations by UHPLC-MS/MS and UHPLC-FD methods sheds light on the fact that, thanks to its higher specificity, especially concerning 5-HTP, UHPLC-MS/MS should be the reference method. The described UHPLC-FD method is still an interesting alternative for

the quantification of monoamine metabolites in CSF, especially for laboratories not equipped with a UHPLC-MS/MS system.

V.7. REFERENCES

Akiyama, T., Hayashi, Y., Hanaoka, Y., Shibata, T., Akiyama, M., Nakamura, K., Tsuyusaki, Y., Kubota, M., Yoshinaga, H., & Kobayashi, K. (2017). Simultaneous measurement of monoamine metabolites and 5-methyltetrahydrofolate in the cerebrospinal fluid of children. *Clinica Chimica Acta, 465*, 5-10. https://doi.org/10.1016/j.cca.2016.12.005

An, J. H., Su, Y., Radman, T., & Bikson, M. (2008). Effects of glucose and glutamine concentration in the formulation of the artificial cerebrospinal fluid (ACSF). *Brain Research, 1218*, 77-86. https://doi.org/10.1016/j.brainres.2008.04.007

Banki, C. M., & Molnár, G. (1981). Cerebrospinal fluid 5-hydroxyindoleacetic acid as an index of central serotonergic processes. *Psychiatry Research, 5*(1), 23-32. https://doi.org/10.1016/0165-1781(81)90057-3

Bicker, J., Fortuna, A., Alves, G., & Falcão, A. (2013). Liquid chromatographic methods for the quantification of catecholamines and their metabolites in several biological samples—A review. *Analytica Chimica Acta, 768*, 12-34. https://doi.org/10.1016/j.aca.2012.12.030

Bioanalytical method validation. (2018, septembre 17). [Text]. European Medicines Agency. https://www.ema.europa.eu/en/bioanalytical-method-validation

Birnbacher, R., Scheibenreiter, S., Blau, N., Bieglmayer, C., Frisch, H., & Waldhauser, F. (1998). Hyperprolactinemia, a Tool in Treatment Control of Tetrahydrobiopterin Deficiency : Endocrine Studies in an Affected Girl. *Pediatric Research, 43*(4), 472-477. https://doi.org/10.1203/00006450-199804000-00006

Boulghobra, A., Bonose, M., Billault, I., & Pallandre, A. (2022). A rapid and sensitive method for the quantification of dopamine and serotonin metabolites in cerebrospinal fluid based on UHPLC with fluorescence detection. *Journal of Chromatography B*, 123264. https://doi.org/10.1016/j.jchromb.2022.123264

Brennenstuhl, H., Jung-Klawitter, S., Assmann, B., & Opladen, T. (2019). Inherited Disorders of Neurotransmitters : Classification and Practical Approaches for Diagnosis and Treatment. *Neuropediatrics, 50*(01), 002-014. https://doi.org/10.1055/s-0038-1673630

Burton, B. K. (1998). Inborn Errors of Metabolism in Infancy : A Guide to Diagnosis. *PEDIATRICS, 102*(6), e69-e69. https://doi.org/10.1542/peds.102.6.e69

Cameron, S., Gillio-Meina, C., Ranger, A., Choong, K., & Fraser, D. D. (2019). Collection and Analyses of Cerebrospinal Fluid for Pediatric Translational Research. *Pediatric Neurology*, *98*, 3-17. https://doi.org/10.1016/j.pediatrneurol.2019.05.011

Galla, Z., Rajda, C., Rácz, G., Grecsó, N., Baráth, Á., Vécsei, L., Bereczki, C., & Monostori, P. (2021). Simultaneous determination of 30 neurologically and metabolically important molecules : A sensitive and selective way to measure tyrosine and tryptophan pathway metabolites and other biomarkers in human serum and cerebrospinal fluid. *Journal of Chromatography A*, *1635*, 461775. https://doi.org/10.1016/j.chroma.2020.461775

Garcia-Cazorla, A., & Duarte, S. T. (2014). Parkinsonism and inborn errors of metabolism. *Journal of Inherited Metabolic Disease*, *37*(4), 627-642. https://doi.org/10.1007/s10545-014-9723-6

Hollak, C. E. M., & Lachmann, R. (2016). *Inherited Metabolic Disease in Adults : A Clinical Guide*. Oxford University Press.

Hyland, K. (1999). Presentation, diagnosis, and treatment of the disorders of monoamine neurotransmitter metabolism. *Inherited Metabolic Disorders in the Neonate*, *23*(2), 194-203. https://doi.org/10.1016/S0146-0005(99)80051-2

Hyland, K. (2008). Clinical Utility of Monoamine Neurotransmitter Metabolite Analysis in Cerebrospinal Fluid. *Clinical Chemistry*, *54*(4), 633-641. https://doi.org/10.1373/clinchem.2007.099986

Hyland, K., Surtees, R. A. H., Heales, S. J. R., Bowron, A., Howells, D. W., & Smith, I. (1993). Cerebrospinal Fluid Concentrations of Pterins and Metabolites of Serotonin and Dopamine in a Pediatric Reference Population. *Pediatric Research*, *34*(1), 10-14. https://doi.org/10.1203/00006450-199307000-00003

Jeanmonod, R., Asuka, E., & Jeanmonod, D. (2022). Inborn Errors Of Metabolism. In *StatPearls*. StatPearls Publishing. http://www.ncbi.nlm.nih.gov/books/NBK459183/

Jung-Klawitter, S., & Kuseyri Hübschmann, O. (2019). Analysis of Catecholamines and Pterins in Inborn Errors of Monoamine Neurotransmitter Metabolism—From Past to Future. *Cells*, *8*(8), 867. https://doi.org/10.3390/cells8080867

Kurian, M. A., Gissen, P., Smith, M., Heales, S. J., & Clayton, P. T. (2011). The monoamine neurotransmitter disorders : An expanding range of neurological syndromes. *The Lancet Neurology*, *10*(8), 721-733. https://doi.org/10.1016/S1474-4422(11)70141-7

Kuster, A., Arnoux, J.-B., Barth, M., Lamireau, D., Houcinat, N., Goizet, C., Doray, B., Gobin, S., Schiff, M., Cano, A., Amsallem, D., Barnerias, C., Chaumette, B., Plaze, M., Slama, A., Ioos, C., Desguerre, I., Lebre, A.-S., de Lonlay, P., … Individual contributors who contributed to this work. (2018). Diagnostic approach to neurotransmitter monoamine disorders : Experience from clinical, biochemical, and genetic profiles. *Journal of Inherited Metabolic Disease*, *41*(1), 129-139. https://doi.org/10.1007/s10545-017-0079-6

Lo, A., Guibal, P., Doummar, D., Rodriguez, D., Hautem, J.-Y., Couderc, R., Billette De Villemeur, T., Roze, E., Chaminade, P., & Moussa, F. (2017). Single-Step Rapid Diagnosis of Dopamine and Serotonin Metabolism Disorders. *ACS Omega*, *2*(9), 5962-5972. https://doi.org/10.1021/acsomega.7b01008

Maas, R. P. P. W. M., Wassenberg, T., Lin, J.-P., van de Warrenburg, B. P. C., & Willemsen, M. A. A. P. (2017). L-Dopa in dystonia. *Neurology*, *88*(19), 1865. https://doi.org/10.1212/WNL.0000000000003897

Marecos, C., Ng, J., & Kurian, M. A. (2014). What is new for monoamine neurotransmitter disorders? *Journal of Inherited Metabolic Disease*, *37*(4), 619-626. https://doi.org/10.1007/s10545-014-9697-4

Ng, J., Heales, S. J. R., & Kurian, M. A. (2014). Clinical Features and Pharmacotherapy of Childhood Monoamine Neurotransmitter Disorders. *Pediatric Drugs*, *16*(4), 275-291. https://doi.org/10.1007/s40272-014-0079-z

Opladen, T., Cortès-Saladelafont, E., Mastrangelo, M., Horvath, G., Pons, R., Lopez-Laso, E., Fernández-Ramos, J. A., Honzik, T., Pearson, T., Friedman, J., Scholl-Bürgi, S., Wassenberg, T., Jung-Klawitter, S., Kuseyri, O., Jeltsch, K., Kurian, M. A., & Garcia-Cazorla, À. (2016). The International Working Group on Neurotransmitter related Disorders (iNTD) : A worldwide research project focused on primary and secondary neurotransmitter disorders. *Molecular Genetics and Metabolism Reports*, *9*, 61-66. https://doi.org/10.1016/j.ymgmr.2016.09.006

Ormazabal, A., García-Cazorla, A., Fernández, Y., Fernández-Álvarez, E., Campistol, J., & Artuch, R. (2005). HPLC with electrochemical and fluorescence detection procedures for the

diagnosis of inborn errors of biogenic amines and pterins. *Journal of Neuroscience Methods*, *142*(1), 153-158. https://doi.org/10.1016/j.jneumeth.2004.08.007

Pearl, P. L., Taylor, J. L., Trzcinski, S., & Sokohl, A. (2007). The Pediatric Neurotransmitter Disorders. *Journal of Child Neurology*, *22*(5), 606-616. https://doi.org/10.1177/0883073807302619

Rilstone, J. J., Alkhater, R. A., & Minassian, B. A. (2013). Brain Dopamine–Serotonin Vesicular Transport Disease and Its Treatment. *New England Journal of Medicine*, *368*(6), 543-550. https://doi.org/10.1056/NEJMoa1207281

Saudubray, J.-M., & Garcia-Cazorla, A. (2018). An overview of inborn errors of metabolism affecting the brain : From neurodevelopment to neurodegenerative disorders. *Dialogues in Clinical Neuroscience*, *20*(4), 301-325. PubMed. https://doi.org/10.31887/DCNS.2018.20.4/jmsaudubray

Sedel, F., Baumann, N., Turpin, J.-C., Lyon-Caen, O., Saudubray, J.-M., & Cohen, D. (2007). Psychiatric manifestations revealing inborn errors of metabolism in adolescents and adults. *Journal of Inherited Metabolic Disease*, *30*(5), 631-641. https://doi.org/10.1007/s10545-007-0661-4

Stanley, M., Traskman-Bendz, L., & Dorovini-Zis, K. (1985). Correlations between aminergic metabolites simultaneously obtained from human CSF and brain. *Life Sciences*, *37*(14), 1279-1286. https://doi.org/10.1016/0024-3205(85)90242-5

Walterfang, M., Bonnot, O., Mocellin, R., & Velakoulis, D. (2013). The neuropsychiatry of inborn errors of metabolism. *Journal of Inherited Metabolic Disease*, *36*(4), 687-702. https://doi.org/10.1007/s10545-013-9618-y

Wassenberg, T., Geurtz, B. P. H., Monnens, L., Wevers, R. A., Willemsen, M. A., & Verbeek, M. M. (2021). Blood, urine and cerebrospinal fluid analysis in TH and AADC deficiency and the effect of treatment. *Molecular Genetics and Metabolism Reports*, *27*, 100762. https://doi.org/10.1016/j.ymgmr.2021.100762

V.8. SUPPLEMENTARY MATERIAL

Quantification of monoamine biomarkers in cerebrospinal fluid: comparison of a UHPLC-MS/MS method to a UHPLC coupled to fluorescence detection method

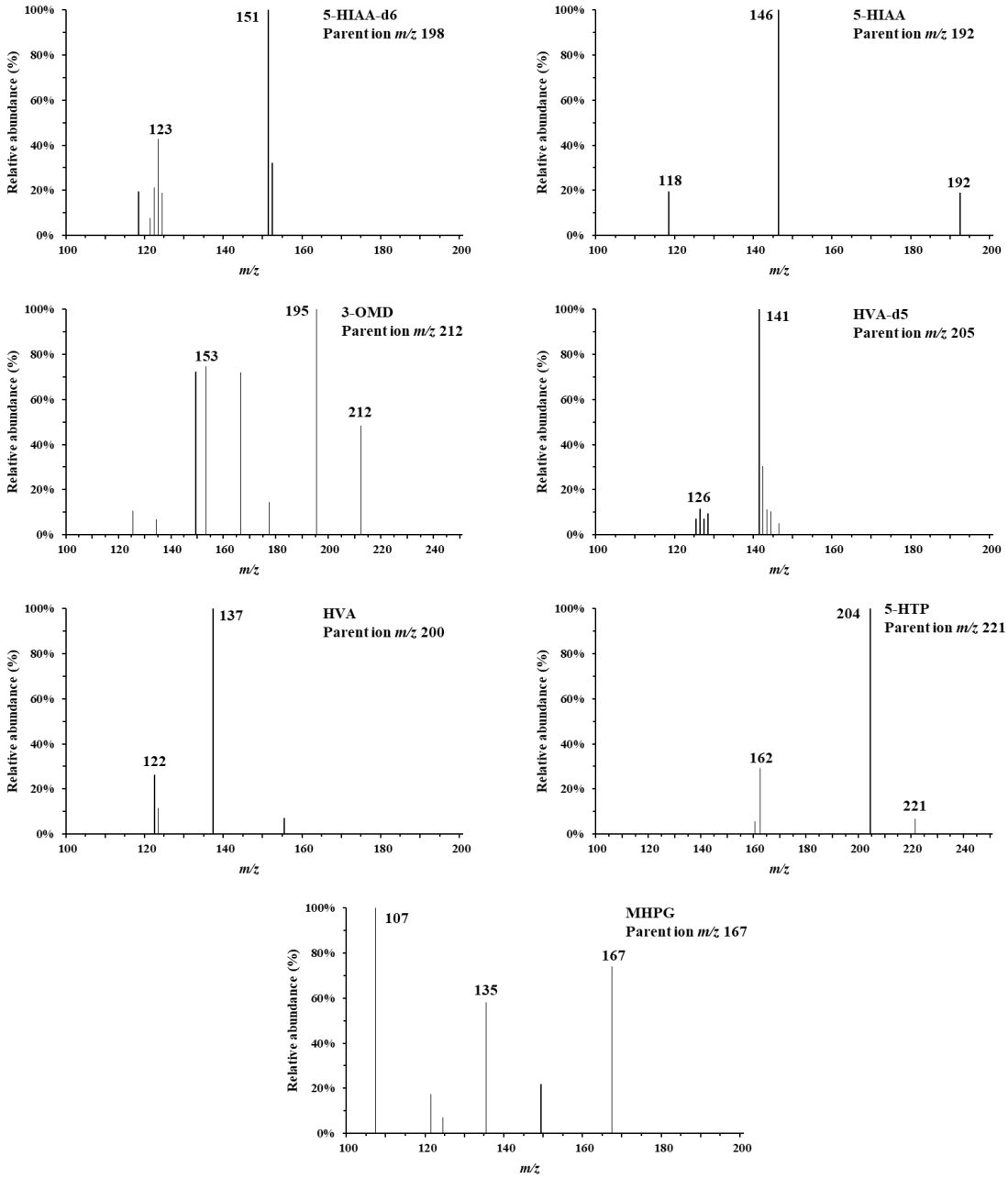

Figure V.5: Product ion spectra of dopamine and serotonin metabolites and their internal standard.

CHAPITRE 6 : ETUDE DE L'EFFET DU PHOSPHATE SUR L'IONISATION EN ELECTROSPRAY

VI.1. PRESENTATION DE L'ARTICLE

Au cours des développements des méthodes d'analyse des ptérines et des métabolites de la dopamine et de la sérotonine, nous avons observé, par pure sérendipité, que de faibles concentrations en phosphate pouvaient entrainer une augmentation du signal obtenu après ionisation par electrospray. Dans un premier temps, l'objectif a été de confirmer cet effet. Pour cela, étant donné que de précédents développements ont permis de bien connaître le comportement en terme de rétention et d'ionisation en electrospray des métabolites de la dopamine et de la sérotonine, dans l'article qui suit, l'ionisation de ces analytes a été étudiée en présence de phosphate. Pour cela, ce dernier a été utilisé comme additif dans la phase mobile à des concentrations allant de 0 à 20 µM. Nous avons étudié l'amélioration de l'ionisation positive basée sur le phosphate en fonction de la nature et du pH du tampon constituant la phase mobile. Cet effet d'amélioration du signal a bien été vérifié et il dépend de manière importante de la constitution de la phase mobile et de l'analyte considéré. L'amélioration du signal en ionisation positive a été confirmée avec un autre groupe de composés, à savoir : la tétrahydrobioptérine, la 7,8-dihydrobioptérine, la bioptérine, la dihydronéoptérine et la néoptérine.

Plusieurs hypothèses ont été formulées pour expliquer ce phénomène. L'explication la plus pertinente repose sur le fait que les faibles concentrations en phosphate diminuent les adduits alcalins des analytes, augmentant, par là même, le signal de l'analyte protoné. En effet, les spectres de masse confirment bien une augmentation du signal au fur et à mesure de l'augmentation de la concentration en phosphate.

Statut de l'article : En cours de soumission

Journal : Analytica Chimica Acta

Electrospray ionization enhancement: phosphate as an additive to eliminate alkali metal ion adducts

Authors

Ayoub Boulghobra, Myriam Bonose

Affiliation

Université Paris-Saclay, CNRS, Institut de Chimie Physique, UMR8000, 91405 Orsay, FRANCE

VI.2. ABSTRACT

Electrospray ionization is an ionization technique particularly inclined to alkali metal ion adduct formation in positive mode. These adducts may reduce the ionization efficiency of the analyzed molecules and, thus, the sensitivity. Therefore, eliminating sodium and potassium adducts allows to improve the sensitivity and the precision of electrospray ionization signal, especially in biological fluids. In the present work, we propose the use of phosphate as additive in the mobile phase to reduce, nay to eliminate, alkali metal ion adducts. Phosphate was used at concentrations ranging between 5 µM and 20 µM and allowed to enhance electrospray ionization signal for 3-ortho-methyl-DOPA, 5-hydroxytryptophan, 3-metoxy-4-hydroxy-phenylglycol, homovanillic acid and 5-hydroxyindole acetic acid. Phosphate-based positive electrospray ionization enhancement was importantly affected by the mobile phase buffer nature and pH and by the analyte. To determine the optimal conditions for each analyte, a full-factorial design of experiment (3 buffers x 5 pHs x 4 phosphate concentrations) was set up. Nevertheless, in negative mode, the opposite effect was observed with a signal decrease with phosphate addition. The enhancement was confirmed in positive mode for five other compounds, namely,

tetrahydrobiopterin, dihydrobiopterin, biopterin, dihydroneopterin and neopterin. Mass spectrometry spectra exhibited a decrease of alkali metal ion adducts, when increasing phosphate concentration in the mobile phase. Phosphate addition allowed to improve the signal to noise ratios with gain factors between 1.4 and 103.4 depending on the analyte and the mobile phase. Therefore, the proposed desalting method is easy-to-handle and highly effective.

VI.3. INTRODUCTION

Electrospray ionization (ESI) is an atmospheric pressure ionization technique widely used in mass spectrometry (MS) after high-performance liquid chromatography (HPLC) separation [1–6]. ESI is adapted to the analysis of small molecules, especially in biological samples since it allows to reach high sensitivity [6–9]. Indeed, its high ionization efficiency enables to detect as low as femtomoles of sample [10–12]. Nevertheless, sensitivity can be significantly reduced when some interfering compounds, namely salts, are present in the sample [13–16]. Sodium chloride being ubiquitous in biological samples, it may lead to ion suppression by competing with the analytes during ESI process [13–15]. Therefore, ESI sensitivity may be insufficient when analyzing trace amounts of molecules in complex mixtures.

Many strategies have been proposed to improve the sensitivity of ESI. First, salts can be removed before introduction in the ESI source, whether during sample treatment [17], during HPLC analysis [18] or after the chromatographic separation [19]. Desalting sample treatment consists mainly in solid-phase extraction [20,21] or in dialysis [22]. Concerning solid-phase extraction, salts are whether retained by the sorbent and the analytes are directly eluted or salts are eluted while the analytes are retained [17]. In both cases, analytes are separated from the interfering salts. During HPLC analysis in reversed-phase, many salts are eluted in the void time, hence their separation from the analytes [20,23]. Desalting may also be performed after chromatographic separation with ions retaining resins [22]. Second, sensitivity of Moreover, ESI can be enhanced by derivatizing the analytes [24,25]. This technique consists

in chemically modifying the analytes to facilitate their ionization in ESI. Indeed, chemical moieties are added to the analyzed molecules making proton affinity or electron affinity increase for positive or negative ESI, respectively [25]. Thus, the analytes are ionized with higher effectiveness. Third, additives may be added to the mobile phase to enhance the obtained signal. Commonly used mobile phase additives are volatile acids, bases and salts [25,26]. The addition of these charged volatile compounds allows to improve coulomb fission during ESI process, and hence, the ionization efficiency [27,28].

ESI may favor adduct formation leading to a lower signal intensity for the molecular ion, especially for the analysis of salts-containing complex samples [29–31]. Thus, another strategy to enhance ESI is to limit adduct formation or even to eliminate them. For this purpose, techniques involving desalting additives have been described [12,32–34]. These additives correspond to supercharging reagents [33], phthalic acid [34] and anions such as tartrate and citrate [12]. The use of desalting additives reduce sodium and potassium adduct formation whether by enhancing analyte protonation or by binding alkali metal ions, then making them less available for adduct formation [12,32–34]. Other additives such as ion-pairing reagents were also used to reduce adduct formation [35–37]. For example, the addition of 15 mM triethylamine and 400 mM hexafluoro-2-propanol to mobile phase was found to induce a significant decrease of sodium adduct abundance in mass spectra [35]. This is explained by the fact that, hexafluoro-2-propanol is negatively charged and complexes cations like sodium. Ion-pairing reagent may modify chromatographic retention of the analytes and this parameter must be considered during method optimization. Nevertheless, some ion-pairing reagents lead to ion suppression [38]. Indeed, given their ability to non-covalently bind cations, they can complex the positively-charged analytes in solution, before the ESI process.

Among the ion-pairing molecules, phosphate can be used to improve chromatographic separation [39–41]. However, phosphate is barely used in ESI-MS since it is involatile and may lead to ion suppression [42,43]. Indeed, phosphate reduces the evaporation efficiency during ESI

process, hence, leading to ion suppression [42]. Moreover, to avoid deteriorating the surfaces of ESI source, phosphate concentration must not exceed 50 µM in the mobile phase [44,45].

In the present work, we studied the effect of the mobile phase composition, specifically, the buffer nature and pH on this ESI enhancement. We explained this phenomenon by showing that, increasing concentrations of phosphate reduce sodium and potassium nonspecific adduction and enhance the protonated analyte.

VI.4. MATERIALS AND METHODS

VI.4.1. Chemicals and reagents

Ultrapure water was obtained from a LabWater ultrapurification system (Veolia). HPLC-grade methanol was purchased from Carlo Erba (Val-de-Reuil, France). Ammonium formate, ammonium acetate, and ammonium carbonate were purchased from Sigma-Aldrich (Kappelweg, Germany). Phosphoric acid and ammonium hydroxide were obtained from Carlo Erba (Val-de-Reuil, France).

The standards of HVA, 5-HIAA, 5-HTP, 3-OMD, MHPG as a hemipiperazinium salt, BH4 as hydrochloric salt, BH2, B, NH2 and N were ordered from Sigma-Aldrich (Kappelweg, Germany) and were used without further purification.

Ammonium phosphate solution were prepared by diluting phosphoric acid in water to reach a concentration of 50 mM. The pH of the obtained solution was adjusted to 2.5 with ammonium. Dilutions were set up in the mobile phase to reach final concentrations of 5 µM, 10 µM and 20 µM.

Stock solutions of each analyte were prepared in water at a concentration of 1 mM, were aliquoted and stored and -20°C. Working solutions for the first group of analytes were prepared by mixing and diluting stock solutions of 5-HIAA, 3-OMD, 5-HTP, MHPG and HVA to reach a final concentration of 1 µM, except for HVA whose concentration was of 10 µM. Dilution was

made in the corresponding mobile phase. Likewise, for the second group of analytes, working solutions were prepared by mixing stock solutions of BH4, BH2, B, NH2 and N and by diluting them in the corresponding mobile phase to obtain a final concentration of 1 µM.

VI.4.2. Materials

UHPLC-MS/MS analyses were carried out on a Shimadzu Nexera LC-20 system coupled to a Shimadzu LCMS-8040 triple quadrupole equipped with an electrospray ionization source.

VI.4.3. UHPLC method

Chromatographic analyses were performed with an Acquity UPLC HSS T3 column (2.1 x 100 mm, 1.8µm; Waters) protected by an Acquity UPLC HSS T3 Vanguard pre-column (2.1 x 5 mm, 1.8µm; Waters) maintained at 30°C. Isocratic mode was used and the mobile phase consisted of a mixture aqueous phase/methanol (97/3, v/v). The aqueous phase corresponded to a buffer solution at an ionic strength of 5 mM where we varied the pH and the buffer nature. Flow rate was of 0.4 mL/min and the injection volume was of 10 µL.

VI.4.4. Mass spectrometry conditions

MS/MS detection was set up after positive ESI whose conditions were as follows: heat block and desolvation line temperatures were of 400°C and 250°C, respectively; N_2 was both the drying gas and the nebulizing gas at a flow rate of 15 L/min and 3 L/min, respectively. ESI voltage was of 4.5 kV. Conversion dynode and detector voltages were of 6.0 and 1.7 kV.

MS/MS detection was also performed in negative ESI mode with the same source parameters, except the voltage which was at -4.5 kV.

MS/MS detection was performed in multiple reaction monitoring (MRM) mode with two mass transitions for each analyte (Table VI.1). Argon was used as collision-induced dissociation (CID) gas at a pressure of 230 kPa. MRM transitions in both positive and negative ESI are summarized in Table VI.1[46].

Table VI.1: MRM conditions for each analyte.

Analyte	Polarity	MRM transitions				
		Parent ion (m/z)	Fragment ions (m/z)	Q1 Voltage (V)	Collision energy (V)	Q3 Voltage (V)
5-HTP	ESI +	221	**204**	-25	-13	-22
			162	-12	-20	-17
	ESI -	237	**144**	18	21	26
			132	18	18	24
3-OMD	ESI +	212	195	-24	-11	-21
			153	-24	-18	-27
	ESI -	210	193	16	13	13
			135	16	19	25
HVA	ESI +	200	**137**	-11	-18	-24
			122	-24	-32	-23
	ESI -	181	**137**	13	10	27
			122	13	15	24
5-HIAA	ESI +	192	**146**	-15	-15	-14
			118	-22	-32	-21
	ESI -	190	**146**	14	11	27
			116	14	40	19
MHPG	ESI +	167	135	-19	-16	-25
			107	-19	-16	-19
	ESI -	183	165	14	9	12
			150	13	14	29
NH2	ESI +	256	238	-28	-17	-21
			208	-14	-13	-26
N	ESI +	254	236	-29	-19	-21
			206	-29	-16	-25
BH4	ESI +	242	206	-13	-18	-21
			166	-27	-20	-30
BH2	ESI +	240	**196**	-27	-14	-20
			165	-27	-21	-16
B	ESI +	238	220	-27	-16	-23
			178	-27	-21	-19

VI.4.5. Design of experiment

In order to evaluate the parameters that could influence phosphate-based ESI enhancement, a full factorial design of experiment was set up (Table VI.2). For 5-HIAA, 3-OMD, 5-HTP, MHPG and HVA, the variables were: buffer nature, buffer pH and phosphate concentration.

Table VI.2: Design of experiment parameters for phosphate-based ESI enhancement for 5-HIAA, 3-OMD, 5-HTP, MHPG and HVA.

Analytes	Design of experiment parameters (3 x 5 x 4)		
	Buffer nature	pH of the mobile phase	Phosphate concentration (µM)
3-OMD	Ammonium formate	5.0	0
5-HTP		5.5	5
MHPG	Ammonium acetate	6.0	10
5-HIAA	Ammonium carbonate	6.5	20
HVA		7.0	

Table VI.2 shows that buffer nature was investigated as part of this design of experiment at five different pHs. All these buffers had an ionic strength of 5 mM and were used to prepare the aqueous part of the chromatographic mobile phase, still with 3% methanol. Phosphate concentration did not exceed 20 µM, in order to avoid any instrument alteration, especially the oxidation of metal surfaces. Each experiment was performed in five replicates.

Concerning phosphate-based ESI enhancement for pterins, namely BH4, BH2, B, NH2 and N, given that their separation is set up at acidic pH, only ammonium formate was adapted. Three

pHs were evaluated (2.5, 3.0 and 3.5). For each pH, four phosphate concentrations (0, 5, 10 and 20 µM) were prepared to observe a potential effect. Each experiment was realized in five replicates.

VI.4.6. Data treatment

In order to observe the effect of the buffer type, the pH and phosphate concentration on ESI enhancement, signal to noise ratio (S/N) was measured. For this purpose, signal corresponds to each peak height whereas the noise is the height of the baseline measured with a blank sample consisting in the mobile phase. Such as the signal, the noise was determined in five replicates. Thanks to the mean measure of S/N, for a given buffer, for each analyte a 3 dimension (3D) graphic showing S/N as a function of pH and phosphate concentration was plotted. Relative standard deviations (RSD) were also calculated for each series of measures of S/N.

VI.5. RESULTS AND DISCUSSION

VI.5.1. Effect of phosphate on positive ESI

To observe phosphate effect on positive ESI, a solution of 5-HIAA, 3-OMD, 5-HTP, MHPG and HVA was analyzed by UHPLC-MS/MS. The mobile phase consisted of pH 5.0 ammonium formate/ methanol (97/3, v/v) with three different concentrations of phosphate: 0 µM, 5 µM and 10 µM. MS/MS was performed in MRM mode with specific mass transitions after positive electrospray ionization.

Figure VI.1 and Table VI.3 show that the addition of phosphate in the mobile phase leads to an increase of peak heights for the five analytes. Indeed, even though peak intensities at 5 µM phosphate are similar to 0 µM, for 10 µM phosphate, a significant increase in peak height is observed regardless of the analyzed molecule.

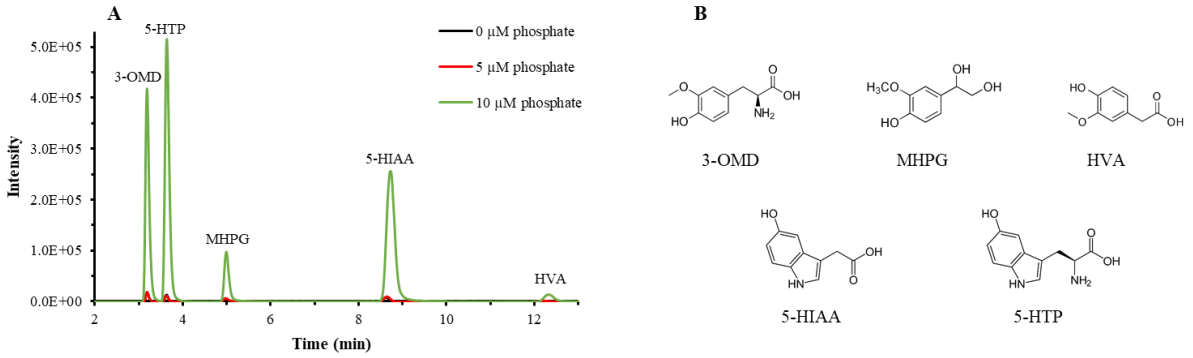

Figure VI.1: (A) Reconstituted chromatograms of a mixture of 5-HIAA, 3-OMD, 5-HTP, MHPG and HVA for three mobile phases consisting of 5 mM; pH 5.0 ammonium formate / methanol (97/3, v/v) varying in terms of phosphate concentrations and (B) Molecular structures of the analytes.

Table VI.3: Peak intensity variation for 5-HIAA, 3-OMD, 5-HTP, MHPG and HVA for three mobile phases consisting of 5 mM; pH 5.0 ammonium formate / methanol (97/3, v/v) varying in terms of phosphate concentrations.

Analytes	Peak intensity		
	0 µM of phosphate	5 µM of phosphate	10 µM of phosphate
3-OMD	12088	18728	411291
5-HTP	6513	11424	507865
MHPG	3353	6696	96221
5-HIAA	6854	9706	245654
HVA	1426	1606	12910

However, Figure VI.1 and Table VI.3 indicate the increase in peak intensities is heterogeneous regarding the analytes. In fact, when comparing 10 µM phosphate to 0 µM, an increase by 21 times is measured for 3-OMD and 5-HIAA, by 28 times for 5-HTP and by 9 times for MHPG and HVA. Therefore, phosphate enhances ESI of the analytes in positive mode. The scale of the improvement depends on the analyte.

VI.5.2. Effect of buffer pH on phosphate-based positive ESI enhancement

In order to investigate how buffer pH would affect phosphate-based ESI enhancement, we varied the pH of ammonium formate buffer contained in the mobile phase. For each pH, four phosphate concentration were evaluated: 0, 5, 10 and 20 µM.

Figure VI.2 shows the evolution of S/N of each analyte as a function of the pH of the mobile phase and of phosphate concentration.

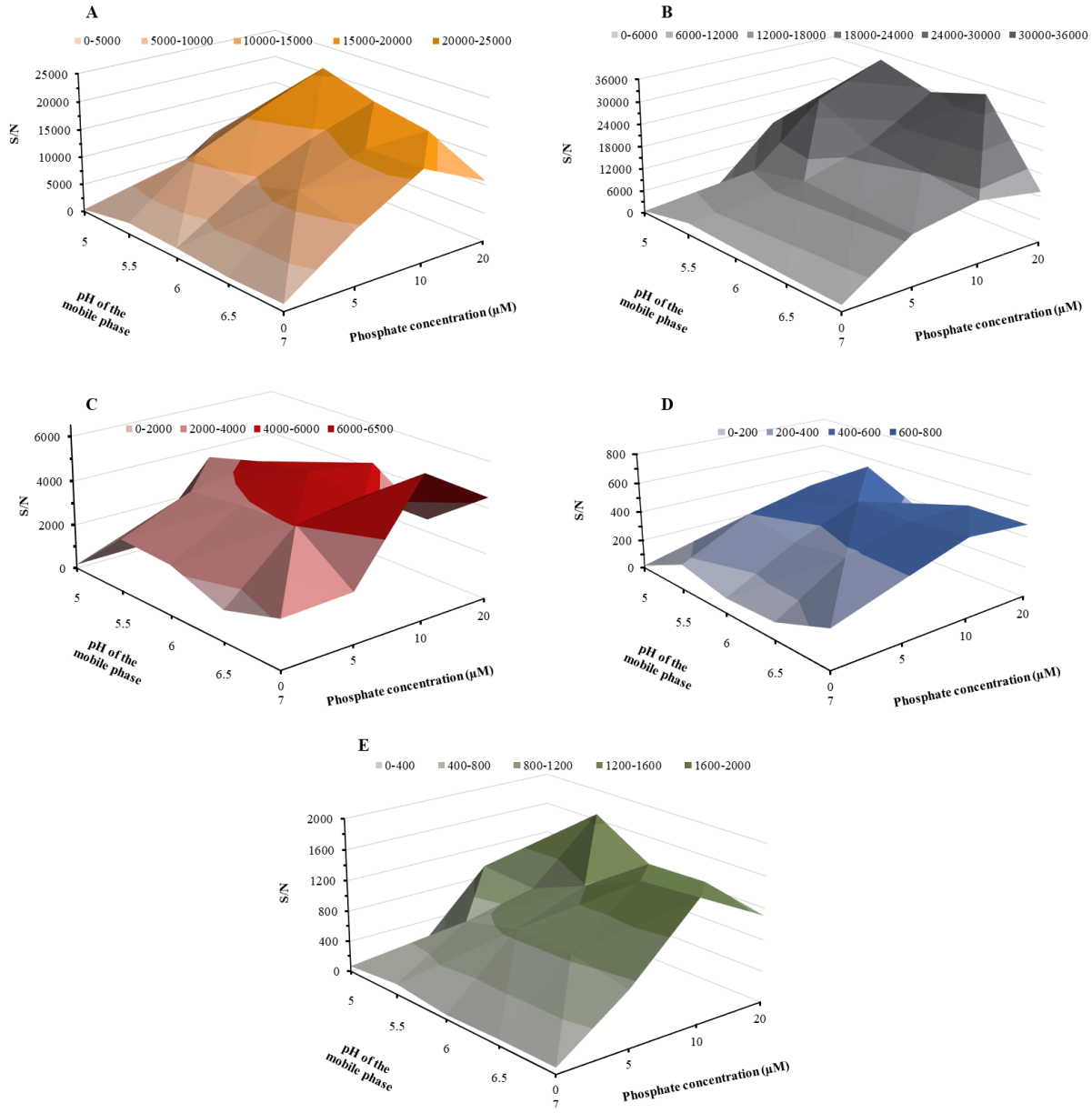

Figure VI.2: Evolution of S/N as a function of the mobile phase pH and of phosphate concentration for 3-OMD (A), 5-HTP (B), 5-HIAA (C), HVA (D) and MHPG (E). The mobile phase consisted of a mixture of 5 mM ammonium formate / methanol (97/3, v/v). ESI was performed in positive mode. For each graph, the darker the color, the higher the S/N.

Figure VI.2 indicates that for all the analytes, regardless of the mobile phase pH, phosphate leads to an increase of S/N. However, the optimal phosphate concentration to reach the highest S/N depends on the pH and on the analyte. Indeed, for 3-OMD (Figure VI.2A) and 5-HTP

(Figure VI.2B), at pH 5.0, 5.5, 6.0 and 6.5, S/N increases continuously with phosphate concentration and the optimal phosphate concentration is of 20 µM, whereas at pH 7.0, S/N increases until 10 µM of phosphate, then it decreases. Likewise, for HVA (Figure VI.2D) and MHPG (Figure VI.2E), the optimal phosphate concentration varies between 10 µM and 20 µM depending on the pH. Concerning 5-HIAA, the optimal phosphate concentration is of 10 µM regardless of the pH. Figure VI.2 shows the combinations (pH; phosphate concentration) allowing to reach the highest S/N are as follow: for 3-OMD, 5-HTP, HVA and MHPG (pH 5.5; 20 µM) and for 5-HIAA (pH 7; 10 µM).

Phosphate-based positive signal enhancement is effective in ammonium formate for all the tested pHs by increasing the positive ESI of parent ions. This enhancement is importantly influenced by the buffer pH given the variation of the optimal phosphate concentration with the buffer pH. Moreover, Figure VI.3 indicates this effect can be saturated since the S/N augmentation may stop with a phosphate concentration of 10 µM and a decrease is then observed between 10 µM and 20 µM phosphate. Phosphate-based positive ESI enhancement is also highly affected by the analyzed molecule whether in terms of optimal combination (pH; phosphate concentration) or in terms of enhancement scale.

VI.5.3. Effect of buffer nature on phosphate-based positive ESI enhancement

Buffer nature influence on phosphate-based positive ESI enhancement was investigated. For this purpose, three ammonium-based buffers were evaluated: formate, acetate and carbonate. Figure VI.3 shows the evolution of S/N for HVA and 3-OMD as a function of the mobile phase pH and of phosphate concentration using these three buffers in the mobile phase.

Figure VI.3A, indicates, in ammonium formate, S/N increased with phosphate concentration in ammonium formate. Similarly, Figure VI.3B shows a continuous increase of the S/N of HVA in ammonium acetate, regardless of the pH. Nevertheless, in ammonium carbonate, Figure VI.3C indicates S/N did not increase with phosphate concentration, except at pH 7.0, where a signif-

icant improvement of S/N is observed between 0 and 10 µM. In terms of optimal S/N, in ammonium formate it was of 537 at pH 5.5 with 20 µM of phosphate whereas it was of 517 at pH 6.5 with 5 µM of phosphate and of 2200 at pH 7.0 with 5 µM of phosphate.

Given the observed differences in the evolution of the S/N of HVA when comparing the three buffers, buffer nature appears as an important parameter that influences phosphate-based positive ESI enhancement. Moreover, for HVA, even though this effect was less observed in ammonium carbonate compared to the other buffers, the maximal S/N is reached in this buffer. Furthermore, interestingly, regardless of the buffer nature and of the pH, Figure VI.3 shows that when phosphate-based positive ESI enhancement was observed, it saturated for high phosphate concentrations.

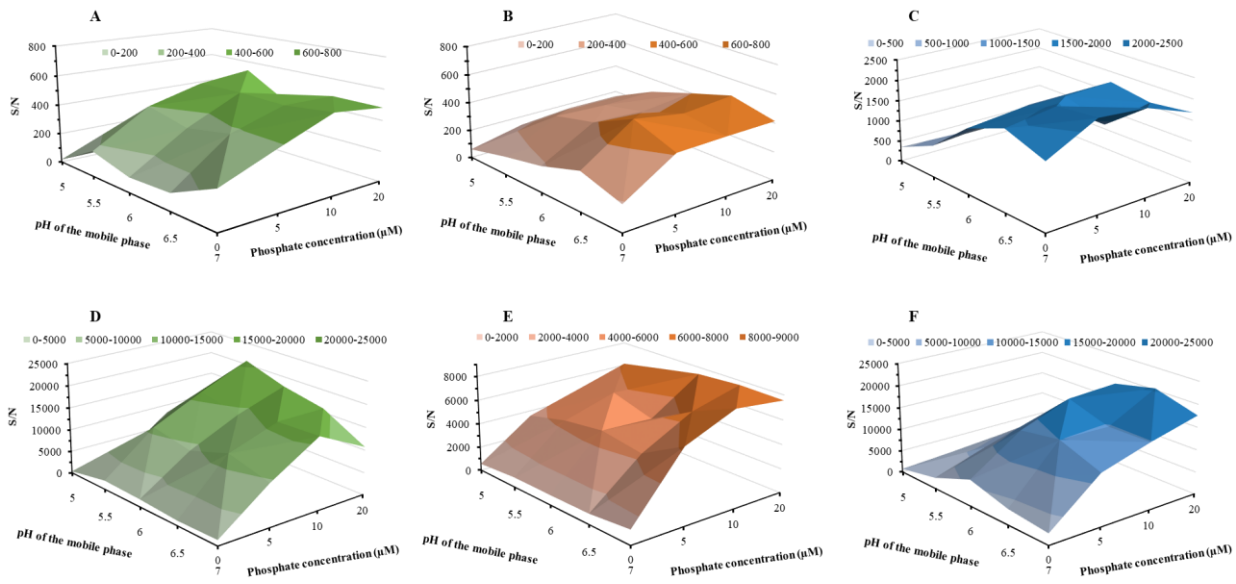

Figure VI.3: Evolution of S/N as a function of the mobile phase pH and of phosphate concentration for HVA (in ammonium formate (A), ammonium acetate (B) and ammonium carbonate (C)) and 3-OMD (in ammonium formate (D), ammonium acetate (E) and ammonium carbonate (F)). The mobile phase consisted of a mixture of 5 mM ionic strength buffer with different pHs/methanol (97/3, v/v). ESI was performed in positive mode. For each graph, the darker the color, the higher the S/N.

Figure VI.3D, 3E and 3F show the S/N of 3-OMD increases with phosphate concentration, regardless of the buffer nature and pH. However, the optimal S/N was of 20820 in ammonium formate at pH 5.5 with 20 µM of phosphate, 8006 in ammonium acetate at pH 7.0 with 10 µM

of phosphate and of 20370 in ammonium carbonate at pH 6.5 with 20 µM of phosphate. 3-OMD exhibits higher S/N in ammonium formate and carbonate compared to acetate. This confirms the buffer-effect on phosphate-based positive ESI enhancement described for HVA. Moreover, the enhancement was significant for 3-OMD in ammonium carbonate whereas it was negligible for HVA in the same buffer. In addition, the optimal combinations (pH; phosphate concentration) were different between these two analytes. Therefore, phosphate addition to the mobile phase at concentration between 5 and 20 µM is confirmed to enhance the positive ESI of the analytes. This enhancement depends on the buffer nature and pH and on the analyte.

VI.5.4. Effect of phosphate on negative electrospray ionization

In order to study if phosphate effect in positive ESI is also observed in negative mode, 3-OMD, 5-HIAA, 5-HTP, HVA and MHPG were analyzed with a mobile phase consisting of 5 mM; pH 5 ammonium acetate / methanol (97/3) with different concentrations of phosphate ranging between 0 and 20 µM (Figure VI.4).

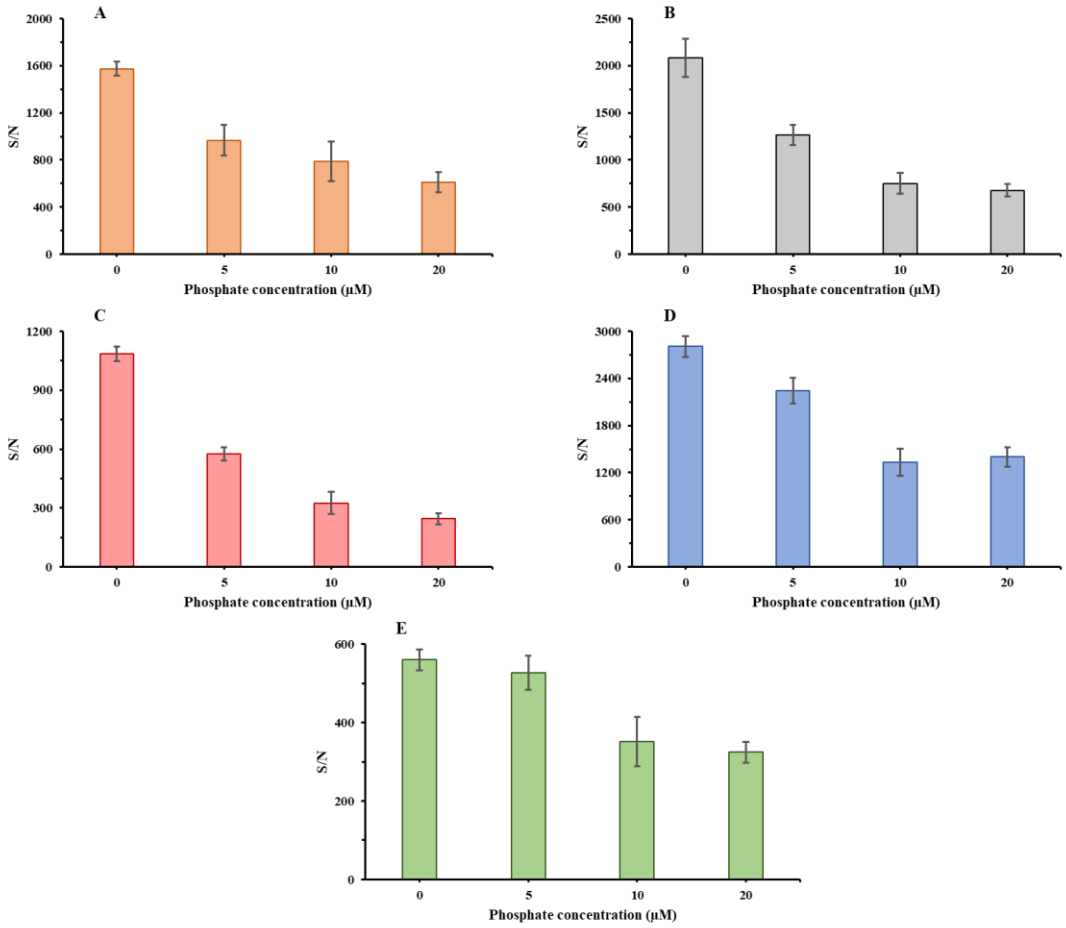

Figure VI.4: Evolution of S/N as a function of phosphate concentration in the mobile phase for 3-OMD (A), 5-HTP (B), 5-HIAA (C), HVA (D) and MHPG (E). The mobile phase consisted of a mixture of pH 5 ammonium acetate with different / methanol (97/3, v/v). ESI was performed in negative mode and MS/MS in MRM mode. Error bars represent the 95% confidence intervals.

Figure VI.4 indicates the S/N of all the analytes decreases significantly when increasing phosphate concentration. Indeed, for 3-OMD, 5-HTP, 5-HIAA and HVA, the decrease is continuous and it is significant starting from 5 µM of phosphate while for MHPG, S/N decreases significantly at 10 µM of phosphate. Therefore, contrary to what was previously described in positive ESI, in negative mode, phosphate inhibit the ionization of the analytes with a concentration-dependent effect. This is explained by the fact that at pH 5, phosphate is mostly in its basic form, thus charged negatively. During negative ESI, negatively charged phosphate is in competition with the analytes which lead to a partial ion suppression and a decrease of S/N. The ion suppression cannot be observed in positive mode since phosphate is negatively charged

and does not compete with the analytes. Moreover, phosphate counter ion, ammonium is highly volatile and is therefore at negligible amounts in the ESI nanodroplets.

VI.5.5. Confirmation of phosphate-based positive electrospray ionization enhancement

In order to determine if phosphate effect on positive ESI is specific or not to the set of analyzed molecules, another set of molecule, namely pterins, was analyzed. These molecules are structurally close to the first set of analytes with some remarkable differences since they contain more nitrogens including an amino function which makes them more inonisable in positive ESI. During these analyses, the mobile consisted of 97% 5 mM ammonium formate adjusted at three different pHs (2.5, 3.0 and 3.5) and 3% of methanol (Figure VI.5). As for the first group of analytes, for each mobile phase pH, four phosphate concentrations were tested: 0, 5, 10 and 20 µM (Figure VI.5). S/N was measured for each analyte in MRM mode in every mobile phase evaluated.

Figure VI.5 shows the S/N of all the analytes increased with phosphate concentration regardless of the mobile phase pH. However, the shape of the graph depended importantly on the analyte. Indeed, for BH2, B, N and NH2, the increase of S/N was continuous with phosphate concentration, whereas for BH4, S/N increased until its maximum then it decreased for higher phosphate concentration. Therefore, for BH2, B, N and NH2 the optimal phosphate concentration is of 20 µM regardless of the pH while for BH4, it is of 10 µM at pH 2.5 and 3.0 and of 5 µM at pH 3.5.

Moreover, Figure VI.5 indicates the optimal combination (pH; phosphate concentration) were as follows: BH4 (pH 3.5; 5 µM), BH2 (pH 3.5; 20 µM), NH2 (pH 3.5; 20 µM), B and N (pH 2.5; 20 µM). Thus, pH impacted significantly phosphate effect on S/N.

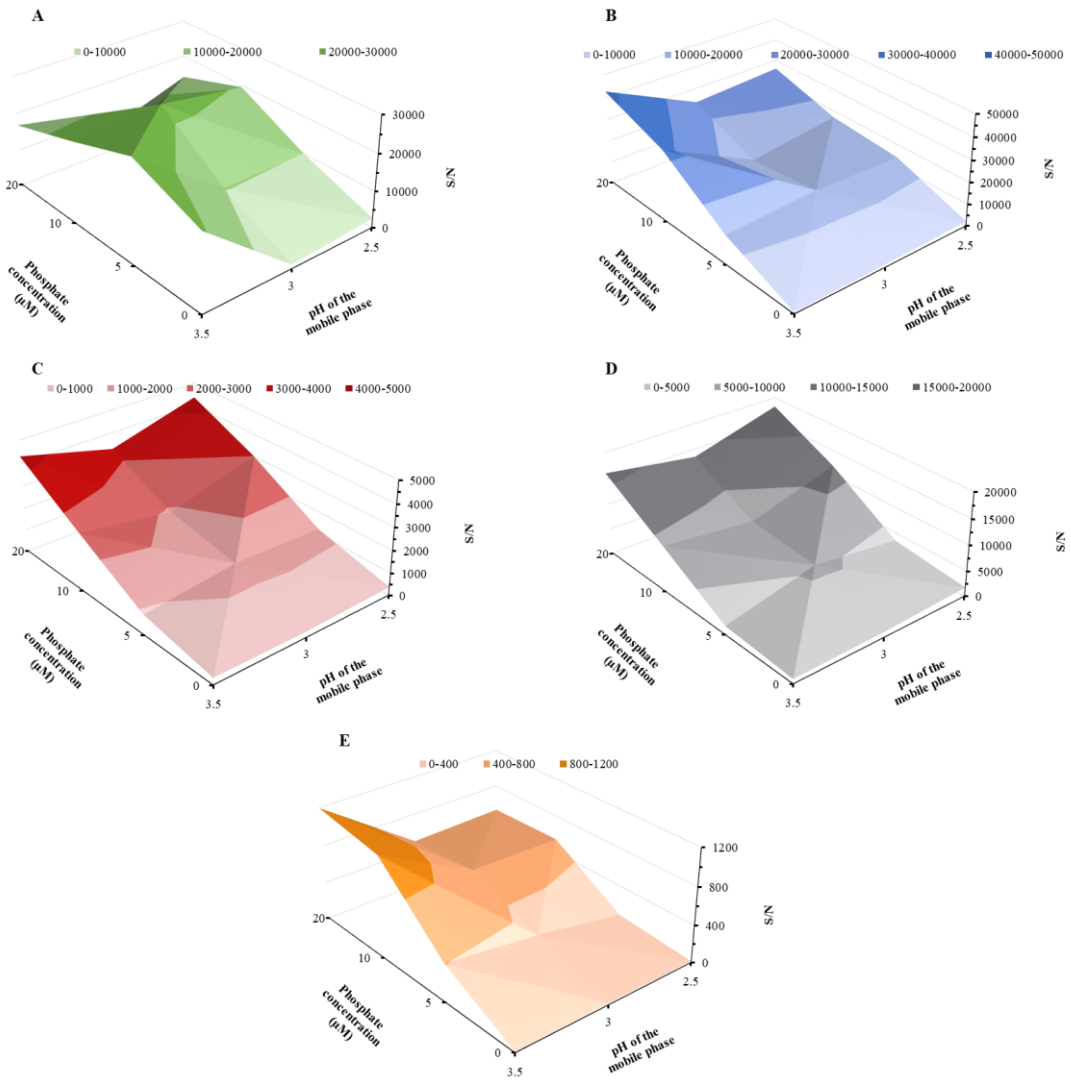

Figure VI.5: Evolution of S/N as a function of the mobile phase pH and of phosphate concentration for BH4 (A), BH2 (B), B (C), N (D) and NH2 (E). The mobile phase consisted of a mixture of 5 mM ammonium formate with different pHs / methanol (97/3, v/v). ESI was performed in positive mode. For each graph, the darker the color, the higher the S/N.

Figure VI.5 indicates for pterins, such as previously described for the first set of analytes, phosphate enhances positive ESI with a pH-dependent and analyte-dependent effect, hence, confirming it is not specific to the first set of molecules. Given the structural differences between the two groups of analytes, the enhancement is not specific to any chemical moiety.

Therefore, considering that phosphate-based positive ESI enhancement depends on the analyte, on the buffer nature and pH, that the aqueous and organic phases were kept constant and that phosphate leads to ion suppression in negative mode, it appears clearly that this effect

involves the ionization during ESI process, not the desolvation part. To explain, this phenomenon, four hypotheses were proposed:

1) Phosphate could decrease significantly the pH of the mobile phase, enabling a higher ESI efficiency.
2) Phosphate would lead to an increase of gas phase proton affinity of the analytes, enhancing by the way their positive ESI.
3) Negatively charged phosphate could form a low-energy complex with the positively-charged analyte based on electrostatic interactions in the ESI droplets, stabilizing the analyte. During the desolvation process, ammonium and formate ions being evaporated first, the complex is not stable anymore and the analyte goes to the gas phase in higher amounts because of the phosphate stabilization.
4) Phosphate could complex alkali metal ions, namely sodium and potassium, leading to a decrease of alkali metal ion adducts, thus to an increase of the signal of the analyte.

VI.5.6. Explanation of phosphate-based positive electrospray ionization enhancement

Hypothesis 1 was evaluated by measuring the aqueous phase pH after addition of the same phosphate concentrations as for the design of experiment. The measured pH did not vary of more than 0.01 with phosphate addition since the added concentrations are very low. Therefore, hypothesis 1 was denied.

To verify hypothesis 2, it was necessary to measure proton affinity of the analytes with different phosphate concentrations, after positive ESI. For this purpose, the kinetic method [47,48] was used. This method relies on the fragmentation of a protonated heterodimer composed of the analyte and a base which leads to the formation of the protonated base and the protonated analyte [47,48]. The proportion of these two fragmentation pathways allows to estimate the relative proton affinity of the analyte. For 3-OMD, HVA, 5-HTP, 5-HIAA and MHPG, the measurement was performed after chromatographic separation. We used ammonium as the base with a mobile phase consisting of a mixture of pH 5 ammonium acetate/ methanol (97/3, v/v).

In these conditions, MHPG did not exhibit any ammonium cluster in its spectrum. 3-OMD, 5-HTP and 5-HIAA had a protonated ammonium heterodimer however, it did not fragment into ammonium regardless of the collision energy. HVA did exhibit an ammonium cluster and it fragmented into both ammonium and the protonated analyte. Therefore, the kinetic method was only performed for HVA with four different concentrations of phosphate: 0, 5, 10 and 20 µM. The relative proportion of the protonated HVA and of ammonia did not vary significantly while increasing phosphate concentration, thus indicating that proton affinity was not affected by phosphate. Hence, hypothesis 2 was denied.

To confirm or deny hypothesis 3, five concentrations of the analytes were tested considering that if a complex is formed between the molecules and phosphate, the optimal phosphate concentration in terms of S/N would shift with analyte concentration. The optimum S/N was at the same phosphate concentration for a given analyte regardless of its concentration. This demonstrates that phosphate did not form a low-energy complex with the analytes that is why, hypothesis 3 was denied.

To verify hypothesis 4, MS spectra were measured for each analyte after chromatographic separation in positive ESI, using a mobile phase consisting of a mixture of pH 5 ammonium acetate / methanol (97/3, v/v) with four phosphate concentration (0, 5, 10 and 20 µM). The measured spectra were compared to phosphate-based S/N increase in the same mobile phase (Figure VI.6). Figure VI.6 shows S/N of all the analytes increase with phosphate concentration. MS spectra (Figure VI.6) indicates phosphate lead to a significant decrease of sodium and potassium adducts and an increase of the protonated analyte for 3-OMD (Figure VI.6A'), 5-HTP (Figure VI.6B'), MHPG (Figure VI.6C') and 5-HIAA (Figure VI.6D'). For HVA (Figure VI.6E'), alkali metal ion adducts decrease in favor of the increase of ammonium adduct. The latter was used as parent ion in the MRM transitions of HVA (Table VI.1) and its repeatability was previously verified [46].

It should be noted that S/N enhancement is not always correlated in proportions to the increase of the parent ion (Figure VI.6). This is explained by the fact that the two analyses were not

performed at the same concentrations of analytes. Indeed, for S/N measurements in MRM, concentrations were of 1 µM for 3-OMD, 5-HTP, MHPG and 5-HIAA and of 10 µM for HVA whereas to measure MS spectra, these concentrations were of 50 µM and 100 µM, respectively. Therefore, MS spectra were measured at concentrations exceeding the linearity range which explains why S/N increases at higher rate than the intensity of parent ions.

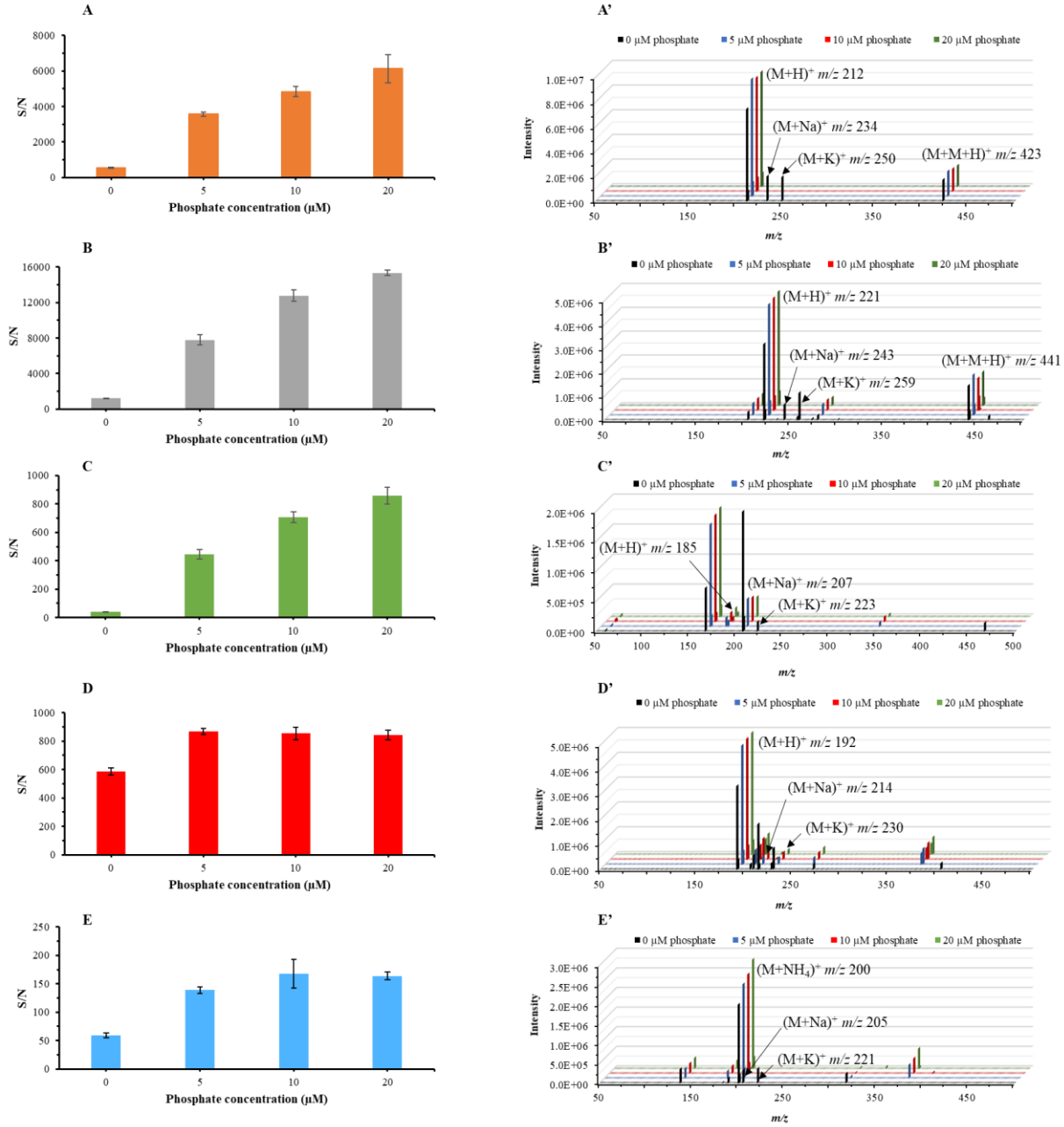

Figure VI.6: Evolution of S/N as a function of phosphate concentration in the mobile phase for 3-OMD (A), 5-HTP (B), MHPG (C), 5-HIAA (D) and HVA (E). The mobile phase consisted of a mixture of 5 mM ammonium acetate pH 5.0 / methanol (97/3, v/v). ESI was performed in positive mode and MS/MS in MRM mode. Error bars represent the 95% confidence intervals. Full scan MS spectra of 3-OMD (A'), 5-HTP (B'), MHPG (C'), 5-HIAA (D') and HVA (E') measured for different phosphate concentration in the mobile phase after positive ESI.

Figure VI.6 indicates phosphate decreases alkali metal ion adduct with a concentration-dependent effect. Since every analyte behaves differently in terms of adduct formation, it explains why phosphate-based positive ESI enhancement highly depends on the analyte. Moreover, alkali metal ion adduct formation is determined by buffer nature and pH [30,36] such as their elimination by the addition of phosphate. Furthermore, we observed previously that phosphate effect on S/N was saturable and may even lead to a decrease of S/N at high concentrations. Indeed, the addition of phosphate complexes sodium and potassium, until there is no more alkali metal ion to complex. Then, phosphate complex the protonated analyte, yielding by the way, a neutral cluster which is not detected, hence the decrease of S/N. Therefore, hypothesis 4 fits perfectly with the previously made observations and it is confirmed.

Phosphate complexation to alkali metal ions could be explained by two processes. First, phosphate binds sodium and potassium in solution with a sufficiently high affinity to form a neutral complex, before the desolvation of the analyte. Second, phosphate has a gas-phase proton affinity of 327.9-328.2 kcal.mol^{-1} as described by Moser *et al.* [49] leading to a weak protonation efficiency. Phosphate being negatively charged and exhibiting a low affinity to protons, it complexes alkali metal ions. The first process occurs in solution and in the electrospray droplets while the second one set up in the gas phase, after the complete desolvation.

Other desalting methods based on anion addition were previously reported [12,32–34]. Flick *et al.* evaluated the ability of citrate and tartrate to reduce nonspecific sodium adduction [12]. It was reported that these anions decreased significantly sodium adduction. This effect was explained to the low proton affinities of both anions (lower than 315 kcal.mol^{-1}). Indeed, citrate and tartrate had a weak affinity to sodium in solution, indicating they could not sequester sodium before ion formation [12]. For phosphate complexation to alkali metal ions, since the proton affinity of phosphate is higher than 315 kcal.mol^{-1}, it is likely that the in-solution process is predominant and that the gas-phase process has only a weak occurrence. This is supported

by the observed important influence of solution pH on phosphate-based positive ESI enhancement.

VI.6. CONCLUSIONS

Phosphate can increase the S/N of molecules analyzed after positive ESI by enhancing their ionization. This enhancement depends on the analyte, the nature and pH of the buffer used in the mobile phase. Depending on the analyte, the buffer nature and pH, gain factors in terms of S/N are ranging between 1.4 and 103.4. Hence, phosphate addition may be highly powerful to improve sensitivity. Nevertheless, phosphate concentration needs to be optimized for each chromatographic mobile phase used and for every analyte. Phosphate-based positive ESI enhancement involves the elimination of sodium and potassium adducts and corresponds therefore to a desalting method. Indeed, negatively charged phosphate complexes alkali metal ions, thus resulting in the decrease of their adducts.

This desalting method in positive ESI is easy-to-handle and effective with very high increase factor of S/N. It does not require any instrumental adaptation and can significantly improve lower limits of quantification and detection. Moreover, by reducing the adduction of analytes, it should allow to enhance precision and accuracy. Thus, the desalting method could be applied to the analytical development of quantification methods especially in biological fluids, namely biomarker quantification or pharmacokinetic monitoring. These methods require high analytical performances in terms of sensitivity, accuracy and precision.

VI.7. REFERENCES

[1] Fenn John B., Mann Matthias, Meng Chin Kai, Wong Shek Fu, Whitehouse Craig M., Electrospray Ionization for Mass Spectrometry of Large Biomolecules, Science. 246 (1989) 64–71. https://doi.org/10.1126/science.2675315.

[2] J.B. Fenn, M. Mann, C.K. Meng, S.F. Wong, C.M. Whitehouse, Electrospray ionization-principles and practice, Mass Spectrom. Rev. 9 (1990) 37–70. https://doi.org/10.1002/mas.1280090103.

[3] M. de Raad, C.R. Fischer, T.R. Northen, High-throughput platforms for metabolomics, Curr. Opin. Chem. Biol. 30 (2016) 7–13. https://doi.org/10.1016/j.cbpa.2015.10.012.

[4] C.M. Whitehouse, R.N. Dreyer, Masamichi. Yamashita, J.B. Fenn, Electrospray interface for liquid chromatographs and mass spectrometers, Anal. Chem. 57 (1985) 675–679. https://doi.org/10.1021/ac00280a023.

[5] H. Mizuno, K. Ueda, Y. Kobayashi, N. Tsuyama, K. Todoroki, J.Z. Min, T. Toyo'oka, The great importance of normalization of LC–MS data for highly-accurate non-targeted metabolomics, Biomed. Chromatogr. 31 (2017) e3864. https://doi.org/10.1002/bmc.3864.

[6] T. Fuhrer, N. Zamboni, High-throughput discovery metabolomics, Anal. Biotechnol. 31 (2015) 73–78. https://doi.org/10.1016/j.copbio.2014.08.006.

[7] K. Dettmer, P.A. Aronov, B.D. Hammock, Mass spectrometry-based metabolomics, Mass Spectrom. Rev. 26 (2007) 51–78. https://doi.org/10.1002/mas.20108.

[8] L. Yi, N. Dong, Y. Yun, B. Deng, D. Ren, S. Liu, Y. Liang, Chemometric methods in data processing of mass spectrometry-based metabolomics: A review, Anal. Chim. Acta. 914 (2016) 17–34. https://doi.org/10.1016/j.aca.2016.02.001.

[9] D. Dudzik, C. Barbas-Bernardos, A. García, C. Barbas, Quality assurance procedures for mass spectrometry untargeted metabolomics. a review, Rev. Issue 2017. 147 (2018) 149–173. https://doi.org/10.1016/j.jpba.2017.07.044.

[10] M. Wilm, Principles of Electrospray Ionization, Mol. Cell. Proteomics. 10 (2011) M111.009407. https://doi.org/10.1074/mcp.M111.009407.

[11] A.P. Bruins, Mechanistic aspects of electrospray ionization, J. Chromatogr. A. 794 (1998) 345–357. https://doi.org/10.1016/S0021-9673(97)01110-2.

[12] T.G. Flick, C.A. Cassou, T.M. Chang, E.R. Williams, Solution Additives that Desalt Protein Ions in Native Mass Spectrometry, Anal. Chem. 84 (2012) 7511–7517. https://doi.org/10.1021/ac301629s.

[13] P.J. Taylor, Matrix effects: the Achilles heel of quantitative high-performance liquid chromatography–electrospray–tandem mass spectrometry, LC Mass Spectrom. Recent Dev. Clin. Chem. 38 (2005) 328–334. https://doi.org/10.1016/j.clinbiochem.2004.11.007.

[14] A. Furey, M. Moriarty, V. Bane, B. Kinsella, M. Lehane, Ion suppression; A critical review on causes, evaluation, prevention and applications, Talanta. 115 (2013) 104–122. https://doi.org/10.1016/j.talanta.2013.03.048.

[15] I. Erngren, J. Haglöf, M.K.R. Engskog, M. Nestor, M. Hedeland, T. Arvidsson, C. Pettersson, Adduct formation in electrospray ionisation-mass spectrometry with hydrophilic interaction liquid chromatography is strongly affected by the inorganic ion concentration of the samples, J. Chromatogr. A. 1600 (2019) 174–182. https://doi.org/10.1016/j.chroma.2019.04.049.

[16] H.J. Sterling, J.D. Batchelor, D.E. Wemmer, E.R. Williams, Effects of buffer loading for electrospray ionization mass spectrometry of a noncovalent protein complex that requires high concentrations of essential salts, J. Am. Soc. Mass Spectrom. 21 (2010) 1045–1049. https://doi.org/10.1016/j.jasms.2010.02.003.

[17] R.M. Tubaon, P.R. Haddad, J.P. Quirino, Sample Clean-up Strategies for ESI Mass Spectrometry Applications in Bottom-up Proteomics: Trends from 2012 to 2016, PROTEOMICS. 17 (2017) 1700011. https://doi.org/10.1002/pmic.201700011.

[18] K. Lanckmans, S. Sarre, I. Smolders, Y. Michotte, Quantitative liquid chromatography/mass spectrometry for the analysis of microdialysates, Talanta. 74 (2008) 458–469. https://doi.org/10.1016/j.talanta.2007.07.027.

[19] K. Nozaki, A. Tarui, I. Osaka, H. Kawasaki, R. Arakawa, Elimination Technique for Alkali Metal Ion Adducts from an Electrospray Ionization Process Using an On-line Ion Suppressor, Anal. Sci. 26 (2010) 715–718. https://doi.org/10.2116/analsci.26.715.

[20] M. Fischnaller, R. Köck, R. Bakry, G.K. Bonn, Enrichment and desalting of tryptic protein digests and the protein depletion using boron nitride, Anal. Chim. Acta. 823 (2014) 40–50. https://doi.org/10.1016/j.aca.2014.03.008.

[21] M.J. Boundy, A.I. Selwood, D.T. Harwood, P.S. McNabb, A.D. Turner, Development of a sensitive and selective liquid chromatography–mass spectrometry method for high throughput analysis of paralytic shellfish toxins using graphitised carbon solid phase extraction, J. Chromatogr. A. 1387 (2015) 1–12. https://doi.org/10.1016/j.chroma.2015.01.086.

[22] I.A. Tibavinsky, P.A. Kottke, A.G. Fedorov, Microfabricated Ultrarapid Desalting Device for Nanoelectrospray Ionization Mass Spectrometry, Anal. Chem. 87 (2015) 351–356. https://doi.org/10.1021/ac5040083.

[23] L. Bräutigam, M. Seegel, I. Tegeder, H. Schmidt, S. Meier, M. Podda, R. Kaufmann, M. Grundmann-Kollmann, G. Geisslinger, Determination of 8-methoxypsoralen in human plasma, and microdialysates using liquid chromatography–tandem mass spectrometry, J. Chromatogr. B. 798 (2003) 223–229. https://doi.org/10.1016/j.jchromb.2003.09.051.

[24] V.G. Zaikin, J.M. Halket, Derivatization in Mass Spectrometry—8. Soft Ionization Mass Spectrometry of Small Molecules, Eur. J. Mass Spectrom. 12 (2006) 79–115. https://doi.org/10.1255/ejms.798.

[25] S. Gao, Z.-P. Zhang, H.T. Karnes, Sensitivity enhancement in liquid chromatography/atmospheric pressure ionization mass spectrometry using derivatization and mobile phase additives, Improv. Sensit. Liq. Chromatogr.-MASS Spectrom. 825 (2005) 98–110. https://doi.org/10.1016/j.jchromb.2005.04.021.

[26] M.C. García, The effect of the mobile phase additives on sensitivity in the analysis of peptides and proteins by high-performance liquid chromatography–electrospray mass spectrometry, Improv. Sensit. Liq. Chromatogr.-MASS Spectrom. 825 (2005) 111–123. https://doi.org/10.1016/j.jchromb.2005.03.041.

[27] T.L. Constantopoulos, G.S. Jackson, C.G. Enke, Challenges in achieving a fundamental model for ESI, Anal. Chim. Acta. 406 (2000) 37–52. https://doi.org/10.1016/S0003-2670(99)00600-5.

[28] P. Kebarle, M. Peschke, On the mechanisms by which the charged droplets produced by electrospray lead to gas phase ions, Anal. Chim. Acta. 406 (2000) 11–35. https://doi.org/10.1016/S0003-2670(99)00598-X.

[29] É. Alechaga, E. Moyano, M.T. Galceran, Ion-molecule adduct formation in tandem mass spectrometry, Anal. Bioanal. Chem. 408 (2016) 1269–1277. https://doi.org/10.1007/s00216-015-9237-6.

[30] R. Costalunga, S. Tshepelevitsh, H. Sepman, M. Kull, A. Kruve, Sodium adduct formation with graph-based machine learning can aid structural elucidation in non-targeted LC/ESI/HRMS, Anal. Chim. Acta. 1204 (2022) 339402. https://doi.org/10.1016/j.aca.2021.339402.

[31] T. Shamai Yamin, H. Prihed, M. Madmon, A. Shifrovitch, A. Baratz, A. Weissberg, Structural elucidation of phenidate analogues via the ESI-MS/MS spectra of their sodium adduct ions, Forensic Sci. Int. 306 (2020) 110044. https://doi.org/10.1016/j.forsciint.2019.110044.

[32] A. Kruve, K. Kaupmees, Adduct Formation in ESI/MS by Mobile Phase Additives, J. Am. Soc. Mass Spectrom. 28 (2017) 887–894. https://doi.org/10.1007/s13361-017-1626-y.

[33] C. A. Cassou, E. R. Williams, Desalting protein ions in native mass spectrometry using supercharging reagents, Analyst. 139 (2014) 4810–4819. https://doi.org/10.1039/C4AN01085J.

[34] W. Qi, Q. Guan, T. Sun, Y. Cao, L. Zhang, Y. Guo, Improving detection sensitivity of amino acids in thyroid tissues by using phthalic acid as a mobile phase additive in hydrophilic interaction chromatography-electrospray ionization-tandem mass spectrometry, Anal. Chim. Acta. 870 (2015) 75–82. https://doi.org/10.1016/j.aca.2015.02.048.

[35] R.E. Birdsall, M. Gilar, H. Shion, Y.Q. Yu, W. Chen, Reduction of metal adducts in oligonucleotide mass spectra in ion-pair reversed-phase chromatography/mass spectrometry analysis, Rapid Commun. Mass Spectrom. 30 (2016) 1667–1679. https://doi.org/10.1002/rcm.7596.

[36] R.E. Birdsall, J. Kellett, Y.Q. Yu, W. Chen, Application of mobile phase additives to reduce metal-ion mediated adsorption of non-phosphorylated peptides in RPLC/MS-based assays, J. Chromatogr. B. 1126–1127 (2019) 121773. https://doi.org/10.1016/j.jchromb.2019.121773.

[37] N. Li, N.M. El Zahar, J.G. Saad, E.R.E. van der Hage, M.G. Bartlett, Alkylamine ion-pairing reagents and the chromatographic separation of oligonucleotides, J. Chromatogr. A. 1580 (2018) 110–119. https://doi.org/10.1016/j.chroma.2018.10.040.

[38] S.Å. Gustavsson, J. Samskog, K.E. Markides, B. Långström, Studies of signal suppression in liquid chromatography–electrospray ionization mass spectrometry using volatile ion-pairing reagents, J. Chromatogr. A. 937 (2001) 41–47. https://doi.org/10.1016/S0021-9673(01)01328-0.

[39] M. Shibue, C.T. Mant, R.S. Hodges, Effect of anionic ion-pairing reagent concentration (1–60mM) on reversed-phase liquid chromatography elution behaviour of peptides, 24th Int. Symp. Sep. Proteins Pept. Polynucleotides. 1080 (2005) 58–67. https://doi.org/10.1016/j.chroma.2005.02.047.

[40] M. Shibue, C.T. Mant, R.S. Hodges, Effect of anionic ion-pairing reagent hydrophobicity on selectivity of peptide separations by reversed-phase liquid chromatography, 24th Int. Symp. Sep. Proteins Pept. Polynucleotides. 1080 (2005) 68–75. https://doi.org/10.1016/j.chroma.2005.03.035.

[41] K. Brak, E.N. Jacobsen, Asymmetric Ion-Pairing Catalysis, Angew. Chem. Int. Ed. 52 (2013) 534–561. https://doi.org/10.1002/anie.201205449.

[42] J.-P. Antignac, K. de Wasch, F. Monteau, H. De Brabander, F. Andre, B. Le Bizec, The ion suppression phenomenon in liquid chromatography–mass spectrometry and its consequences in the field of residue analysis, Anal. Chim. Acta. 529 (2005) 129–136. https://doi.org/10.1016/j.aca.2004.08.055.

[43] D.L. Buhrman, P.I. Price, P.J. Rudewicz, Quantitation of SR 27417 in human plasma using electrospray liquid chromatography-tandem mass spectrometry: A study of ion suppression, J. Am. Soc. Mass Spectrom. 7 (1996) 1099–1105. https://doi.org/10.1016/S1044-0305(96)00072-4.

[44] G. Gunasekaran, L.R. Chauhan, Eco friendly inhibitor for corrosion inhibition of mild steel in phosphoric acid medium, Electrochimica Acta. 49 (2004) 4387–4395. https://doi.org/10.1016/j.electacta.2004.04.030.

[45] A.A. Khadom, S.N. Farhan, Corrosion inhibition of steel in phosphoric acid, Corros. Rev. 36 (2018) 267–280. https://doi.org/10.1515/corrrev-2017-0104.

[46] A. Boulghobra, T. Abar, F. Moussa, B. Baudin, D. Rodriguez, A. Pallandre, M. Bonose, Quantification of monoamine biomarkers in cerebrospinal fluid: comparison of a UHPLC-MS/MS method to a UHPLC coupled to fluorescence detection method, Biomed. Chromatogr. n/a (n.d.) e5502. https://doi.org/10.1002/bmc.5502.

[47] G. Cooks, J. Patrick, T. Kotiaho, S. McLuckey, Thermochemical determinations by the kinetic method, Mass Spectrom. Rev. 13 (1994) 287–339. https://doi.org/10.1002/mas.1280130402.

[48] S.A. McLuckey, D. Cameron, R.G. Cooks, Proton affinities from dissociations of proton-bound dimers, J. Am. Chem. Soc. 103 (1981) 1313–1317. https://doi.org/10.1021/ja00396a001.

[49] A. Moser, K. Range, D.M. York, Accurate Proton Affinity and Gas-Phase Basicity Values for Molecules Important in Biocatalysis, J. Phys. Chem. B. 114 (2010) 13911–13921. https://doi.org/10.1021/jp107450n.

CONCLUSION ET PERSPECTIVES

Depuis plusieurs années, le diagnostic des EIM de la dopamine et de la sérotonine repose sur l'analyse quantitative de biomarqueurs identifiés et validés dans le LCR. Du fait de la complexité de cette quantification, seuls quelques laboratoires dans le monde sont capables de réaliser ce type d'analyse. En effet, le dosage des biomarqueurs des EIM de la dopamine et de la sérotonine dans le LCR présente plusieurs difficultés. Certaines sont liées à la nature de l'échantillon biologique et à la stabilité des biomarqueurs : le LCR doit être stocké à -80°C et analysé très rapidement après décongélation. D'autres défis sont liés aux performances de la méthode analytique utilisée. Elle doit permettre une analyse sensible, exacte, précise et suffisamment rapide pour une utilisation en routine clinique. Par ailleurs, la méthode analytique doit, de par les profils métaboliques, rendre possible un diagnostic de certitude en identifiant les échantillons de patients atteints d'EIM. Enfin, du fait du caractère hautement précieux du LCR, qui plus est, prélevé chez des nourrissons ou des enfants, la prise en compte du volume disponible est primordiale pour l'analyse quantitative, notamment lors de la préparation de l'échantillon.

L'état de l'art des méthodes de dosages des biomarqueurs des EIM dans le LCR a permis de mettre en évidence les différentes façons de relever les défis liés au diagnostic de ces maladies. En termes de traitement d'échantillon, la simplicité ainsi que la rapidité sont privilégiées pour un meilleur débit d'analyse en routine. En effet, la dilution et/ou la filtration sont les préparations d'échantillons de choix pour analyser les LCR. L'état de l'art a également permis d'identifier la technique de référence pour la séparation de ces composés : l'HPLC. Par ailleurs, plusieurs modes de détection peuvent être envisagés pour l'analyse de ces composés, à savoir la détection électrochimique (ECD), la détection par fluorescence (FD) et la spectrométrie de masse en tandem (MS/MS). Du fait de sa spécificité, la tendance est à l'utilisation de la MS/MS dans des méthodes quantifiant plus de 20 analytes. Ceci permet d'affiner le diagnostic en explorant plus de pathologies potentielles, tout en utilisant le même volume d'échantillon.

Dans cette thèse, avant de proposer des méthodes quantitatives pour le dosage des ptérines, nous avons étudié la stabilité de la BH4 dans les conditions d'analyse. Cette étude a mis en évidence que ce biomarqueur est sujet à de l'auto-oxydation spontanée. Effectivement, la BH4 se dégrade très rapidement et ce, quel que soit le milieu étudié. Par ailleurs, les produits de dégradation et la cinétique d'auto-oxydation varient en fonction du tampon de dissolution. Ces résultats sont déterminants quant à la façon d'appréhender le dosage de ce biomarqueur. Ainsi, pour les prochains développements de méthodes, la BH4 ne peut être quantifiée sans que sa cinétique d'auto-oxydation et ses produits de dégradation ne soient pris en compte. Pour cela, une détection en MS/MS sera à privilégier du fait de sa grande spécificité. La séparation en HPLC peut être délicate, étant donnée la proximité des structures des produits de dégradation et de la BH4. Une dimension de séparation supplémentaire pourrait alors être utilisé pour une séparation efficace. Avec l'avènement d'instrumentation de plus en plus robuste et permettant des analyses reproductibles en mobilité ionique, celle-ci pourrait être envisagée. Cependant, sa compatibilité avec le diagnostic doit préalablement être vérifiée, en particulier concernant la sensibilité, la précision et le temps d'analyse.

Au cours de cette thèse, nous nous sommes intéressés au second groupe de biomarqueurs des EIM de la dopamine et de la sérotonine, à savoir les métabolites de type monoamine. Pour ces composés, nous avons proposé et validé deux méthodes quantitatives adaptées au diagnostic des maladies étudiées. Les deux méthodes varient essentiellement en termes de mode de détection : l'une est basée sur la FD et l'autre sur la MS/MS. La comparaison des deux a montré que, dans un laboratoire désirant quantifier ces biomarqueurs dans le LCR, l'une ou l'autre pouvait être choisie en fonction des critères pris en compte : si la priorité est la rapidité de l'analyse, la méthode UHPLC-MS/MS sera privilégiée, tandis que si le premier critère de choix est le coût de l'instrumentation, celle en UHPLC-FD sera choisie.

Une avancée majeure obtenue au cours de cette thèse correspond à la méthode de dessalage en ionisation par electrospray (ESI) en mode positif, lors d'une détection par MS. Cette étape n'était pas prévue dans le plan de départ de la thèse. Cependant, après avoir

observé le phénomène d'amélioration du signal en ESI avec de faibles concentrations de phosphate, il nous a paru judicieux d'approfondir cet aspect afin de comprendre et d'expliquer le phénomène. Dans un premier temps, l'amélioration du signal en ESI en mode positif avec le phosphate a été confirmé et nous avons observé qu'elle dépend de la nature et du pH du tampon utilisé dans la phase mobile. Après avoir formulé plusieurs hypothèses pouvant expliquer ces observations, nous les avons testées. Celle qui a été vérifiée est que le phosphate ajouté complexe le sodium et le potassium présents dans la solution et permet le dessalage en ESI à polarité positive. Cette méthode simple et efficace pourrait être utilisée pour améliorer la sensibilité de méthodes quantitatives en particulier pour le dosage de biomarqueurs.

Ainsi, au cours de cette thèse, nous avons pu proposer des méthodes fiables pour la quantification des biomarqueurs validés des EIM de la dopamine et de la sérotonine. La perspective serait de mieux comprendre ces pathologies afin d'identifier de nouveaux biomarqueurs, de nouvelles cibles thérapeutiques et pour envisager un suivi thérapeutique après la mise en place d'un traitement. Pour cela, étant donné la nature métabolique de ces maladies, il faudrait, dans un premier temps, étudier le métabolome du LCR chez les individus non atteints d'EIM et le comparer à chacune des EIM de la dopamine et de la sérotonine. Ceci permettrait de mieux comprendre la physiopathologie de ces maladies au niveau du SNC. Par la suite, l'étude métabolomique du LCR devrait être corrélée à une recherche métabolomique dans le plasma et dans les urines chez les mêmes patients. D'éventuels biomarqueurs dans ces fluides biologiques plus accessibles et prélevés de manière moins invasive pourraient alors être identifiés. Il s'agit donc de mettre en place une étude clinique de grande envergure pour corréler les métabolomes du LCR, du plasma et des urines de chaque individu. Ceci correspond à la continuité scientifique du projet. Cependant, avant d'envisager cette continuité, il convient de se poser certaines questions éthiques : la pratique clinique (diagnostic et traitement) actuelle n'est-elle pas suffisamment efficace dans la prise en charge des patients atteints d'EIM ?